Educational Handbook

Nuclear and Particle Physics Experiments

2025 Edition

CAEN Educational Handbook

Nuclear and Particle Physics Experiments

2025 Edition

https://edu.caen.it

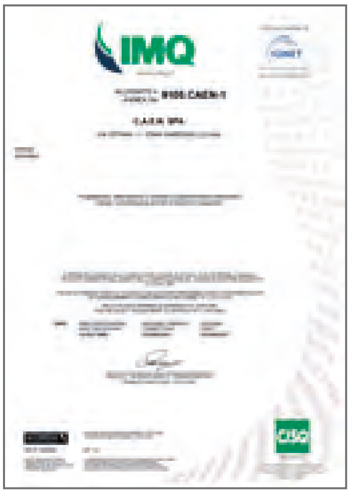

We are proud of the high quality of our products.

ISO 9001

ISO 9001:2015 approved quality system ensures all our internal processes.

From R&D to the registration of the incoming purchase orders, through:
- Resource Planning
- Scheduling
- Production

Our quality system is responsible for the proper functioning of all our internal processes and is subject to regularly audits, carried out by the National Standards Authority.

From the initial product design and its development stages, till the delivery of the production batches, we follow documented procedures that cover every aspect of our business.

The quality of CAEN S.p.A. products is constantly monitored by the application of the UNI EN ISO 9001:2015 standard. CAEN S.p.A. is ISO 9001 certified since 1998.

ISO9001:2015
certified Company

Authorised research laboratory of the MIUR

CAEN CAEN draws upon over 45 years of collaboration with the High Energy & Nuclear Physics community to enhance university educational laboratories. This includes providing advanced instrumentation developed for major experiments worldwide and leveraging teaching experience at esteemed institutions like the University of Insubria (Como, Italy), University of Ferrara (Italy), and Aveiro University (Portugal), as well as partnerships with prestigious academic programs such as the Erasmus Mundus in Nuclear Physics and LA CoNGA Physics.

In addition to offering detailed Educational Notes showcasing a variety of experiments based on the latest technologies and instrumentations, CAEN also provides dedicated training sessions. These sessions, led by expert staff, are tailored to meet specific customer needs. The goal is to inspire students and facilitate their understanding of diverse physics phenomena through state-of-the-art technologies, instruments, and methodologies.

In collaboration with:

University of Insubria, Italy
University of Aveiro, Portugal
Nuclear Instruments srl, Italy,
University of Ferrara, Italy
Erasmus Mundus
LA CoNGA Physics

CAEN *Tools for Discovery* **Electronic Instrumentation**

CAEN SpA is a worldwide leading company provider of a comprehensive range of high/low voltage power systems and data acquisition/front-end modules compliant with IEEE standards for nuclear and particle physics.

Extensive research and development capabilities allowed **CAEN SpA** to play an important long-term role in this field. Thanks to years of close collaborations with the most important Research Centres of the world, CAEN strikes to deliver innovative products and services worldwide.

CAEN portfolio includes over a thousand products and solutions for nuclear measurements, whose quality is monitored throughout the entire production cycle and guaranteed by UNI EN ISO 9001:2015 standard. Its products appeal to a wide range of customers including engineers, scientists and technical professionals who all trust them to achieve their goals quickly and effectively.

Thanks to plenty of experience in physics research, CAEN instruments are now used in several advanced industrial applications.

Products

- Modular Pulse Processing Electronics
- Waveform Digitizers
- Digital Spectroscopy
- Electronics for SiPM
- Power Supplies
- Digital Detector Emulators
- Educational Kits

Applications

- High Energy Physics
- Astrophysics
- Neutrino Physics
- Dark Matter Investigation
- Nuclear Physics
- Material Science
- Medical Imaging Applications
- Homeland Security
- Industrial Applications

Discover, Learn, and Innovate with
CAEN EduLab Learning Platform

Where science and technology meet your curiosity

CAEN EduLab Learning Platform is the dedicated portal for scientific and technological education, designed to support students, teachers, and enthusiasts in their STEM (Science, Technology, Engineering, and Mathematics) education. The platform offers a wide range of educational resources, including tutorials, virtual labs, and interactive learning materials, all aimed at facilitating the teaching and learning of the most advanced technologies.

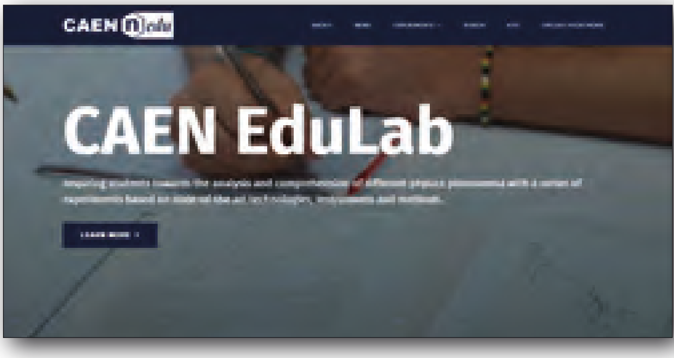

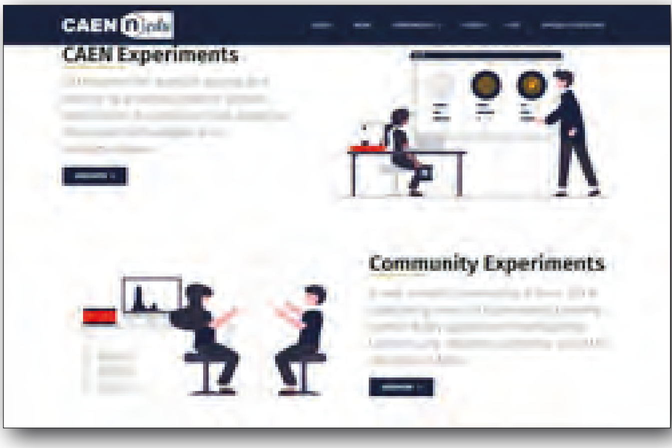

Key Sections of the Platform:

Lab Toolkit
A section dedicated to educational toolkits, providing practical guides and tools to conduct experiments and laboratory activities effectively and safely.

Tutorials
Step-by-step video tutorials and guides that help students and educators explore scientific and technical applications, with a particular focus on CAEN products and solutions.

Courses
Structured learning paths that cover various levels of expertise, offering the opportunity to learn progressively and in-depth.

Resources
A repository of educational materials, including handouts, articles, and technical manuals, accessible to enrich the learning process.

Support
A dedicated support service to answer questions and provide technical assistance, ensuring a smooth and uninterrupted learning experience.

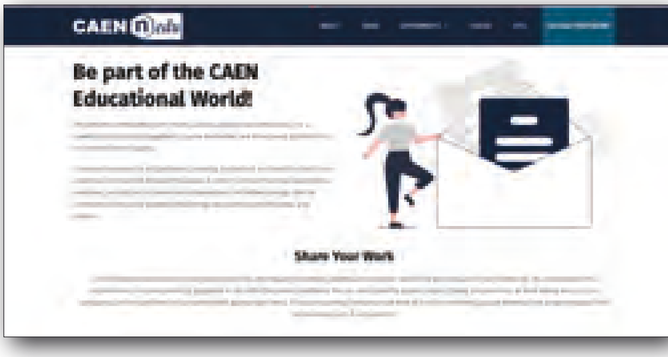

Additionally, **registered users have the opportunity to collaborate with the platform by proposing new experiments and sharing their scientific experiences using CAEN Edu products.** This collaborative approach not only enhances the platform's content but also fosters a community of learners who can socialize and grow together through shared knowledge and experiences.

CAEN EduLab Learning Platform stands as a key resource for anyone looking to deepen their knowledge of cutting-edge sciences and technologies, offering tools and resources for innovative and engaging learning.

Detailed Information on https://edu.caen.it

Navigating the Experiment Framework

How to read this Handbook

This handbook is divided into four sections:

1. Indexes: a list of experiments (p. 10-11) and an index that cross-references the experiments with the kits required for their execution (pp. 12-15)
2. Experience Short Guides, which include details of the kits and products used (pp. 16-147). Below and to the right, you will find a key explaining how our Short Guides model is organized.

Experiment name

Section & Subsection name

B. Nuclear Physics and Radioactivity - B.4 β Spectroscopy

Experiment Reference ID

Experiment Name

B.1.4 System Calibration: Linearity and Resolution

SG6114

Experimental Setup

Ordering option

Dedicated kit	
Description	pp.
SP5600C Educational Gamma Kit	178

Experiment summary table

Difficulty	Execution Time	Data Analysis	Radioactive Sources
		NO	YES

Additional requirements

Requirements

Gamma Radioactive Source

Equipment list

Equipment

SP5600C - Educational Gamma Kit

Model	SP5600	DT5720A	A315	SP5606	SP5607
Description	Power Supply and Amplification Unit	Desktop Digitizer 250 MS/s	Splitter	Mini-Spectrometer	Absorption tool
	p. 184	p. 184	p. 186	p. 186	p. 187

Experiment task

Purpose of the experiment

Recording and comparing the γ energy spectra of several radioactive sources is the main goal of the experiment. The photo-peaks are used to calibrate the response of the system and to measure the energy resolution.

Experiment description (Web version)

See the Application

Short description

Fundamentals

Linearity and energy resolution are the main figures of merit of a spectrometric system. In the proposed experiment, based on a scintillating crystal coupled to a Silicon Photomultipliers, deviations in the linearity may be due to the sensor or the front-end electronics saturation. The student is guided through the analysis of the response curve using a series of isotopes up to the MeV energy by a ^{60}Co source and to disentangle the different effects. At the same time, the energy resolution of the system is measured by the width of the photo-peaks and the results compared to what is expected by the fluctuations in the number of detected scintillation photons, the system noise, the sensor stochastic effects, the intrinsic resolution of the scintillator.

This is following an initial activity on the optimization of the operating parameters by an analysis of the photo-peak position and the resolution for a single isotope.the scintillation light and, last but not least, cost. The choice of the scintillator is essentially dependent on the specific targeted application.

32

How to read this Handbook

3. **Collection of some Application Notes related to SiPM Applications (pp. 148-172)**
4. **Short Catalog of CAEN Educational products (pp. 173-194)**

Quick Guide

Block diagram

Experimental result

Data plots

Alternative Kits & Qr Code

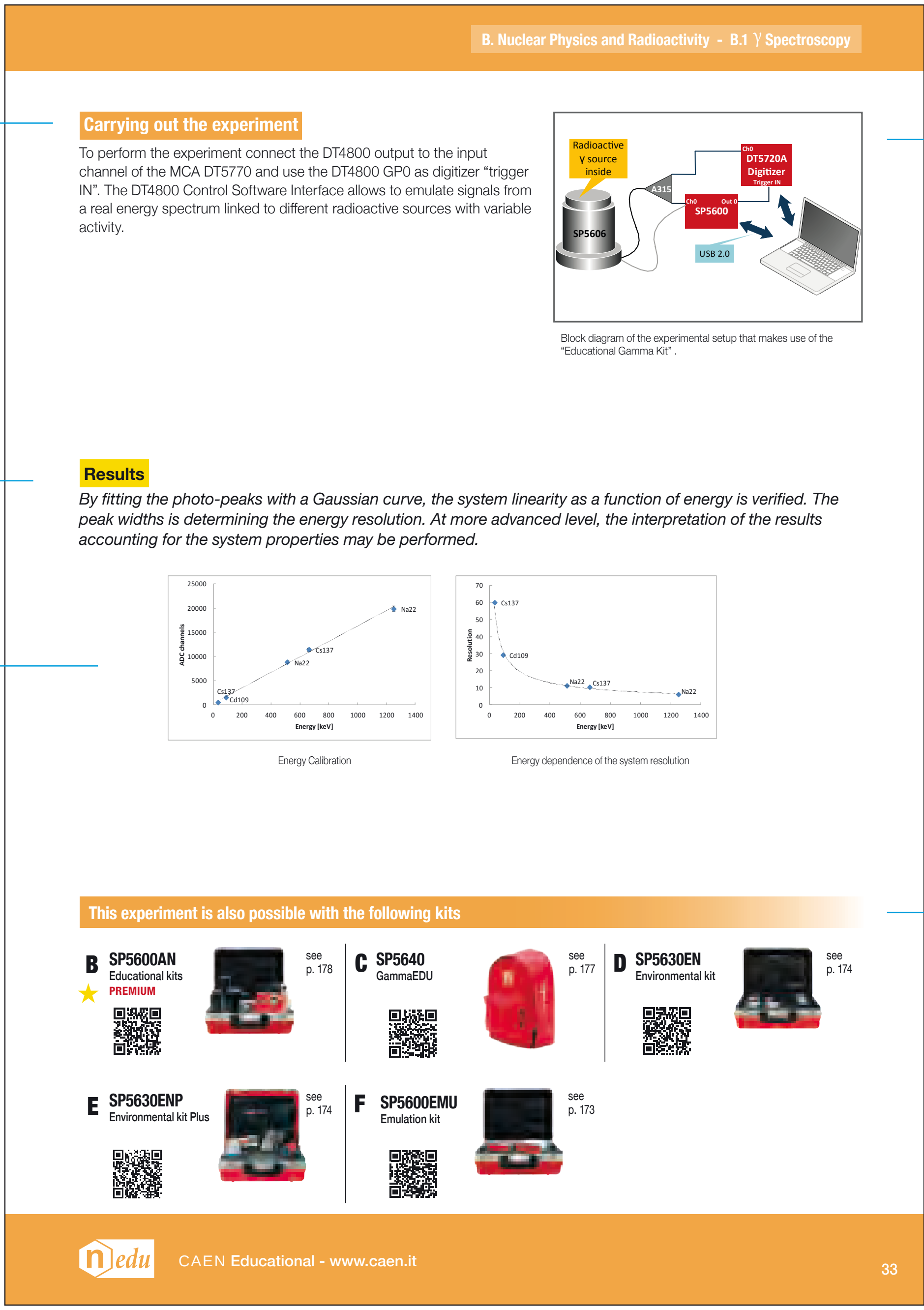

Symbols Guide

Experiments with radioactive sources.

Data analysis code developed in MATLAB is available.
MATLAB® is a registered trademark of The MathWorks, Inc.

Table of Contents

Choose Your Educational Kit!

The table is a simple guide to associate each physics experiment to the kit used to perform it.
For all Physics Application fields, identified in "Section" column, one or more topics are associated as shown in "subsection" column. A series of applications linked to each topic and listed in "Experiment" column is allowed by using the modular kit.

The conclusive matrix of the table allows to associate the equipments to the experiments. Each column is connected to one of the modular kits presented for educational purpose. The checked cells identify the experiments allowed by the chosen kit.

Section	Subsection	N. Exp.	Experiment	SP5600C Educational Gamma Kit	SP5600D Educational Beta Kit
				p. 177	p. 177/180
A. Particle Detector Characterization	A1. Silicon Photomultiplier (SiPM)	3	A.1.1 SiPM Characterization	-	-
			A.1.2 Dependence of the SiPM Properties on the Bias Voltage	-	-
			A.1.3 Temperature Effects on SiPM Properties	-	-
	A2. Photomultiplier Tube (PMT)	1	A.2 Measurement of Photomultiplier Plateau Curves	-	-
B. Nuclear Physics and Radioactivity	B.1 γ Spectroscopy	9	B.1.1 Detecting γ-Radiation	●	-
			B.1.2 Poisson and Gaussian Distributions	●	-
			B.1.3 Energy Resolution	●	-
			B.1.4 System Calibration: Linearity and Resolution	●	-
			B.1.5 A Comparison of Different Scintillating Crystals: Light Yield, Decay Time and Resolution	●	-
			B.1.6 γ Radiation Absorption	●	-
			B.1.7 Photonuclear cross-section/Compton Scattering cross-section	●	-
			B.1.8 Study of the ^{137}Cs spectrumç the backscatter peak and X rays	●	-
			B.1.9 Activity of the ^{60}Co	●	-
	B.2 γ Environmental Radioactivity Indoor	7	B.2.1 Energy calibration of System based on LYSO crystal and Fertilizer sample	-	-
			B.2.2 Background Measurements	-	-
			B.2.3 Fertilizer and photopeak identification	-	-
			B.2.4 Soil sample identification	-	-
			B.2.5 Samples Comparison	-	-
			B.2.6 Test Sample Identification	-	-
			B.2.7 Radon passive measurement	-	-
	B.3 γ Environmental Radioactivity Outdoor	9	B.3.1 Environmental monitoring in field	-	-
			B.3.2 Ground Coverage Effect on the Environmental Monitoring.	-	-
			B.3.3 Human Body Radioactivity	-	-
			B.3.4 γ Environmental detection as a function of the soil distance	-	-
			B.3.5 Radioactivity maps production	-	-
			B.3.6 Radiological evaluation of the building materials	-	-
			B.3.7 Mapping of potential radon-prone areas - **coming soon**	-	-
			B.3.8 Soil water content evaluation with gamma ray spectroscopy - **coming soon**	-	-
			B.3.9 Geochemical and mineral exploration	-	-

EQUIPMENTS

	SP5600E Educational Photon Kit	SP5600AN Educational Kit Premium Version	SP5640 GammaEDU	SP5630EN Environmental Kit	SP5630ENP Environmental Kit Plus	SP5600EMU Emulation Kit	SP5620CH Cosmic Hunter	SP5700 EasyPet	SP5701 EasyPet Kit	SP5660 Portable geiger
	p. 177	p. 177	p. 181	p. 179	p. 179	p. 178	p. 180	p. 176/193	p. 176	p. 182
	●	●	-	-	-	-	-	-	-	-
	●	●	-	-	-	-	-	-	-	-
	●	●	-	-	-	-	-	-	-	-
	-	-	●	-	-	-	-	-	-	-
	-	●	●	●	●	●	-	-	-	-
	-	●	●	●	●	●	-	-	-	●
	-	●	●	●	●	●	-	-	-	-
	-	●	●	●	●	●	-	-	-	-
	-	●	-	-	●	-	-	-	-	-
	-	●	●	-	●	-	-	-	-	-
	-	●	●	●	●	●	-	-	-	-
	-	●	●	●	●	●	-	-	-	-
	-	●	●	●	●	●	-	-	-	-
	-	-	-	●	●	-	-	-	-	-
	-	-	-	●	●	-	-	-	-	-
	-	-	-	●	●	-	-	-	-	-
	-	-	-	●	●	-	-	-	-	-
	-	-	-	●	●	-	-	-	-	-
	-	-	-	●	●	-	-			
	-	-	-	●	●	-	-	-	-	-
	-	-	●	-	-	-	-	-	-	-
	-	-	●	-	-	-	-	-	-	-
	-	-	●	-	-	-	-	-	-	-
	-	-	●	-	-	-	-	-	-	-
	-	-	●	-	-	-	-	-	-	-
	-	-	●	-	-	-	-	-	-	-
	-	-	●	-	-	-	-	-	-	-
	-	-	●	-	-	-	-	-	-	-
	-	-	●	-	-	-	-			

Choose Your Educational Kit! (continued)

Section	Subsection	N. Exp.	Experiment	SP5600C Educational Gamma Kit p. 177	SP5600D Educational Beta Kit p. 177/180
B. Nuclear Physics and Radioactivity (CONTINUED)	B.4 β Spectroscopy	5	B.4.1 Response of a Plastic Scintillating Tile	-	●
			B.4.2 β Spectroscopy	-	●
			B.4.3 β-Radiation: Transmission through Matter	-	●
			B.4.4 β-Radiation as a Method to Measure Paper Sheet Grammage and Thin Layer Thickness	-	●
			B.4.5 Coating effect on the Light Collection	-	●
B. Nuclear Physics and Radioactivity	B.5 Nuclear Imaging - PET	4	B.5.1 Basic Measurements: γ Spectroscopy and System Linearity	-	-
			B.5.2 Positron Annihilation Detection	-	-
			B.5.3 Two-dimensional Reconstruction of a Radioactive Source	-	-
			B.5.4 Spatial Resolution	-	-
	B.6 GM Detector	5	B.6.1 Statistics: Uncertainty as a function of live time	-	-
			B.6.2 Environmental Background	-	-
			B.6.3 Lead Shielding Effect on Environmental Radioactive Background	-	-
			B.6.4 Detecting Ionizing-Radiation	-	-
			B.6.5 Samples Comparison	-	-
C. Particle Physics	C.1 Cosmic Rays	12	C.1.1 Muons Spectrum - **coming soon**	-	●
			C.1.2 Statistics	-	●
			C.1.3 Muons Detection	-	●
			C.1.4 Muons Vertical Flux on Horizontal Detector	-	●
			C.1.5 Random Coincidence	-	●
			C.1.6 Detection Efficiency	-	-
			C.1.7 Cosmic Flux as a function of the altitude	-	-
			C.1.8 Zenith Dependence of Muons Flux	-	●
			C.1.9 Cosmic Shower Detection	-	-
			C.1.10 Environmental and Cosmic Radiation	-	-
			C.1.11 Absorption Measurements	-	-
			C.1.12 Solar Activity Monitoring	-	-
	C.2 Photons	2	C.2.1 Quantum Nature of Light	-	-
			C.2.2 Hands-on Photon Counting Statistics	-	-

EQUIPMENTS

	SP5600E Educational Photon Kit	SP5600AN Educational Kit Premium Version	SP5640 GammaEDU	SP5630EN Environmental Kit	SP5630ENP Environmental Kit Plus	SP5600EMU Emulation Kit	SP5620CH Cosmic Hunter	SP5700 EasyPet	SP5701 EasyPet Kit	SP5660 Portable geiger
	p. 177	p. 177	p. 181	p. 179	p. 179	p. 178	p. 180	p. 176/193	p. 176	p. 182
	-	●	-	-	-	-	-	-	-	-
	-	●	-	-	-	-	-	-	-	-
	-	●	-	-	-	-	-	-	-	-
	-	●	-	-	-	-	-	-	-	-
	-	●	-	-	-	-	-	-	-	-
	-	-	-	-	-	-	-	-	●	-
	-	-	-	-	-	-	-	●	●	-
	-	-	-	-	-	-	-	●	●	-
	-	-	-	-	-	-	-	●	●	-
	-	-	-	-	-	-	-	-	-	●
	-	-	-	-	-	-	-	-	-	●
	-	-	-	-	-	-	-	-	-	●
	-	-	-	-	-	-	-	-	-	●
	-	-	-	-	-	-	-	-	-	●
	-	●	-	-	-	-	-	-	-	-
	-	●	-	-	-	-	●	-	-	-
	-	●	-	-	-	-	●	-	-	-
	-	●	-	-	-	-	●	-	-	-
	-	●	-	-	-	-	●	-	-	-
	-	-	-	-	-	-	●	-	-	-
	-	-	-	-	-	-	●	-	-	-
	-	●	-	-	-	-	●	-	-	-
	-	-	-	-	-	-	●	-	-	-
	-	-	-	-	-	-	●	-	-	-
	-	-	-	-	-	-	●	-	-	-
	-	-	-	-	-	-	●	-	-	-
	●	●	-	-	-	-	-	-	-	-
	●	●	-	-	-	-	-	-	-	-

A. Particle Detector Characterization

A.1 Silicon Photomultipliers (SiPM)

Exploring the quantum nature of phenomena is one of the most exiting experiences a physics student can live.

What is being proposed here has to do with light quanta, radioactive decays (β and γ rays) and cosmic rays. The experiments address the essence of the phenomenon as well as exemplary illustrations of their use in medical imaging and industry, complemented by basic and advanced statistical exercises.

The set-up are all based on Silicon Photomultipliers (SiPM) state of-the-art sensor of light with single photon sensitivity and unprecedented photon number capability. In the field of light sensing and related appliances and instrumentation, SiPM are expected to have the same impact the transistor had: well beyond the replacement of thermoionic valves, it triggered a revolution opening up new and unforeseen perspectives. As a consequence, it is quite natural to get started with activities aimed to introduce the student to the knowledge of the features of this class of sensors.

Recommended kits

A **SP5600E**
Educational kits

see p. 179

B **SP5600AN**
Educational kits
PREMIUM

see p. 179

Experiment	★ SP5600E	★ SP5600AN
A.1.1 SiPM Characterization	•	•
A.1.2 Dependence of the SiPM Properties on the Bias Voltage	•	•
A.1.3 Temperature Effects on SiPM Properties	•	•

★ The star indicates the recommended Kits while the yellow color highlights the Kits especially dedicated to the experiences of this Section. If you are also interested in other experiences, the PREMIUM Kit is recommended.

A.1.1 SiPM Characterization

SG6011

Dedicated kit	
Description	**pp.**
SP5600E Educational Photon Kit	179

Difficulty	Execution Time	Data Analysis	Radioactive Sources
2/5	1/5	YES	NO

Requirements

No other tools are needed.

Equipment

SP5600E - Educational Photon Kit

Model	SP5600	DT5720A	SP5601	SP5650C
Description	Power Supply and Amplification Unit 	Desktop Digitizer 250 MS/s 	LED Driver 	Sensor Holder for SP5600 with SiPM 
	p. 190	p. 190	p. 191	p. 191

Purpose of the experiment

Characterization of a SiPM detector using an ultra-fast pulsed LED. Estimation of the main features of the detector at fixed bias voltage.

See the Application

Fundamentals

Silicon Photomultipliers (SiPM) consist of a high-density (up to ~$10^4/mm^2$) matrix of diodes connected in parallel on a common Si substrate. Each diode is an Avalanche Photo Diode (APD) operated in a limited Geiger-Müller regime connected in series with a quenching resistor, in order to achieve gain at level of ~10^6. As a consequence, these detectors are sensitive to single photons (even at room temperature) feature a dynamic range well above 100 photons/burst and have a high Photon Detection Efficiency (PDE) up to 50%. SiPM measure the light intensity simply by the number of fired cells. However, this information is affected and biased by stochastic effects characteristic of the sensor and occurring within the time window: spurious avalanches due to thermally generated carriers (a.k.a. Dark Counts), delayed avalanches associated to the release of carriers trapped in metastable states (a.k.a. Afterpulses) and an excess of fired cells due to photons produced in the primary avalanche, travelling in Silicon and triggering neighboring cells (a phenomenon called Optical Cross Talk).

The typical SiPM response to a light pulse is characterized by multiple traces, each one corresponds to different numbers of fired cells, proportional to the number of impinging photons. Because of the high gain compared to the noise level, the traces are well separated, providing a photon number resolved detection of the light field.

Carrying out the experiment

The selected scintillator crystal shall be coupled to the SiPM in the SP5607, through a thin layer of index matching grease to maximize the light collection. In order to avoid saturation, the output of the SiPM is divided using the A315 splitter: one branch is connected to the DT5720A and will be digitized. The other branch will be amplified by the SP5600 module, generating the trigger for the integration signal by the on-board leading edge discriminator or simply counting the pulses induced by the detected gamma ray

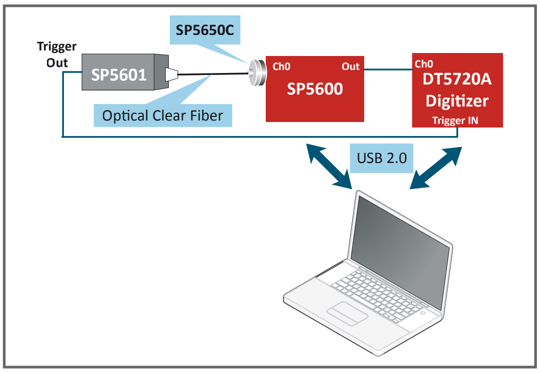

Experimental setup block diagram.

Results

The gain of the SiPM is evaluated from the output charge of the sensor. After the estimation of the ADC channel conversion factor ($ADC_{c.r.}$) and the distance between adjacent peaks (ΔPP(ADC_ch), the SiPM gain can be calculated according to the following equation:

$$Gain = \frac{\Delta PP(ADC\_ch) * ADCc.r.}{e}$$

The resolution power of the system can be evaluated plotting the σ of each peaks versus the number of peaks. The counts frequency, in absence of light, at 0.5 p.e. threshold represents the DCR. The ratio between the dark count at 1.5 p.e. threshold ($DCR_{1.5}$) and the value at 0.5 p.e. threshold ($DCR_{0.5}$) give the crosstalk estimation of the detector.

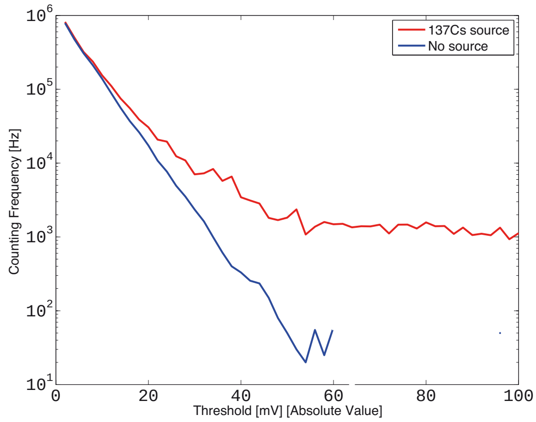

Sensor output frequency as a function of the threshold in mV, with and without ^{137}Cs source.

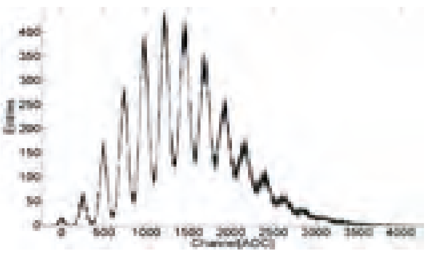

Spectrum of Hamamatsu S10362-11-100C.

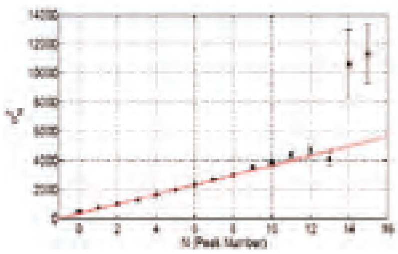

Peak σ versus peak number for Hamamatsu S10362-11-100C.

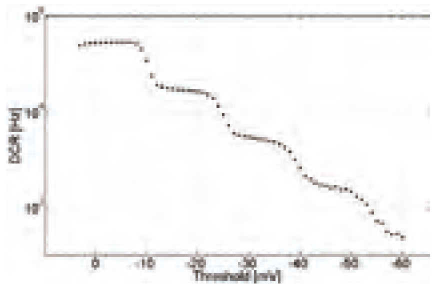

Sensor Dark Count frequency versus discrimination threshold.

This experiment is also possible with the following kits

B **SP5600AN**
Educational kits
PREMIUM

see p. 179

A.1.2 Dependence of the SiPM Properties on the Bias Voltage

SG6012

Dedicated kit	
Description	**pp.**
SP5600E Educational Photon kit	179

Difficulty	Execution Time	Data Analysis	Radioactive Sources
2/5	2/5	YES	NO

Requirements

No other tools are needed.

Equipment

SP5600E - Educational Photon Kit

Model	SP5600	DT5720A	SP5601	SP5650C
Description	Power Supply and Amplification Unit 	Desktop Digitizer 250 MS/s 	LED Driver 	Sensor Holder for SP5600 with SiPM 
	p. 190	p. 190	p. 191	p. 191

Purpose of the experiment

Study the dependence of the main SiPM figures of merit on the bias voltage. Measurement of the breakdown voltage and identification of the optimal working point. The experiment requires the use of the LED source included in the kit.

See the Application

Fundamentals

The main features of the SiPM are expected to depend on the bias voltage or, more specifically, on the overvoltage, the voltage in excess of the breakdown value:

- The gain is expected to depend linearly on the overvoltage
- The triggering efficiency, i.e. the probability for a charge carrier to generate an avalanche by impact ionization, increases with the overvoltage till a saturation value is achieved. As a consequence, the Photon Detection Efficiency (PDE) increases together with the stochastic events (Dark Count Rate, Cross Talk and After Pulses) affecting the sensor response.

Actually, spurious events are expected to grow super-linearly and the determination of the optimal working point requires the definition of a proper figure of merit. Referring to the photon number resolving capability of the SiPM, the bias can be set to optimize the resolution power, i.e. the maximum number of resolved photons.

Carrying out the experiment

Mount one of the sensors (SP5650C) on the SP5600 and connect the analog output to the input of the DT5720A digitizer. Optically couple the LED and the sensor via the optical fiber, after having used the index matching grease on the tips. Set the internal trigger mode on the SP5601 and connect its trigger output on the DT5720A trigger IN. Connect via USB the modules to the PC and power ON the devices. Through the LabView graphical user interface (GUI), properly synchronize the signal integration and, for every voltage value, record the photon spectrum and measure directly the Dark Count and the Optical Cross talk. The measurement of the After Pulse is also possible but it requires most advanced analysis techniques.

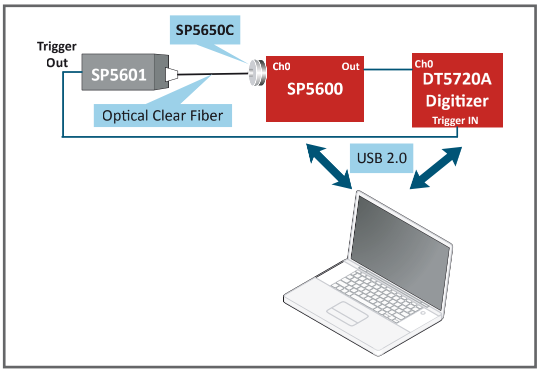

Experimental setup block diagram.

Results

As exemplary illustration, the trend of the gain vs. the bias voltage is shown, allowing as well the measurement of the breakdown voltage corresponding to the value at zero gain. The optimal working point by a measurement of the resolution power on the multi-photon peak spectrum is also shown.

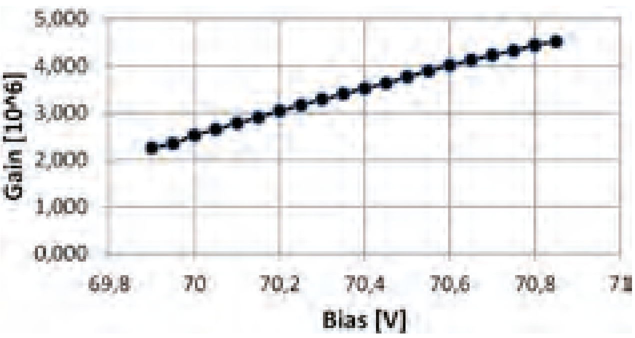

SiPM gain versus bias voltage.

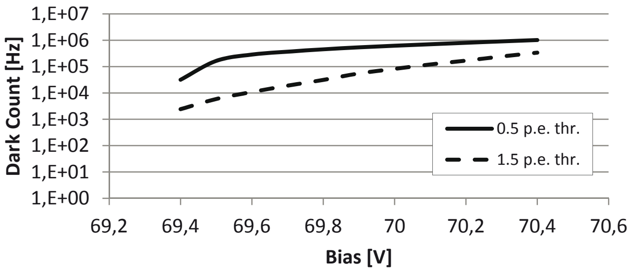

Dark count versus bias voltage.

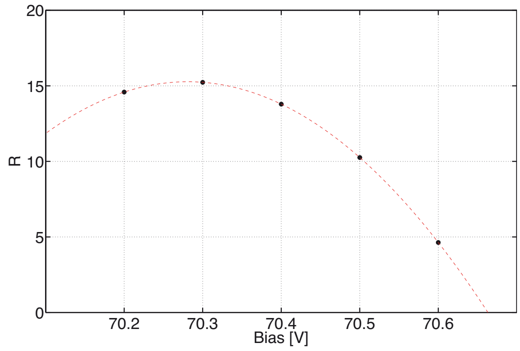

Scan of the resolution power R as a function of the bias voltage.

This experiment is also possible with the following kits

B **SP5600AN**
Educational kits
PREMIUM

see p. 179

A.1.3 Temperature Effects on SiPM Properties

SG6013

Dedicated kit	
Description	**pp.**
SP5600E Educational Photon kit	179

Difficulty	Execution Time	Data Analysis	Radioactive Sources
		YES	NO

Requirements

No other tools are needed.

Equipment

SP5600E - Educational Photon Kit

Model	SP5600	DT5720A	SP5601	SP5650C
Description	Power Supply and Amplification Unit	Desktop Digitizer 250 MS/s	LED Driver	Sensor Holder for SP5600 with SiPM
				
	p. 190	p. 190	p. 191	p. 191

Purpose of the experiment

Gain, noise and photon detection efficiency (at fixed bias voltage) are affected by temperature. The student is driven through the measurement of the dependence of these critical figures.

See the Application

Fundamentals

The gain in a SiPM biased at fixed voltage changes with temperature since the breakdown voltage Vbr does it. Gain stabilization is a must and can be pursued tracking the V_{br} changes and adjusting the bias voltage accordingly. The rate of variation depends on the sensor, through the material properties. Noise depends on the thermal generation of charge carriers, so a significant dependence is expected as well.

Carrying out the experiment

In a temperature controlled box, mount one of the sensors (SP5650C) on the SP5600 and connect the analog output to the input of the DT5720A digitizer. Optically couple the LED and the sensor via the optical fiber, after having used the index matching grease on the tips. Set the internal trigger mode on the P5601 and connect its trigger output on the DT5720A trigger IN. Connect via USB the modules to the PC and power ON the devices. Through the LabView graphical user interface (GUI), properly synchronize the signal integration and, for every temperature & voltage value, record the photon spectrum and measure directly the Dark Count and the Optical Cross talk.

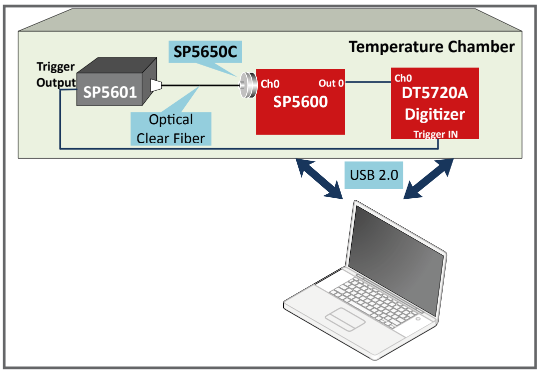

Experimental setup block diagram.

Results

Figures show the dependence of the gain upon temperature at various voltages and the voltage dependence at various temperatures. By the two set of results, the temperature coefficient of the sensor, i.e. the variation of the breakdown voltage with temperature, can be measured.

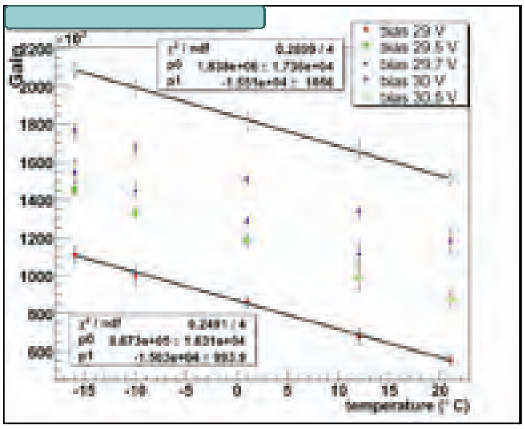

SiPM gain as a function of temperature, at different bias voltage values.

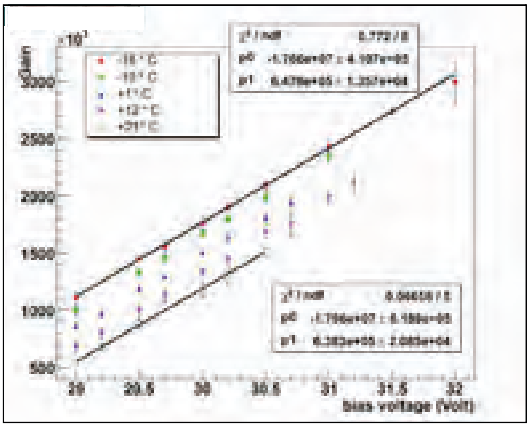

SiPM gain as a function of the bias voltage, at different temperature values.

This experiment is also possible with the following kits

B **SP5600AN**
Educational kits
PREMIUM

see p. 179

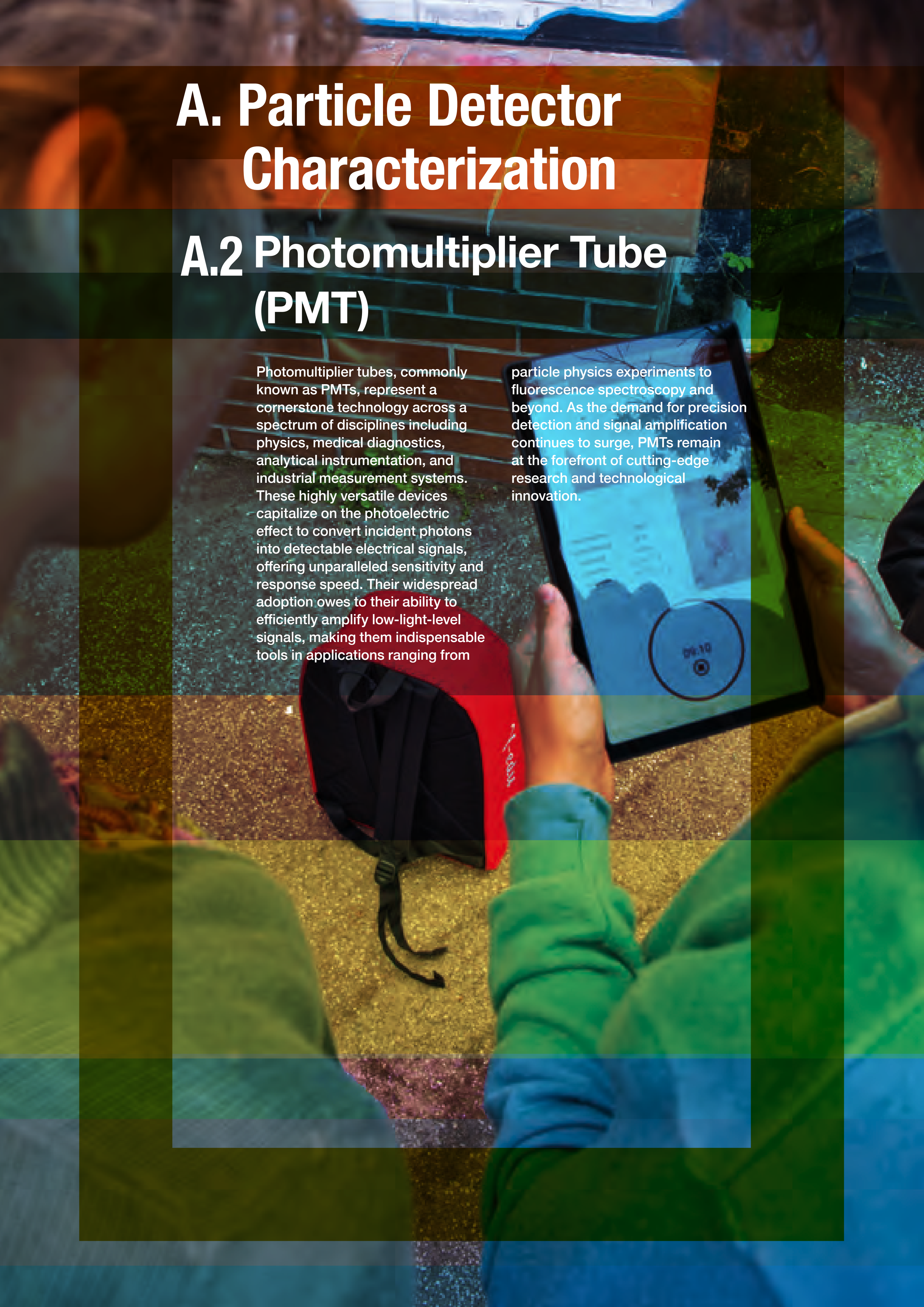

A. Particle Detector Characterization

A.2 Photomultiplier Tube (PMT)

Photomultiplier tubes, commonly known as PMTs, represent a cornerstone technology across a spectrum of disciplines including physics, medical diagnostics, analytical instrumentation, and industrial measurement systems. These highly versatile devices capitalize on the photoelectric effect to convert incident photons into detectable electrical signals, offering unparalleled sensitivity and response speed. Their widespread adoption owes to their ability to efficiently amplify low-light-level signals, making them indispensable tools in applications ranging from particle physics experiments to fluorescence spectroscopy and beyond. As the demand for precision detection and signal amplification continues to surge, PMTs remain at the forefront of cutting-edge research and technological innovation.

Recommended kits

C SP5640
GammaEDU

see p. 183

	Experiment	★ SP5640
A.2	Measurement of Photomultiplier Plateau Curves	•

★ The star indicates the recommended Kits while the yellow color highlights the Kits especially dedicated to the experiences of this Section.

A.2.1 Measurement of photomultiplier plateau curves

SG6020E

Difficulty	Execution Time	Data Analysis	Radioactive Sources
		NO	YES

Dedicated kit	
Description	**pp.**
SP5640 GammaEDU	183

Requirements

The present experiment was performed using ^{137}Cs source but the background can be use in replacement.

Equipment

SP5600E - Educational Gamma Kit

Model	SP5640
Description	Backpack Detector  p. 183

Purpose of the experiment

The goal of this experience is the identification of the working point of a photomultiplier by determining the plateau curve.

See the Application

Fundamentals

Photomultiplier tubes (often abbreviated as PMT) are widely used Physics, in medical equipment, analytical instruments and industrial measurement systems. The PMTs make use of the photoelectric effect and have good response speed and sensitivity (low-light-level detection). Photomultiplier tubes are usually tested in combination with a ^{137}Cs radiation source and a NaI(Tl) scintillator. There are two characterization measurement methods in scintillation counting. One is the spectrum method which uses a pulse height analyzer to measure an energy spectrum. The other one, described in this experimental activity, is the counting method. Plateau characteristics are measured by setting a threshold value and counting all pulses with amplitudes greater than that value while changing the supply voltage for the photomultiplier tube. The plateau region is such that the count rate will not vary even if the supply voltage is changed within this region. The importance of operating the photomultiplier in the plateau zone is then understood for a correct use of each particle detection apparatus that includes this instrument.

Carrying out the experiment

The experiment can be performed both by taking off the instrumentation from the backpack and using the backpack with the open zipper. To power ON γstream, press the ON/OFF button. Take care that the γstream internal battery is charged, otherwise use the external power system. Connect the Ethernet cable from γstream to the PC and configure the Ethernet network of your PC. Connect γstream to the MC2Analyzer software through Ethernet connection. Place the radioactive source close to the scintillator/under the central part of the backpack and run the software. Set the threshold value and keep it fixed for the whole measurement time, by varying the PMT supply voltage.

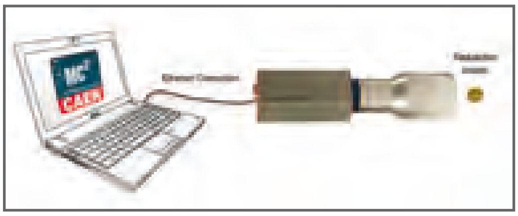

Experimental setup block diagram.

Results

The identification of the working point where the output signals of the photomultiplier are less affected by variations in the power supply voltage.

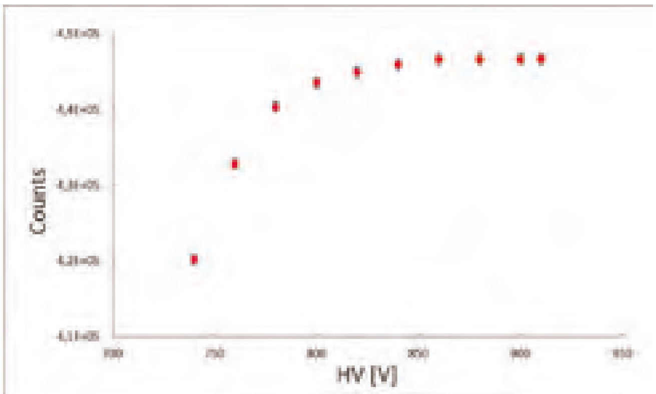

Example of plateau characteristics.

B. Nuclear Physics and Radioactivity

B.1 γ Spectroscopy

In 1895 the radioactivity was discovered by H.Becquerel and in 1903 the Nobel Prize in Physics was assigned to Curie spouses for their studies on these phenomena. Radioactivity is around us and getting to know it experimentally is essential for physics students.

When an unstable nucleus decays in a cascade leading to a stable nuclide, it emits α or β or γ quanta or a combination of them. Gamma rays are high energy photons and the spectroscopy of the emitted γ rays is instrumental for understanding the mechanism of the interaction with matter, the fundamentals about detection and the underlying nuclear physics. Moreover, it is relevant in basic and applied fields of science and technology, from nuclear to medical physics, from archaeomet to homeland security.

The γ spectroscopy experiments can be performed by using differe set-ups: Educational Gamma and Premium kits, Emulation kit, Environmental and Environmental Plus kits, GammaEDU Backpack and Open FPGA Kit.

Recommended kits

A SP5600C
Educational kits

see p. 179

B SP5600AN
Educational kits
PREMIUM

see p. 179

You can also create the experiences in this section with other Kits

C SP5640
GammaEDU

see p. 183

D SP5630EN
Environmental kit

see p. 181

E SP5630ENP
Environmental kit Plus
PREMIUM

see p. 181

F SP5600EMU
Emulation kit

see p. 180

Experiment	pp.	SP5600C ★	SP5600AN ★	SP5640	SP5630EN	SP5630ENP	SP5600EMU
B.1.1 Detecting γ-Radiation	32	•	•	•	•	•	-
B.1.2 Poisson and Gaussian Distributions	34	•	•	•	•	•	•
B.1.3 Energy Resolution	36	•	•	•	•	•	•
B.1.4 System Calibration: Linearity and Resolution	38	•	•	•	•	•	•
B.1.5 A Comparison of Different Scintillating Crystals: Light Yield, Decay Time and Resolution	40	•	•	-	•	•	-
B.1.6 γ Radiation Absorption	42	•	•	•	•	•	
B.1.7 Photonuclear cross-section/Compton Scattering cross-section	42	•	•	•	•	•	•
B.1.8 Study of the ^{137}Cs spectrum the backscatter peak and X rays	44	•	•	•	•	•	•
B.1.9 Activity of the ^{60}Co	46	•	•	•	•	•	•

★ The star indicates the recommended Kits while the yellow color highlights the Kits especially dedicated to the experiences of this Section. If you are also interested in other experiences, the PREMIUM Kit is recommended.

B.1.1 Detecting γ-Radiation

SG6111

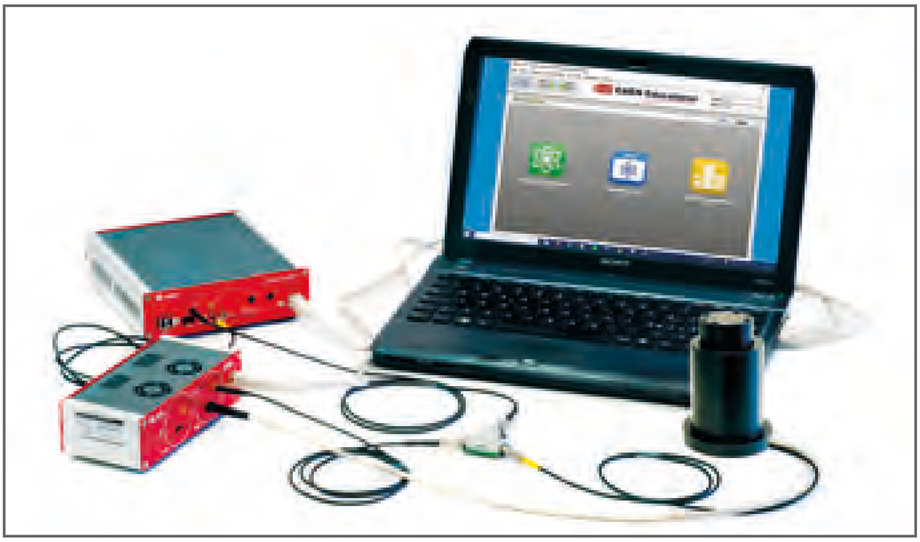

Dedicated kit	
Description	pp.
SP5600C Educational Gamma Kit	179

Difficulty	Execution Time	Data Analysis	Radioactive Sources
		NO	YES

Requirements

Gamma Radioactive Source

Equipment

SP5600C - Educational Gamma Kit

Model	SP5600	DT5720A	A315	SP5606	SP5607
Description	Power Supply and Amplification Unit 	Desktop Digitizer 250 MS/s 	Splitter 	Mini-Spectrometer 	Absorption tool 
	p. 190	p. 190	p. 192	p. 192	p. 193

Purpose of the experiment

Gamma radioactivity detection by using a system composed of a scintillating crystal coupled to a photon detector.

See the Application

Fundamentals

Gamma rays interact with matter by three processes: Compton Scattering, Photoelectric Effect and Pair Production (whenever the energy exceeds the 1.022 MeV threshold corresponding to the e^+e^- rest mass). The cross section of each process depends on the energy of the gamma ray.

The Compton Effect is the inelastic scattering between the incoming photon and an atomic electron. In the Photoelectric Effect, the incident gamma ray transfers all of its energy to a bound electron which acquires a kinetic energy equal to the incoming gamma energy decreased by the binding energy.

These processes convert, totally or partially, the gamma ray energy into kinetic energy of electrons (or positrons, in case of pair production). The interaction of the charged particles with the atomic and molecular systems of the medium results in excited states whose decay, possibly mediated, leads to light in the visible or UV region, eventually detected by the light sensor. A wide range of scintillator products is available today, differing for the light yield, the material properties, the time characteristics of the scintillation light and, last but not least, cost. The choice of the scintillator is essentially dependent on the specific targeted application.

Carrying out the experiment

The selected scintillator crystal shall be coupled to the SiPM in the SP5607, through a thin layer of index matching grease to maximize the light collection. In order to avoid saturation, the output of the SiPM is divided using the A315 splitter: one branch is connected to the DT5720A and will be digitized. The other branch will be amplified by the SP5600 module, generating the trigger for the integration signal by the on-board leading edge discriminator or simply counting the pulses induced by the detected gamma ray

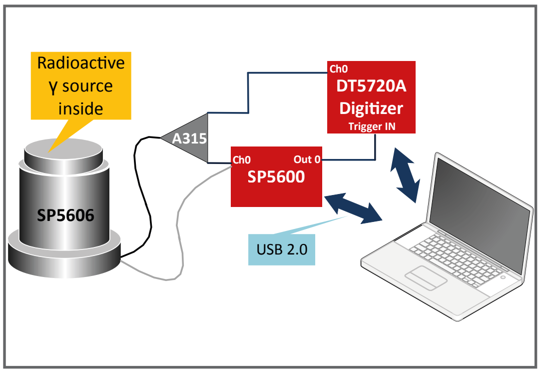

Experimental setup block diagram.

Results

The student may get acquainted with the presence of radioactivity with a simple preliminary measurement, namely comparing the counting frequency as a function of the discriminator threshold with/without the source. Presuming the source, essentially in contact to the crystal, to be point like with respect to the crystal surface, and assuming its activity is known, the student may estimate for every threshold value the detection efficiency and the signal over noise ratio, building up an efficiency-purity plot. Exemplary results obtained with a ^{137}*Cs source are shown. Moving away the source from the crystal, the law governing the variation of the flux can also be investigated.*

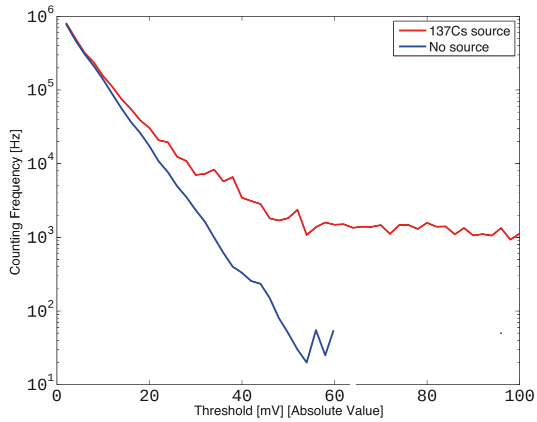

Sensor output frequency as a function of the threshold in mV, with and without ^{137}Cs source.

This experiment is also possible with the following kits

B **SP5600AN**
Educational kits
PREMIUM

see p. 179

C **SP5640**
GammaEDU

see p. 183

D **SP5630EN**
Environmental kit

see p. 181

E **SP5630ENP**
Environmental kit Plus

see p. 181

F **SP5600EMU**
Emulation kit

see p. 180

B.1.2 Poisson and Gaussian Distribution

SG6112A

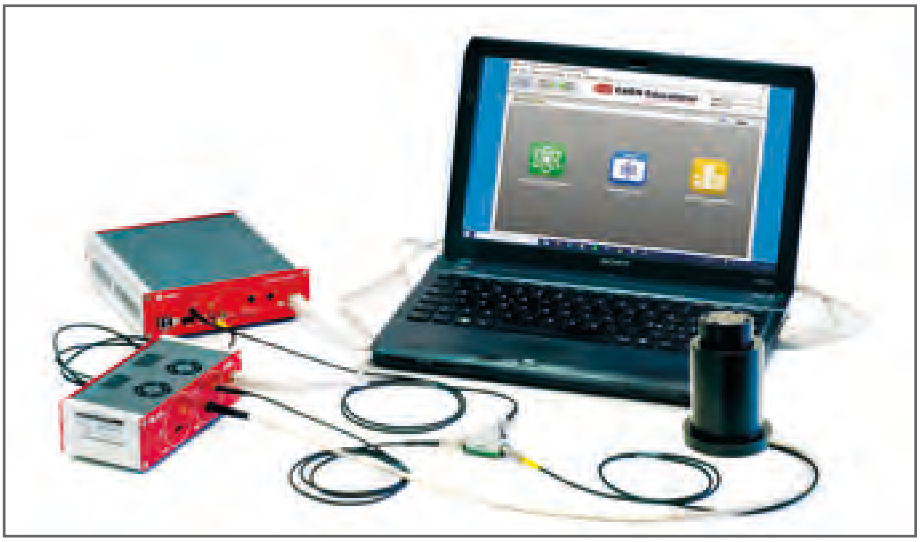

Difficulty	Execution Time	Data Analysis	Radioactive Sources
		YES	YES

Dedicated kit	
Description	**pp.**
SP5600C Educational Gamma Kit	179

Requirements

Gamma Radioactive Source

Equipment

SP5600C - Educational Gamma Kit

Model	**SP5600**	**DT5720A**	**A315**	**SP5606**	**SP5607**
Description	Power Supply and Amplification Unit	Desktop Digitizer 250 MS/s	Splitter	Mini-Spectrometer	Absorption tool
					
	p. 190	p. 190	p. 192	p. 192	p. 193

Purpose of the experiment

Study the statistical distribution of the counting rates of a gamma radioactive source. Comparison of the data to the Poisson distribution, turning into a Gaussian as the mean number of counts grows. The study can be performed both experimentally, with the SiPM kit or simulating it with the emulation kit.

See the Application

Fundamentals

The number of radioactive particles detected over a time Δt is expected to follow a Poisson distribution with mean value μ. It means that for a given radioactive source, the probability that n decays will occur over a given time period Δt is given by:

$$P_\mu(n) = \frac{\mu^n}{n!} e^{-\mu}$$

Where μ is proportional to the sample size and to the time Δt and inversely proportional to the half-life $T_{1/2}$ of the unstable nucleus. As long as μ grows, the probability $P_\mu(n)$ is well approximated by a Gaussian distribution:

$$P(n) = \frac{1}{\sqrt{2\pi\sigma}} e^{\frac{-(n-\mu)^2}{2\sigma^2}}$$

Where $\sigma = \sqrt{\mu}$ is the standard deviation.

Carrying out the experiment

The selected scintillator crystal shall be coupled to the SiPM in the SP5607, through a thin layer of index matching grease to maximize the light collection. In order to avoid saturation, the output of the SiPM is divided using the A315 splitter: one branch is connected to the DT5720A and will be digitized. The other branch will be amplified by the SP5600 module, generating the trigger for the integration signal by the on-board leading edge discriminator or simply counting the pulses induced by the detected gamma ray. The discriminator threshold shall be defined looking at the spectrum and evaluating the dark count rate. Once this is properly set, the counting experiment shall be performed.

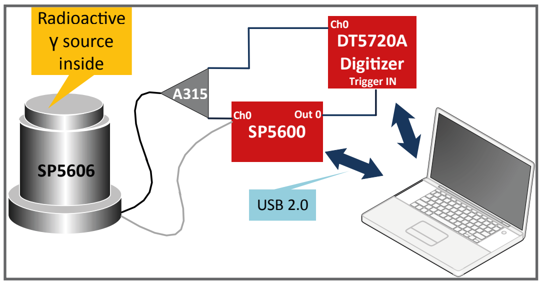

Block diagram of the experimental setup that makes use of the "Educational Gamma Kit" .

Results

Changing the counting window and/or the activity of the source or the threshold, the number of counts changes, with a probability density function moving form a Poissonian to a Gaussian shape. The student may play with the data, fitting them and comparing the expectations to the measurement.

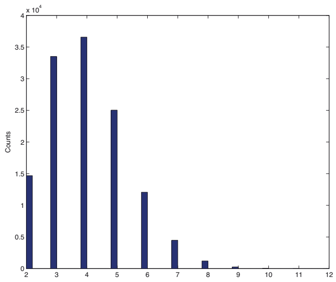

Poissonian distribution.

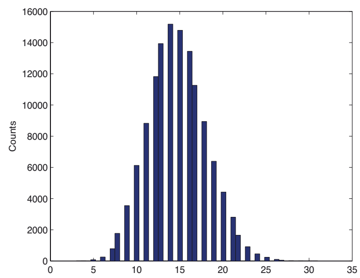

Gaussian distribution.

This experiment is also possible with the following kits

B **SP5600AN**
Educational kits
★ **PREMIUM**

see p. 179

C **SP5640**
GammaEDU

see p. 183

D **SP5630EN**
Environmental kit

see p. 181

E **SP5630ENP**
Environmental kit Plus

see p. 181

F **SP5600EMU**
Emulation kit

see p. 180

B.1.3 Energy Resolution

SG6113

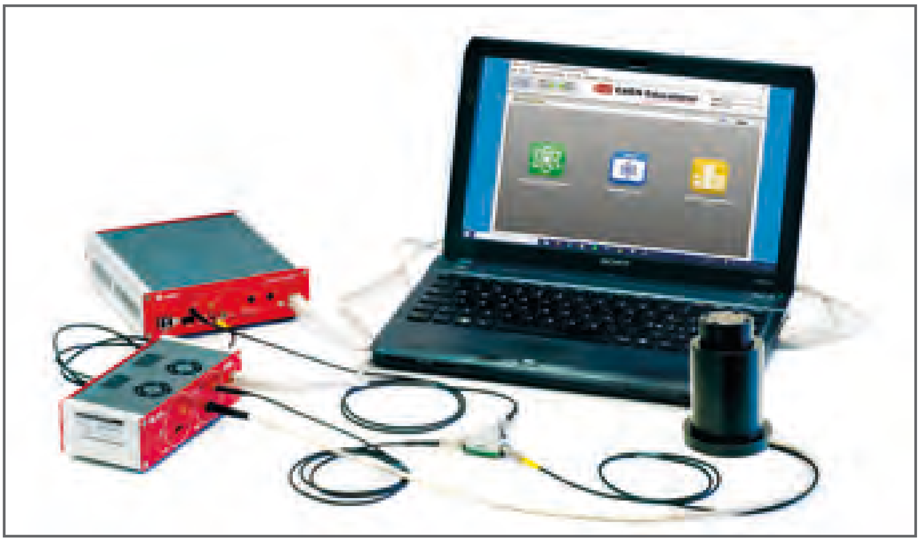

Dedicated kit	
Description	pp.
SP5600C Educational Gamma Kit	179

Difficulty	Execution Time	Data Analysis	Radioactive Sources
		YES	YES

Requirements

Gamma Radioactive Source

Equipment

SP5600C - Educational Gamma Kit

Model	SP5600	DT5720A	A315	SP5606	SP5607
Description	Power Supply and Amplification Unit 	Desktop Digitizer 250 MS/s 	Splitter 	Mini-Spectrometer 	Absorption tool 
	p. 190	p. 190	p. 192	p. 192	p. 193

Purpose of the experiment

Analysis of the spectrum of the deposited energy by a γ ray in a detector discloses the essence of the interaction of high energy photons with matter and allows to learn by doing the detector related effects.

See the Application

Fundamentals

For γ-energy less than 2MeV, the interaction with matter is dominated by Compton scattering and Photo-absorption. The analysis of the Compton continuum of the deposited energy and of the photo-peak conveys information on the characteristics of the decaying isotope as well as the effects due to the system noise, the detected photon statistics, the stochastic terms in the detector and the intrinsic resolution of the scintillator. The experiment presumes to use ^{137}Cs with its decays detected by a CsI crystal coupled to a Silicon Photomultiplier. The ^{137}Cs source is particularly interesting due to its low energy X ray line at 30 keV and the high energy gamma emission at 662 keV. The former is relevant to optimize the lower detection limit of the system; the latter is a standard to evaluate the energy resolution. The use of the 2 lines and the analysis of the Compton spectrum

Carrying out the experiment

The CsI scintillator crystal shall be coupled to the SiPM in the SP5607, through a thin layer of index matching grease to maximize the light collection. In order to avoid saturation, the output of the SiPM is divided using the A315 splitter: one branch is connected to the DT5720A and will be digitized. The other branch will be amplified by the SP5600 module, generating the trigger for the integration signal by the on-board leading edge discriminator. The discriminator threshold shall be defined looking at the spectrum and evaluating the dark count rate. Once this is properly set and the radioactive source is properly positioned, the spectrum can be recorded.

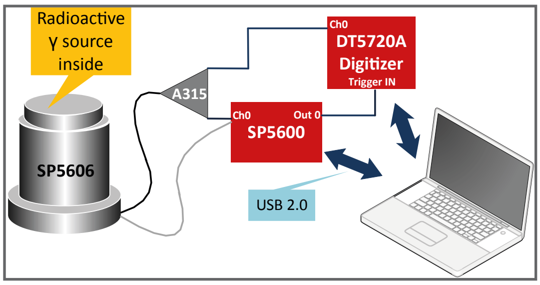

Block diagram of the experimental setup that makes use of the "Educational Gamma Kit" .

Results

The figure shows a typical gamma spectrum, recorded with a very low energy threshold. The left over from the system noise is clearly visible, as well as the low energy line at 30 keV and the photopeak. For this specific spectrum, the energy resolution on the 662 keV peak corresponds to:

$$\text{Energy Resolution} = \frac{FWHM_{peak}}{\mu_{peak}} \cdot 100 \sim 10\%$$

$FWHM_{peak}$ = full width at half maximum of the peak

μ_{peak}= channel number of the peak centroid.

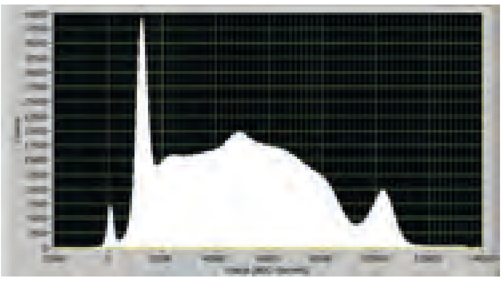

^{137}Cs spectrum.

This experiment is also possible with the following kits

B **SP5600AN**
Educational kits
★ PREMIUM

see p. 179

C **SP5640**
GammaEDU

see p. 183

D **SP5630EN**
Environmental kit

see p. 181

E **SP5630ENP**
Environmental kit Plus

see p. 181

F **SP5600EMU**
Emulation kit

see p. 180

B.1.4 System Calibration: Linearity and Resolution

SG6114

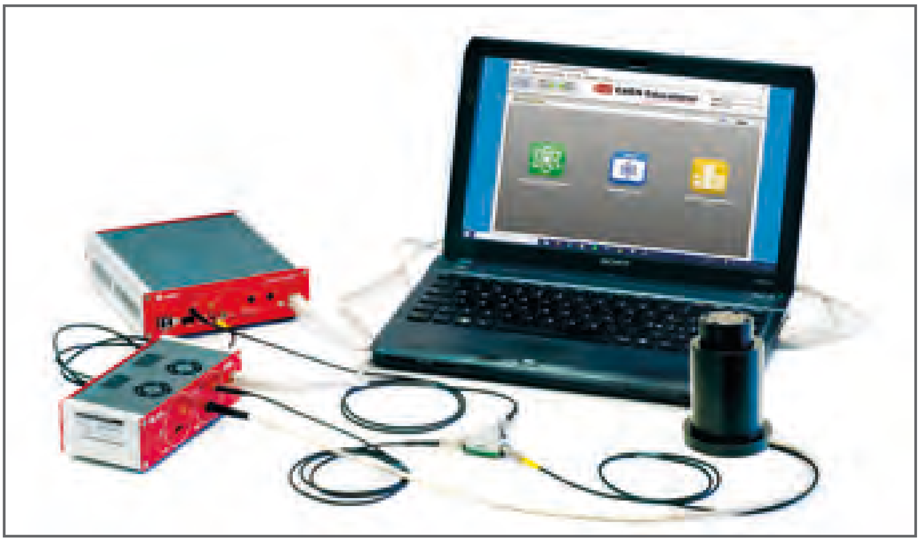

Difficulty	Execution Time	Data Analysis	Radioactive Sources
		YES	YES

Dedicated kit	
Description	pp.
SP5600C Educational Gamma Kit	179

Requirements

Gamma Radioactive Source

Equipment

SP5600C - Educational Gamma Kit

Model	SP5600	DT5720A	A315	SP5606	SP5607
Description	Power Supply and Amplification Unit	Desktop Digitizer 250 MS/s	Splitter	Mini-Spectrometer	Absorption tool
					
	p. 190	p. 190	p. 192	p. 192	p. 193

Purpose of the experiment

Recording and comparing the γ energy spectra of several radioactive sources is the main goal of the experiment. The photo-peaks are used to calibrate the response of the system and to measure the energy resolution.

See the Application

Fundamentals

Linearity and energy resolution are the main figures of merit of a spectrometric system. In the proposed experiment, based on a scintillating crystal coupled to a Silicon Photomultipliers, deviations in the linearity may be due to the sensor or the front-end electronics saturation. The student is guided through the analysis of the response curve using a series of isotopes up to the MeV energy by a ^{60}Co source and to disentangle the different effects. At the same time, the energy resolution of the system is measured by the width of the photo-peaks and the results compared to what is expected by the fluctuations in the number of detected scintillation photons, the system noise, the sensor stochastic effects, the intrinsic resolution of the scintillator.

This is following an initial activity on the optimization of the operating parameters by an analysis of the photo-peak position and the resolution for a single isotope.the scintillation light and, last but not least, cost. The choice of the scintillator is essentially dependent on the specific targeted application.

Carrying out the experiment

The scintillator crystal shall be coupled to the SiPM in the SP5607, through a thin layer of index matching grease to maximize the light collection. In order to avoid saturation, the output of the SiPM is divided using the A315 splitter: one branch is connected to the DT5720A and will be digitized. The other branch will be amplified by the SP5600 module, generating the trigger for the integration signal by the on-board leading-edge discriminator. The discriminator threshold shall be defined looking at the spectrum and evaluating the dark count rate. Once this is set and the radioactive source is properly positioned, the spectrum can be recorded.

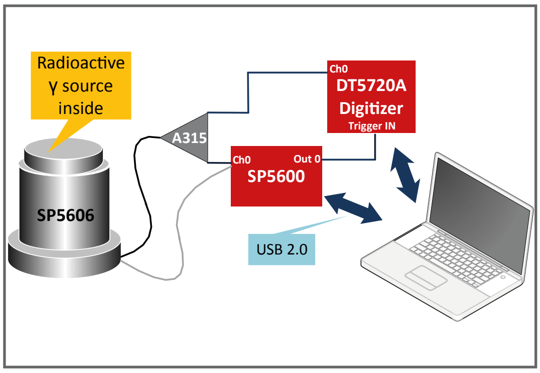

Block diagram of the experimental setup that makes use of the "Educational Gamma Kit" .

Results

By fitting the photo-peaks with a Gaussian curve, the system linearity as a function of energy is verified. The peak widths is determining the energy resolution. At more advanced level, the interpretation of the results accounting for the system properties may be performed.

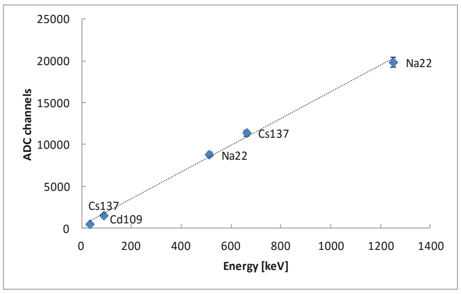

Energy Calibration

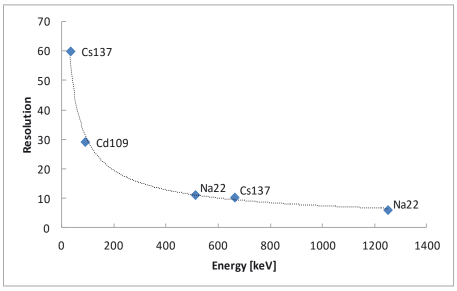

Energy dependence of the system resolution

This experiment is also possible with the following kits

B **SP5600AN**
Educational kits
PREMIUM

see p. 179

C **SP5640**
GammaEDU

see p. 183

D **SP5630EN**
Environmental kit

see p. 181

E **SP5630ENP**
Environmental kit Plus

see p. 181

F **SP5600EMU**
Emulation kit

see p. 180

B.1.5 A Comparison of Different Scintillating Crystals: Light Yield, Decay Time and Resolution

SG6115

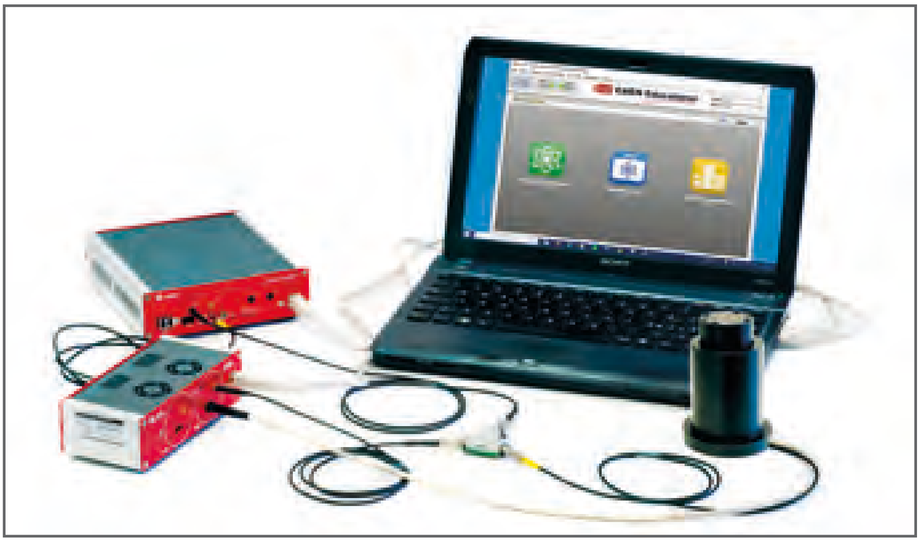

Dedicated kit	
Description	**pp.**
SP5600C Educational Gamma Kit	179

Difficulty	Execution Time	Data Analysis	Radioactive Sources
2/5	3/5	NO	YES

Requirements

Gamma Radioactive Source

Equipment

SP5600C - Educational Gamma Kit

Model	SP5600	DT5720A	A315	SP5606	SP5607
Description	Power Supply and Amplification Unit 	Desktop Digitizer 250 MS/s 	Splitter 	Mini-Spectrometer 	Absorption tool 
	p. 190	p. 190	p. 192	p. 192	p. 193

Purpose of the experiment

Compare the basic characteristics of different scintillating crystals, namely the light yield and the decay time of the scintillation light. Verify the effect on the energy resolution.

See the Application

Fundamentals

Scintillating materials exhibit various characteristics related to light yield and the characteristic time of emission. The CAEN spectrometer is equipped with three different crystals: BGO (Bismuth Germanate), LYSO(Ce) (Cerium-doped Lutetium Yttrium Orthosilicate), CsI(Tl) (Thallium-doped Cesium Iodide). All of them have the same volume (6 x 6 x 15 mm³), are polished on all sides, and coated with a white epoxy on 5 faces. One 6 x 6 mm² face is open to be coupled with the Silicon Photomultiplier. The main characteristics of the crystals are summarized in the table alongside.

	BGO	LYSO(Ce)	CsI(Tl)
Density (g/cm³)	7.13	7.4	4.51
Decay Time (ns)	300	40	1000
Light Yield (ph./MeV)	8200	27000	52000
Peak emission (nm)	480	420	560
Radiation length (cm)	1.13	1.14	1.85
Reflective index	2.15	1.82	1.78

The light yield affects the energy resolution. This is also influenced by the decay time, which constrains the integration time and implies a different effect of the sensor's stochastic effects (dark counts and afterpulses).

Carrying out the experiment

The scintillator crystal shall be coupled to the SiPM in the SP5607, through a thin layer of index matching grease to maximize the light collection. In order to avoid saturation, the output of the SiPM is divided using the A315 splitter: one branch is connected to the DT5720A and will be digitized. The other branch will be amplified by the SP5600 module, generating the trigger for the integration signal by the on-board leading edge discriminator. The discriminator threshold shall be defined looking at the spectrum and evaluating the dark count rate. Once this is set and the radioactive source is properly positioned, the spectrum can be recorded. The procedure shall be repeated for every crystal.

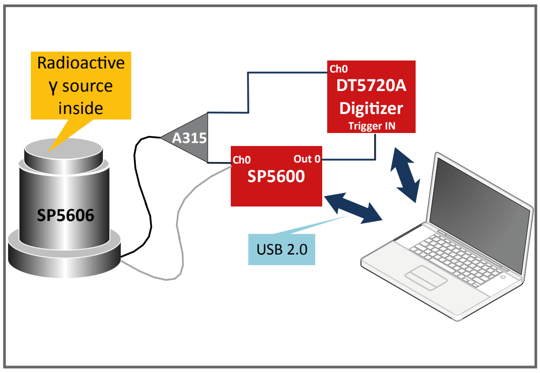

Experimental setup block diagram.

Results

The crystal characteristics are investigated recording a source spectrum (for example ^{137}Cs) with the three different crystals, optimizing the integration time as a function of the scintillation decay time.

According to table, the Light Yield of the three crystal is very different. LYSO(Ce) has a light yield three times greater than the BGO, and CsI(Tl) light yield is twice than LYSO(Ce). The analysis of the signal waveform or the trend of the charge vs integration time leads to the measurement of the time characteristics of the scintillator.

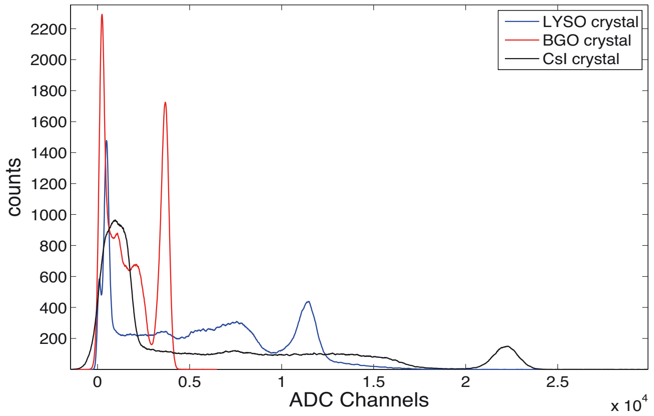

^{137}Cs energy spectra. Blue spectrum corresponds to the acquisition through LYSO crystal, the red and black ones respectively with BGO and CsI crystals.

	Light Yield Ratio (from datasheet)	Peak Position Ratio
LYSO/CsI	0.52	~0.51
LYSO/BGO	3.29	~3.11
BGO/CsI	0.16	~0.16

Experimental results of Light Yield Ratio

This experiment is also possible with the following kits

B **SP5600AN** Educational kits ★

see p. 179

E **SP5630ENP** Environmental kit Plus **PREMIUM**

see p. 181

B.1.6 γ-Radiation Absorption

SG6116

Dedicated kit	
Description	pp.
SP5600C Educational Gamma Kit	179

Difficulty	Execution Time	Data Analysis	Radioactive Sources
		NO	YES

Requirements

Gamma Radioactive Source

Equipment

SP5600C - Educational Gamma Kit

Model	SP5600	DT5720A	A315	SP5606	SP5607
Description	Power Supply and Amplification Unit 	Desktop Digitizer 250 MS/s 	Splitter 	Mini-Spectrometer 	Absorption tool 
	p. 190	p. 190	p. 192	p. 192	p. 193

Purpose of the experiment

The main goal of the experiment is the measurement of the γ radiation attenuation coefficient for different materials and different energies.

See the Application

Fundamentals

The attenuation of a γ radiation flux passing through matter is described by the exponential law

$$I(x)=I_0 * e^{-\mu x}$$

where I0 is the incident photon flux and I(x) measures the flux of γ rays emerging from a layer x of material without having interacted. The coefficient μ depends on the material properties (atomic number, density) and on the energy of the impinging photon.

The student is guided towards the development of complementary measurement techniques based on counting and on the analysis of the spectrum, performing the experiment for different materials (including PMMA, a water equivalent solid state organic material used in medical dosimetry).

Carrying out the experiment

The scintillator crystal shall be coupled to the SiPM in the SP5607, through a thin layer of index matching grease to maximize the light collection. In order to avoid saturation, the output of the SiPM is divided using the A315 splitter: one branch is connected to the DT5720A and will be digitized. The other branch will be amplified by the SP5600 module, generating the trigger for the integration signal by the on-board leading edge discriminator. The discriminator threshold shall be defined looking at the spectrum and evaluating the dark count rate. Once this is set the SP5609 absorption tool shall be mounted. The experiment can be performed for every absorber thickness in counting mode and analysing the spectrum, measuring the events in the photo-peak for a constant predefined time interval.

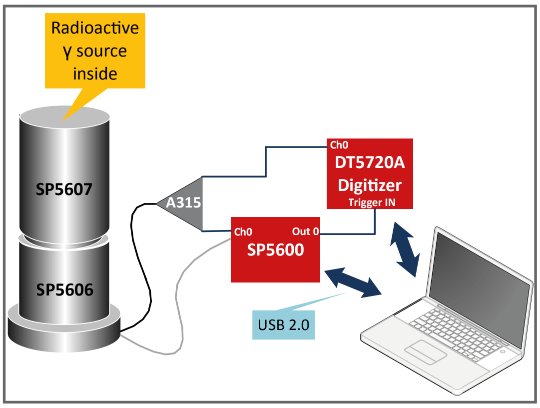

Experimental setup block diagram.

Results

Exemplary results are shown below, reporting the variation of the events in the photopeak for different absorber thickness, a plot verifying the exponential absorption law and the dependence of the absorption coefficient on the energy.

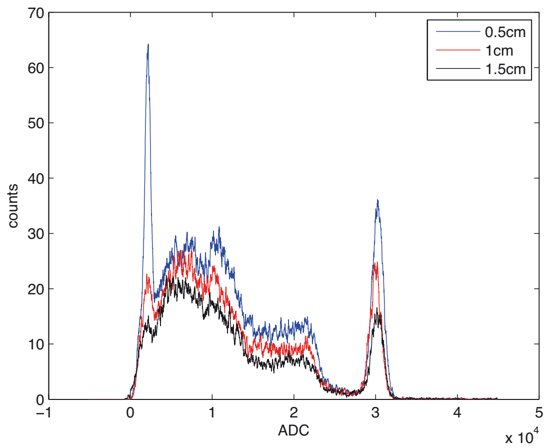

Gamma spectra acquired with different absorber thicknesses.

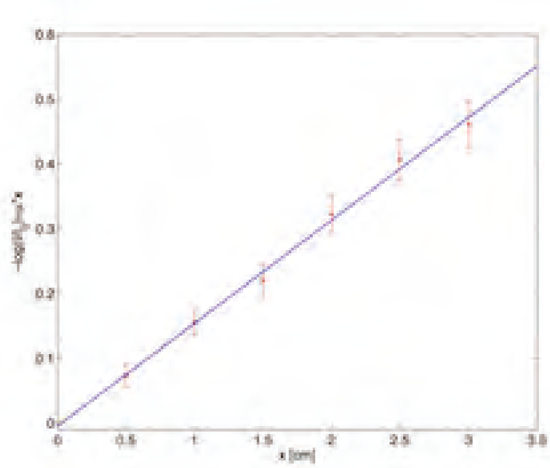

Linear dependence of logarithmic intensity of gamma rays as a function of penetration thickness.

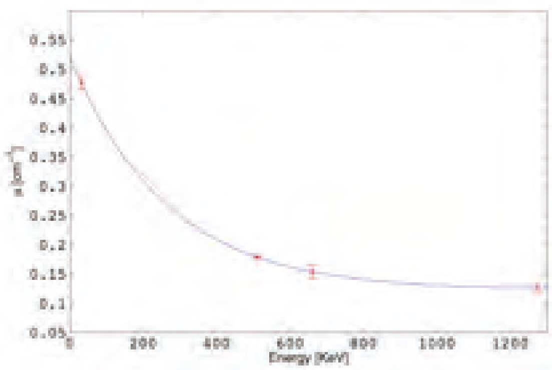

Gamma attenuation coefficient as a function of energy.

This experiment is also possible with the following kits

B ★ **SP5600AN**
Educational kits

see p. 179

C **SP5640**
GammaEDU

see p. 183

E **SP5630ENP**
Environmental kit Plus
PREMIUM

see p. 181

B.1.7 SG6117 Photonuclear cross-section / Compton Scattering cross-section

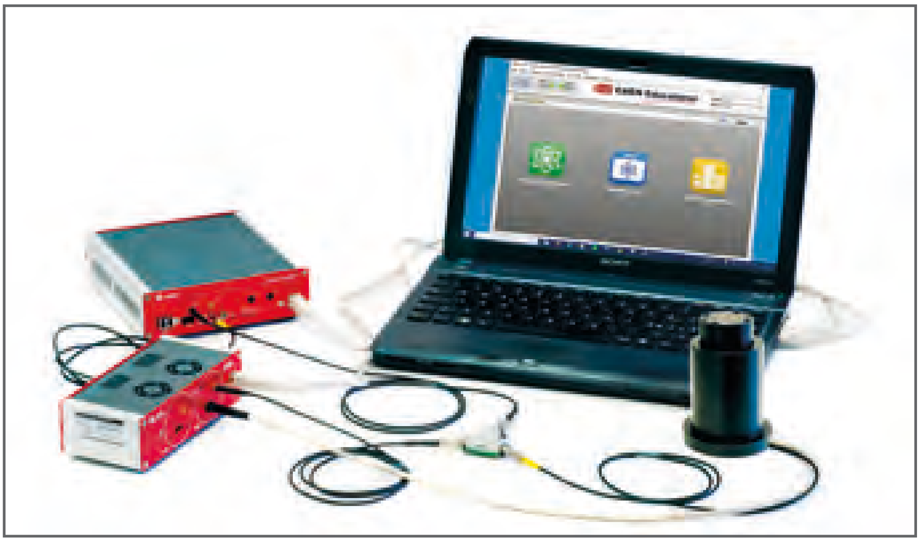

Dedicated kit	
Description	pp.
SP5600C Educational Gamma Kit	179

Difficulty	Execution Time	Data Analysis	Radioactive Sources
1/5	1/5	NO	YES

Requirements

Gamma Radioactive Source

Equipment

SP5600C - Educational Gamma Kit

Model	SP5600	DT5720A	A315	SP5606	SP5607
Description	Power Supply and Amplification Unit	Desktop Digitizer 250 MS/s	Splitter	Mini-Spectrometer	Absorption tool
					
	p. 190	p. 190	p. 192	p. 192	p. 193

Purpose of the experiment

Determination of the ratio of the effective cross-sections due to Compton and Photoelectric effects as a function of photons energy.

See the Application

Fundamentals

Gamma rays interact with matter by three processes: Compton Scattering, Photoelectric Effect and Pair Production (whenever tIn the energy range up to 2MeV, gamma rays interact with matter by two processes:

- Photoelectric Effect, dominant at energy less than 100 KeV. In this process the photon energy is completely transferred to atomic electron bounded

$$\gamma + \text{atom} \rightarrow \text{ion} + e^-$$

- Compton Scattering, linked to the elastic collision between electrons and photons and relevant at 1MeV energy level

$$\gamma + e^{--} \rightarrow \gamma' + e^{-'}$$

The predominant mode of interaction depends on the energy of the incident photons and the atomic number of the material with which they are interacting. From the acquired γ-spectrum, it is possible to estimate the fraction of events due to Compton scattering and those caused by the photoelectric. The ratio of the event fractions is used to determine the ratio of the two effective cross-sections that depends on the detector size.

Carrying out the experiment

Spread the optical grease on the open face of the scintillating crystal, insert this crystal side in the SP5607 spectrometer. Connect the power cable to the SP5600 module and connect the other cable of the spectrometer to the splitter A315. Connect the two split outputs to SP5600 channel 0 and DT5720A channel 0. Use the SP5600 digital output as DT5720A "trigger IN". Use the default software values or optimize the parameters to choose the discriminator cut-off threshold in mV. Switch off the power supply, open the spectrometer and insert the radioactive gamma source to acquire the first spectrum. After that, switch off the power supply, open the spectrometer, change the radioactive gamma source and repeat the measurement.

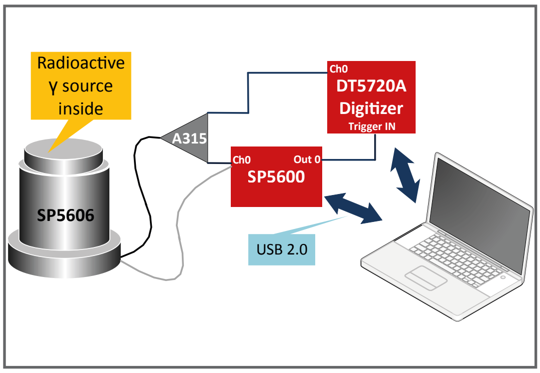

Experimental setup block diagram.

Results

By using several radioactive sources or spectra simulated by DT4800, the energy dependence of the ratio between the cross-sections of two phenomena can be examined, by verifying that the Photoelectric Effect cross section decreases with increasing energy compared to the Compton Scattering cross section for the used detector size.

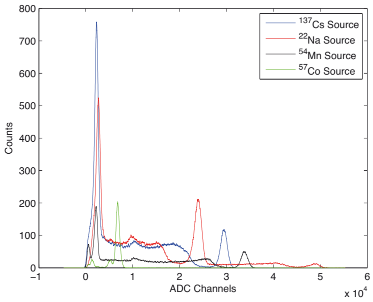

S... of Photonuclear and scattering Compton cross sections.

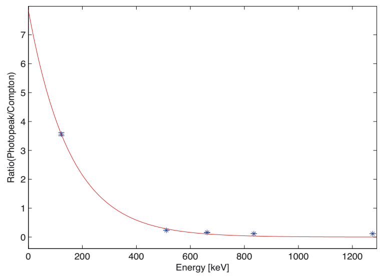

contributions as a function of energy.

This experiment is also possible with the following kits

B **SP5600AN** Educational kits PREMIUM

see p. 179

C **SP5640** GammaEDU

see p. 183

D **SP5630EN** Environmental kit

see p. 181

E **SP5630ENP** Environmental kit Plus

see p. 181

B.1.8 SG6118B Study of the ^{137}Cs spectrum: the backscatter peak and X rays

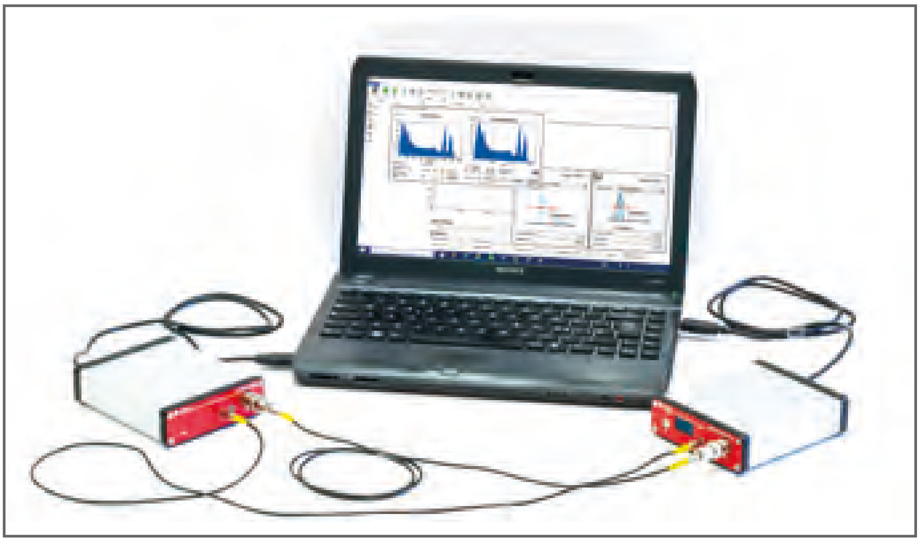

Dedicated kit	
Description	pp.
SP5600EMU Emulation Kit	180

Difficulty	Execution Time	Data Analysis	Radioactive Sources
3/5	3/5	YES	YES

Requirements

Gamma Radioactive Source

Equipment

SP5600EMU - Emulation Kit

Model	DT4800	DT5770
Description	Digital Detector Emulator 	Digital Multi-Channel Analyzer 
	p. 194	p. 194

Purpose of the experiment

Study the characteristics of the ^{137}Cs spectrum, with special relevance given to the low energy spectrum. The student can learn effects related to the experimental observation of a gamma decay and have basic information about the experimental setup used in gamma spectroscopy. Estimate the energy of the backscatter peak and of the K_α line.

See the Application

Fundamentals

The Compton effect is linked with experimental issues, since it is caused by the interaction of photons with the electrons instrument that measure the gamma radiation. In a real detector setup, some photons can and will undergo one or potentially more Compton scattering processes (e.g. in the housing material of the radioactive source, in shielding material or material otherwise surrounding the experiment) before entering the detector material. This leads to a peak structure, the so-called backscatter peak.

The basic principle for the backscatter peak formation is the following: gamma-ray sources emit photons isotropically, some photons will undergo a Compton scattering process with a scattering angle close to 180° and some of these photons will subsequently be detected by the detector. The result is an excess of counts in the Compton part of the spectrum, the so-called backscatter peak. This peak has an energy approximately equal to the photopeak energy minus the Compton edge energy.

The ^{137}Cs gamma photopeak at 661 keV is responsible also for a low energy emission (i.e. emission of an X-ray). This is due to the decay mechanism of ^{137}Cs: it decays via β decay into an excited state of barium-137, which than passes to the ground state, giving rise to the 661 keV photopeak. Emission of a 661 keV γ photon is not the only way excited barium gives off its energy. In some cases barium-137 can transfer its energy to an electron of its 1s atomic shell ("internal conversion"). The hole in the 1s shell is replenished from higher shells. This process gives rise to the emission of the characteristic X radiation of barium, which is the Kα line nearly at 32 keV (X rays are photons in the range 100 eV-100 keV).

Carrying out the experiment

To perform the experiment, connect the DT4800 output to the input channel of the MCA DT5770 and use the DT4800 GP0 as digitizer "trigger IN". The Emulation Control Software Interface allows user to generate exponential decay signals with programmable rise time and fall time and it is possible to emulate signals from ^{137}CsI radioactive. The spectrum can be recorded and analyzed by the MCA.

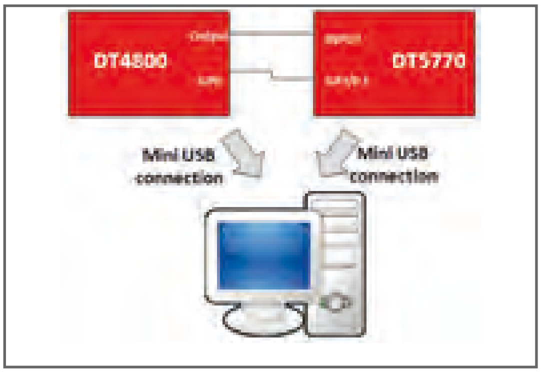

Experimental setup block diagram for the experiment.

Results

The user can calibrate the system by using the spectrum itself. The backscatter peak and the K_α line can be identified. After calibrating the spectrum, it is possible to estimate the energy of the two peaks and compare them with theoretical predictions.

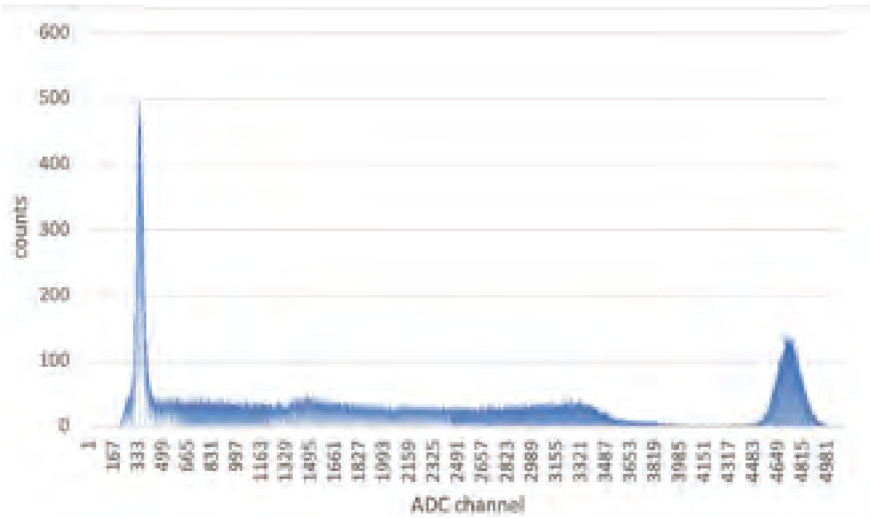

Plot of the ^{137}Cs spectrum acquired by the MCA. The backscatter peak and the Kα line are indicated with the red arrows.

This experiment is also possible with the following kits

A **SP5600C**
Educational kits

see p. 179

B **SP5600AN**
Educational kits
PREMIUM

see p. 179

C **SP5640**
GammaEDU

see p. 183

D **SP5630EN**
Environmental kit

see p. 181

E **SP5600ENP**
Environmental kit Plus

see p. 181

B.1.9

SG6119B

Activity of the ^{60}Co

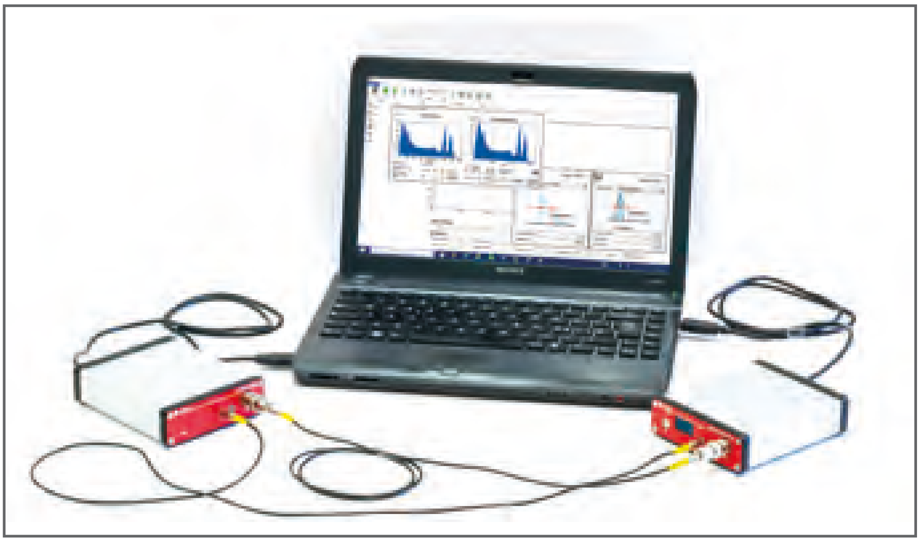

Difficulty	Execution Time	Data Analysis	Radioactive Sources
		NO	YES

Dedicated kit	
Description	**pp.**
SP5600EMU Emulation Kit	180

Requirements

Gamma Radioactive Source

Equipment

SP5600EMU - Emulation Kit

Model	DT4800	DT5770
Description	Digital Detector Emulator  p. 194	Digital Multi-Channel Analyzer  p. 194

Purpose of the experiment

Determine the activity of a ^{60}Co source from its gamma spectrum. Learn about the meaning of the sum peak, visible in the spectrum of some radioactive sources.

See the Application

Fundamentals

The ^{60}Co spectrum presents two distinct gamma photopeak in its spectrum, respectively corresponding to photons γ1 and γ2 at 1.17 MeV and 1.33 MeV. For the purpose of this experiment, we can assume that each of these gamma rays are isotropically distributed. In other words, if γ1 departs in a particular direction, γ2 can go in any direction that it wishes. There is a certain probability that γ2 will go in the same direction as γ1. If this occurs the energies of γ1 and γ2 will be summed in the detector. Hence a sum peak will show up in the spectrum, at nearly 2.5 MeV.

We can estimate the activity of the source by calculating the counts under the two main peaks and under the sum peak, i.e. calculating their area ∑. For the case of ^{60}Co, we have that the counts under the sum peak can be evaluated as

$$\Sigma(SUM) = \frac{\Sigma_1 \Sigma_2}{A\,t}$$

Where A is the activity of the source and t is the acquisition time.

Therefore, fitting the peaks with a gaussian and calculating their area, it is possible to estimate the activity of the ^{60}Co source used to record the available spectrum.

Carrying out the experiment

To perform the experiment, connect the DT4800 output to the input channel of the MCA DT5770 and use the DT4800 GP0 as digitizer "trigger IN". The Emulation Control Software Interface allows user to generate exponential decay signals with programmable rise time and fall time and it is possible to emulate signals from ^{137}CsI radioactive. The spectrum can be recorded and analyzed by the MCA.

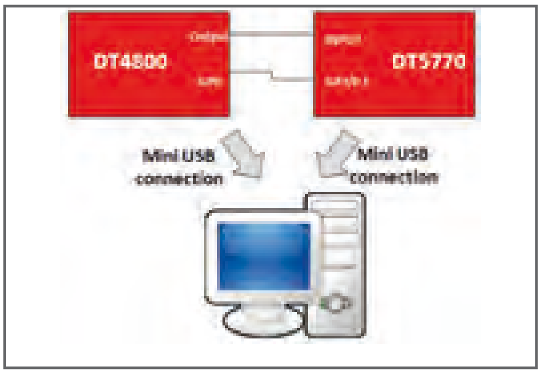

Experimental setup block diagram for the experiment.

Results

The student should verify that, after the spectrum calibration, the sum peak is nearly at 2.5 MeV. From the formula given above, using the live time in seconds, the student can estimate de activity of ^{60}Co directly in Bq. A calculation made for a spectrum acquired in 100 seconds gives an activity of nearly 264 kBq.


The ^{60}Co complete spectrum acquired by the MCA DT5770 and plotted by the Emulation Software

This experiment is also possible with the following kits

A **SP5600C**
Educational kits

see p. 179

B **SP5600AN**
Educational kits
PREMIUM

see p. 179

C **SP5640**
GammaEDU

see p. 183

D **SP5630EN**
Environmental kit

see p. 181

E **SP5600ENP**
Environmental kit Plus

see p. 181

B. Nuclear Physics and Radioactivity

B.2 γ Environmental Radioactivity Indoor

Despite the common misconception associating radioactivity solely with threats like atomic bombs and nuclear waste diseases, it permeates our everyday environment and can be harnessed for beneficial purposes with proper handling and understanding. In our efforts to promote a deeper comprehension of the underlying principles of nuclear physics, we aim to demonstrate the peaceful applications of radioactivity. The "Environmental kit", as well as the "Environmental kit Plus", enables users to explore the behavior of gamma radiation, which emanates from commonplace materials such as soil samples and camping lanterns.

Recommended kits

D SP5630EN
Environmental kit

see p. 181

E SP5630ENP
Environmental kit Plus

see p. 181

Experiment	★ SP5630EN	★ SP5630ENP
B.2.1 Energy calibration of System based on LYSO crystal and Fertilizer sample	•	•
B.2.2 Background Measurements	•	•
B.2.3 Fertilizer and photopeak identification	•	•
B.2.4 Soil sample identification	•	•
B.2.5 Samples Comparison	•	•
B.2.6 Test Sample Identification	•	•
B.2.7 Radon passive measurement	•	•

★ The star indicates the recommended Kits while the yellow color highlights the Kits especially dedicated to the experiences of this Section. If you are also interested in other experiences, the Environmental Kit Plus is recommended.

B.2.1 SG6140C Energy calibration of System based on LYSO crystal and Fertilizer sample

Dedicated kit	
Description	pp.
SP5630EN Environmental kit	181

Difficulty	Execution Time	Data Analysis	Radioactive Sources
3/5	3/5	NO	NO

Requirements

No other tools are needed.

Equipment

SP5630EN - Environmental kit

Model	i-Spector - S2570B	Samples
Description	Intelligent Silicon Photomultiplier Tube  p. 187	Samples 

Purpose of the experiment

Recording γ energy spectra of several radioactive sources and detecting the photo-peaks to calibrate the response of the system is the main goal of the experiment.

See the Application

Fundamentals

The calibration of the spectrum is the first step to be done in a typical experiment. The settings, like the trigger threshold, gate width, etc., used in the calibration should be used in the following measurements proposed in the Environmental kit. It is usually convenient to use radioactive sources with a wide range of energies, from hundreds keV to MeV. In the proposed experiment we take advantage of the LYSO(Ce) (Cerium-doped Lutetium Yttrium Orthosilicate) crystal (202 keV and 307 keV) and the Fertilizer sample (1468 keV) to have a calibration curve for the full spectrum range. The LYSO is also a scintillator material which can be coupled with SiPM or PMTs to detect gamma rays. See for example the SP5600C and SP5600AN kits.

Carrying out the experiment

Put the i-Spector digital into the base and place, one at a time, the radioactive sources to be used for the calibration, like, for example, the LYSO crystal and the Fertilizer to have two/three points for calibration. Power on the i-Spector and connect the Ethernet cable. Wait until the temperature is stable from the web interface (it can take half an hour from power on).

Check the waveform, modify the threshold and gate width, if needed, then start the measurement of the energy spectrum.

Take for example 5 minutes of acquisition with the LYSO crystal sample and 30 minutes of acquisition with the Fertilizer. Acquisition time with laboratory radioactive sources can be reduced according to the source activity. Select the ROIs and use the calibration tool to calibrate the spectrum.

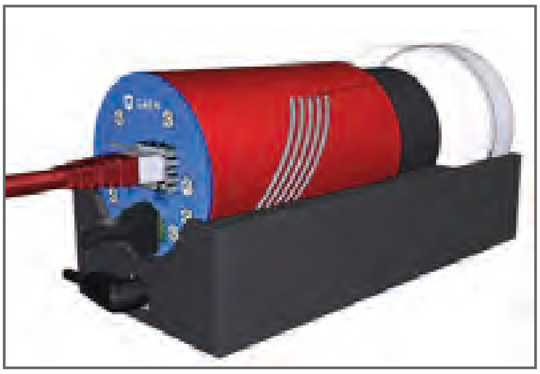

Experimental setup block diagram

Results

By fitting the photo-peaks with a Gaussian curve, the system linearity as a function of energy is verified. The final calibration function is used for the consecutive activities.

Linear dependency in the Energy Calibration

This experiment is also possible with the following kits

E **SP5630ENP**
Environmental kit Plus
★ **PREMIUM**

see p. 181

B.2.2 Background Measurements

SG6141C

Dedicated kit	
Description	pp.
SP5630EN Environmental kit	181

Difficulty	Execution Time	Data Analysis	Radioactive Sources
		NO	NO

Requirements

No other tools are needed.

Equipment

SP5630EN - Environmental kit

Model	i-Spector - S2570B	Samples
Description	Intelligent Silicon Photomultiplier Tube  p. 187	Samples 

Purpose of the experiment

Measurement of the background radioactivity to be subtracted from the energy spectra of the samples.

See the Application

Fundamentals

The main contributors to the background energy spectrum are the gamma radiations that originate from naturally occurring radioactive isotopes dispersed in the environment and the materials that surround the detector, and the radiations whose origin can be traced to cosmic rays. To properly identify the radioactive source and its activity, the background must be acquainted. The background spectrum is obtained by removing the radioactive source and must be acquired in the same conditions of the desired spectra. A possibility is to use lead blocks to cover the system and reject as much as possible environmental radioactivity that could hide interesting peaks.

Carrying out the experiment

Decide whether or not to use the Lead blocks to cover the system. The entire system can be covered by lead blocks, as shown in the figure below, just taking care to leave air flow for the i-Spector base fans. In any case, it is important to make all the measurements on the same conditions of the background one, so that the background subtraction can be made easily. The same software settings must be applied as well, including the acquisition time, so that the background subtraction can be done bin-by-bin in the energy spectrum.

Put the i-Spector digital into the base. No sample is required in this experience. Power on the i-Spector and connect the Ethernet cable. Wait until the temperature is stable from the web interface (it can take half an hour from power on).

Check the waveform, modify the threshold and gate width, if needed, then start the measurement of the energy spectrum. Take for example 30 minutes of spectra acquisition.

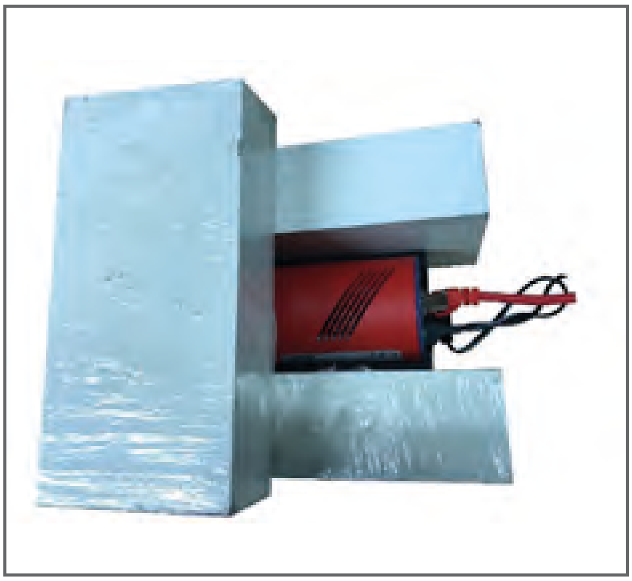

Experimental setup block with Lead blocks covering the active scintillator of i-Spector digital.

Results

The user can easily check how lead blocks reduce the gamma radioactivity, by comparing the spectra with and without lead blocks (left and right respectively). A factor of 4 in the background reduction is visible when using the Lead blocks.

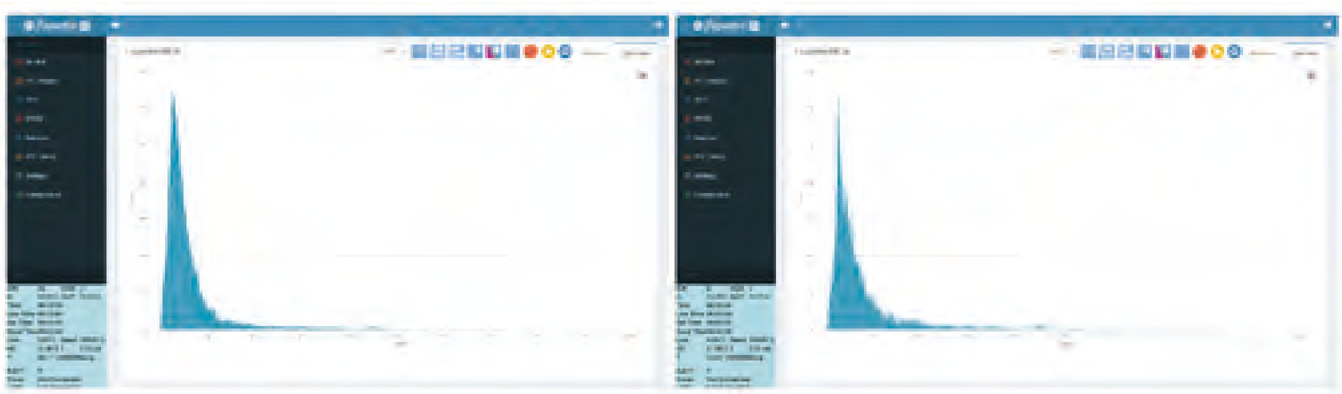

Environmental background acquired without Lead blocks (on the left) and with Lead blocks (on the right). Note the different scale on the y-axis. The radioactivity is reduced by a factor of about 4 when using the blocks.

This experiment is also possible with the following kits

E **SP5630ENP**
Environmental kit Plus
★ **PREMIUM**

see p. 181

B.2.3 Fertilizer and photopeak identification

SG6142C

Dedicated kit	
Description	pp.
SP5630EN Environmental kit	181

Difficulty	Execution Time	Data Analysis	Radioactive Sources
		NO	NO

Requirements

No other tools are needed.

Equipment

SP5630EN - Environmental kit

Model	i-Spector - S2570B	Samples
Description	Intelligent Silicon Photomultiplier Tube  p. 187	Samples 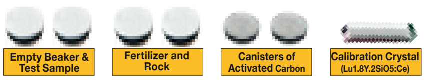

Purpose of the experiment

Record the energy spectrum of Fertilizer sample and identify the Potassium peak. The experience will guide the user to select a ROI and perform a Gaussian fit on the peak. This sample can be used also as a reference for the spectrum calibration.

See the Application

Fundamentals

Potassium is a natural element whose radioactive isotope ^{40}K is widely available on Earth, especially in food and in human bodies. It plays a key role in geologic fields for the dating samples and rocks. Indeed, one of the main decay is in ^{40}Ar, which remains locked up in minerals. Knowing the decay time of ^{40}K into ^{40}Ar, and measuring the ratio between the two elements, it is possible to give a precise estimate about the origin of that material.

Another interesting application is the so-called Banana Equivalent Dose (BED), a "user-friendly" unit to measure radioactivity. Bananas naturally contains ^{40}K and 1 BED corresponds to 0.1 μSi of equivalent dose. To understand the proportions, consider that a dental X-ray corresponds to eating 50 bananas, an average daily dose of natural background is 100 BED, a fatal dose is 100 million bananas. This quantity has been introduced to get users familiar with natural low-radioactive objects.

Carrying out the experiment

Put the i-Spector digital into the base and place the Fertilizer box into the place-holder. Power on the i-Spector and connect the Ethernet cable. Wait until the temperature is stable from the web interface (it can take half an hour from power on).

Check the waveform, modify the threshold and gate width, if needed, then start the measurement of the energy spectrum.

Take 30 minutes of acquisition with the Fertilizer.

NOTE: in case of background measurement, settings and acquisition time must be the same. Lead blocks could help in distinguish a clearer peak but they must be used if just employed in background measurement only.

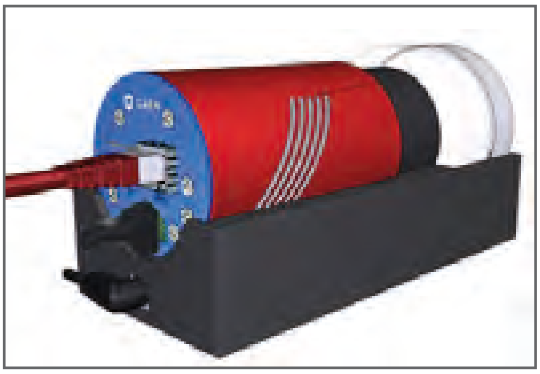

Experimental setup block diagram

Results

Several steps can be done in this experiment. First, the background subtraction by saving the .csv of the two and by making a bin-by-bin subtraction of the two spectra. A small portion of the 40K peak can be seen in the background spectrum too. The ^{40}K peak can be then selected through a ROI and fitted by means of a Gaussian function. The peak can be used together with the LYSO crystal for the energy calibration of the system (ID.6140).

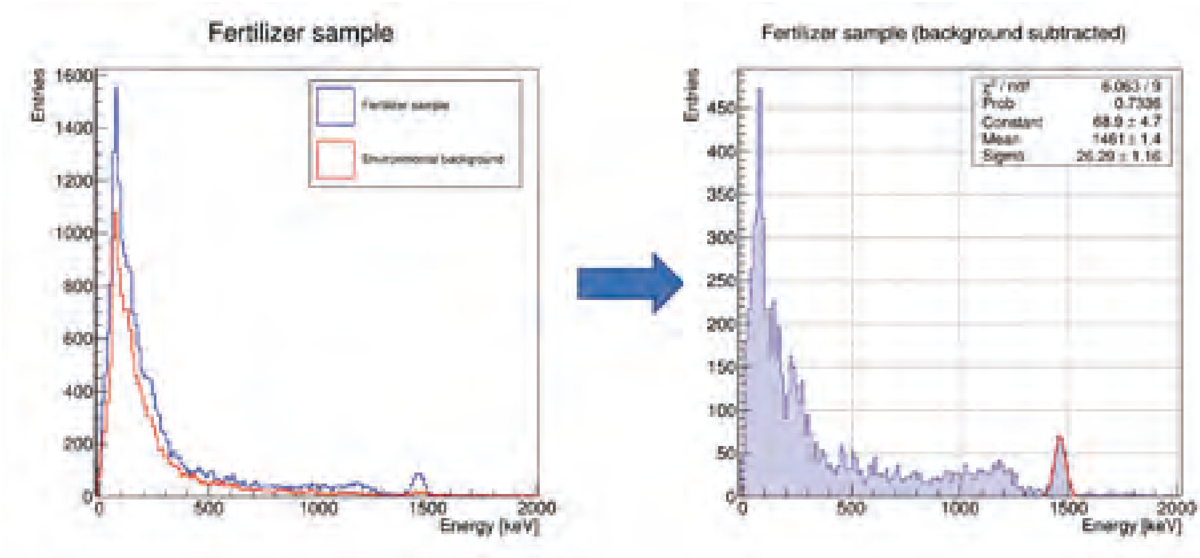

Fertilizer sample: total contribution and background on the left; background subtracted on the right with a Gaussian fit on the ^{40}K peak. The mean value is in agreement with the expected value of 1460.8 keV

This experiment is also possible with the following kits

E SP5630ENP
Environmental kit Plus
★ **PREMIUM**

see p. 181

B.2.4 Soil sample identification

SG6143C

Dedicated kit	
Description	pp.
SP5630EN Environmental kit	181

Difficulty	Execution Time	Data Analysis	Radioactive Sources
		YES	NO

Requirements

No other tools are needed.

Equipment

SP5630EN - Environmental kit

Model	i-Spector - S2570B	Samples
Description	Intelligent Silicon Photomultiplier Tube  p. 187	Samples 

Purpose of the experiment

Record the energy spectrum of the Soil sample and identify the peaks, after the energy calibration, by knowing the decay chain of Thorium and Uranium.

See the Application

Fundamentals

Natural radioactivity has several sources that can be classified into two broad categories: high energy cosmic rays incident on the Earth's atmosphere and releasing secondary radiation (cosmic contribution); and radioactive nuclides generated during the formation of the Earth and still present in the Earth's crust (terrestrial contribution).

The terrestrial contribution is mainly composed of the radionuclides of the uranium and thorium decay chains together with radioactive potassium. In most circumstances, radon, a noble gas produced in the radioactive decay of uranium, is the most important contributor to radiation exposure.

Natural radionuclides, both terrestrial and cosmogenic, migrate in the environment through different pathways: air, water, rock, soil, and the food chain. Radionuclides may then enter the human body through ingestion (food and drinking water) and inhalation giving the so-called internal exposure. External exposure is due to cosmic radiation and radiation from terrestrial radionuclides present in soil, rocks, and building materials.

Carrying out the experiment

Put the i-Spector digital into the base and place the Soil box into the place-holder. Power on the i-Spector and connect the Ethernet cable. Wait until the temperature is stable from the web interface (it can take half an hour from power on).

Check the waveform, modify the threshold and gate width, if needed, then start the measurement of the energy spectrum.

More than 30 minutes of acquisition need with the Soil sample.

NOTE: in case of background measurement (ID.6141), settings and acquisition time must be the same. Lead blocks could help in distinguish clearer peaks but they must be used if just employed in background measurement only.

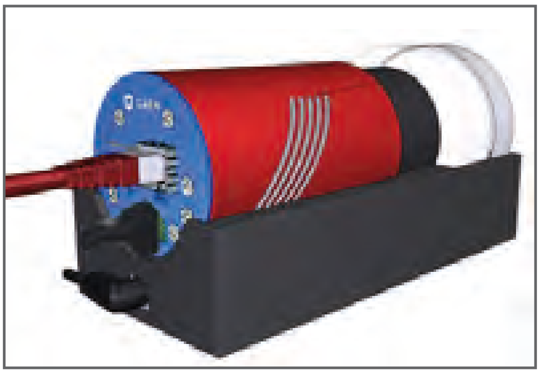

Experimental setup block diagram

Results

After the background subtraction, it is possible to recognize peaks coming from the Uranium or Thorium chain, as shown in the picture below.

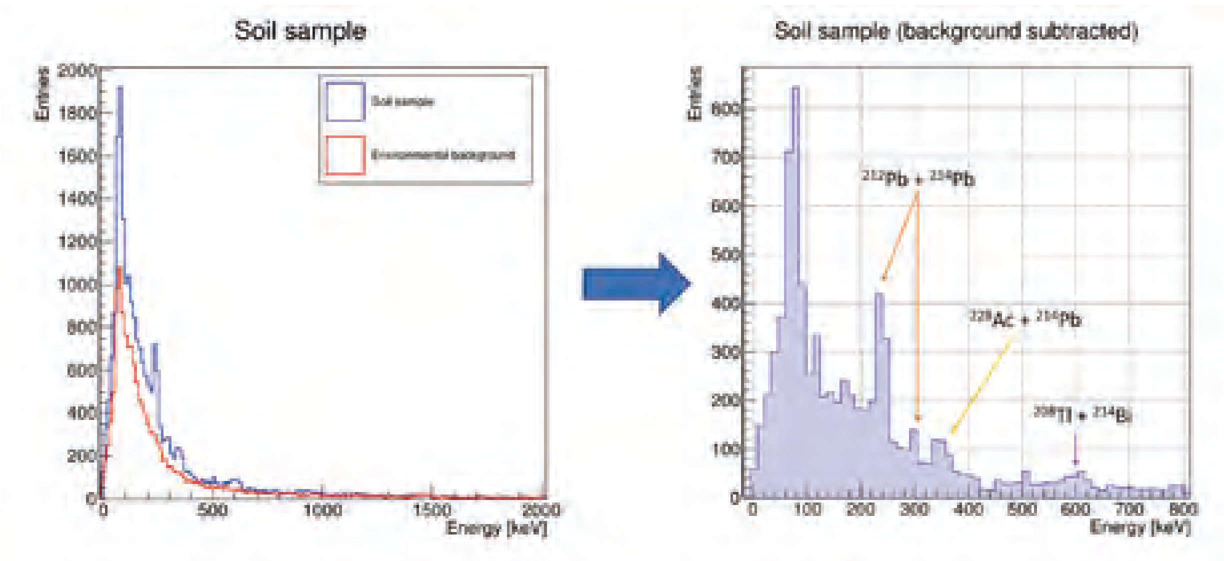

Soil sample: total contribution and background on the left; background subtracted on the right. The visible peaks from the ^{238}U and ^{232}Th are highlighted in the spectrum.

This experiment is also possible with the following kits

E SP5630ENP
Environmental kit Plus
★ **PREMIUM**

see p. 181

B.2.5 Samples Comparison

SG6144C

Dedicated kit	
Description	pp.
SP5630EN Environmental kit	181

Difficulty	Execution Time	Data Analysis	Radioactive Sources
3/5	3/5	YES	NO

Requirements

No other tools are needed.

Equipment

SP5630EN - Environmental kit

Model	i-Spector - S2570B	Samples
Description	Intelligent Silicon Photomultiplier Tube	Samples

p. 187

Purpose of the experiment

This activity shows how to compare different spectra together.

See the Application

Fundamentals

Spectra comparison is a very common procedure in statistics and physics and consist of the superposition of different spectra, taken in the same conditions, or normalized to a common state. For example, radioactive sample and background spectra can be superimposed to visually show the differences and highlight the signal contribution.

Different sample spectra can be superimposed too, like for example the Soil and Fertilizer samples to see how in the same amount of time the two samples emitted. In the case of comparison of radioactive samples with a big activity difference, the normalization could be done for the total number of events.

Another possible comparison is by using a different detector, like the High Purity Germanium detector (HPGe), or a different system, like the GammaEDU backpack SP5640, composed of photomultiplier tube (PMT) coupled to a NaI scintillating crystal (0,3L).

Carrying out the experiment

ut the i-Spector digital into the base and place the Soil box into the place-holder. Power on the i-Spector and connect the Ethernet cable. Wait until the temperature is stable from the web interface (it can take half an hour from power on).

Check the waveform, modify the threshold and gate width, if needed, then start the measurement of the energy spectrum.

Take 30 minutes acquisition with the Soil sample and then repeat the measurement by using Fertilizer sample.

NOTE: Settings and acquisition time must be the same. Lead blocks could help in distinguish clearer peaks but they must be used if just employed in background measurement only.

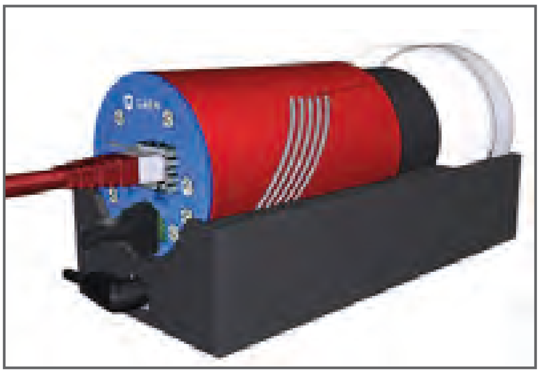

Experimental setup block diagram

Results

Superimpose the Fertilizer and Soil spectra in the same histogram. The different contributions are clearly visible on the left plot below, where the Uranium and Thorium peaks are visible in the region 200-400 keV of the Soil sample, while no contribution appears in the Fertilizer sample, and viceversa, the ^{40}K peak with its Compton edge is visible in the Fertilizer sample, with no contribution in other energy areas.

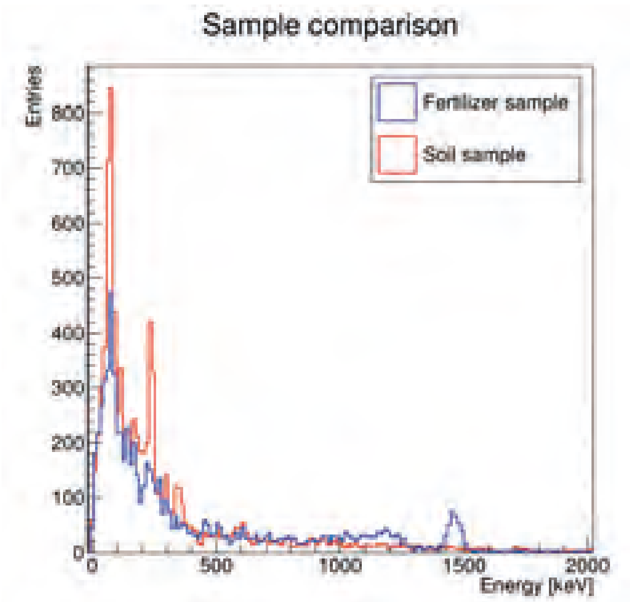

Sample comparison: two samples taken with the same i-Spector in the same experimental conditions

This experiment is also possible with the following kits

E **SP5630ENP**
Environmental kit Plus
★ **PREMIUM**

see p. 181

B.2.6 Test Sample Identification

SG6145C

Dedicated kit	
Description	**pp.**
SP5630EN Environmental kit	181

Difficulty	Execution Time	Data Analysis	Radioactive Sources
3/5	3/5	YES	NO

Requirements

No other tools are needed.

Equipment

SP5630EN - Environmental kit

Model	i-Spector - S2570B	Samples
Description	Intelligent Silicon Photomultiplier Tube  p. 187	Samples 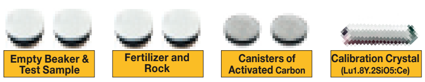

Purpose of the experiment

Record the energy spectrum of the Test sample and identify the peaks, after the energy calibration, by knowing the decay chain of Thorium and Uranium.

See the Application

Fundamentals

Naturally occurring radiative material (NORM) is material found in the environment that contains radioactive elements of natural origin (uranium, thorium, and potassium). NORM is often found in its natural state in rocks or sand but it can also be present in consumer products, including common building products (like brick and cement blocks), granite counter tops, glazed tiles, phosphate fertilizers, and tobacco products. Moreover, there are some of the materials and products sitting around your house could be emitting low levels of radiation. In the past, radioactive materials were employed by humans in objects of common use, like ceramics dishes (once uranium oxides were used to create a bright red-orange dinnerware), drinking glasses (glassmakers widely used uranium to color glasses a transparent yellow or yellow-green), clocks (glow in the dark with radium in the paint), camping lanterns (white light due to thorium), etc.

The test sample available in the kit contains old objects containing radioactive elements. The user can acquire the energy spectrum and try to recognize the source by knowing the decay products of Thorium and Uranium.

Carrying out the experiment

Put the i-Spector digital into the base and place the Test sample box into the place-holder. Power on the i-Spector and connect the Ethernet cable. Wait until the temperature is stable from the web interface (it can take half an hour from power on).

Check the waveform, modify the threshold and gate width, if needed, then start the measurement of the energy spectrum.

Take few minutes of acquisition according to the sample activity

NOTE: in case of background measurement, settings and acquisition time must be the same. Lead blocks could help in distinguish clearer peaks but they must be used if just employed in background measurement only.

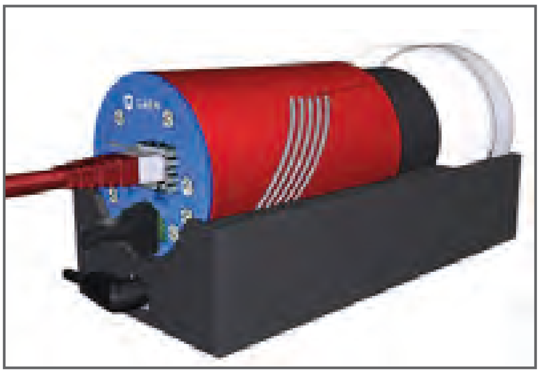

Experimental setup block diagram

Results

The background subtraction can be made with the background spectrum. After that, it is possible to recognize peaks and identify the source, either Thorium, Uranium, or both, as shown in the picture below. The user can identify which source is contained in the Test sample by knowing the product decay of the two elements.

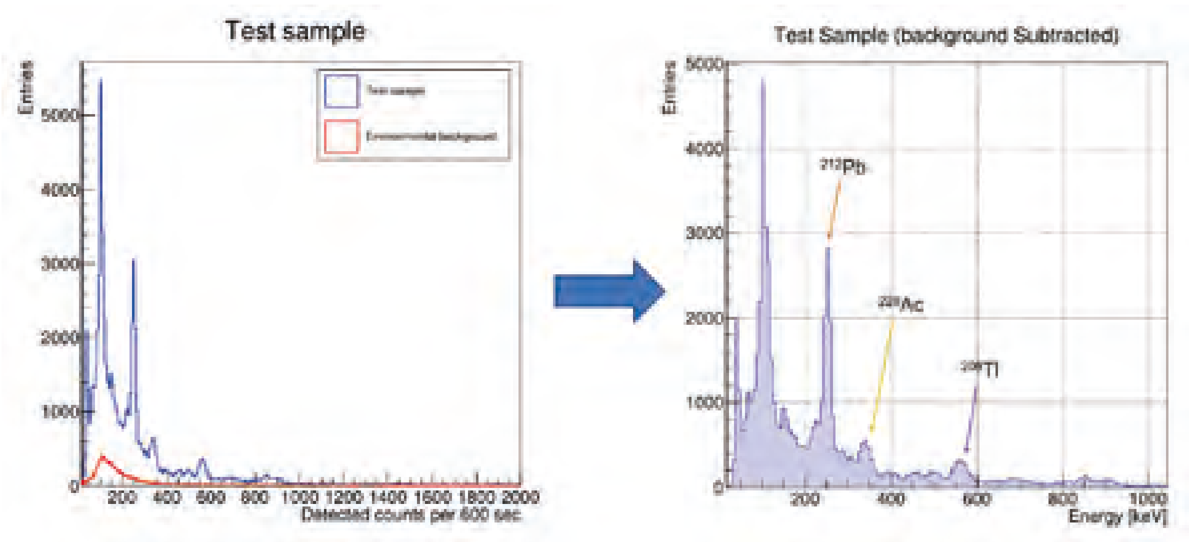

Test sample: total contribution and background on the left; background subtracted on the right. The visible peaks are highlighted in the spectrum

This experiment is also possible with the following kits

E **SP5630ENP**
Environmental kit Plus
PREMIUM

see p. 181

B.2.7 Radon passive measurement

SG6146C

Dedicated kit	
Description	pp.
SP5630EN Environmental kit	181

Difficulty	Execution Time	Data Analysis	Radioactive Sources
3/5		YES	NO

Requirements

No other tools are needed.

Equipment

SP5630EN - Environmental kit

Model	i-Spector - S2570B	Samples
Description	Intelligent Silicon Photomultiplier Tube	Samples

p. 187

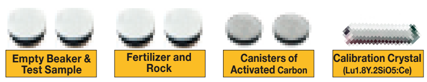

Purpose of the experiment

Get familiar with radon passive measurements by taking care of the proper sample preparation and exposure, as well as of acquiring the spectrum to calculate the Radon concentration.

See the Application

Fundamentals

Radon is a naturally occurring radioactive gas produced by the breakdown of uranium in soil, rock, and water. Radon can be dangerous since it accumulates inside houses or buildings. Air pressure inside your home is usually lower than the pressure in the soil around the building foundation. Because of this difference in pressure, the building acts like a vacuum, drawing radon in through foundation cracks and other openings. Additionally, building materials — such as granite and certain concrete products — can give off radon.

It is usually recommended to make screening measurements to have a quick estimate of the highest concentration and take action in case the measurement exceeds 4 pCi/L (or 100 Bq/m^3), which is the limit for a non-dangerous exposure to this element.

Carrying out the experiment

Detailed instructions for this activity are reported in Sec. ERROR Reference source not found. Error! Reference source not found.. Check the expiration date of the charcoal sample; if expired, or if the sample has already been used, bake it for some hours. Acquire the background spectrum with the i-Spector. Before starting the acquisition, make sure that the temperature is stable from the web interface. Once done, expose the sample for about 5-6 days, following the requirements of the closed house, and far away from wall, windows, etc., according to the Radon measurement procedure. Once ready, seal again the sample, wait at least three hours, and acquire the energy spectrum. Take few hours of acquisition with the exposed sample in the same condition of background acquisition.

Experimental setup block diagram

Results

After the energy calibration and background subtraction, it is possible to select the region of interest (ROI) of the ^{214}Pb and ^{214}Bi decay products at 295 keV, 352 keV, and 609 keV. The counts can be used together with the calibration curves to calculate the Radon concentration. On request, Excel® spreadsheets examples can be provided to customers.

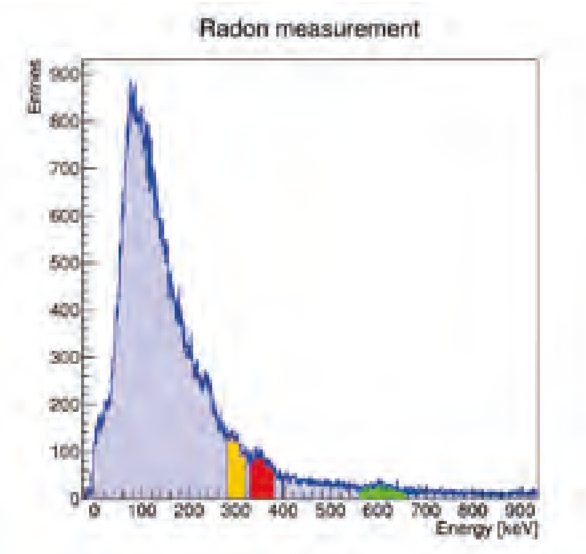

Radon spectrum: counts of the three ROI are summed and combined with the calibration curves. The result is 124 ± 85 Bq/m^3. Longer acquisition time will improve the measurement resolution.

This experiment is also possible with the following kits

E SP5630ENP
Environmental kit Plus
★ **PREMIUM**

see p. 181

B. Nuclear Physics and Radioactivity

B.3 γ Environmental Radioactivity Outdoor

Minerals and materials from the earth soil are the most common sources of natural radiation. “Naturally Occurring Radionuclides” stands for radionuclides that occur naturally in significant quantities on earth. The term is usually used to refer to the primordial radionuclides Potassium-40, Uranium-235, uranium-238 and Thorium-232 (the decay product of primordial uranium-236), their radioactive decay products, and tritium and carbon-14 generated by natural activation processes. GammaEDU backpack allows the user to get acquainted with what concern the gamma environmental radioactivity.

Recommended kits

C SP5640
GammaEDU

see p. 183

★

Experiment	SP5640
B.3.1 Environmental monitoring in land field	•
B.3.2 Ground Coverage Effect on the Environmental Monitoring.	•
B.3.3 Human Body Radioactivity	•
B.3.4 γ Environmental detection as a function of the soil distance	•
B.3.5 Radioactivity maps production	•
B.3.6 Radiological evaluation of the building materials	•
B.3.7 Mapping of potential radon-prone areas - **Coming soon**	•
B.3.8 Soil water content evaluation with gamma ray spectroscopy - **Coming soon**	•
B.3.9 Geochemical and mineral exploration	•

★ The star indicates the recommended Kits while the yellow color highlights the Kits especially dedicated to the experiences of this Section.

B.3.1 Enviromental monitoring in field

SG6150E

Dedicated kit	
Description	**pp.**
SP5640 GammaEDU	183

Difficulty	Execution Time	Data Analysis	Radioactive Sources
1/5	1/5	NO	NO

Requirements

No other tools are needed.

Equipment

SP5640 - Backpack Detector

Model	SP5640
Description	Backpack Detector  p. 183

Purpose of the experiment

Increase of the familiarity with environmental radioactivity topic via measurements in field which combine nuclear engineering and computer science for a better comprehension of basic physics concepts.

See the Application

Fundamentals

Radioactivity is a physical phenomenon occurring when an unstable nucleus undergoes a transition from one energy state to another. In addition to the cosmogenic radionuclides, natural sources include the so-called primordial radionuclides existing since the Earth formed and that have not completely decayed due to their long half-life (~109 years and longer). The most common isotopes in the Earth responsible for the so-called terrestrial radiation are Uranium (^{238}U), Thorium (^{232}Th), and Potassium (^{40}K), together with their multiple daughter products. It is estimated that 80% of the average annual dose for the world's population comes from natural background radiation. While ^{40}K undergoes one single decay, ^{238}U and ^{232}Th produce decay chains that comprise α, β, and/or γ decays.

In the outside environment, especially in case of in-situ γ-ray spectroscopy, there are many variables that could interfere with the measurement, such as the presence of vegetation or buildings and the morphology of the area affecting the field of view of the spectrometer.

Carrying out the experiment

Power on the γstream inside the red backpack. Power on the tablet and associate the two devices via Bluetooth.

Take care that the γstream internal battery is charged, otherwise use the external power system.

Start the measurement campaign in land field and place the backpack on the floor almost 1m far from the trees, manhole or other construction. Set the acquisition time to about 5 minutes and see the results. If the statistic is not enough increasing the acquisition time.

It is good practice to repeat the measurement in order to obtain the mean and standard deviation of the result.

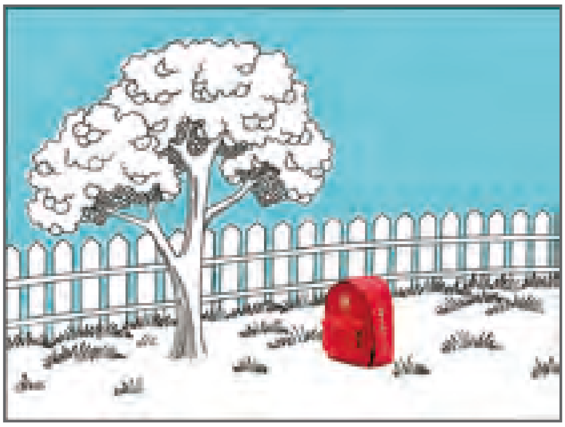

Experimental setup block diagram.

Results

The measurement results are compared to the reference values in the terrestrial crust. The discrepancy in the reference levels can be explained by the building material, distance from soil and more. This kind of measurement is important for the evaluation of natural radiation exposure from building materials [2013/59/ Euratom Directive and by UNSCEAR (United Nations Scientific Committee on the Effects of Atomic Radiation)].

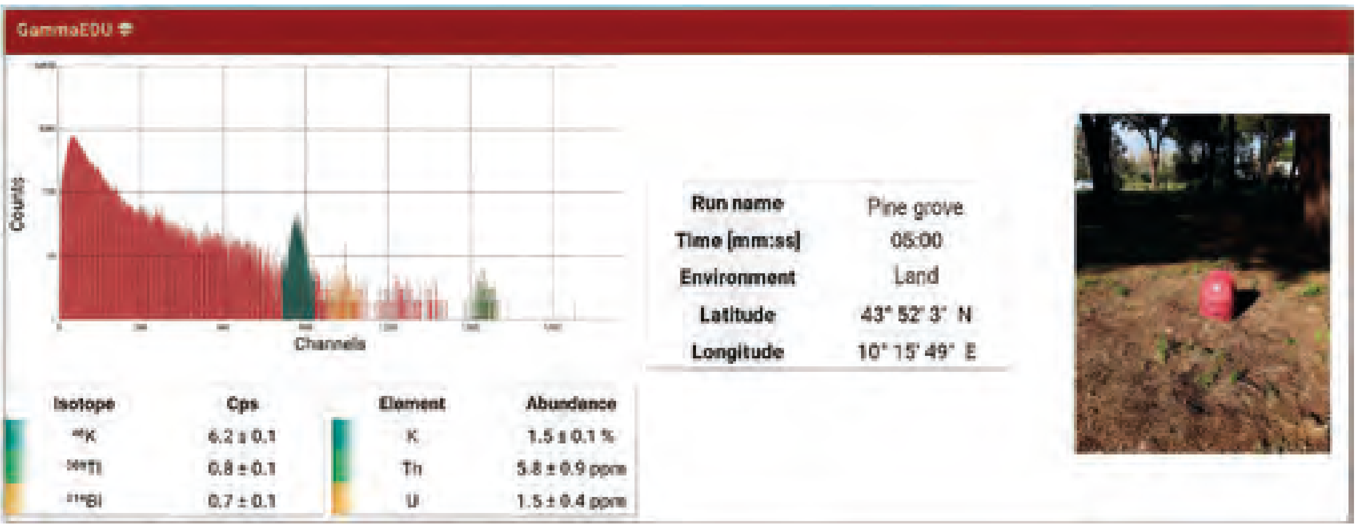

Experimental result of in-situ γ-ray spectroscopy taken place in Viareggio, Italy.

B.3.2 SG6151E Ground coverage Effect on the Environmental Monitoring

Dedicated kit	
Description	**pp.**
SP5640 GammaEDU	183

Difficulty	Execution Time	Data Analysis	Radioactive Sources
		YES	NO

Requirements

No other tools are needed.

Equipment

SP5640 - Backpack Detector

Model	SP5640
Description	Backpack Detector  p. 183

Purpose of the experiment

The experimental activity aims to give to the user a critical understanding of environmental radioactivity phenomenon.

See the Application

Fundamentals

The use of portable gamma-ray spectrometers (NaI) as a probe for exploring the natural radioactivity allows the users to be able to grasp quantitative insights of the spatial distribution of the terrestrial radionuclides (i.e. U, Th and K) in the daily environment.

In the specific case of in-situ gamma ray spectroscopy, there are many variables that could interfere with the measurement, such as the presence of vegetation or buildings and the morphology of the area affecting the field of view of the spectrometer. In addition, soil humidity has an attenuating effect on gamma radiation and sources having weak intensities need longer acquisition times. Moreover, the different types of ground coverage (like asphalt, grass, or brick) affect the measurement considerably. It is interesting to observe and understand how some type of ground coverage can be most or least abundant in natural radioactivity terms.

Carrying out the experiment

Power on the γstream inside the red backpack.
Power on the tablet and associate the two devices via Bluetooth.

Take care that the γstream internal battery is charged, otherwise use the external power system.

Start the measurement campaign in field and place the backpack on the floor almost 1m far from the trees, manhole or other construction. Set the acquisition time to about 5 minutes and see the results. If the statistic is not enough increasing the acquisition time. Repeat the measurements for the different types of ground coverage, like asphalt, grass, or brick and compare the results.

Experimental setup block diagram.

Results

Different ground coverage types are investigated by recording in-situ γ-ray spectra. The mean and standard deviation of the ^{40}K, ^{238}U, and ^{232}Th concentrations can be compared and discussed critically.

Ground Coverage	Number of Measurements	^{40}K [10^{-2} g/g]	^{238}U [µg/g]	^{232}Th [µg/g]
Brick	7	0.82 ± 0.19	1.8 ± 0.5	4.1 ± 1.0
Grass	28	2.08 ± 0.32	1.7 ± 0.4	9.5 ± 1.8
Asphalt	7	1.20 ± 0.10	1.9 ± 0.4	5.1 ± 0.7

Mean and standard deviation of the K, U, and Th concentrations that were obtained from the in-situ -ray measurements distinguished according to the different ground coverage types (Data from University of Ferrara).

B.3.3 Human body radioactivity

SG6151E

Dedicated kit	
Description	pp.
SP5640 GammaEDU	183

Difficulty	Execution Time	Data Analysis	Radioactive Sources
		YES	NO

Requirements

No other tools are needed.

Equipment

SP5640 - Backpack Detector

Model	SP5640
Description	Backpack Detector 

p. 183

Purpose of the experiment

The purpose of the experiment is to become aware of the radioactivity of the human body.

See the Application

Fundamentals

Potassium is essential to all living beings, including humans, where it's found especially in the muscle tissue. It can be found in most soils, building materials, plants and animals and it is typically used in fertilizers.

In nature there are only three isotopes of potassium: ^{39}K (93.3% of weight abundance), ^{41}K (6.7%) and ^{40}K (0.0117%). While ^{39}K and ^{41}K are stable, ^{40}K is a radioactive isotope with a half-life of $1.28 \cdot 10^9$ years and it is one of the most common responsible for the so-called *terrestrial radiation*.

Considering the relative abundance, only twelve of a hundred thousand potassium atoms are actually radioactive, i.e. approximately for 1 g of potassium, 31 nuclei decay per second [~ 31 Bq /g]. This fact implies that one banana of 150 g contains about 525 mg of potassium which corresponds to ~16 Bq activity, and similarly, an adult man (70 kg) has about 140 g of potassium which corresponds to ~ 4400 Bq.

^{40}K decays 89.3% of the time to the ground state of ^{40}Ca by pure β-emission and 10.7% of the time by electron capture to an excited state of ^{40}Ar which then decays γ reaching the stability. The emitted photon has an energy of 1460.86 keV and can be used in order to identify and quantify the activity concentration of ^{40}K in sites of measurement and in the environmental samples.

Carrying out the experiment

Power on the γstream inside the red backpack.
Power on the tablet and associate the two devices via Bluetooth. Take care that the γstream internal battery is charged, otherwise use the external power system.

Start the experiment by placing the backpack on the ground and be sure that your presence is far enough from the measure point not to be revealed (A). Set the acquisition time to about 5 minutes and see the results. If the statistic is not enough increasing the acquisition time. Repeat the measurements leaving the backpack in the same position together with just your presence or more (B).

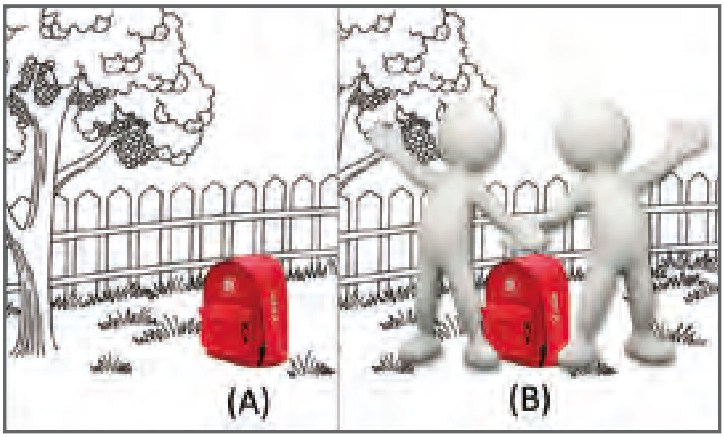

Results

The measurements results show how the detection of the ^{40}K in situ is dependent of the human presence weakly.

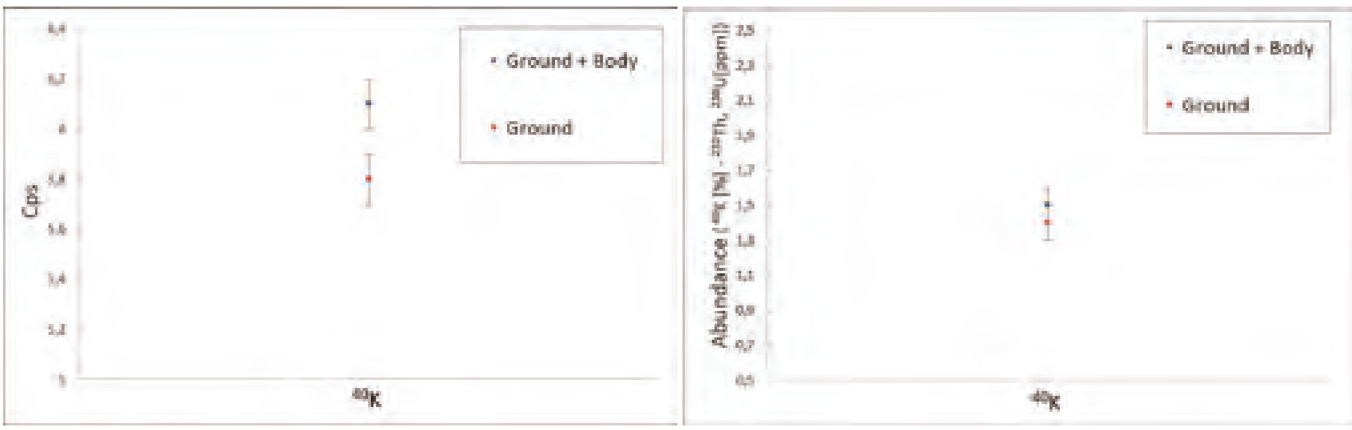

Experimental result of in-situ γ-ray coming from ^{40}K [1460 keV] with and without people presence.

B.3.4 Enviromental detection as a function of the soil distance

SG6153E

Dedicated kit	
Description	**pp.**
SP5640 GammaEDU	183

Difficulty	Execution Time	Data Analysis	Radioactive Sources
2/5	1/5	YES	NO

Requirements

No other tools are needed.

Equipment

SP5640 - Backpack Detector

Model	SP5640
Description	Backpack Detector 

p. 183

Purpose of the experiment

The main goal of the experiment is to understand how the measurement of the γ environmental radiation can be affect by the distance of the point of measurement.

See the Application

Fundamentals

The linear attenuation coefficient of gamma radiation μ represents the inverse of the distance at which the number of photons is reduced by a factor 1/e, as can be inferred by the following equation: N = N0e−μx , where μ in cm−1. This Equation is the key for understanding the lateral horizon of in-situ gamma ray spectroscopy. The horizontal field of view of a gamma-ray detector expresses the relative contribution to the total signal that is produced within a given radial distance from the detector vertical axis. The lateral horizon depends on the height of the detector: for instance, a spectrometer that was placed at ground level detect gammas coming from the first 25 cm of depth and it receives 90% of the signal from a radius of ~0.5 m. At a height of 0.5 m, 95% of the signal come from a radius of ~8 m and the maximum percentage contribution to the flux comes from the concentric hollow cylinder of soil having a ~0.6 m radius centered at the detector vertical axis. When it's carried on the shoulders of the operator (1.5

m of height) the signal reaches ~95% at ~20 m and the maximum percentage contribution to the flux comes from the concentric hollow cylinder with a radius of ~1.2 m.

Carrying out the experiment

Power on the γstream inside the red backpack.
Power on the tablet and associate the two devices via Bluetooth.

Take care that the γstream internal battery is charged, otherwise use the external power system.

Start the experiment by placing the backpack on the floor/soil. Set the acquisition time to about 5 minutes and see the results. If the statistic is not enough increasing the acquisition time.

Repeat the measurements at different heights/ distances from soil and pay attention to perform the measurements in the same conditions exactly.

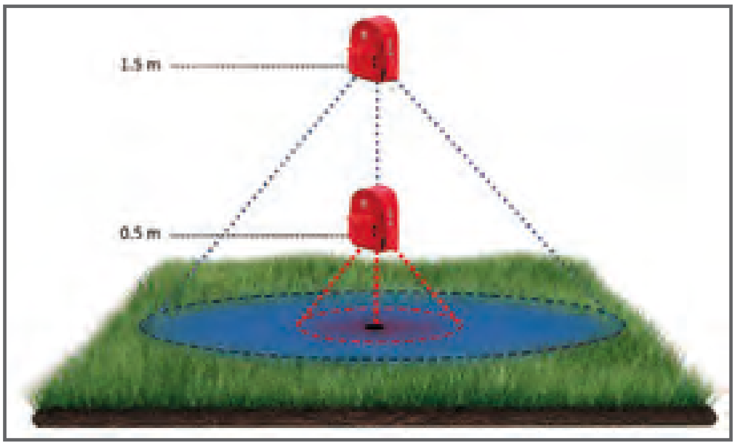

Results

The measurements results show how the detection of the ^{40}K in situ is dependent of the human presence weakly.

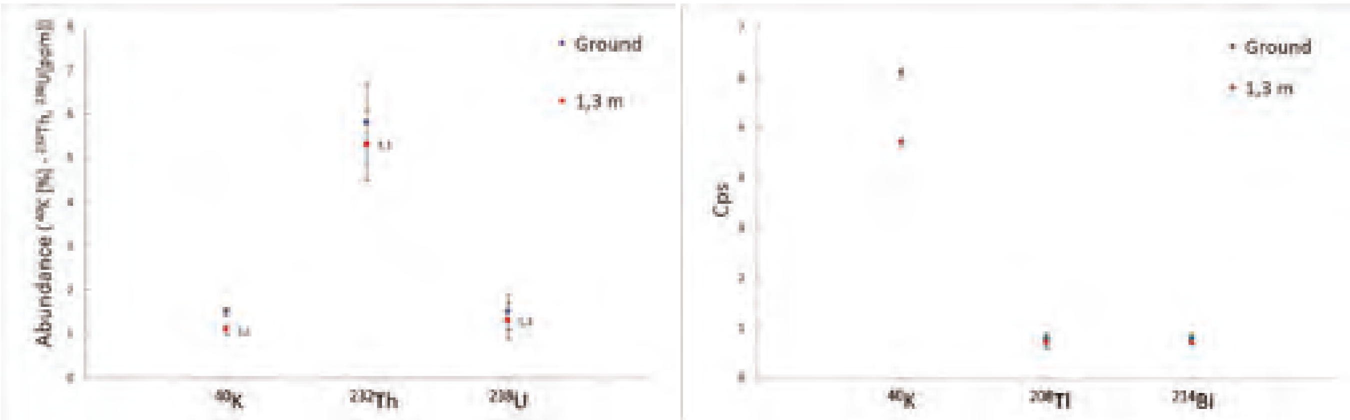

Result of the in-situ-y-ray measurements that were performed at different heights: the counts per second go three isotopes (a) and the abundance (b).

B.3.5 Radioactivity maps production

SG6154E

Dedicated kit	
Description	pp.
SP5640 GammaEDU	183

Difficulty	Execution Time	Data Analysis	Radioactive Sources
		YES	NO

Requirements

No other tools are needed.

Equipment

SP5640 - Backpack Detector

Model	SP5640
Description	Backpack Detector

p. 183

Purpose of the experiment

Starting from outdoor spectroscopy measurements to create the map of the natural radioactivity expressed in total specific activity in Bq/kg of the investigated area.

See the Application

Fundamentals

The human population is continuously exposed to ionizing radiation from various natural sources (cosmic and terrestrial ones). Moreover, the exposure to natural sources exceeds that of all artificial, i.e., due to medical use, power generation and associated fuel cycle facilities, radioisotope production waste management and from military ones. In this context, the radiological monitoring of the geographical areas became very important. All over the World, several institutions are missioned to develop collections of maps showing the levels of natural radioactivity caused by different sources (e.g., indoor radon, cosmic radiation, terrestrial gamma radiation, and natural radionuclides in soil and bedrock).

Carrying out the experiment

Power on the γstream inside the red backpack.
Power on the tablet and associate the two devices via Bluetooth.

Take care that the γstream internal battery is charged, otherwise use the external power system.

The in-situ survey must be planned to keep in mind the spatial resolution of the desired information: it is important choosing the sampling points in order to cover the surveyed area comprehensively for the different types of ground coverage, like asphalt, grass, or brick.

Start the measurement campaign and place the backpack on the floor almost 1m far from the buildings, manhole or other construction. Set the acquisition time to about 5 minutes and see the results. If the statistic is not enough increasing the acquisition time.

Results

The results that were obtained during the outdoor experiment in terms of total activity originating from ^{40}K, ^{238}U, and ^{232}Th are visualized via Google Earth. From these data, a natural radioactivity map of the investigated area can be developed.

Maps of the measurement points (yellow triangles) reported in the Google Earth app and the example of the measurement result reporting total activity concentration and Isotopic abundances [Viareggio, Italy].

B.3.6 SG6155E Radiological evaluation of the building materials

Dedicated kit	
Description	pp.
SP5640 GammaEDU	183

Difficulty	Execution Time	Data Analysis	Radioactive Sources
3/5	3/5	YES	NO

Requirements

No other tools are needed.

Equipment

SP5640 - Backpack Detector

Model	SP5640
Description	Backpack Detector 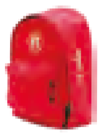

p. 183

Purpose of the experiment

The main goal of the experiment is the estimation of the natural radioactivity content in several dwellings and/or buildings representative of the different geological construction materials and commonly used in building constructions.

See the Application

Fundamentals

The main contributors on the overall natural indoor effective dose to which population is exposed are ^{222}Rn and ^{220}Rn isotopes of radon gas, by-products of the ^{238}U and ^{232}Th series.

Only a fraction of radon atoms preserves enough kinetic energy to leave the grain of the material where it has been generated and to reach the empty space in the porous materials (emanation process that depends on the material itself). Moreover, only a fraction of the radon atoms reaching the pore volume of the material mass can escape into the air and reaches the spaces where people live (exhalation process). The exhalation rate and the emanation coefficient.

The study of the natural radionuclides ^{232}Th, ^{40}K, ^{226}Ra, and the radon emanation coefficient exhalation rate is essential to estimate the actual risk for human health associated to a given natural material used for building construction. The natural radioactivity content of building materials depends on the local geology of each region on Earth. One of the requirements of estimate the radiation hazards in closed spaces, aiming to better protect against natural ionizing radiations exposure, is the assessment of the radiation hazards arising from the use of natural building materials in the construction of dwellings, since the majority of people in the World spend most time in indoor environments.

Carrying out the experiment

Power on the γstream inside the red backpack. Power on the tablet and associate the two devices via Bluetooth.

Take care that the γstream internal battery is charged, otherwise use the external power system.

Start the measurement campaign and place the backpack on the floor far from the room walls. Set the acquisition time to about 5 minutes and see the results. If the statistic is not enough increasing the acquisition time. Repeat the measurements in a different place where the building material is different and compare the results.

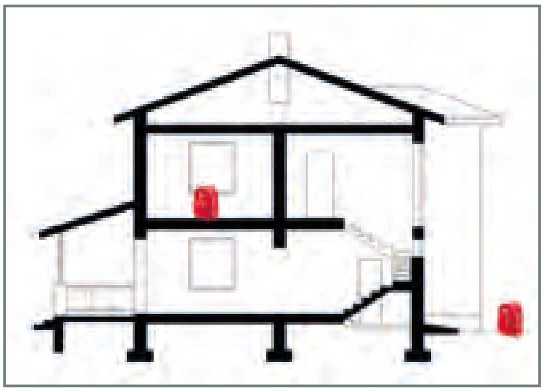

Experimental setup block diagram.

Results

The measurement results are compared to the reference values in the terrestrial crust. The discrepancy in the reference levels can be explained by the building material, distance from soil and more. This kind of measurement is important for the evaluation of natural radiation exposure from building materials [2013/59/ Euratom Directive and by UNSCEAR (United Nations Scientific Committee on the Effects of Atomic Radiation)].

	Isotopic Abundances		
	^{238}eU [ppm]	^{232}eTh [ppm]	^{40}K [%]
Reference Values Range	[2 ; 2.5]]	[8 ; 12]]	[2 ; 2.5]]
Tuff Dwelling (4° floor)	10 ± 1	31 ± 1	6.9 ± 0.2
Modern Building (1° floor)	2.8 ± 0.6	8.8 ± 1.1	1.6 ± 0.1
Country House (0° floor)	6.8 ± 0.9	17.6 ± 1.6	3.4 ± 0.2

Isotopic abundances evaluated in buildings located in different places and made with several construction materials

B.3.7 Mapping of potential radon-prone areas

SG6156E

Dedicated kit	
Description	pp.
SP5640 GammaEDU	183

Requirements

No other tools are needed.

Equipment

SP5640 - Backpack Detector

Model	SP5640
Description	Backpack Detector 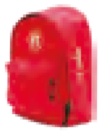

p. 183

Purpose of the experiment

The experiment topic is aimed to study and understanding the radioactive radon gas produced in uranium decays.

See the Application

COMING SOON

Fundamentals

It is now widely known that radon inhalation, in particular its progeny, significantly contributes to the public exposure. Radon is widely distributed in our living and working environment, soil and building materials contain meaningful tracks of its source and its exhalation rates must be determined in order to prevent human health. Radon concentration measurements, both in air and in gas from the soil are very important. The latest ones are used to realize geogenic maps. These maps link the gas to the geology and lithology of the area, allowing the development of more strict criteria for assessing the risk associated with the presence of radon. The radon monitoring is important also for another essential aspect: it is an indicator of the earth crust dynamics. In recent decades, many attempts to connect it to earthquakes prediction have been developed. Currently there is no confirmation about that, but, certainly, the correct radon measurement gives a valuable tool for taking information from the deeper Earth crust layers. As a noble gas, the radon produced by radium alpha decay is relatively free to move. All the rocks contain some empty interstices through which the gas can migrate. The features of gas production areas are function of temperature, pressure, mechanical stress, precipitation and chemical reactions. Only a fraction of the radon, called the "emanation coefficient", generated in soil leaves the solid grains and enters the pore volume of the soil.

The study of the natural radionuclides ^{232}Th, ^{40}K, ^{226}Ra, and the radon emanation coefficient exhalation rate is essential to estimate the actual risk for human health associated to a given natural material used for building construction. The natural radioactivity content of building materials depends on the local geology of each region on Earth. One of the requirements of estimate the radiation hazards in closed spaces, aiming to better protect against natural ionizing radiations exposure, is the assessment of the radiation hazards arising from the use of natural building materials in the construction of dwellings, since the majority of people in the World spend most time in indoor environments.

Carrying out the experiment

Power on the γstream inside the red backpack. Power on the tablet and associate the two devices via Bluetooth.

Take care that the γstream internal battery is charged, otherwise use the external power system.

Start the measurement campaign in land field and place the backpack on the floor almost 1m far from the trees, manhole or other construction. Set the acquisition time to about 5 minutes and see the results. If the statistic is not enough increasing the acquisition time.

It is good practice to repeat the measurement to obtain the mean and standard deviation of the result.

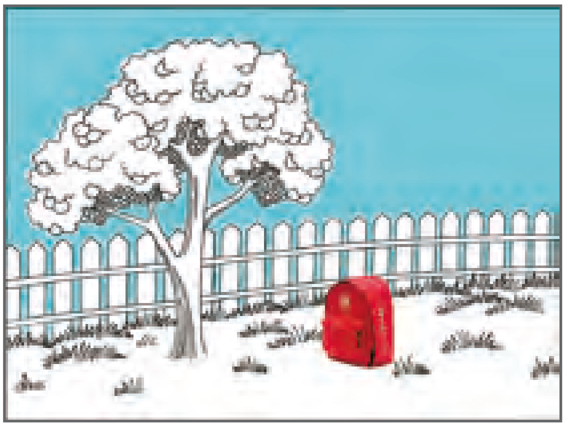

Experimental setup block diagram.

Results

The radon emanation has a big dependence on humidity variations, namely from the water content in the material. It is interesting to observe how this phenomenon affects the measurement of the Uranium concentration in the same place with different weather conditions.

COMING SOON

B.3.8 SG6157E Soil water content evaluation with gamma ray spectroscopy

Dedicated kit	
Description	pp.
SP5640 GammaEDU	183

Requirements

No other tools are needed.

Equipment

SP5640 - Backpack Detector

Model	SP5640
Description	Backpack Detector 

p. 183

Purpose of the experiment

The experiment topic is aimed at understanding how gamma-ray measurements can provide information about the water content of the soil.

See the Application

COMING SOON

Fundamentals

The global warming effects put in danger global water availability and make it necessary to decrease water wastage. A lot of researchers are focusing their attention on monitoring global irrigation due to global irrigation information is scarce due to the absence of a solid estimation technique. Recent studies show that proximal gamma-ray spectroscopy represents an innovative approach able to fill the spatial gap between punctual and satellite soil water content measurements.

A gamma-ray station measures the ^{40}K in the soil and monitors the moisture for the rational use of irrigation water. When it rains, the gamma signal is attenuated by the water and it drops down, while when the soil dries up, the gamma signal rises again.

Carrying out the experiment

Power on the γstream inside the red backpack. Power on the tablet and associate the two devices via Bluetooth. Take care that the γstream internal battery is charged, otherwise use the external power system.

Start the measurement campaign in the land field and place the backpack on the floor almost 1m far from the trees, manhole or other construction. Set the acquisition time to about 5 minutes and see the results. If the statistic is not enough to increase the acquisition time.

Repeat the measurements in the same place but in different weather conditions. Remember that it is good practice to repeat the measurement to obtain the mean and standard deviation of the result.

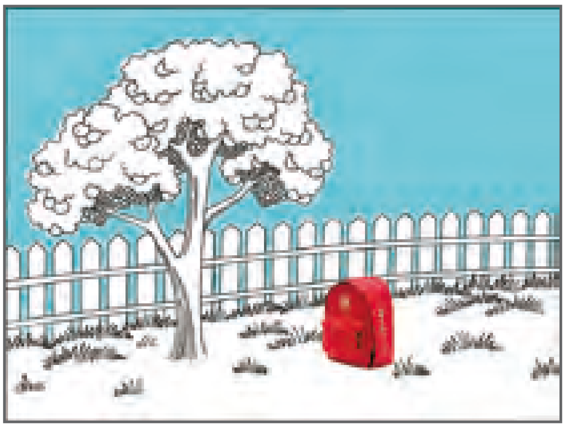

Experimental setup block diagram.

Results

This experiment represents a simple way to observe how Potassium 40 detection is affected by the water content in the soil.

COMING SOON

B.3.9 Geochimical and mineral exploration

SG6158E

Dedicated kit	
Description	pp.
SP5640 GammaEDU	183

Difficulty	Execution Time	Data Analysis	Radioactive Sources
		YES	NO

Requirements

No other tools are needed.

Equipment

SP5640 - Backpack Detector

Model	SP5640
Description	Backpack Detector 

p. 183

Purpose of the experiment

Large area survey to evaluate the radioactivity concentration of Uranium, Thorium, and Potassium.

See the Application

Fundamentals

A geochemical exploration campaign aims at locating economic mineral deposits through the recognition of concentrations of chemical components, to be called as geochemical anomaly, in surface materials such as rocks, soils, stream sediments, glacial till, water, plants, and air. The radiological characterization of surface soil, in terms of Uranium, Thorium and Potassium, proves to be also a good tool to direct excavations for mines. The main advantages of using in situ measurements are quick feedback, a large sample size, immediate repeatability of the measurement and low management costs. The areas with an enormous geodiversity have a considerable variety of stone materials that can be used both as building materials and as ornamental elements. This enormous variety also corresponds to considerable variability in the abundance of radionuclides. The world average radioactivity content in the upper continental crust is (33 ± 7) Bq/kg for ^{238}U, (43 ± 4) Bq/kg for ^{232}Th and (727 ± 60) Bq/

kg for ^{40}K. Igneous plutonic rocks are characterized by relatively high concentrations of natural radionuclides varying over a wide range of up to 2000 Bq/kg for ^{40}K, 600 Bq/kg for ^{238}U and 900 Bq/kg for ^{232}Th.

Carrying out the experiment

Power on the γstream inside the red backpack. Power on the tablet and associate the two devices via Bluetooth. Take care that the γstream internal battery is charged, otherwise use the external power system.

Start the measurement campaign in land field and place the backpack on the floor almost 1m far from the trees, manhole or other construction. Set the acquisition time to about 5 minutes and see the results. If the statistic is not enough increasing the acquisition time. Repeat the measurements along the survey area.

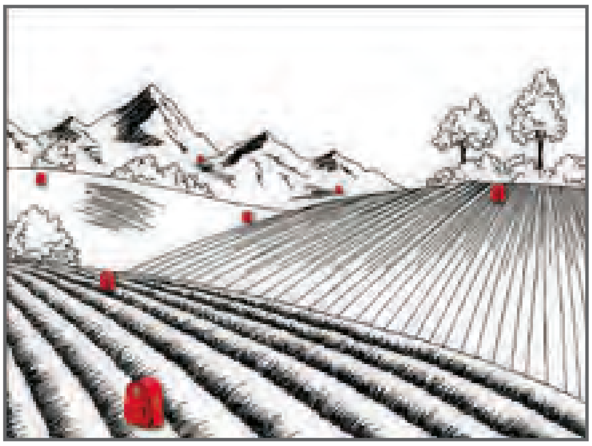

Experimental setup block diagram.

Results

Exemplary of in situ survey performed by using a portable NaI(Tl) scintillation detector for the determination of the radioactivity concentration of ^{40}K, ^{238}U and ^{232}Th on intrusive granite outcrops in Corsica-Sardinia (FR-IT) (*).

(*) Radiological characterization of granitoid outcrops and dimension stones of the Variscan Corsica-Sardinia Batholith, Puccini, A., Xhixha, G., Cuccuru, S., Oggiano, G., Xhixha, M. K., Mantovani, F., Alvarez, C. R., and Casini, L., Environmental Earth Sciences, 71, 393-405, (2014).

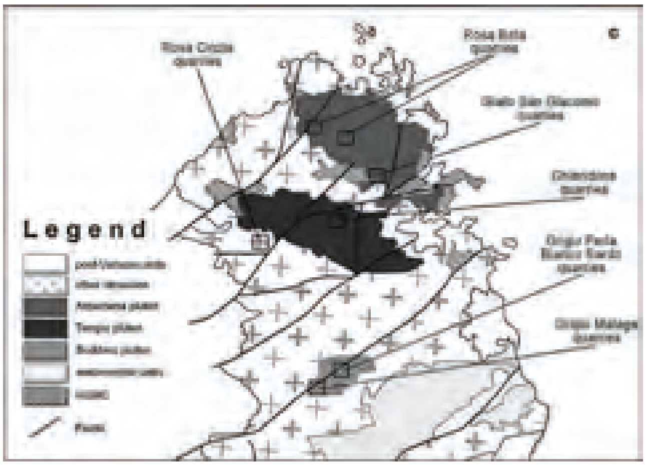

Position of extractive districts in Sardinia where in situ measurements were performed.

Granite Quarries	^{40}K [Bq/kg]	^{238}U [Bq/kg]	^{232}Th [Bq/kg]
Rosa Beta	1144 ± 120	42.3 ± 7.1	55.0 ± 6.3
Ghiandone	1092 ± 198	56.3 ± 12.7	68.9 ± 10.4
G. San Giacomo	1335 ± 206	50.1 ± 13.8	61.9 ±9.4
Rosa Cinzia	1313 ± 64	56.0 ± 6.8	69.4 ± 3.4
Grigio Malaga	848 ± 121	34.5 ± 4.6	61.1 ± 5.5
Grigio Perla	1222 ± 155	39.1 ±5.2	60.6 ±5.7
Bianco Sardo	1269 ±64	44.8 ±7.1	51.6 ±8.8

Activity concentration of ^{40}K, ^{238}U and ^{232}Th in situ measurements.

B. Nuclear Physics and Radioactivity

B.4 β Spectroscopy

After radioactivity discovery, E. Rutherford separated radioactive emissions into two types: alpha (α) and beta (β-) radiations, based on matter penetration and ability to cause ionization. The β-particles have higher penetration and lower specific ionization than alpha particles. Beta particles are electrons (β-) or positrons (β+), resulting by nucleon decays in unstable nuclei. Since beta decay is a three body process, the β energy spectrum is continuum.

CAEN offers β spectroscopy experiments that can be conducted using the "Educational Beta Kit" or, alternatively, the "Premium Kit."

Recommended kits

A SP5600D
Educational kits

see p. 182, 179

B SP5600AN
Educational kits
PREMIUM

see p. 179

Experiment	SP5600D ★	SP5600AN ★
B.4.1 Response of a Plastic Scintillating Tile	•	•
B.4.2 β Spectroscopy	•	•
B.4.3 β-Radiation: Transmission through Matter	•	•
B.4.4 β-Radiation as a Method to Measure Paper Sheet Grammage and Thin Layer Thickness	•	•
B.4.5 Coating effect on the Light Collection	•	•

★ The star indicates the recommended Kits while the yellow color highlights the Kits especially dedicated to the experiences of this Section. If you are also interested in other experiences, the PREMIUM Kit is recommended.

B.4.1 Response of a Plastic Scintillating Tile

SG6121

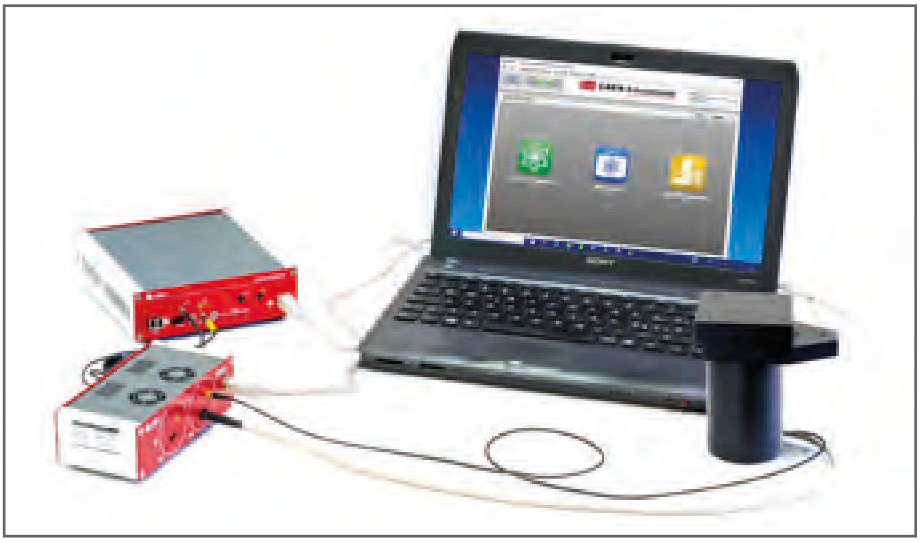

Dedicated kit	
Description	**pp.**
SP5600D Educational Beta Kit	182 179

Difficulty	Execution Time	Data Analysis	Radioactive Sources
		NO	YES

Requirements

Beta Radioactive Source

Equipment

SP5600D – Educational Beta Kit

Model	SP5600	DT5720A	SP5608
Description	Power Supply and Amplification Unit 	Desktop Digitizer 250 MS/s 	Scintillating tile 
	p. 190	p. 190	p. 193

Purpose of the experiment

To get acquainted with a set-up based on a plastic scintillator tile coupled to a Silicon Photo-multiplier.

See the Application

Fundamentals

Particle detectors based on scintillating material coupled to a photosensor are in common use in nuclear and particle physics, medical, industrial and environmental applications. The choice of the scintillator is dependent on the end-user specifications but for a large set of applications plastic scintillators represent a cost effective viable solution. The CAEN kit comprises a plastic scintillator tile of 5 x 5 x 1 cm^3 volume, directly coupled to a 6 x 6 mm^2 SiPM. The sensitive area is a trade off between the requests for some of applications (e.g. cosmic ray detection or inspection of thin layers or filters) and the homogeneity of the response of the system.

Before addressing a variety of lab applications, the student is guided through the basics of the system.

Carrying out the experiment

Connect the power and the MCX cables of the SP5608 tile to one channel of the SP5600. Connect the two channel outputs to DT5720A: the analog output to the channel 0 and the digital output to "trigger IN" of the digitizer. Use the GUI to optimize the system parameters (bias, gain, discriminator threshold). Once this is done, switch off the power supply, open the SP5608 top cover and position the beta source on the scintillating tile in the center. Close the support top, switch ON the power supply and measure the counting rate. Repeat the measurement moving the source in several positions over the tile and acquiring the signal/background ratio.

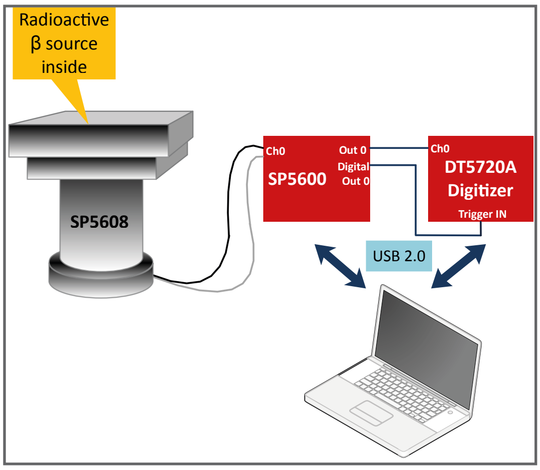

Experimental setup block diagram.

Results

In response to the incoming beta particles, the system is designed to deliver a high signal. However, the student shall consider the optimal setting of the discriminator threshold, taking into account the dark count rate, the variation in the beta source counts, the signal to noise ratio and the quality of the recorded beta spectrum. Moreover, for the optimal setting it is significant to monitor the homogeneity of the response as the source is moved across the tile.

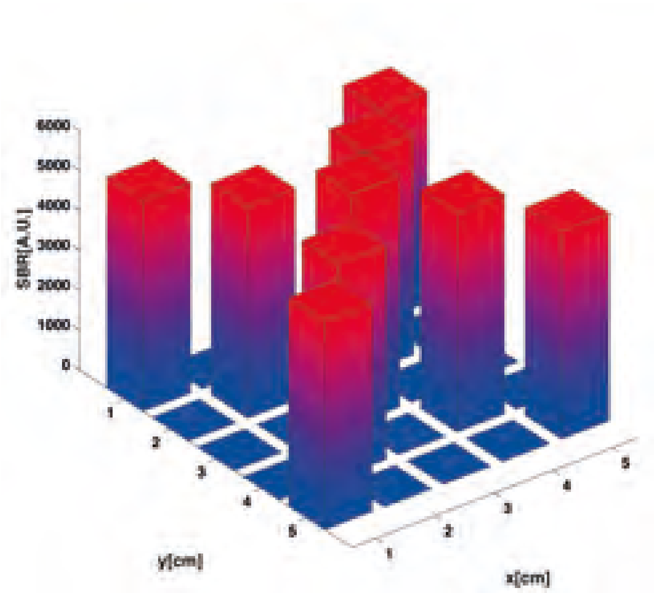

Homogeneity of tile response to a beta source.

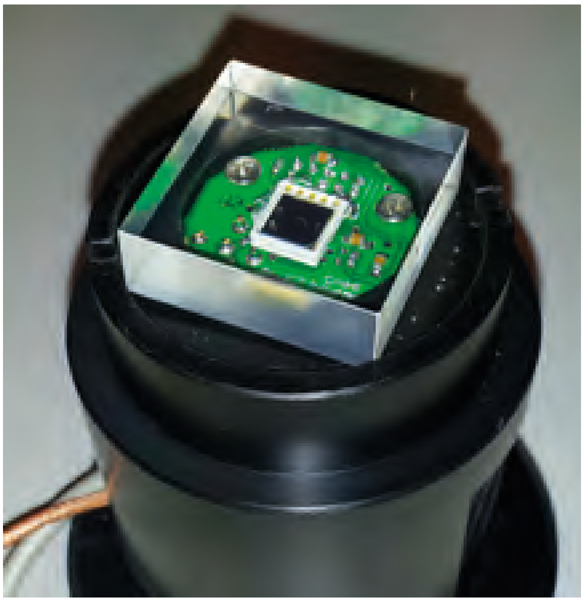

Scintillating tile coupled to a sensor.

This experiment is also possible with the following kits

B **SP5600AN**
Educational kits
PREMIUM

see p. 179

B.4.2 β Spectroscopy

SG6122A

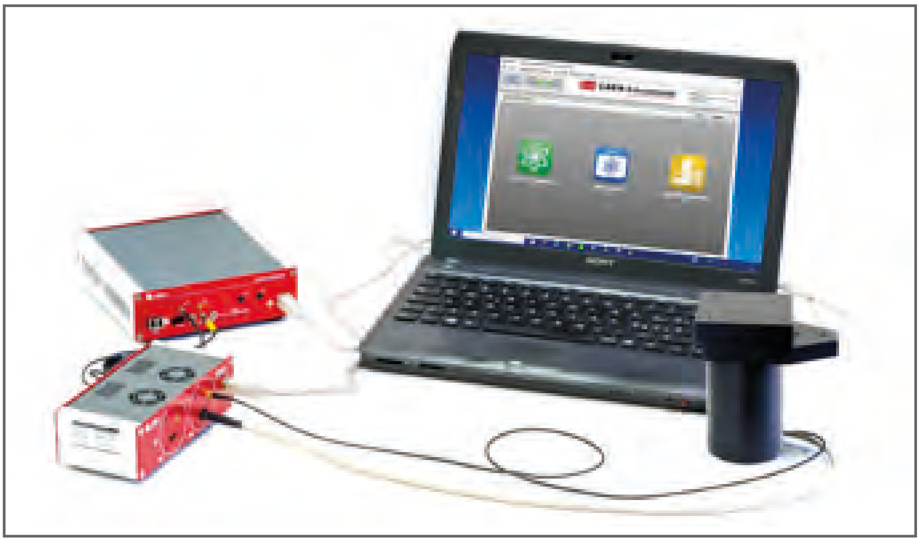

Dedicated kit	
Description	**pp.**
SP5600D Educational Beta Kit	182 179

Difficulty	Execution Time	Data Analysis	Radioactive Sources
1/5	1/5	NO	YES

Requirements

Beta Radioactive Source

Equipment

SP5600D – Educational Beta Kit

Model	SP5600	DT5720A	SP5608
Description	Power Supply and Amplification Unit 	Desktop Digitizer 250 MS/s 	Scintillating tile 
	p. 190	p. 190	p. 193

Purpose of the experiment

After gamma spectrometry, the student is introduced to the measurement and interpretation of β spectra, using a plastic scintillator tile.

See the Application

Fundamentals

There are three different beta decays:

β⁻ decay (electron emission): $n \rightarrow p+ \;\; e^- + \nu_e$

β+ decay (positron emission): $p \rightarrow n + e+ + \nu_e$

Electron capture (EC): $p + e^- \rightarrow n + \nu_e$

Where p identifies the proton, n the neutron and ν the weakly interacting neutrino. Because of the three body kinematics and the energy associated to the neutrino, the β spectrum is continuum up to a maximum energy depending on the isotope under study (and the neutrino mass)

Carrying out the experiment

Connect the power and the MCX cables of the SP5608 tile to one channel of the SP5600. Connect the two channel outputs to DT5720A: the analog output to the channel 0 and the digital output to “trigger IN“ of the digitizer. Use the default software values or optimize the parameters to evaluate the contribution not coming from the beta source and choose the discrimination threshold in mV. After that, switch off the power supply, open the SP5608 top and place the beta source on the scintillating tile. close the support top, switch ON the power supply and acquire the beta spectrum.

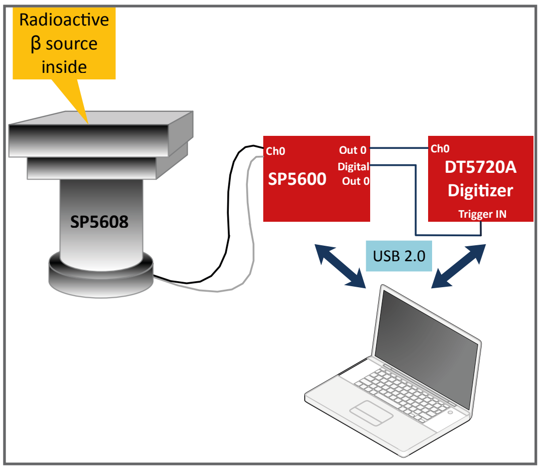

Experimental setup block diagram.

Results

Measurement and interpretation of β spectra introduce the student into the field of special relativity and weak interactions of radioactive decays. Observation of the beta spectrum is very important to understand the theory of beta decay. Historically, experimental beta-ray spectra introduced enormous problems in the interpretation of beta decay due to the ostensible violation of the energy conservation. The introduction of neutrinos explaining the continuous beta-ray spectra solved not the problem conservation of energy, momentum and lepton number.

As first approach to beta spectroscopy, it is interesting to determine the maximum energy available in the decay process and to verify that the most probable energy value Eavg can be expressed as:

$$E_{avg} \cong 1/3 * E_{max}$$

By using several β-sources, different energy values E_{avg} can be estimated, each one corresponds to the total energy released in the specified β decay.

An example of ^{90}Sr spectrum is shown in the figure. For a most complete analysis on beta spectrum, other application notes are recommended.

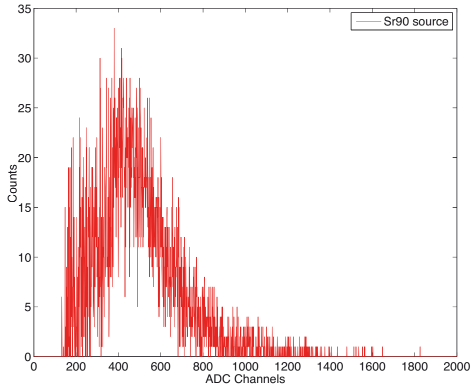

Experimental beta spectrum of ^{90}Sr radioactive source.

This experiment is also possible with the following kits

B **SP5600AN**
Educational kits
PREMIUM

see p. 179

B.4.3 β Radiation: Transmission through Matter

SG6123A

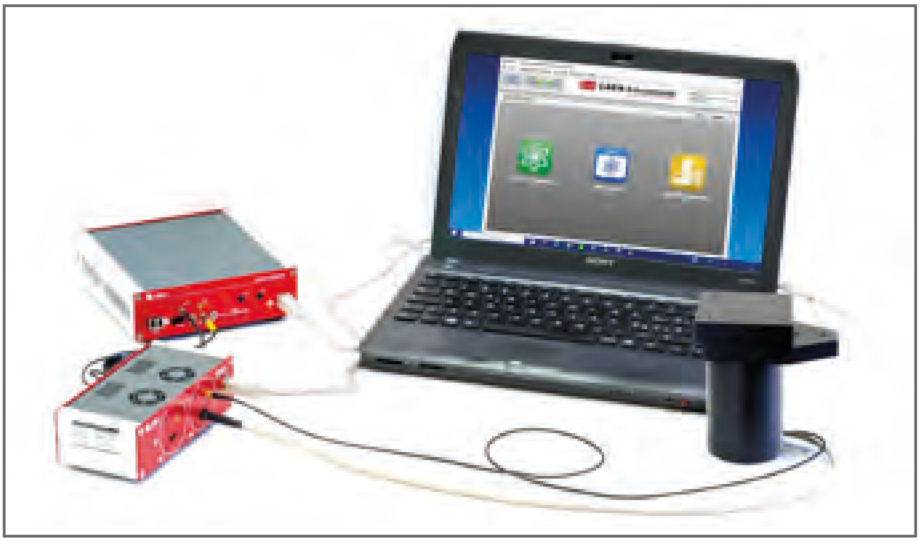

Dedicated kit	
Description	**pp.**
SP5600D Educational Beta Kit	182 179

Difficulty	Execution Time	Data Analysis	Radioactive Sources
1/5	1/5	NO	YES

Requirements

Beta Radioactive Source

Equipment

SP5600D – Educational Beta Kit

Model	SP5600	DT5720A	SP5608
Description	Power Supply and Amplification Unit 	Desktop Digitizer 250 MS/s 	Scintillating tile 
	p. 190	p. 190	p. 193

Purpose of the experiment

Attenuation measurement of the intensity of β radioactive source as a function of the absorber thickness by using two absorber materials: aluminium and paper sheets.

See the Application

Fundamentals

β-particle is a charged particle that interacts with matter in several ways depending on its initial energy: ionization process, Bremsstrahlung process, Cherenkov and Transition radiation. When β-radiation crosses a matter thickness, it releases completely or part of its energy due to collisions with absorber atoms; this phenomenon depends on the initial β-energy and on the crossed material density. Beta particles are less massive than alpha particles and only carry a charge of 1e; consequently, beta particles can appreciably penetrate many potential shielding materials although their penetrating capacity is considerably lower compared with γ-rays. These different radiation behaviours are essential for those attempting to shield locations from gamma radiation, either for sensitive experiments or for the safety of humans.

The transmission of beta particles is frequently calculated in the same fashion as that of gamma rays, where the mass attenuation coefficient is defined by the slope of the exponential function. Due to the fact that the β-particles with lower energies are less penetrating hence they are completely absorbed at smaller values of thickness, the initial decrease of the absorption curve is too rapid to be fit by exponential function. This approximation is verified only in a particular region of the transmission curve: a minimal absorber thickness so that the beta counting are very well separated from the "background level".

Carrying out the experiment

Insert the beta source support in the SP5608 and connect power and MCX cables to one channel of the SP5600. Connect the two channel outputs to DT5720A: the analog output to the channel 0 and the digital output to "trigger IN" of the digitizer. Use the default software values or optimize the parameters to evaluate the contribution not coming from the beta source and choose the discrimination threshold in mV. After that, switch off the power supply, open the SP5608 top and place the beta source on the plastic support and close the support top. Switch ON the power supply and measure the counting rate. Repeat the measurement by adding layers of the same absorber and later change the absorber type.

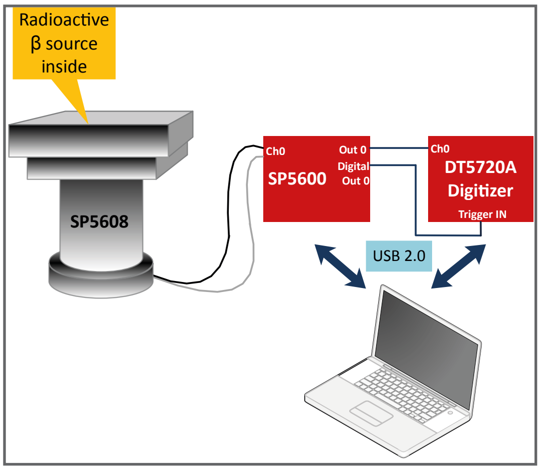

Experimental setup block diagram.

Results

By using different absorber thicknesses, the near-exponential decreasing of β-radiation intensity I as a function of the absorber thickness x, is verified. This behaviour does not have a fundamental basis like gamma rays attenuation, but it is very well described by

$$I = I_0 * e^{-nx}$$

where n is the absorption coefficient. This coefficient correlates the endpoint energy of beta source for a particular absorbing material. From absorption curves of beta particles , the absorption coefficients and ranges of β particles in aluminium and in paper sheets can be determined.

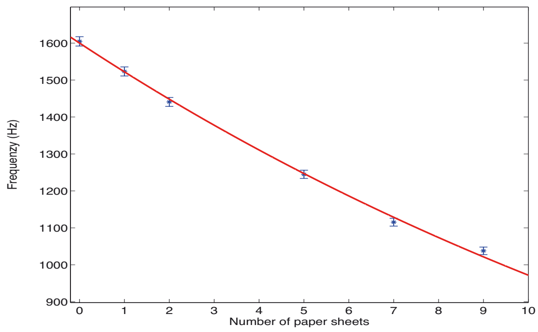

Exponential behaviour of the transmitted counting rate of Sr90 source with respect to number of paper sheets.

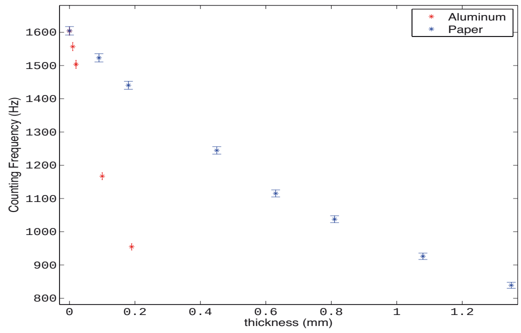

Behaviour of the transmitted counting rate of Sr90 source as a function of different absorbing materials.

This experiment is also possible with the following kits

B SP5600AN
Educational kits
PREMIUM

see p. 179

B.4.4 SG6124A β Radiation as a Method to Measure Paper Sheet Grammage and Thin Layer Thickness

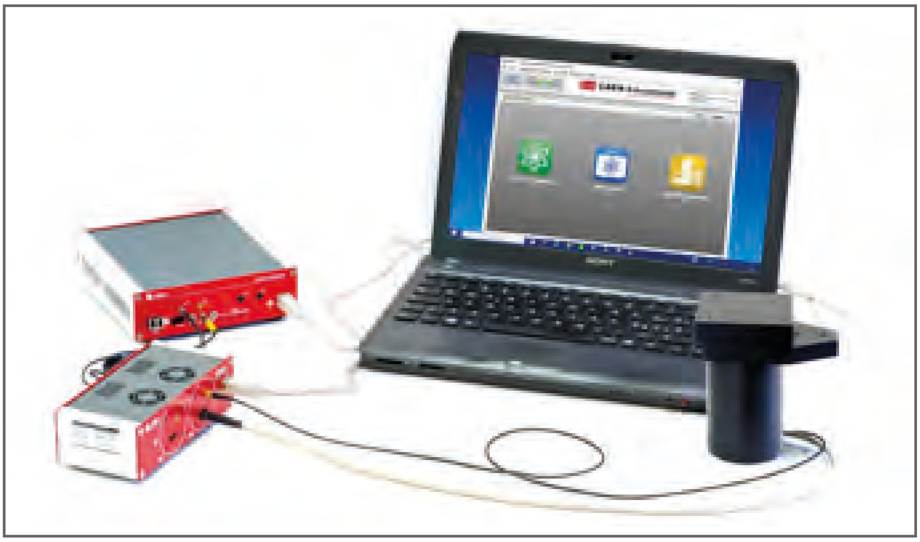

Dedicated kit	
Description	pp.
SP5600D Educational Beta Kit	182 179

Difficulty	Execution Time	Data Analysis	Radioactive Sources
		NO	YES

Requirements

Beta Radioactive Source

Equipment

SP5600D – Educational Beta Kit

Model	SP5600	DT5720A	SP5608
Description	Power Supply and Amplification Unit 	Desktop Digitizer 250 MS/s 	Scintillating tile 
	p. 190	p. 190	p. 193

Purpose of the experiment

Estimate of the instrument sensitivity in the measurement of thin layer thickness by beta particle attenuation.

See the Application

Fundamentals

Beta attenuation represents a golden standard in the quality control of paper industry and in the measurement of thin layer thickness. The latter has several applications, including the concentration of fine particulate matter deposited on a filter. The use of high activity sources with relatively soft spectrum and highly efficient detectors guarantees that this technique, used since the 50's, is yet today a standard.

Carrying out the experiment

Insert the beta source support in the SP5608 and connect power and MCX cables to one channel of the SP5600. Connect the two channel outputs to DT5720A: the analog output to the channel 0 and the digital output to "trigger IN" of the digitizer. Use the default software values or optimize the parameters to evaluate the contribution not coming from the beta source and choose the discrimination threshold in mV. After that, switch off the power supply, open the SP5608 top and place the beta source on the plastic support and close the support top. Switch ON the power supply and measure the counting rate. Repeat the measurement by adding paper sheets.

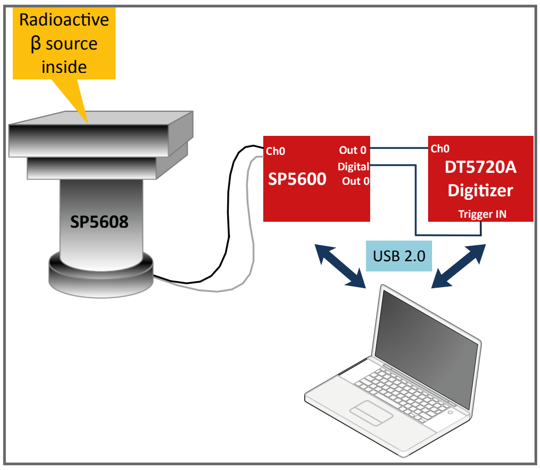

Experimental setup block diagram.

Results

The industrial results are provided by using high activity β source (1 GBq). This experiment allows to estimate the instrument sensibility and the time needed to obtain a certain percentage of sensibility through the attenuation curve of a β source with "student compliant" activity. The results are very surprising: 3σ of confidence level to distinguish one or two post-it in 250 ms and 25 seconds to reach sensibility 10%.

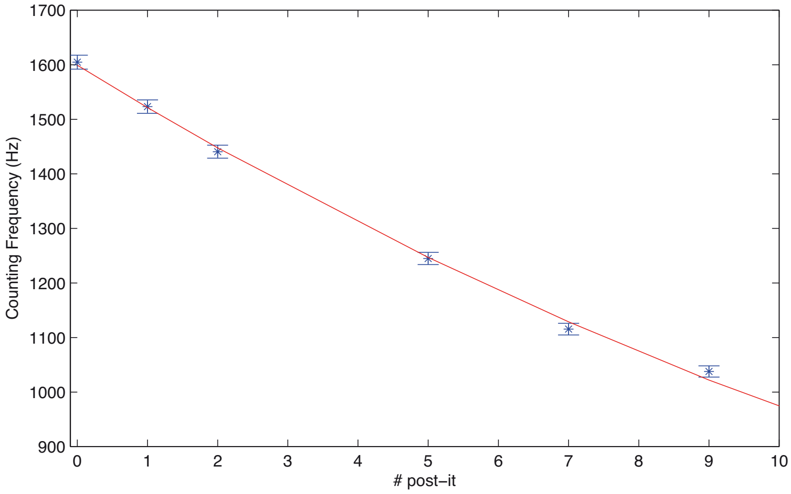

Counting frequency of the beta rays as a function of the number of crossed paper sheets.

This experiment is also possible with the following kits

B **SP5600AN**
Educational kits
PREMIUM

see
p. 179

B.4.5 Coating effect on the Light Collection

SG6125A

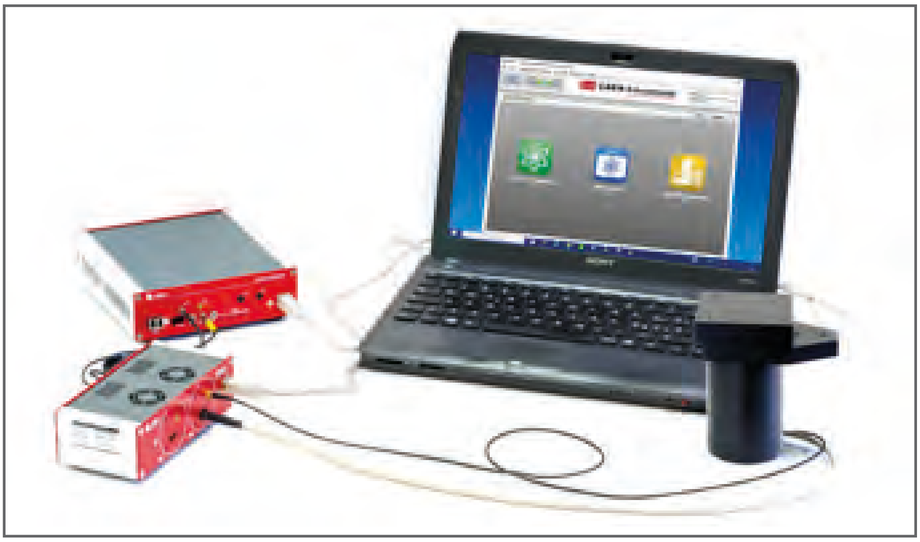

Dedicated kit	
Description	**pp.**
SP5600D Beta Kit	182 179

Difficulty	Execution Time	Data Analysis	Radioactive Sources
2/5	2/5	NO	YES

Requirements

Beta Radioactive Source

Equipment

SP5600D – Educational Beta Kit

Model	SP5600	DT5720A	SP5608
Description	Power Supply and Amplification Unit	Desktop Digitizer 250 MS/s	Scintillating tile
			
	p. 190	p. 190	p. 193

Purpose of the experiment

This experiment investigates the impact of a reflective coating on the light collection efficiency in a plastic scintillating tile.

See the Application

Fundamentals

Scintillating materials are commonly used in high energy physics and medical applications because of their capability to convert high energy radiation into optical photons and they are usually coupled with a photosensor. Scintillator has a key tole in the detection chains and it is often mandatory to extract and detect the generated scintillation light as efficiently as possible. The amount of light generated during the scintillation process is, in standard configurations, only a small percentage of this light reaches the photodetector. Extracting as much light as possible from the crystal becomes this crucial, given that both energy and time resolution depend strongly on the amount of detected light. Indeed, extracting more light enables a more accurate estimation of the energy absorption in the scintillator itself, and, moreover, if not covered by any material, the scintillator can let light escape through its lateral surfaces, thus losing a significant number of optical photons.

Carrying out the experiment

Connect the power and the MCX cables of the SP5608 tile to one channel of the SP5600. Connect the two channel outputs to DT5720A: the analog output to channel 0 and the digital output to "trigger IN" of the digitizer. Use the default software values or optimize the parameters to evaluate the contribution not coming from the beta source and choose the discrimination threshold in mV. After that, switch off the power supply, open the SP5608 top and place the beta source on the scintillating tile. Close the support top, switch ON the power supply and acquire the beta spectrum. Repeat the spectrum acquisition after having uniformly covered the scintillator with the Teflon tape leaving only a window open for the optical coupling with the SiPM.

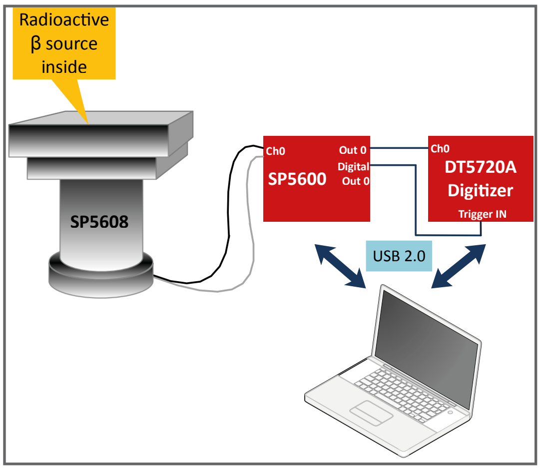

Experimental setup block diagram.

Results

The presence of a white coating allows the user to observe the improvement of the light collection via the acquisition of ^{90}Sr spectrum.

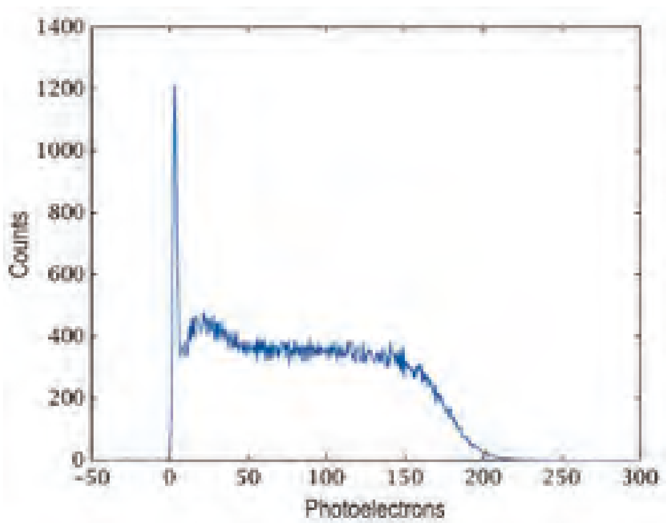

^{90}Sr spectrum acquired just by using optical grease as coupling between scintillator and SiPM.

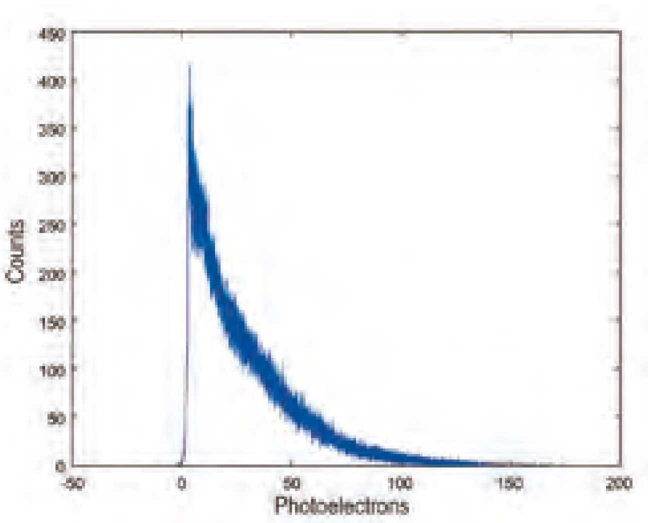

^{90}Sr spectrum acquired by using Teflon coating and Optical interface sheet between scintillator and SiPM.

This experiment is also possible with the following kits

B **SP5600AN**
Educational kits
PREMIUM

see p. 179

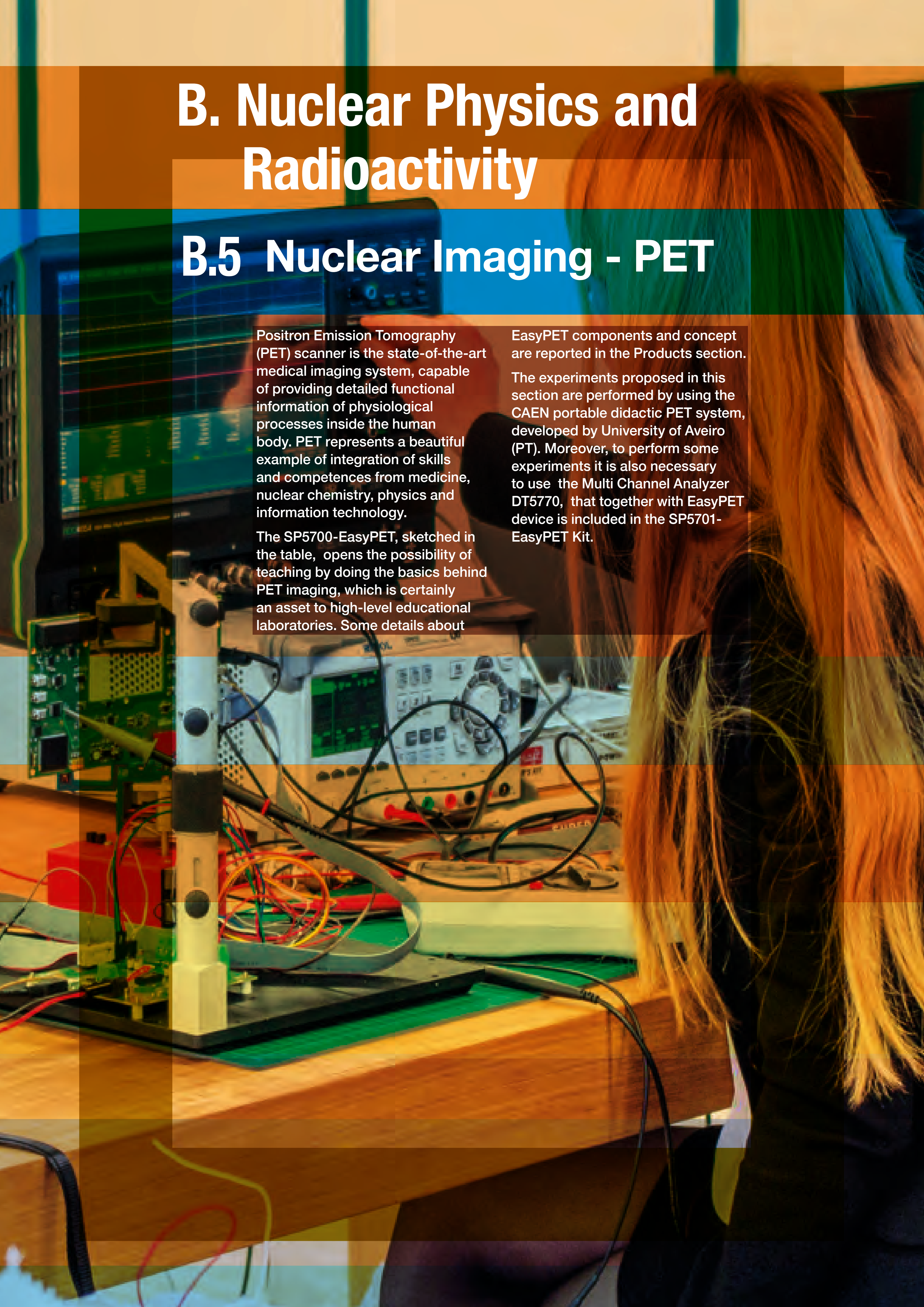

B. Nuclear Physics and Radioactivity

B.5 Nuclear Imaging - PET

Positron Emission Tomography (PET) scanner is the state-of-the-art medical imaging system, capable of providing detailed functional information of physiological processes inside the human body. PET represents a beautiful example of integration of skills and competences from medicine, nuclear chemistry, physics and information technology.

The SP5700-EasyPET, sketched in the table, opens the possibility of teaching by doing the basics behind PET imaging, which is certainly an asset to high-level educational laboratories. Some details about EasyPET components and concept are reported in the Products section.

The experiments proposed in this section are performed by using the CAEN portable didactic PET system, developed by University of Aveiro (PT). Moreover, to perform some experiments it is also necessary to use the Multi Channel Analyzer DT5770, that together with EasyPET device is included in the SP5701-EasyPET Kit.

Recommended kits

G SP5700
EasyPET

see pp. 178, 195

G SP5701
EasyPET kit

see p. 178

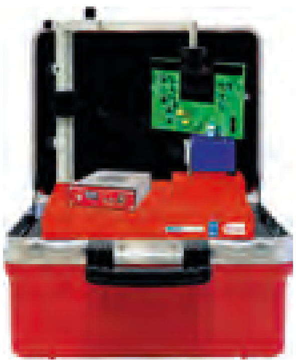

Experiment	★ SP5701	★ SP5700
B.5.1 Basic Measurements: γ Spectroscopy and System Linearity	•	
B.5.2 Positron Annihilation Detection	•	•
B.5.3 Two-dimensional Reconstruction of a Radioactive Source	•	•
B.5.4 Spatial Resolution	•	•

★ The star indicates the recommended Kits while the yellow color highlights the Kits especially dedicated to the experiences of this Section.

B.5.1 SG6131G Basic Measurements: γ Spectroscopy and System Linearity

Difficulty	Execution Time	Data Analysis	Radioactive Sources
		NO	YES

Dedicated kit	
Description	pp.
SP5701 EasyPET kit	178

Requirements

^{22}Na Radioactive source
(recommended: 1/2 inch disc, 10 μCi)

Equipment

SP5701 - EasyPET Kit

Model	SP5700	DT5770
Description	EasyPET 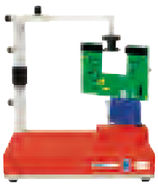 p. 178	Desktop Multi-Channel Analyzer  p. 194

Purpose of the experiment

Gamma spectroscopy studies by using a gamma radioactive sources and by analysing the signals produced by the interaction of the gamma with one of the scintillating crystals of the system.

See the Application

Fundamentals

The EasyPET detector system is composed of two Silicon Photomultipliers (SiPM) coupled to scintillating crystals. The EasyPET operation principle is simple: the two small detector cells, each composed of a small scintillator crystal coupled to a silicon photomultiplier (SiPM), develop a signal when they detect a photon emitted by the source. In order to perform the gamma spectroscopy measurements using one of the two detector systems, it is important underline that the detector is characterized by a noise component, caused by spurious events occurring randomly and independently from the illumination field. This noise, called Dark Count Rate (DCR), depends mainly on the sensor technology and on the operating temperature, with a rate from 100kHz up to several MHz per mm^2 at 25 °C. The DCR decreases with the lowering of the temperature (about a factor 2 of DCR reduction every 8 °C). In addition, the operating voltage has an impact on the DCR since it's connected to the electric field and as a consequence to the active volume of the sensor and to the triggering probability of the charge carrier. This noise component affects the resolution of a generic gamma spectrum composed of system noise peak, Compton distribution and Photo-peak.

Carrying out the experiment

Mount the arm of the source holder on the column fixed to the system base, fix the U-shaped board to the top stepper motor and connect the flat cable to the U-shaped board and to the control unit. Connect to PC and power ON the system. Choose one detection system and connect its analog output to channel input of the DT5770, then use the comparator output to trigger the MCA and choose the threshold in mV of the signal output. Place the radioactive source as close as possible to the detector chosen and acquire the energy spectrum thanks to a Multi Channel Analyzer. Repeat the measurements with several gamma radioactive source in order to study the linearity system.

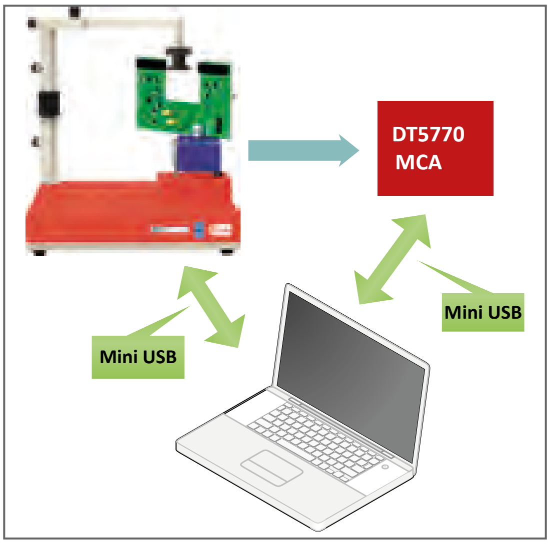

Experimental setup block diagram.

Results

The γ spectrum shows the Compton continuum, related to the continuum of energies released by the Compton scattered electrons, and the Photo-Peak, the full-energy peak corresponding to the photoelectric absorption of the incident gamma. The peak around zero represents the system noise. The conversion between the channels number and the energy can be performed by a calibration. The system linearity is checked by using several radioactive sources. If the response of the system is linear, the output signals are directly proportional to the incident gamma energies.

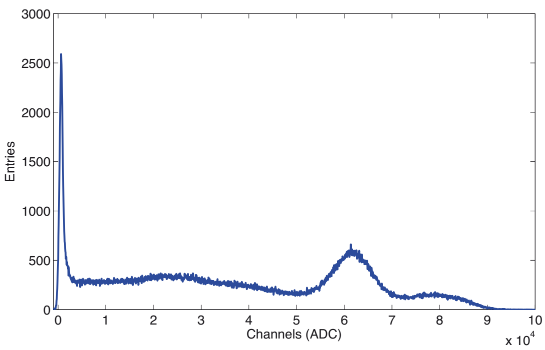

Energy spectrum of ^{22}Na source.

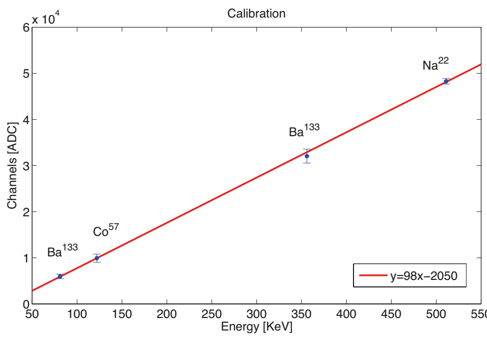

Energy Calibration.

B.5.2 Positron Annihilation Detection

SG6132G

Difficulty	Execution Time	Data Analysis	Radioactive Sources
		NO	YES

Dedicated kit	
Description	pp.
SP5701 EasyPET kit	178

Requirements

^{22}Na Radioactive source
(recommended: 1/2 inch disc, 10 µCi)

Equipment

SP5701 - EasyPET Kit

Model	SP5700	DT5770
Description	EasyPET 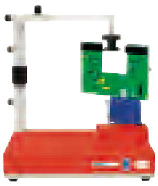 p. 178	Desktop Multi-Channel Analyzer  p. 194

Purpose of the experiment

Positron annihilation detection by using a couple of detectors composed of a LYSO scintillating crystal coupled to a Silicon Photomultiplier (SiPM).

See the Application

Fundamentals

The underlying principle to PET systems is the detection of high energy radiation emitted from a chemical marker, a molecule labelled with a radioisotope, administered to a patient. The marker is properly chosen in order to associate to molecules involved in biochemical or metabolic processes under investigation. This allows studying the function of a particular organ or evaluating the presence of disease, revealed by the excessive concentration of the marker in specific locations of the body. The radioisotope emits positrons which, after annihilating with atomic electrons, result in the isotropic emission of two photons back to back with an energy of 511 keV. The two photons are detected by a ring of detectors, which allows a pair of them to detect two back to back photons in any direction. EasyPET comprehends only two detector modules that move together and execute two types of independent movements, around two rotation axes, so as to cover a field of view similar to that of a complete ring of detectors. A fast electronic readout system allows detecting coincident events resulting from the same decay process.

Carrying out the experiment

Mount the arm of the source holder on the column fixed on the system base, fix the U–shaped board to the top stepper motor and connect the flat cable to the U-shaped board and to control unit. Connect to PC and power ON the system. Connect the analog output of one detector to channel input of the DT5770 and use as MCA “trigger IN” the coincidence output characterized by the occurring of the comparator output of each detector within a time window. Place the source holder between the two detectors and measure the DCR frequency as a function of the threshold. Place the ^{22}Na radioactive source in the holder and repeat the measurement. Chose a threshold and acquire the coincidence spectrum thanks to a Multi Channel Analyzer.

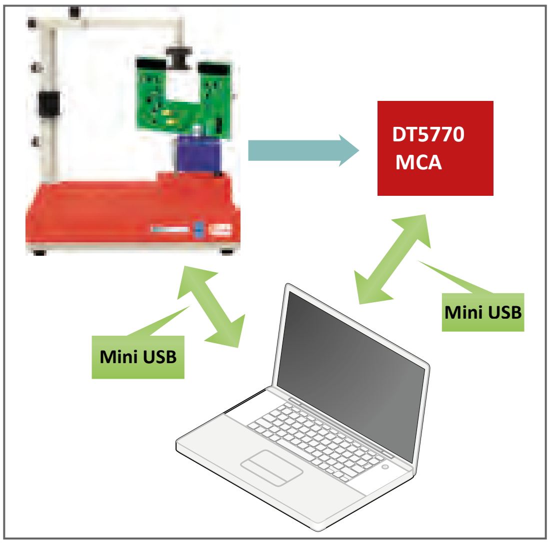

Experimental setup block diagram.

Results

The coincidence detection allows to reduce significantly the system noise due to the SiPM DCR. In the optimization of the acquisition conditions, the coincidence detection introduces the parameter of the time window width in addition to the bias voltage and the threshold. In order to find the best parameter values is necessary to analyse the response of the system in coincidence mode to the radioactive source with respect to the random events, at fixed operating voltage. The simple geometry of the system with only two opposite and aligned detectors and the implementation of the coincidence detection ensures that, in the energy distribution, the Compton scattering occurring in one or even in both scintillating crystals comes from the same annihilation event.

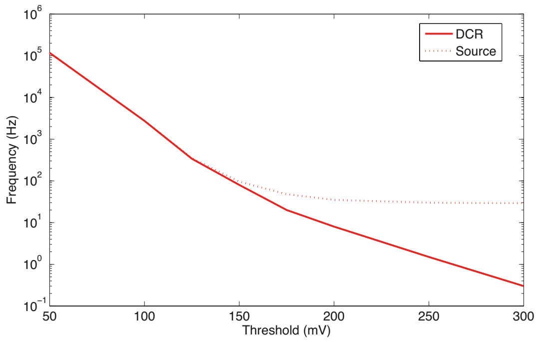

Coincidence frequency, with and without ^{22}Na source, as a function of the threshold.

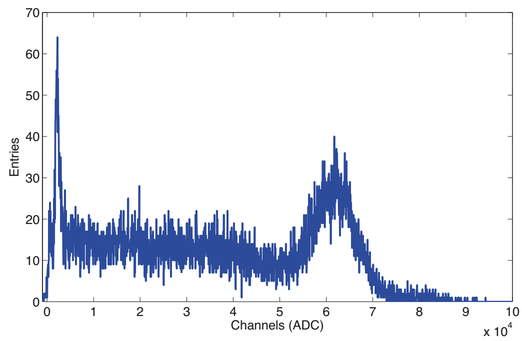

Coincidence spectrum of ^{22}Na radioactive source.

This experiment is also possible with the following kits

B **SP5700**
EasyPET

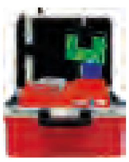

see pp. 178, 195

B.5.3 Two-dimensional Reconstruction of a Radioactive Source

SG6133G

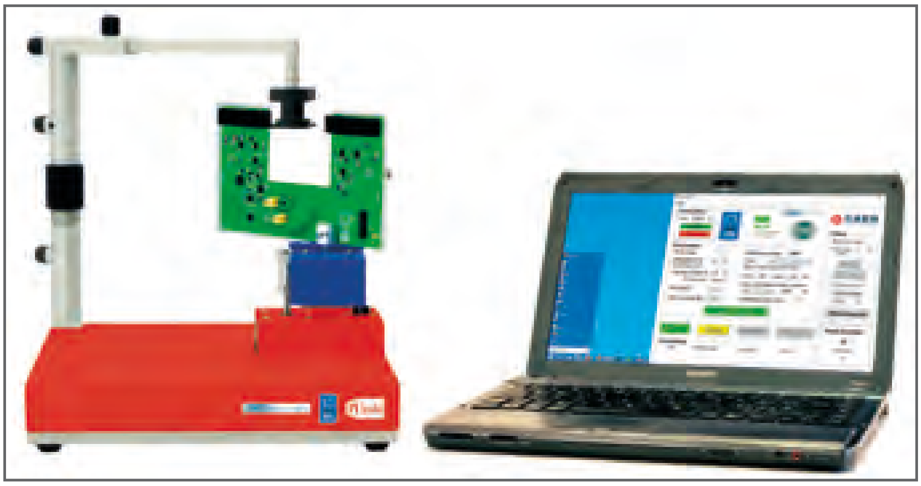

Dedicated kit	
Description	pp.
SP5700 EasyPET	178

Difficulty	Execution Time	Data Analysis	Radioactive Sources
		NO	YES

Requirements

^{22}Na Radioactive source
(recommended: 1/2 inch disc, 10 μCi)

Equipment

SP5700 - EasyPET

Model	SP5700
Description	EasyPET 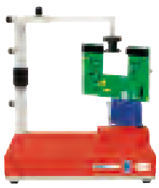 p. 178

Purpose of the experiment

Understanding the technique of the nuclear imaging and the setup optimization of the parameters by performing two-dimensional image reconstruction of ^{22}Na radioactive source.

See the Application

Fundamentals

The EasyPET operation principle is simple: two detector modules move together and execute two types of independent movements, around two rotation axes, so as to cover a field of view similar to that of a complete ring of detectors.

The rotation movements are executed by two stepper motors. The bottom motor has a fixed axis, whose position defines the center of the field of view. The bottom motor supports and performs a complete rotation of a second motor, in predefined steps of amplitude α. The axis of the top motor is thus always positioned within a circumference of radius equal to the distance between the two axes. The top motor, in its turn, supports and moves a U-shaped printed circuit board, where a pair of aligned and collinear detector modules is mounted, performing a symmetric scan of range θ around the center, for each position of the bottom motor. In this way, EasyPET can reconstruct an image of a radioactive source placed anywhere within a cylindrical field of view between the pair of detectors. The diameter of the field of view is defined by the amplitude of θ, the range of the top motor scan.

Carrying out the experiment

Mount the arm of the source holder on the column fixed on the system base, fix the U–shaped board to the top stepper motor and connect the flat cable to the U-shaped board and to control unit. Connect to PC and power ON the system. The parameters involved in the setup optimization for the two-dimensional reconstruction of the source image are three: the detectors operating voltage, the coincidence time window and the threshold. Place the source holder between the two detector modules and tune the parameters to estimate the DCR contribution.

Place the ^{22}Na radioactive source in the holder and repeat the measurement tuning the parameters in order to obtain a good image reconstruction of the radioactive source.

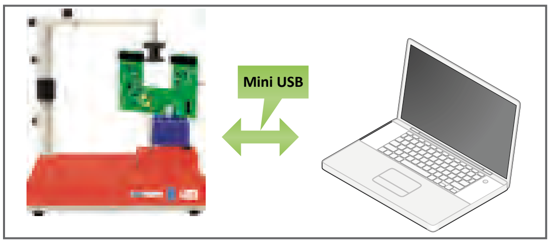

Experimental setup block diagram.

Results

Tuning the parameters, the students can directly observe and understand their effects on the imaging measurements. At fixed threshold, the image contrast changes due to the time window width. The use of the lowest possible coincidence time window of the system is mandatory to achieve a good image contrast. Fixing the bias voltage and the time window, it is interesting to observe how the threshold affects the image contrast. This parameter choice is dictated by a trade off between the signal to noise ratio and efficiency maximization. The threshold value and the coincidence time window should be set by choosing the best compromise.

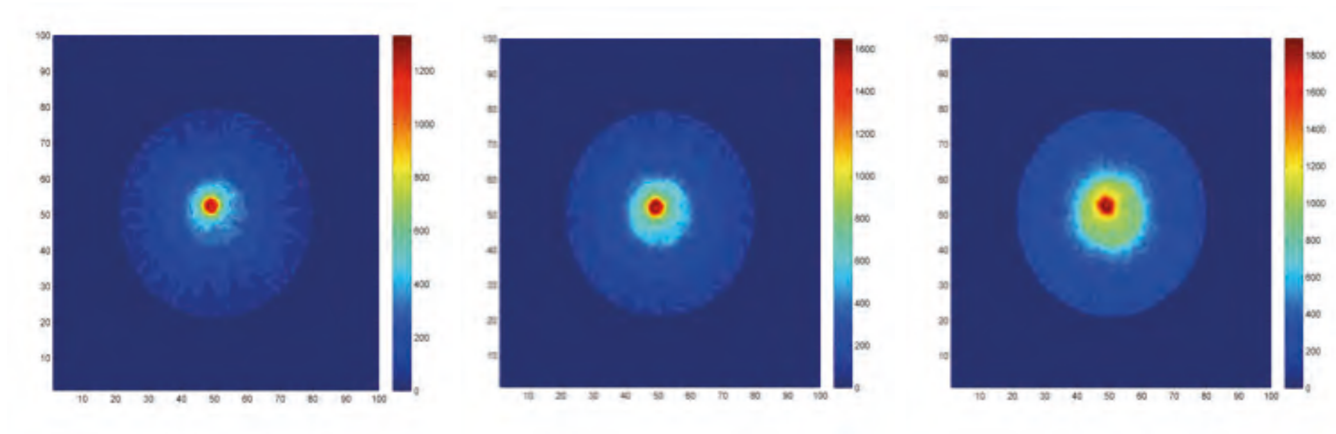

^{22}Na source distribution image as a function of coincidence time window , at fixed threshold and bias voltage.

This experiment is also possible with the following kits

B **SP5701**
EasyPET Kit

see pp. 178

B.5.4 Spatial Resolution

SG6134G

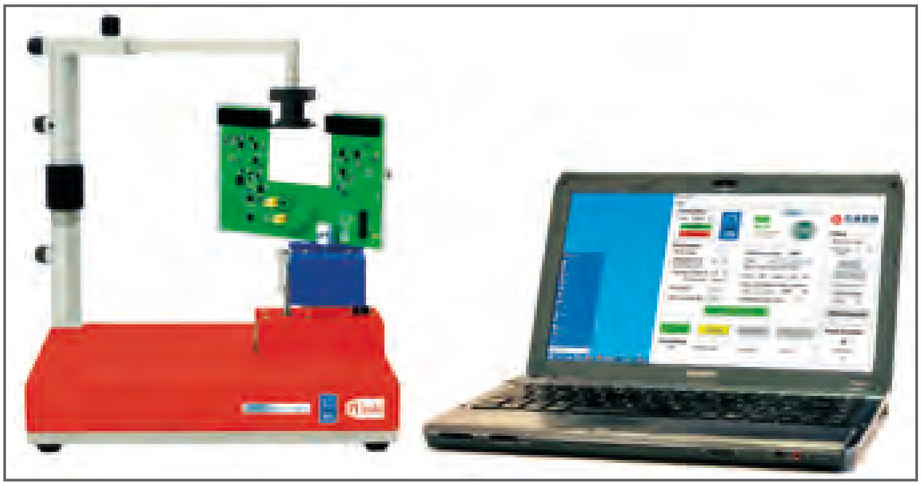

Difficulty	Execution Time	Data Analysis	Radioactive Sources
		NO	YES

Dedicated kit	
Description	**pp.**
SP5700 EasyPET	178

Requirements

^{22}Na Radioactive source
(recommended: 1/2 inch disc, 10 µCi)

Equipment

SP5700 - EasyPET

Model	SP5700
Description	EasyPET 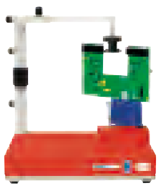

p. 178

Purpose of the experiment

Evaluation of the spatial resolution of a PET system composed of two detector modules.

See the Application

Fundamentals

The main goal of the PET studies is to obtain a good quality and detailed image of an object by the PET scanner. The parameters involved and critical to good quality image formation are several: spatial resolution, sensitivity, noise, scattered radiations, and contrast.

The spatial resolution is a fundamental characteristics of a tomographic system and its determination is mandatory for a PET system. The spatial resolution of a PET scanner is a measure of the ability of the device to faithfully reproduce the image of an object. It is empirically defined as the minimum distance between two points in an image that can be detected by a scanner.

In the EasyPET the dominant factor determining the spatial resolution is represented by the width of the scintillating crystals. Another effect that degrades the spatial resolution of the system is the so-called sampling error. It is associated to the distribution of the lines of response in the field of view and is a direct consequence of the rotation and scanning granularity.

Carrying out the experiment

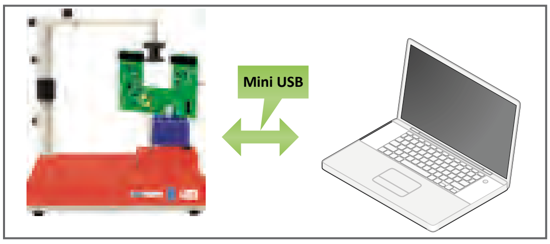

Experimental setup block diagram.

Mount the arm of the source holder on the column fixed on the system base, fix the U–shaped board to the top stepper motor and connect the flat cable to the U-shaped board and to control unit. Connect to PC and power ON the system. Set and optimize the parameters as bias voltage, threshold and coincidence time windows. In order to perform the spatial resolution measurement, the radioactive source is placed between the two detectors, on the line of response passing through the center. Its position is kept fixed while the system acquires the number of coincidence counts for successive scanning positions of the detector pair. The acquisition time is chosen in relation to the source activity to have enough statistics. The system response function is obtained plotting the number of coincidence counts for each position as a function of the distance between the source and the line of response (the distance is calculated as the product of the source-scanning axis distance and the scanning angle tangent). The resulting curve can be interpreted as the radioactive source distribution convoluted with the system spatial resolution.

Results

The estimated spatial resolution is ~ (1.45 ± 0.4) mm, which is comparable to the spatial resolution of the small animal PET systems.

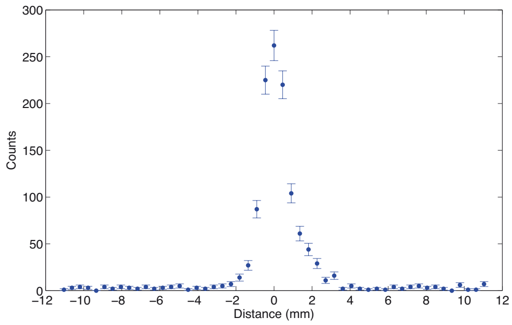

Counting frequency of the beta rays as a function of the number of crossed paper sheets.

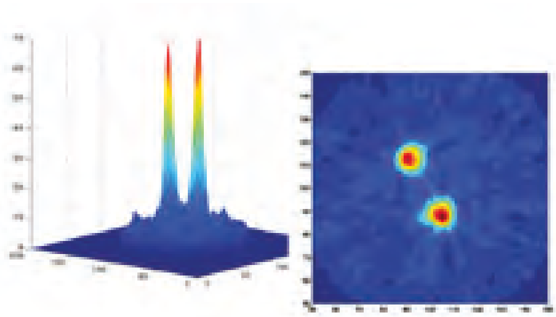

^{22}Na sources, 5 µCi, 2.7 mm Ø and 9 mm apart.

This experiment is also possible with the following kits

B **SP5701**
EasyPET Kit

see pp. 178

B. Nuclear Physics and Radioactivity

B.6 GM Detector

Geiger-Müller (GM) detectors, named after the physicists Hans Geiger and Walther Müller who invented them in the early 20th century, are widely used radiation detectors with applications ranging from scientific research to everyday life. These detectors operate based on the ionization produced by radiation in a gas-filled chamber, enabling them to detect various types of ionizing radiation. Despite their origins in scientific exploration, Geiger-Müller detectors have found practical use in numerous real-world scenarios due to their simplicity, reliability, and versatility. They play a crucial role in safeguarding public health and the environment. In this section, a series of experiments, based on CAEN "RockyRAD", are presented to explore the principles behind Geiger-Müller detectors and their diverse applications in everyday life.

Recommended kits

H SP5660
RockyRAD

see p. 184

Experiment	★ SP5660
B.6.1 Statistics: Uncertainty as a function of live time	•
B.6.2 Environmental Background	•
B.6.3 Lead Shielding Effect on Environmental Radioactive Background	•
B.6.4 Detecting Ionizing-Radiation	•
B.6.5 Samples Comparison	•

★ The star indicates the recommended Kits while the yellow color highlights the Kits especially dedicated to the experiences of this Section.

B.6.1 SG6160H Statistics: Uncertainty as a function of live time

Dedicated kit	
Description	pp.
SP5660 RockyRAD	184

Difficulty	Execution Time	Data Analysis	Radioactive Sources
		NO	NO

Requirements

No other tools are needed.

Equipment

SP5660 - RockyRAD

Model	SP5660
Description	RockyRAD  p. 184

Purpose of the experiment

Study of relationship between uncertainty analysis and the duration of data acquisition.

See the Application

Fundamentals

In the experimental Physics field, the accurate assessment of uncertainties is paramount to ensure the reliability and precision of measurements.

Measurement, an essential aspect of scientific inquiry, inherently involves some degree of uncertainty. Uncertainty refers to the range within which the true value of a physical quantity is expected to lie. Two key dimensions of uncertainty are relative uncertainty and absolute uncertainty. Relative uncertainty, often expressed as a percentage, gauges the precision of a measurement in relation to the size of the measured quantity. It is calculated by dividing the absolute uncertainty by the measured value and multiplying by 100. Absolute uncertainty is the quantitative measure of the range within which the true value of a measured quantity is expected to lie. It is typically expressed in the same units as the measured quantity. The determination of absolute uncertainty involves considering various factors, including instrumental limitations and experimental procedures.

Live time, as a parameter in this experiment, represents the duration for which data is actively collected. By systematically varying the live time during measurements, we aim to observe the influence of this temporal factor on both relative and absolute uncertainties. The statistical nature of measurements becomes apparent as we analyze how uncertainties change as a function of live time.

Carrying out the experiment

The experiment involves several data-taking with different acquisition time.

Begin by placing the GM detector on the desk and powering on the system. The experiment could be performed with or without a rock sample. GM detector will immediately initiate measurements and record data every minute during acquisition. The detected particles are counted and displayed on the monitor (CNTS), along with the average counts per minute (CPM) and dose (nSv/h). The system produces a sound for each detection.

Experimental setup block diagram.

Results

The experiment explores how the relative uncertainty evolves with varying live times, providing insights into the impact of data acquisition duration on the precision of our measurements. This experiment not only provides valuable insights into the statistical aspects of measurements but also sheds light on the dynamic relationship between uncertainty and the temporal dimension of data acquisition.

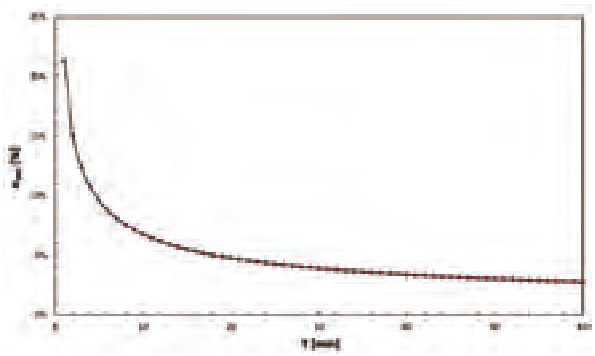

Relative uncertainty as a function of the live time.

T [min]	σ_{REL} [%]	σ_{ABS} [cpm]
1	21	4.7
5	10	2.1
15	6	1.2
30	4	0.9
60	3	0.6
120	2	0.4

Experimental results.

B.6.2 Environmental Background

SG6161H

Dedicated kit	
Description	**pp.**
SP5660 RockyRAD	184

Difficulty	Execution Time	Data Analysis	Radioactive Sources
		NO	NO

Requirements

No other tools are needed.

Equipment

SP5660 - RockyRAD

Model	**SP5660**
Description	RockyRAD  p. 184

Purpose of the experiment

Study of relationship between uncertainty analysis and the duration of data acquisition.

See the Application

Fundamentals

The main contributors to the background energy spectrum are the gamma radiations that originate from naturally occurring radioactive isotopes dispersed in the environment and the materials that surround the detector, and the radiations whose origin can be traced to cosmic rays. To properly identify a sample from radioactivity point of view, the background must be acquainted. The background radioactivity measurement must be obtained without using any sample, specifically with the GM tube window free.

Carrying out the experiment

Place the GM detector on the desk if you are indoors or on an outdoor surface. Power ON the system. The GM detector immediately starts measurements and records data every minute of acquisition. The background counts must be acquired in the absence of samples, specifically with the GM tube window uncovered. The detected particles are counted and displayed on the monitor (CNTS), along with the average counts per minute (CPM) and dose (nSv/h). The system produces a sound for each detection. A significant statistical dataset is necessary for an accurate estimation of the environmental background. It is recommended to conduct an acquisition for at least 24 hours.

Experimental setup block diagram.

Results

The user can check for the presence of environmental radiation by observing non-zero counts on the GM counter. The statistical analysis of the distribution of this background plays a crucial role in accurately estimating the radioactive contribution of the samples under investigation.

An example of the typical measurement outcome is shown in the table and figures provided below. However, it is important to note that the measured background value strongly depends on the environment in which the detection is carried out.

CPM Max	37.0
CPM Min	11.0
CPM Mean	22.0
σ_{STAT}	0.1
STD	4.5
Live Time [m]	3739

Experimental results.

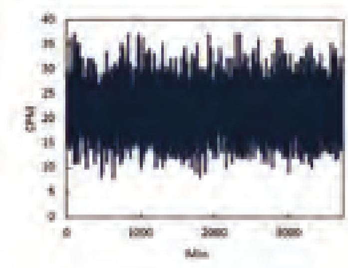

CPM - Raw data.

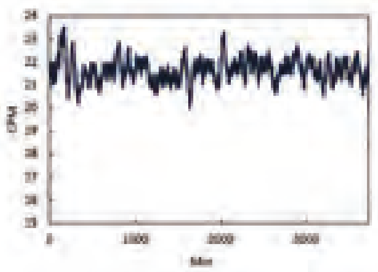

CPM - Moving average (1h)

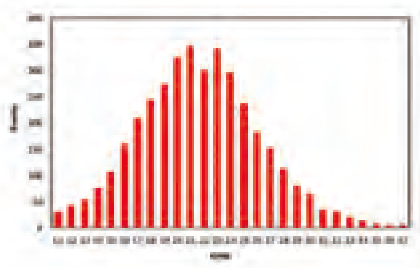

CPM Distribution

B.6.3 SG6162H Lead Shielding Effect on Environmental Radioactive Background

Dedicated kit	
Description	**pp.**
SP5660 RockyRAD	184

Difficulty	Execution Time	Data Analysis	Radioactive Sources
		NO	NO

Requirements

Lead blocks are required

Equipment

SP5660 - RockyRAD

Model	**SP5660**
Description	RockyRAD  p. 184

Purpose of the experiment

The experiment aims to analyze the impact of lead shielding on the environmental background particles detected by the GM detector.

See the Application

Fundamentals

For precise spectral measurements, resolution in energy and signal-to-noise ratio are the key parameters. Therefore, it is crucial to shield the detector with lead to minimize background. Lead is the most widely used material for shielding due to its high density and atomic number. The photoelectric absorption cross-section predominates at energies above 0.5 MeV, making it effective in easily absorbing relatively hard external background gamma rays (such as those at 1.46 MeV from ^{40}K). Owing to its high density, thin layers of a few centimeters of Pb significantly reduce background for typical gamma-ray detectors. Additionally, it can eliminate many components of cosmic rays, although thicknesses of about 10 cm contribute to the background with secondary radiation due to cosmic interaction with the lead itself. It is often used in the form of rectangular "bricks." Common lead exhibits a notable level of natural radioactivity; if refined, it may still contain ^{210}Pb, a product of the decay of ^{226}Ra, with a half-life of 20.4 years. While some types of Pb exhibit an activity of around 1.5 Bq/g, more refined lead is an order of magnitude or two below this value.

Carrying out the experiment

The experiment involves two data-taking phases: one with lead blocks covering and one without. Begin by placing the GM detector on the desk and powering on the system. The GM detector will immediately initiate measurements and record data every minute during acquisition. Background counts, essential for calibration, should be obtained in the absence of samples, specifically with the GM tube window uncovered. It is advisable to conduct a background acquisition for a minimum of 2 hours.

Upon completing the background measurement, cover the GM detector entirely with lead blocks. Maintain the same acquisition time to facilitate straightforward background subtraction.

Experimental setup block diagram.

Results

The user can easily check how lead blocks reduce the gamma radioactivity from the background, by comparing the results obtained by GM detector with and without lead blocks. The subsequent results illustrate how the mean counts per minute (CPM) decrease from approximately 24 to around 15 when lead shielding is employed.

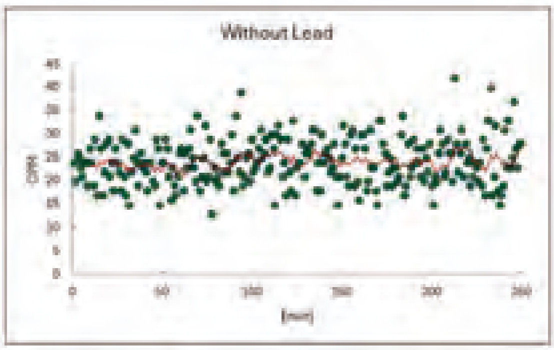

No shielding. CPM - Raw data in green and moving average (10 min) in red.

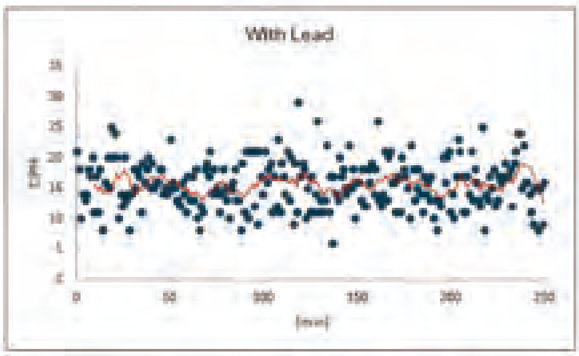

Lead Shielding. CPM - Raw data in blue and moving average (10 min) in red.

B.6.4 Detecting Ionizing-Radiation

SG6163H

Dedicated kit	
Description	pp.
SP5660 RockyRAD	184

Difficulty	Execution Time	Data Analysis	Radioactive Sources
1/5	1/5	NO	NO

Requirements

Lead blocks are required

Equipment

SP5660 - RockyRAD

Model	SP5660
Description	RockyRAD  p. 184

Purpose of the experiment

Radioactivity detection by using a GM detector.

See the Application

Fundamentals

In the Nuclear Physics field, ionizing particles play a pivotal role in understanding the fundamental building blocks of matter. These particles possess sufficient energy to liberate electrons from atoms, a process known as ionization. This ionization capability stems from their inherent ability to penetrate matter and impart energy to atomic structures. Ionizing particles in nuclear physics include alpha particles, beta particles, and gamma rays. Alpha particles consist of two protons and two neutrons, making them relatively massive and charged. Beta particles can be either electrons (β^-) or positrons (β^+) and can interact with atomic electrons. Gamma rays are electromagnetic waves of extremely high energy and no mass.

A GM detector is a device specifically designed to detect ionizing radiation. The operational principle of the GM detector hinges on the ionization generated by incoming radiation. Within the GM detector, there exists a gas-filled chamber, typically containing a low-pressure inert gas, and a central wire electrode running along the chamber's axis. The detector applies a high voltage between its outer casing (anode) and the central wire electrode (cathode), thereby creating an electric field within the gas-filled chamber. When ionizing radiation enters the detector, it interacts with the gas atoms, leading to the formation of ion pairs positively charged ions and free electrons. These free electrons, accelerated by the electric field, travel towards the central wire, inducing additional ionization events through collisions with other gas atoms. This cumulative effect, known as an electron avalanche, generates a detectable electrical pulse. This signal is then amplified and processed by the detector's electronics.

Carrying out the experiment

The experiment involves two data-taking phases: one with rock sample and one without. Begin by placing the GM detector on the desk and powering on the system. The GM detector will immediately initiate measurements and record data every minute during acquisition. Background counts, essential for calibration, should be obtained in the absence of samples, specifically with the GM tube window uncovered. It is advisable to conduct a background acquisition for a minimum of 2 hours. Upon completing the background measurement, place the rock sample in the middle of the open window of the GM detector. Start the new acquisition maintaing the same acquisition time to facilitate straightforward background subtraction.

Experimental setup block diagram.

Results

The student is provided with an opportunity to familiarize themselves with the presence of radioactivity within a given rock sample through a straightforward measurement technique. This involves a comparative analysis of the detected counts using a GM (Geiger-Muller) detector, both in the presence and absence of the rock sample. The comparison between the counts with and without the rock sample serves as a means of assessing the radioactivity associated with the specific geological material. An increase in detected counts when the rock sample is present suggests the emission of ionizing radiation from the sample. This increase is indicative of the radioactive properties of the rock, as certain minerals within the sample may naturally emit alpha, beta, or gamma particles, contributing to the overall ionization observed by the GM detector.

CPM Max	37.0
CPM Min	11.0
CPM Mean	22.0
σ_{stat}	0.1
STD	4.5
Live Time [m]	197

Environmental background

CPM Max	37.0
CPM Min	15.0
CPM Mean	27.2
σ_{stat}	1.3
STD	5.9
Live Time [m]	197

Rhyolite Rock

B.6.5 Samples Comparison

SG6164H

Dedicated kit	
Description	**pp.**
SP5660 RockyRAD	184

Difficulty	Execution Time	Data Analysis	Radioactive Sources
		NO	NO

Requirements

No other tools are needed.

Equipment

SP5660 - RockyRAD

Model	SP5660
Description	RockyRAD  p. 184

Purpose of the experiment

The objective of the experiment is to analyze and compare the detected counts originating from rocks of different origins.

See the Application

Fundamentals

The radioactivity of rocks varies significantly depending on their geological origin, with different types of rocks contributing distinctively to the overall radiation background. The composition of the Earth's crust contains various radioactive elements, and the concentration of these elements in rocks can vary based on factors such as the rock type and the geological processes that formed them.

Granitic rocks, for example, often exhibit higher concentrations of radioactive elements such as uranium, thorium, and potassium. These rocks contribute to elevated levels of ionizing radiation due to the decay of these radioactive isotopes. On the other hand, sedimentary rocks like limestone may have lower concentrations of these radioactive elements, resulting in comparatively lower radioactivity.

The different contributions of rocks to radioactivity are crucial in understanding natural background radiation and its variations across geological regions. This knowledge not only has implications for scientific studies but also plays a role in applications such as radiological assessments, mineral exploration, and environmental monitoring. Additionally, it underscores the importance of considering the geological context when interpreting measurements from radiation detection experiments, as the types of rocks present can influence the observed radiation levels.

Carrying out the experiment

The experiment involves several data-taking sessions, depending on the number of rocks under investigation. Begin by placing the GM detector on the desk and powering on the system. The GM detector will immediately initiate measurements and record data every minute during acquisition. Background counts, essential for calibration, should be obtained in the absence of samples, specifically with the GM tube window uncovered. It is advisable to conduct an acquisition for a minimum of 2 hours.

Upon completing the background measurement, place the first rock sample in the middle of the open window of the GM detector. Start the new acquisition, maintaining the same acquisition time to facilitate straightforward background subtraction. Repeat the procedure by using the other rock samples.

Experimental setup block diagram.

Results

The primary aim of this experience is to investigate the variations in ionizing radiation levels exhibited by several geological samples. Furthermore, it not only serves as a practical application of radiation detection principles but also encourages participants to apply scientific methods in data analysis and interpretation. The experiment opens avenues for discussions on the geological factors influencing radioactivity, contributing to a broader understanding of the complex interplay between rocks and ionizing radiation.

	Background	Leucitic Tephrite	Granite	Porphyry	Trachyte
Max	37.0	47.0	40.0	40.0	33.0
Min	11.0	20.0	15.0	15.0	15.0
Mean	22.0	33.6	25.4	25.4	24.8
σ_{STAT}	0.1	0.4	0.9	0.9	0.9
STD	4.5	5.6	5.4	5.4	4.6
Live Time [m]	197	197	121	35	28

CPM Comparison: Analyzing experimental results obtained with various rock samples.

C. Particle Physics

C.1 Cosmic Rays

The cosmic radiation, discovered by Victor Hess1 in 1912, includes all stable charged particles and it is composed by two component: “primary” and “secondary” cosmic rays. Essentially, the first ones are composed by heavy nucleus, protons (~90%) and helium (~10%), but also electrons, neutrinos, photons, some light nucleus and antimatter (positron and antiprotons). These particles are accelerated by astrophysical sources and by interacting with the terrestrial atmosphere, they mainly produce the “secondary” cosmic rays: pions, kaons and electromagnetic showers. Muons and neutrinos are products of the decay chain of charged mesons, while electrons and photons originate in decays of neutral mesons.

The experiments on cosmic rays proposed in this section are performed by using the “Educational Beta KIT” and the “Cosmic Hunter”.

For both kits, the mechanical structure to build a cosmic telescope to measure the flux azimuthal variation is also available.

Recommended kits

D **SP5620CH**
Cosmic Hunter

see p. 182

B **SP5600AN**
Educational kits
PREMIUM

see p. 179

A **SP5600D**
Educational kits

see pp. 182, 179

	★ K12		★
Experiment	**SP5620CH**	**SP5600AN**	**SP5600D**
C.1.1 Muons Spectrum - **Coming soon**		•	•
C.1.2 Statistics	•	•	•
C.1.3 Muons Detection	•	•	•
C.1.4 Muons Vertical Flux on Horizontal Detector	•	•	•
C.1.5 Random Coincidence	•	•	•
C.1.6 Detection Efficiency	•		
C.1.7 Cosmic Flux as a function of the altitude	•		
C.1.8 Zenith Dependence of Muons Flux	•	•	•
C.1.9 Cosmic Shower Detection	•		
C.1.10 Environmental and Cosmic Radiation	•		
C.1.11 Absorption Measurements	•		
C.1.12 Solar Activity Monitoring	•		

★ The star indicates the recommended Kits while the yellow color highlights the Kits especially dedicated to the experiences of this Section. If you are also interested in other experiences, the PREMIUM Kit is recommended.

K12 This symbol indicates that the Kit is also suitable for educational use with young students

C.1.2 Statistics

SG6210D

Difficulty	Execution Time	Data Analysis	Radioactive Sources
1/5	1/5	NO	YES

Dedicated kit	
Description	pp.
SP5620CH Cosmic Hunter	182

Requirements

No other tools are needed.

Equipment

SP5620CH - Cosmic Hunter

Model	SP5621	SP5622 (x2)
Description	Coincidence Module 	Detection System 
	p. 182	p. 187

Purpose of the experiment

Statistical properties of the cosmic rays.

See the Application

Fundamentals

The event number in a given time interval is one of the most interesting points in many Physics phenomena. This number is often affected by statistical fluctuations around an average value determined by the type of phenomenon. Multiple factors may cause fluctuations and influence the measurement result. Thus, the exact value is not always the same (as in the case of particles that decay may derive from space or from a radioactive source).

The most important goal in the experimental approach is to understand which values can occur in a series of measurements as well as their probability, i.e. the probability distribution. The Poisson distribution describes with good approximation events comings from radioactive phenomena or from counting cosmic rays. This distribution expresses the probability of a given number of events occurring in a fixed interval of time or space, and can be expressed as:

$$P_{\mu}(n) = (\mu^n / n!) * e^{-\mu}$$

where μ is the average number of events in a fixed interval and n is the number of events.

Carrying out the experiment

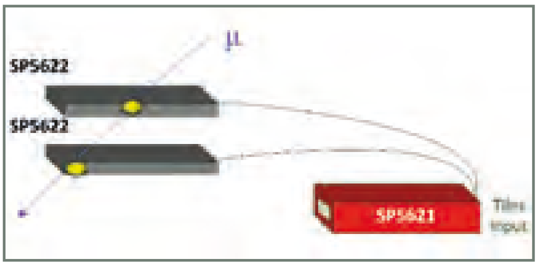

Experimental setup block diagram.

Connect the cable connector from each SP5622 Detection System to the input located on the rear panel of of the SP5621 module. Power on the SP5621 module and start acquisition via the START button on the front panel. When a charged particle crosses the black tile its energy is converted into scintillation light. The photons produced are detected by the photosensor and converted into an electrical signal. The number of counts for each scintillator is available via the SP5621 display. Note that spurious electrical signals will likely also be detected by the photosensor, thus producing noise. Coincidence between two SP5622 will greatly reduce the number of spurious events. However, the statistical fluctuations cannot be totally removed. Select the scintillators coincidence via the related button on the front panel, then select the integration time of the measurement. Before starting acquisition choose the system geometry. Be sure to keep this geometry constant for the duration of the experiment. Take and record more data to obtain statistical significance.

Results

The Poisson distribution of cosmic rays can be experimentally verified via data analysis and the treatment of their statistical uncertainty.

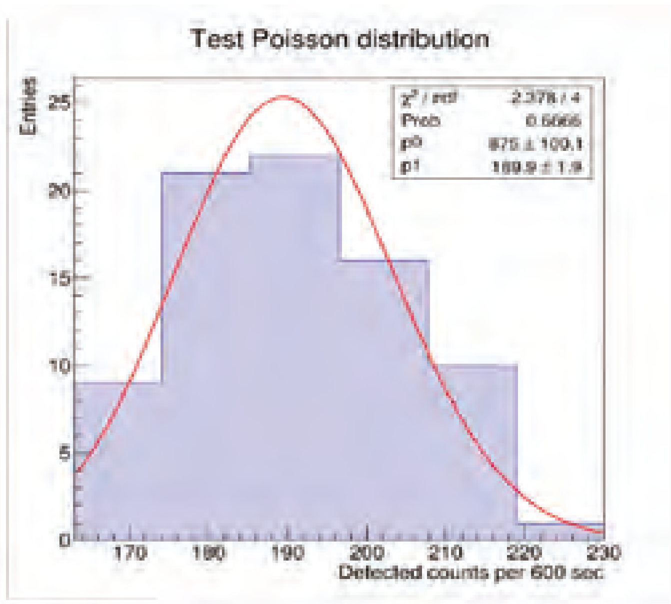

Poissonian distribution of cosmic rays [Fit: $y = p0^* (p1^x/x!)^* e^{-p1}$]

This experiment is also possible with the following kits

A **SP5600D**
Educational kits

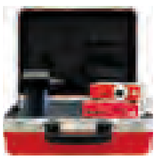

see pp. 182, 179

B **SP5600AN**
Educational kits
PREMIUM

see p. 179

C.1.3 Muons Detection

SG6211A

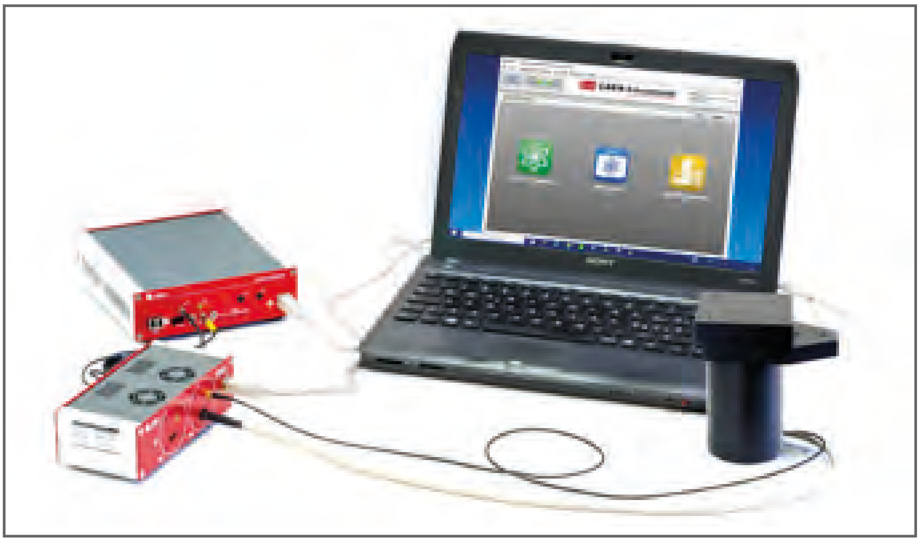

Dedicated kit	
Description	pp.
SP5600D Educational Beta Kit	182 179

Difficulty	Execution Time	Data Analysis	Radioactive Sources
		NO	YES

Requirements

No other tools are needed.

Equipment

SP5600D - Educational Beta Kit

Model	SP5600	DT5720A	SP5608
Description	Power Supply and Amplification Unit 	Desktop Digitizer 250 MS/s 	Scintillating tile 
	p. 190	p. 190	p. 193

Purpose of the experiment

Cosmic rays detection by using a system composed of a plastic scintillating tile directly coupled to a Silicon Photomultiplier detector.

See the Application

Fundamentals

The muons, produced by the decay of pions and kaons generated by the hadronic interaction of the primary cosmic rays with atmospheric nuclei, are the most cosmic rays at sea level.

Cosmic muons are charged particles, produced high in the atmosphere (typically 15 km) with highest penetration capability in matter. Their mass (~ 200 times the electron mass), the absence of strong interactions and their long lifetime ($\tau \sim 2{,}2 \times 10^{-6}$ s), allow muons to cross the atmosphere and reach the Earth's surface.

The muon average energy at sea level is around 4 GeV.

Carrying out the experiment

Open the SP5608 and remove the plastic scintillating tile. Close the SP5608 and connect its power cable and its MCX cable to one channel of the SP5600. Connect the two outputs of the chosen channel to DT5720A: the analog output to the channel 0 and the digital output to “trigger IN“ of the digitizer. Use the default software values or optimize the parameters to evaluate the noise contribution of the sensor, called Dark Count Rate (DCR). Measure the DCR as a function of the discrimination threshold in mV. Because of the DCR, the system has to be made sensitive to the cosmic ray flux relying on the acquisition time of the sensor signal. Switch off the power supply, open the SP5608 top, spread the optical grease on the SiPM and insert the scintillating tile. Close the support top, switch ON the power supply and restore the previous configuration parameters. Measure the counting rate scanning the values of the threshold.

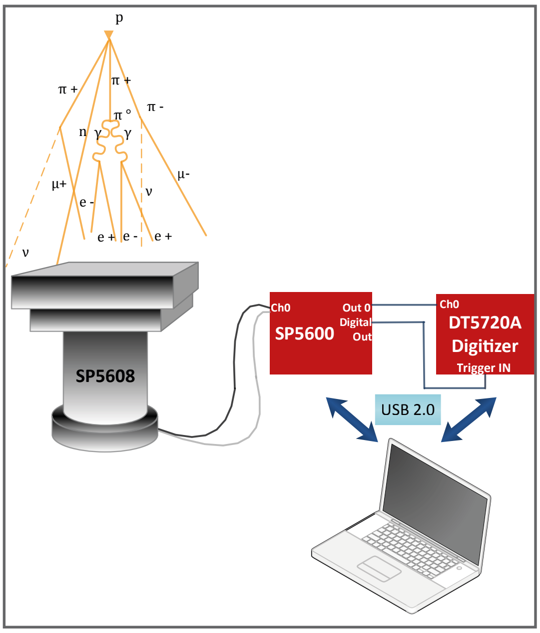

Experimental setup block diagram.

Results

The cut-off threshold has a key role in the cosmic ray detection and it shall be set to reduce the random coincidence rate below the Hertz level and measure the cosmic rate.

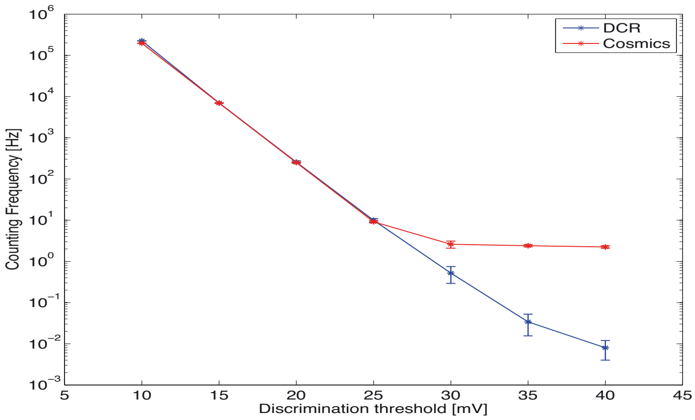

Signal frequency as a function of discriminator threshold. The red line represents the cosmic contribution, the black one the noise.

This experiment is also possible with the following kits

B **SP5600AN**
Educational kits
PREMIUM

see p. 179

D **SP5620CH**
Cosmic Hunter

see p. 182

C.1.4 Muons Vertical Flux on Horizontal Detector

SG6212A

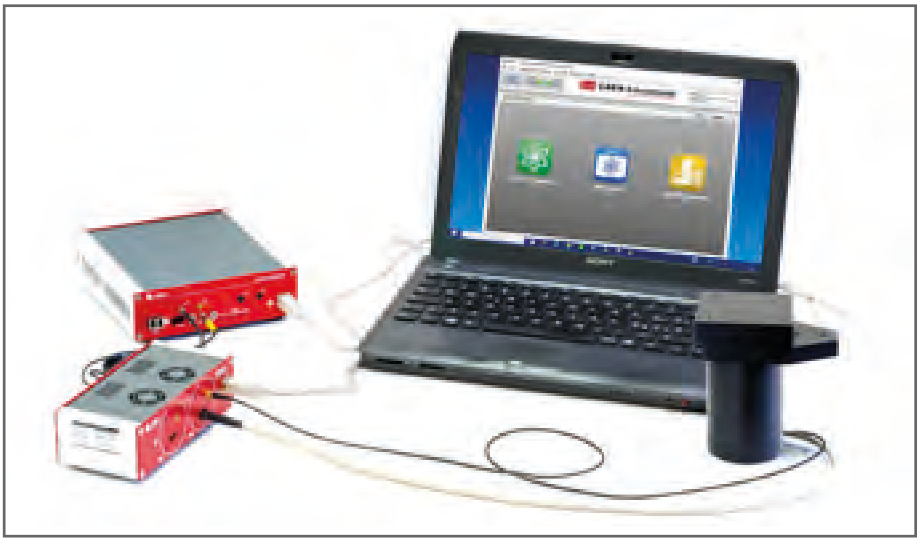

Dedicated kit	
Description	pp.
SP5600D Educational Beta Kit	182 179

Difficulty	Execution Time	Data Analysis	Radioactive Sources
		NO	YES

Requirements

No other tools are needed.

Equipment

SP5600D - Educational Beta Kit

Model	SP5600	DT5720A	SP5608
Description	Power Supply and Amplification Unit  p. 190	Desktop Digitizer 250 MS/s  p. 190	Scintillating tile  p. 193

Purpose of the experiment

Measurement of the muon vertical flux on a plastic scintillating tile. Estimation of the detection efficiency of the system by comparison between the expected rate and the measured one.

See the Application

Fundamentals

Muons lose about 2 GeV to ionization before reaching the ground with average energy around 4 GeV. The production spectrum, energy loss in the atmosphere and decay of the muons are convoluted in their energy and angular distribution. The integral intensity of vertical muons is

$$I_V \approx 82\ m^{-2}s^{-1}sr^{-1}$$

and their flux for horizontal detectors is ≈ 1 $cm^{-2}min^{-1}$ at energies higher than 1 GeV at sea level, as know in literature[2].

Carrying out the experiment

Open the SP5608 and remove the plastic scintillating tile. Close the SP5608 and connect its power cable and its MCX cable to one channel of the SP5600. Connect the two outputs of the chosen channel to DT5720A: the analog output to the channel 0 and the digital output to "trigger IN" of the digitizer. Use the default software values or optimize the operating voltage of the sensor to reach an higher photon detection efficiency (PDE). The first measurement step is the evaluation of the noise (Dark Count Rate) as a function of the discriminator threshold. Because of the DCR, the system has to be made sensitive to the cosmic ray flux relying on the acquisition time of the sensor signal. The thresholds shall be set to reduce the random coincidence rate below the Hertz level. Switch off the power supply, open the SP5608 top, spread the optical grease on the SiPM and insert the scintillating tile. Close the support top, switch ON the power supply and reset the previous configuration parameters. Measure the muons counting rate and estimate the cosmic flux.

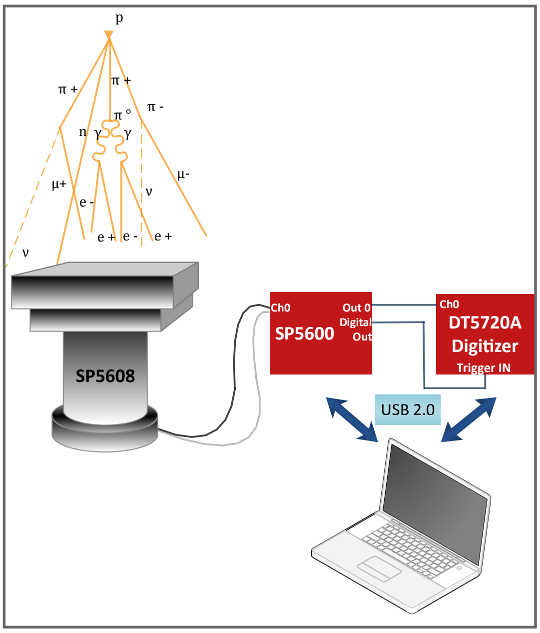

Experimental setup block diagram.

Results

The expected rate of muons across the scintillating tile is very low, requiring a fine tuning of the system in order to achieve a significant reduction of the random count rate and enhance the system sensitivity.

Considering the zenith dependence of flux ($I(\theta)=I_v \cos\theta^2$) and the integration over the solid angle, the expected cosmic rate due to the geometry system can be estimated and the detection efficiency can be evaluated.

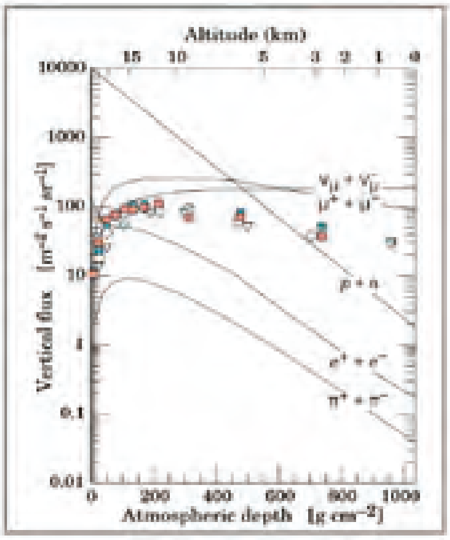

Cosmic vertical flux as a function of altitude and atmospheric depth[2].

[2] K.A. Olive et al. (Particle Data Group), Chin. Phys. C, 38, 090001 (2014).

This experiment is also possible with the following kits

B **SP5600AN**
Educational kits
★ **PREMIUM**

see p. 179

D **SP5620CH**
Cosmic Hunter

see p. 182

C.1.5 Random Coincidence

SG6213D

Dedicated kit	
Description	pp.
SP5620CH Cosmic Hunter	182

Requirements

No other tools are needed.

Difficulty	Execution Time	Data Analysis	Radioactive Sources
		YES	YES

Equipment

SP5620CH - Cosmic Hunter

Model	SP5621	SP5622 (x2)
Description	Coincidence Module  p. 182	Detection System  p. 187

Purpose of the experiment

To understand the potential for accidental counts coming from double tile coincidence.

See the Application

Fundamentals

Once the geometry of the detectors has been defined and coincidence is confirmed it becomes important to estimate the number of random coincidences. Random coincidences derive from simultaneous or nearly-simultaneous pulses caused by accidental discharges (i.e. noise), and not by particles with a trajectory within the volume determined by the solid angle of the geometry. The probability that a particle crosses the detector is a function of the surface of the tile itself and of the average rate. Therefore, the probability of a random coincidence is proportional to the pulse duration.

An evaluation of random coincidence contribution [R_{random}] can be obtained by a simple theoretical calculation, Janossy method based Error! Reference source not found:

$$R_{random} = 2*R_A*R_C*\tau$$

Where τ is the pulse duration (*700 ns*), and R_A and R_C are the event rate of each scintillating tile.

Carrying out the experiment

Connect the cable connectors of the two SP5622 to the tile inputs located on the rear panel of the SP5621 module. Power on the SP5621 module and start the acquisition via the front panel START button. When a charged particle crosses the black tile it's energy is converted into scintillation light. The photons which are produced are detected by the photosensor and converted into an electrical signal. The number of counts for each scintillator may be viewed via the SP5621 display. Select the scintillators coincidence via the related button on the front panel, then select the integration time of the measurement.

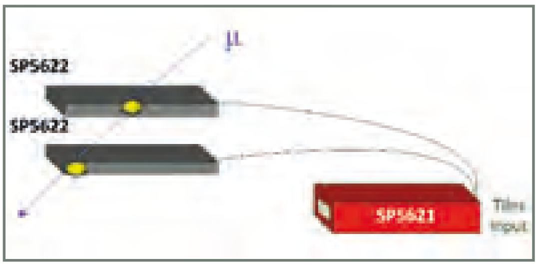

Experimental setup block diagram.

Before starting acquisition choose the system geometry. Be sure to keep this geometry constant for the duration of the experiment. Take and record more data to obtain statistical significance.

Results

Double tile coincidence plays a key role in a great many Physics experiments. The random coincidence rate allows you to evaluate the data quality via estimation of the Signal to Background ratio [SBR].

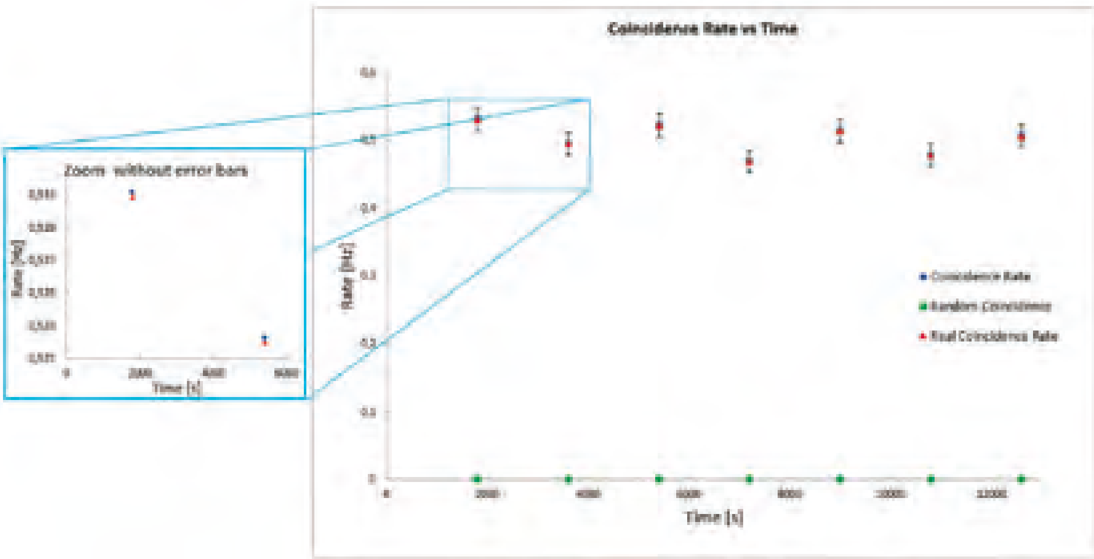

Trend of the Count Rate and Random Rate as a function of the time. The plot on the left side is an enlargement of the main plot and underlines the deviation between the measured coincidence rate and the real one, obtained via the random rate subtraction.

This experiment is also possible with the following kits

A **SP5600D**
Educational kits

see pp. 182, 179

B **SP5600AN**
Educational kits
★ **PREMIUM**

see p. 179

C.1.6 Detection Efficiency

SG6214D

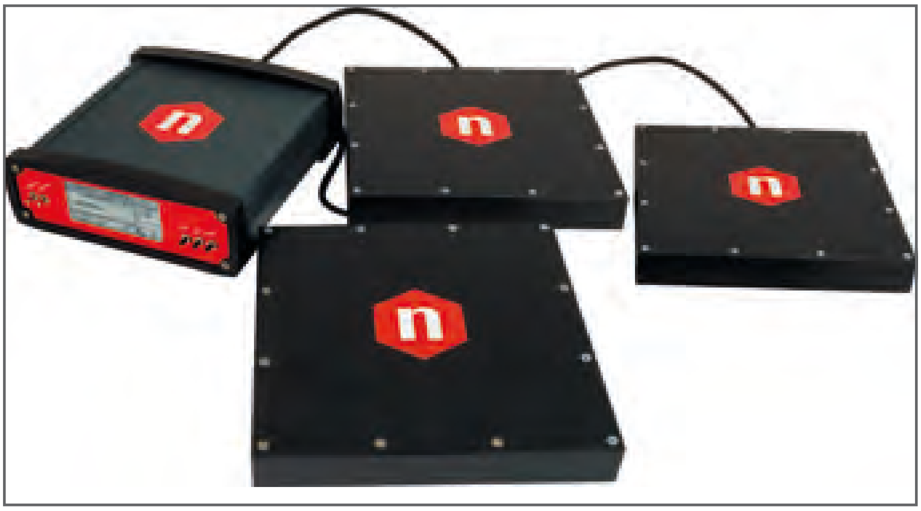

Dedicated kit	
Description	**pp.**
SP5620CH Cosmic Hunter	182

Difficulty	Execution Time	Data Analysis	Radioactive Sources
		YES	NO

Requirements

Additional:

- SP5622 - Detection System
- DT1081A - Four-Fold Programmable Logic Unit (Discriminator, Coincidence and Scaler modules in one solution
- Cable Adapter

are needed.

Equipment

SP5620CH - Cosmic Hunter

Model	SP5621	SP5622 (x2)
Description	Coincidence Module 	Detection System 
	p. 182	p. 187

Purpose of the experiment

To goal of the experiment is the evaluation of the detection efficiency of the scintillating tiles that make up the system.

See the Application

Fundamentals

Detection efficiency is the probability that a particle is detected after crossing the sensitive volume of the detector. Detection efficiency is dependent upon the incidence angle, the cross-section through which the particle interacts with the scintillator, and on its physical dimensions. The efficiency of a detector can change depending upon the bias voltage applied and upon the particle type and energy. The efficiency (ε) is defined experimentally as the ratio between the number of detected particles (N_0) and the number of particles incident upon the detector surface (N):

$$\varepsilon = N_0 / N$$

The number of the particles detected in coincidence between additional detectors can be expressed as the product between the impinging particles and the efficiency of each detector. The following expressions can be assumed for the double and triple coincidences:

$$N_{AC} = \varepsilon_A * \varepsilon_C * N_0 \qquad \text{and} \qquad N_{ABC} = \varepsilon_A * \varepsilon_B * \varepsilon_C * N_0$$

Thus, the detection efficiency of the scintillating tile positioned in the middle can be expressed as:

$$\varepsilon_B = N_{ABC} / N_{AC}$$

Carrying out the experiment

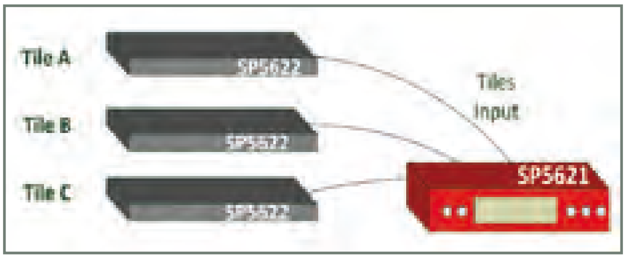

Experimental setup block diagram.

Connect the cable connectors of the three SP5622 to the tile inputs located on the rear panel of the SP5621 module. Power on the SP5621 module and start the acquisition via the front panel START button. When a charged particle crosses the black tile it's energy is converted into scintillation light. The photons which are produced are detected by the photosensor and converted into an electrical signal. The number of counts for each scintillator may be viewed via the SP5621 display. Select triple scintillator coincidence mode via the related button on the front panel, then select the integration time of the measurement. Arrange the geometry of the detectors as depicted in the diagram above. Be sure to keep this geometry for the duration of the experiment. This system configuration allows the user to test the efficiency of the central scintillating tile. Connect the signal outputs of the three scintillating tiles to an external apparatus in order to identify double and triple counts at the same time, which correspond to the same cosmic ray.

To estimate the detection efficiency of the upper and lower scintillating tiles change the detector positions and repeat the measurement.

Results

The efficiency value for each detector should be very close to one another.

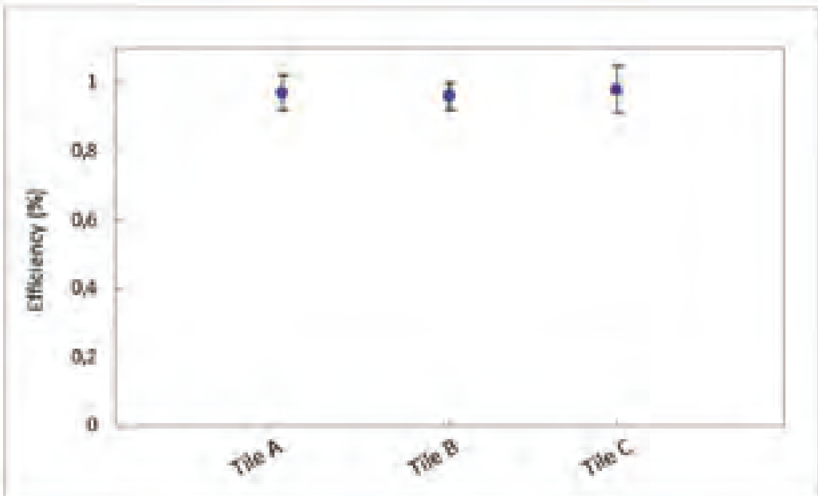

Detection efficiency of the three scintillating tiles – SP5622

C.1.7 Cosmic Flux as a function of the altitude

SG6215D

Dedicated kit	
Description	**pp.**
SP5620CH Cosmic Hunter	182

Requirements

No other tools are needed.

Difficulty	Execution Time	Data Analysis	Radioactive Sources
		YES	NO

Equipment

SP5620CH - Cosmic Hunter

Model	SP5621	SP5622 (x2)
Description	Coincidence Module 	Detection System 
	p. 182	p. 187

Purpose of the experiment

The measurement of cosmic ray flux as a function of altitude. The goal of this experiment is analyse muon rate behaviour by performing measurements at different altitude levels. For example, one may perform such measurements on different floors of a building, at different elevations of a hill, or even by using a hot-air balloon.

See the Application

Fundamentals

The origin of cosmic radiation represents one of the most fascinating Physics discoveries of the 20th century. The first evidence of natural and non-terrestrial ionizing radiation in the atmosphere was observed in the early 1900s and subsequently studied via different typology of electroscopes by several scientists: from the Jesuit monk Theodor Wulf to the Italian physicist Domenico Pacini, to the Austrian-American physicist Victor Hess (Nobel Prize in 1936).

The measurement of the cosmic ray flux as a function of the altitude played a key role in the comprehension of the nature of both primary and secondary cosmic rays. The Earth's atmosphere acts as a filter by absorbing most of the secondary particles produced by the interaction of the primary ones with the external layers of the atmosphere itself. Muons and Pions are the most have the greatest penetrating capability and can reach the Earth's surface. For that reason they constitute the hard component of the secondary cosmic radiation. The soft component consists mainly of gamma, positrons, and electrons that are easily absorbed by the Earth's atmosphere. Initially, the flux of the secondary cosmic rays as a function of the altitude endures a slight decrease due to the loss of the contribution of natural radioactivity from the terrestrial crust. However, evident increase in the flow of revealed particles is then observed.

Carrying out the experiment

Connect the cable connectors of the two SP5622 to the tile inputs located on the rear panel of the SP5621 module. Power on the SP5621 module and start the acquisition via the front panel START button. When a charged particle crosses the black tile it's energy is converted into scintillation light. The photons which are produced are detected by the photosensor and converted into an electrical signal. The number of counts for each scintillator may be viewed via the SP5621 display. Select double scintillators coincidence mode via the related button on the front panel, and then select measurement integration time. Because the acquisition of events takes place only in the presence of the coincidence, all such events coming from a cosmic particle that crosses only one scintillating tile will automatically be discarded.

Before starting acquisition choose the system geometry. Be sure to keep this geometry constant even at different altitude levels. Take and record more data to obtain statistical significance

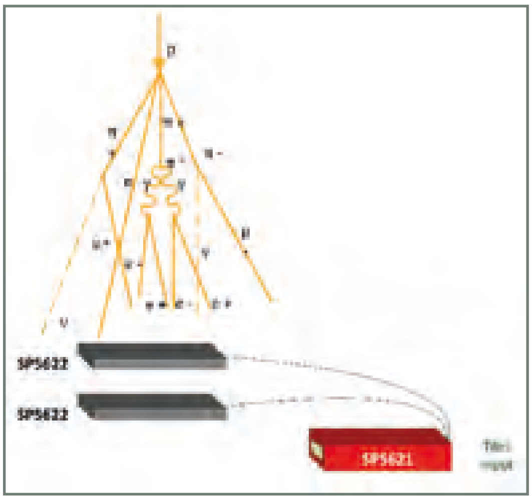

Experimental setup block diagram.

Results

This experiment is a simple way to identify and prove the non-terrestrial origin of cosmic radiation. For better comprehension of the cosmic flux behaviour as a function of the altitude the user may cover the floor with lead bricks.

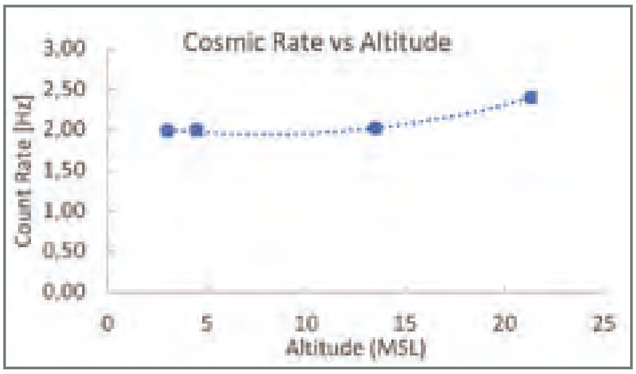

Cosmic flux as a function of altitude.

C.1.8 Zenith Dependence of Muons Flux

SG6215D

Dedicated kit	
Description	**pp.**
SP5620CH Cosmic Hunter	182

Requirements

SP5609 – Telescope Mechanics or a similar structure

Difficulty	Execution Time	Data Analysis	Radioactive Sources
		YES	NO

Equipment

SP5620CH - Cosmic Hunter

Model	SP5621	SP5622 (x2)
Description	Coincidence Module  p. 182	Detection System  p. 187

See the Application

Purpose of the experiment

Measurement of the zenith dependence of the cosmic ray flux as a function of altitude. The goal of the experiment is to analyse zenith dependence by performing a series of measurements at different zenith angle values.

Fundamentals

Most muons are produced in the upper atmosphere, typically 15km above the surface of the earth. Muons typically lose about 2GeV to ionization before reaching the ground. The average energy of muons on the ground is around 4GeV. When their decay (E_μ> 100 / cosθ GeV) and the curvature of the Earth (for θ> 70°) can be disregarded the flux of cosmic muons can be expressed as follows:

$$\frac{dN_\mu}{dS\,dt\,dE_\mu\,d\Omega} = 0.14E_\mu^{-2.7}\left\{\frac{1}{1+\frac{1.1E_\mu\cos\theta}{115GeV}} + \frac{0.054}{1+\frac{1.1E_\mu\cos\theta}{850GeV}}\right\}[cm^2\, s\, GeV\, sr]^{-1}$$

Where θ is the zenith angle, and the two terms in the brackets indicate the contribution of the charged pions and kaons. For E_μ ~ 3GeV, the angular distribution of muons is proportional to cos2θ at sea level. The intensity of cosmic muons is only determined by the angular dependence of the zenith on their energy spectrum and their energy. As first approximation, the dependence of the muon flow from ϕ is considered negligible, which is in fact less than 10% (*).

(*) A. A. Ivanov et al., JETP letters, V69 N4(1999)288

Carrying out the experiment

Connect the cable connectors of the two SP5622 to the tile inputs located on the rear panel of the SP5621 module. Power on the SP5621 module and start the acquisition via the front panel START button. When a charged particle crosses the black tile it's energy is converted into scintillation light. The photons which are produced are detected by the photosensor and converted into an electrical signal. The number of counts for each scintillator may be viewed via the SP5621 display. Select the scintillators coincidence via the related button on the front panel, then select the integration time of the measurement.

Before starting acquisition choose the system geometry. Be sure to keep this geometry constant for the duration of the experiment. Take and record more data to obtain statistical significance.

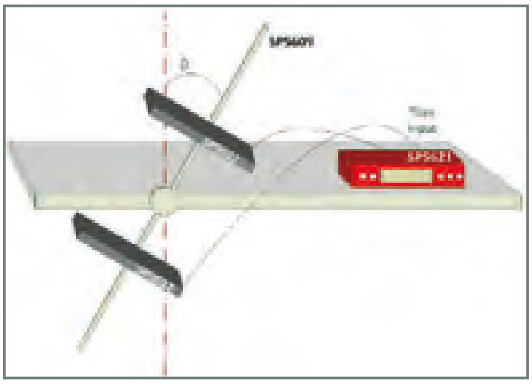

Experimental setup block diagram.

Results

The following plot shows the result obtained by positioning the two detectors at 20 cm distance. The count rate was measured at four values of the zenith angle, θ=[0, 10°, 50°, 70°], to verify the cos2(θ) theoretical trend of the muons flux.

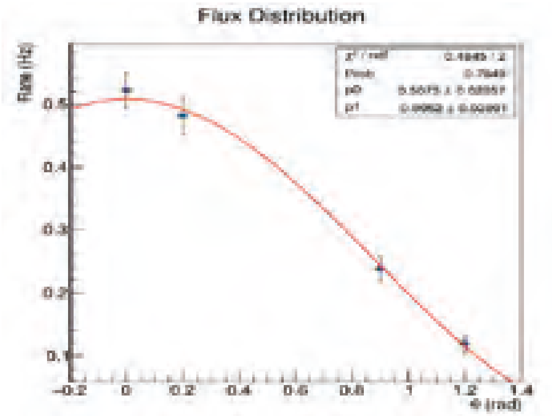

Zenith angle dependence of the muons flux [Fit: *y = p0*cos² (p1*x)*]

This experiment is also possible with the following kits

A **SP5600D**
Educational kits

see pp. 182, 179

B **SP5600AN**
Educational kits
★ **PREMIUM**

see p. 179

C.1.9 Cosmic Shower Detection

SG6217D

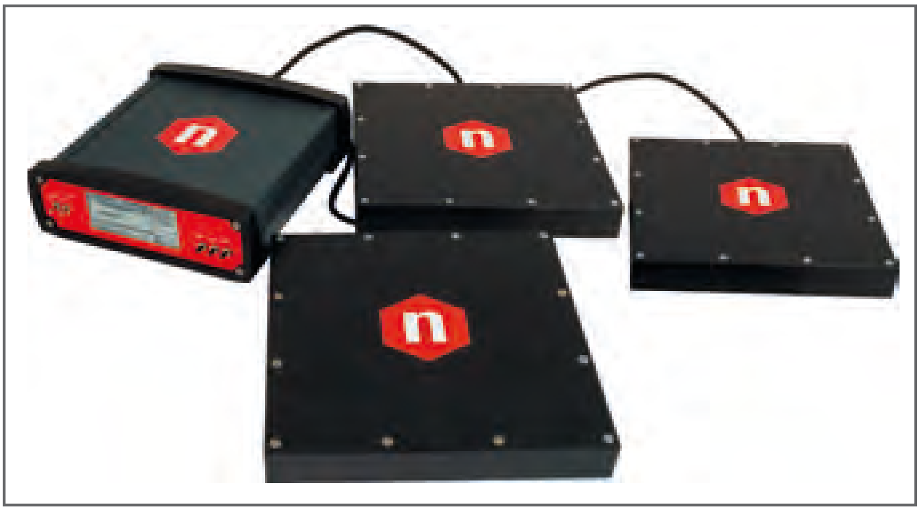

Difficulty	Execution Time	Data Analysis	Radioactive Sources
		NO	NO

Dedicated kit	
Description	**pp.**
SP5620CH Cosmic Hunter	182

Requirements

Additional SP5622 - Detection System is needed.

Equipment

SP5620CH - Cosmic Hunter

Model	SP5621	SP5622 (x2)
Description	Coincidence Module  p. 182	Detection System  p. 187

Purpose of the experiment

Detection of the cosmic showers by using the coincidence of three scintillating tiles located adjacent to one another on a flat surface.

See the Application

Fundamentals

Cosmic ray showers are cascades generated by cosmic rays interacting with the atmosphere. They were originally discovered by chance during the application of coincidence counters for the study of the cosmic rays. In some of these experiments coincident events were detected when the detectors were not assembled in telescopic structure, but rather were organized near one another on a flat surface.

The intuition of this new physical phenomenon was formulated by Bruno Rossi in 1934 and is considered to be the first evidence of the existence of extended atmospheric showers. The Italian physicist was the first to deduce that the multiplicative processes made by the cosmic rays produced in the atmosphere are identical to those observed in dense materials such as lead. Several groups of scientists studied this phenomenon. In particular, Auger and Maze undertook a campaign of systematic studies of these showers and even managed to measure coincident events between detectors as far apart as 300 meters! Auger and collaborators discovered the Extensive Atmospheric Showers [EAS] of very high energy, i.e. the energy of the primary particles at the origin of these events is around 10^{16} eV.

Carrying out the experiment

Connect the cable connectors of the three SP5622 to the tile inputs located on the rear panel of the SP5621 module. Arrange the tiles on a flat surface some distance apart from one another. Power on the SP5621 module and start the acquisition via the front panel START button. When a charged particle crosses the black tile it's energy is converted into scintillation light. The photons which are produced are detected by the photosensor and converted into an electrical signal. The number of counts for each scintillator may be viewed via the SP5621 display. Select triple scintillator coincidence mode via the related button on the front panel, then select the integration time of the measurement. Because event acquisition will only take place only in the presence of the coincidence, all those events coming from a cosmic particle that crosses only one scintillating tile will be automatically discarded.

An extended geometry can be realized simply by using additional Cosmic Hunter. Additionally, it could be interesting to observe Air Showers as a function of the altitude.

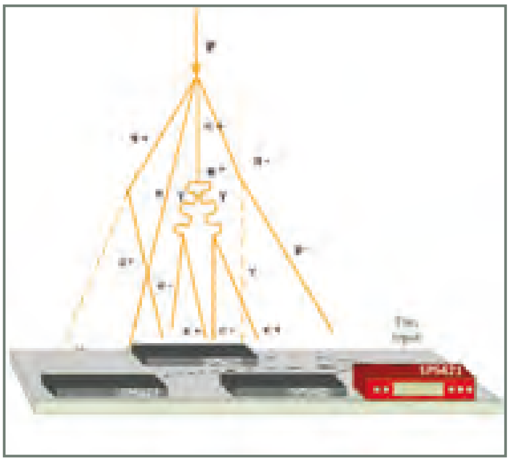

Experimental setup block diagram.

Results

Observation of the cosmic shower phenomenon.

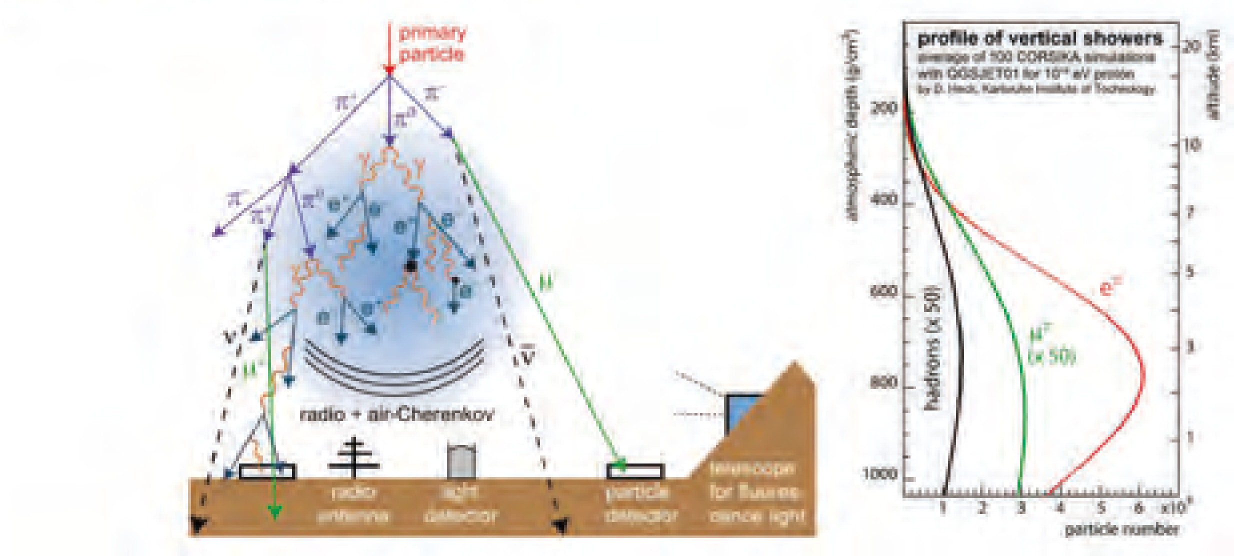

Scheme of an air shower detected by several detectors and its vertical profile (Ref. Frank G.Schröder, Radio detection of cosmic-ray air showers and high energy neutrinos, 2017, https://doi.org/10.1016/j.ppnp.2016.12.002).

C.1.10 Environmental and Cosmic Radiation

SG6218D

Dedicated kit	
Description	pp.
SP5620CH Cosmic Hunter	182

Requirements

No other tools are needed.

Difficulty	Execution Time	Data Analysis	Radioactive Sources
2/5	4/5	YES	NO

Equipment

SP5620CH - Cosmic Hunter

Model	SP5621	SP5622 (x2)
Description	Coincidence Module  p. 182	Detection System  p. 187

Purpose of the experiment

To estimate the contribution of environmental radiation during the detection of the cosmic radiation.

See the Application

Fundamentals

Natural radiation is composed of two components: Environmental (primarily derived from soil, but also water, air and food) and Cosmic radiation. Gamma rays coming from soil will have mean energy lower than 2MeV and will descend from the decay chains of three natural radioactive elements: Potassium [^{40}K], Thorium [^{232}Th] and Uranium [^{238}U]. However, there is a not null probability that a soil-derived gamma interacts with the scintillating tile and deposits 1MeV of energy. This potential could cause confusion or inaccuracies in cosmic rays counting measurement. However, the high threshold of the electronics and the low probability of this phenomenon, when compared to the cosmic ray high detection probability, should typically avoid this inconvenient situation.

Carrying out the experiment

Connect the cable connectors of the two SP5622 to the tile inputs located on the rear panel of the SP5621 module. Power on the SP5621 module and start the acquisition via the front panel START button. When a charged particle crosses the black tile it's energy is converted into scintillation light. The photons which are produced are detected by the photosensor and converted into an electrical signal. The number of counts for each scintillator may be viewed via the SP5621 display. Select double scintillators coincidence mode via the related button on the front panel, and then select measurement integration time.

Before beginning acquisition the geometry of the system must be determined. Be sure to keep this geometry for the duration of the experiment. To get acquainted with environmental radiation detected by the Cosmic Hunter place the system over bare soil and record data. Once complete, place the detectors a few meters above bare soil and place an iron or lead shield between the soil and the tiles. Acquire the data again with identical tile geometry and compare the results.

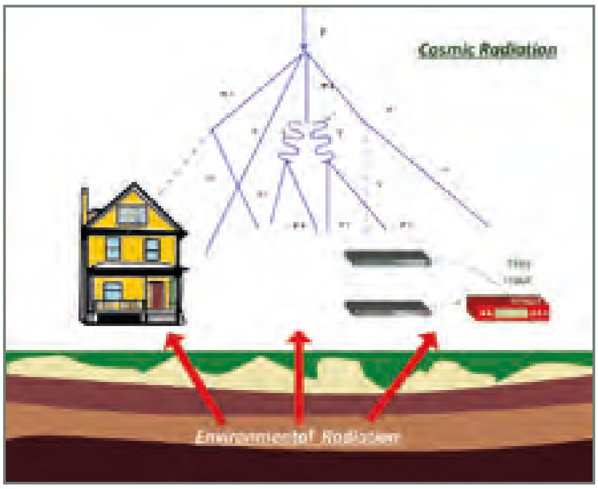

Experimental setup block diagram.

Results

Students may become acquainted with the presence of natural radioactivity by identifying environmental and cosmic contributions via simple comparison of the counting measurements at different heights.

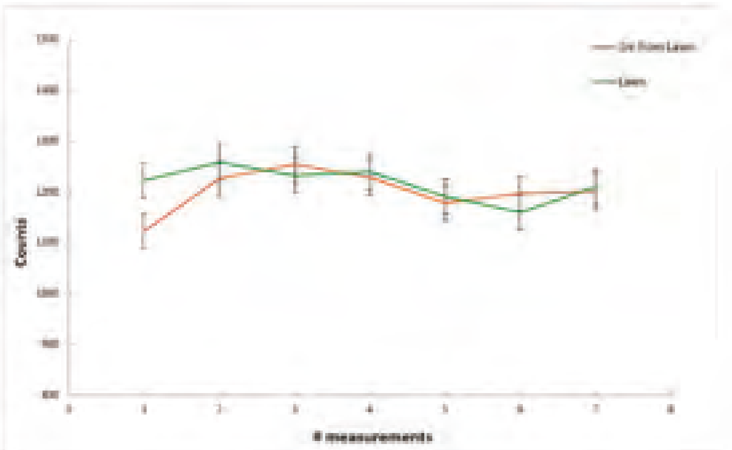

Comparison between the count rates of the measurements acquired on soil and again 1 meter above soil. The comparison plot demonstrates that the parameter settings (Bias Voltage and Threshold) are such that cosmic ray detection is not affected by environmental radiation

C.1.11 Absorption Measurements

SG6219D

Difficulty	Execution Time	Data Analysis	Radioactive Sources
		YES	NO

Dedicated kit	
Description	pp.
SP5620CH Cosmic Hunter	182

Requirements

No other tools are needed.

Equipment

SP5620CH - Cosmic Hunter

Model	SP5621	SP5622 (x2)
Description	Coincidence Module  p. 182	Detection System  p. 187

Purpose of the experiment

The main goal of this experiment is verify the absorption of the cosmic rays passing through solid matter and understand related observations about the material which has been traversed by the cosmic rays.

See the Application

Fundamentals

Before reaching the ground cosmic muons lose energy by ionization and through processes such as bremsstrahlung, creation of pairs ($e^+ e^-$), and nuclear interactions. If a detector is located within a building or below the earth's surface the detected muon flux decreases in relation to the thickness of the crossed rock/material. The expression of the average energy lost by a muon through matter is:

$$-dE / dx = k(E) + b_b(E)\,E + b_p(E)\,E + b_n E$$

where the $b_b(E)$, $b_p(E)$ and b_n are proportionally connected to the losses due to bremsstrahlung, to pairs creation, and to the nuclear interactions respectively. Interesting applications which explore the absorption of cosmic rays are represented by muon radiography and tomography. Muon radiography and tomography are based on the measurement of the absorption undergone by high energy muons when they cross solid objects. Good measurement techniques can provide precise maps of the average density of the object under investigation. These methods are used in several fields, from the geophysical application (volcanoes, caves, etc.) to the control of illicit traffic of radioactive materials, and much more. Typically, the average energy loss is about 1.7 MeV $g^{-1}cm^2$, therefore in the case of 1 Km of crossed rock whose density is equal to 2 g cm^{-3}, the muons lose about 0.5 TeV.

Carrying out the experiment

Connect the cable connectors of the two SP5622 to the tile inputs located on the rear panel of the SP5621 module. Power on the SP5621 module and start the acquisition via the front panel START button. When a charged particle crosses the black tile it's energy is converted into scintillation light. The photons which are produced are detected by the photosensor and converted into an electrical signal. The number of counts for each scintillator may be viewed via the SP5621 display. Select double scintillators coincidence mode via the related button on the front panel, and then select measurement integration time.

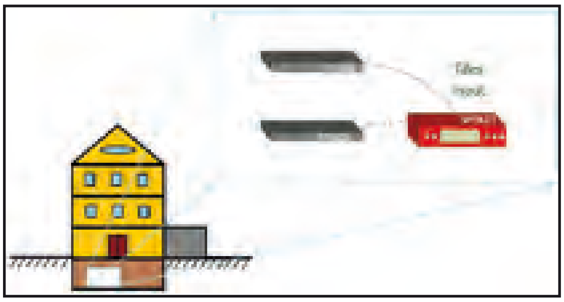

Experimental setup block diagram.

Before beginning acquisition the geometry of the tile must be determined. Be sure to keep this geometry for the duration of the experiment. Acquire data in a cave or solid structure. Then repeat acquisition, keeping the tiles in an identical geometric orientation, outside of the structure or cave.

Results

Students can estimate absorption extent by comparing the results of the measurements performed underground or inside a cave to measurements performed outdoors and without any solid obstructions. Additionally, if the thickness of the overburden material or structure is known then some hypothesis about the average density of the material can be determined.

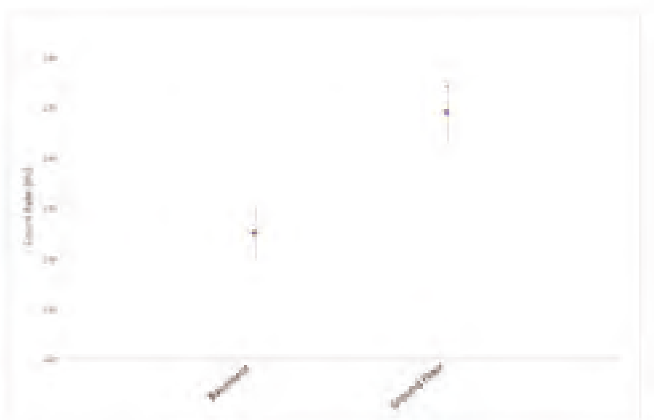

An example of absorption measurement has been performed in the basement of a building. As shown in the plot, the counting rate in thebasement is reduced by 14%

C.1.12 Solar Activity Monitoring

SG6220D

Difficulty	Execution Time	Data Analysis	Radioactive Sources
		NO	NO

Dedicated kit	
Description	pp.
SP5620CH Cosmic Hunter	182

Requirements

No other tools are needed.

Equipment

SP5620CH - Cosmic Hunter

Model	SP5621	SP5622 (x2)
Description	Coincidence Module 	Detection System 
	p. 182	p. 187

Purpose of the experiment

Observation of cosmic flux variation due to solar activity.

See the Application

Fundamentals

The intensity of the cosmic rays observed at the surface of the Earth is influenced and modulated by geomagnetic effects, by the location where the measurement takes place, and by the solar activity. There is a strong connection between the Sun and its effects on the Earth. The most visible effect relates to sunlight. But another effect relates to cosmic rays. Cosmic rays can be divided into two types: galactic cosmic rays and extragalactic cosmic rays (high-energy particles originating outside the solar system), and solar energetic particles (high-energy particles emitted by Solar activity). The solar wind which is continuously produced by the Sun is not constant due to changes in solar activity. The unsteady nature of the solar wind is responsible for the flux variations of incoming cosmic rays observed at the top of the Earth's atmosphere. Multiple studies have shown that the sunspot cycle is not correlated with cosmic rays detected. This is caused by the solar magnetic field being stronger at the solar maximum which lets fewer cosmic rays penetrate into the Earth's atmosphere. Hence, cosmic rays are at a minimum when solar activity is at a maximum.

Carrying out the experiment

Connect the cable connectors of the two SP5622 to the tile inputs located on the rear panel of the SP5621 module. Power on the SP5621 module and start the acquisition via the front panel START button. When a charged particle crosses the black tile it's energy is converted into scintillation light. The photons which are produced are detected by the photosensor and converted into an electrical signal. The number of counts for each scintillator may be viewed via the SP5621 display. Select double scintillators coincidence mode via the related button on the front panel, and then select measurement integration time. Because the acquisition of events takes place only in the presence of the coincidence, all such events coming from a cosmic particle that crosses only one scintillating tile will automatically be discarded.

Determine the system geometry and keep this geometry constant the duration of the measurement. Try to collect as much data as possible, over the period of days or even weeks, in order to perform and understand several theoretical considerations about the night-day trend, the solar wind, etc

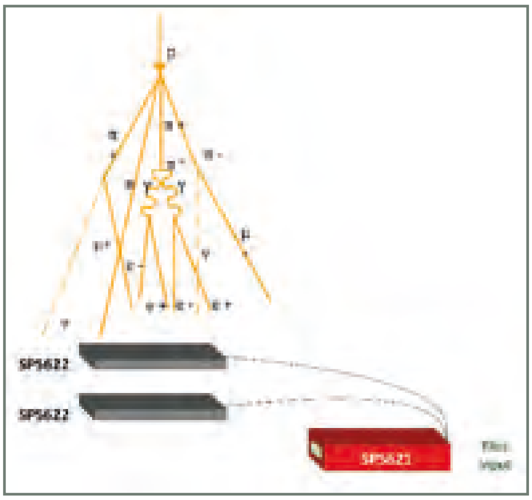

Experimental setup block diagram.

Results

This experiment leads the students to an intriguing and critical analysis of acquired data. Collected data can be compared to data from several websites which are designed allow the user to monitor the solar activity in real-time [RD7]. When comparing such data it is possible to find correlations between the trend of the cosmic rays detected by the system and the solar activity itself, the solar wind speed, the geomagnetic field, etc.

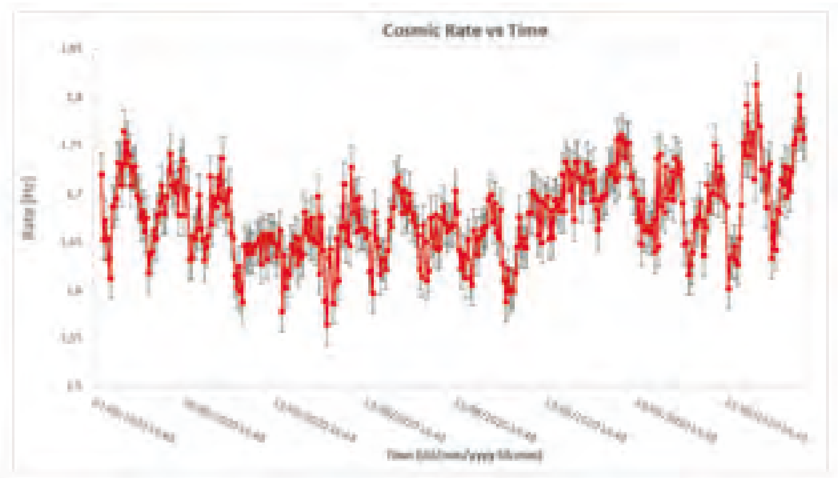

The typical cosmic rate night /day trend can be sometimes modified due to solar activity changes

C. Particle Physics

C.2 Photons

The Elementary Particles can be divided into fermions, which are matter or antimatter particles as quarks, antiquarks, electrons, antielectrons and so on, and bosons which generally are "force particles" that mediate interactions among fermions.

Photon is an elementary particle belonging to the boson family. It is massless, stable and it has no electric charge. As a boson, it has an integer spin and it obeys to Bose-Einstein Statistics.

The photon is the gauge boson for electromagnetism.

The experiments related the photons are performed thanks to the CAEN “Educational Photon Kit”.

Recommended kits

A SP5600E
Educational kits

see p. 179

B SP5600AN
Educational kits
PREMIUM

see p. 179

Experiment	SP5600E ★	SP5600AN ★
C.2.1 Quantum Nature of Light	•	•
C.2.2 Hands-on Photon Counting Statistics	•	•

★ The star indicates the recommended Kits while the yellow color highlights the Kits especially dedicated to the experiences of this Section.
If you are also interested in other experiences, the PREMIUM Kit is recommended.

C.2.1 Quantum Nature of Light

SG6221A

Dedicated kit	
Description	pp.
SP5600E Educational Photon Kit	179

Difficulty	Execution Time	Data Analysis	Radioactive Sources
1/5	1/5	NO	YES

Requirements

No other tools are needed.

Equipment

SP5600E - Educational Photon Kit

Model	SP5600	DT5720A	SP5601	SP5650C
Description	Power Supply and Amplification Unit 	Desktop Digitizer 250 MS/s 	LED Driver 	Sensor Holder for SP5600 with SiPM 
	p. 190	p. 190	p. 191	p. 191

Purpose of the experiment

Exploring the quantum nature of light thanks to bunches of photons emitted in a few nanoseconds by an ultra-fast LED and sensed by a state-of-the-art detector, a Silicon Photomultiplier (SiPM).

See the Application

Fundamentals

In the XVII century the concept of wave-particle duality was developed, starting from the wave nature of light postulated by Huygens to the Einstein Photoelectric Effect, which postulates light quanta existence.

A basic principle of quantum mechanics is complementarity: each quantum-mechanical object has both wave-like and particle-like properties. With this approach the photon is at the same time wave and particle, but they can never be observed simultaneously in the same experiment, not even if the uncertainty principle is successfully bypassed

Carrying out the experiment

Plug in the SP5650A into one channel of SP5600 and connect the analog output to DT5720A channel 0. Remove the protection cover of the SP5601 and SP5650A, spread the optical grease on both ends of the optical fiber and connect them. Use internal trigger mode on SP5601 and connect its trigger output on the DT5720A trigger IN. Connect via USB the modules to PC and power ON the devices. Use the default software values or optimize the parameters to acquire the light spectrum.

In the spectrum of the SiPM response to a light pulse, every entry corresponds to the digitized released charge, measured integrating the electrical current spike during a predefined time interval. The peaks correspond to different number of cells fired at the same time by incoming photons.

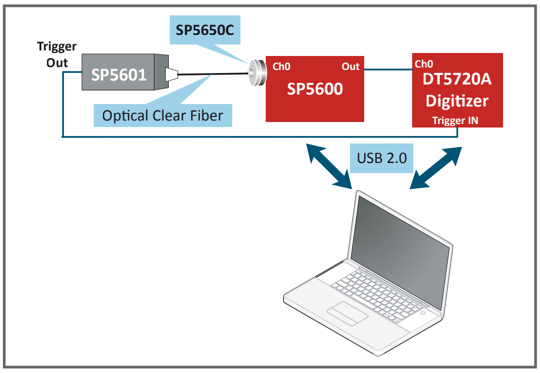

Experimental setup block diagram.

Results

This detector can count the number of impacting photons, shot by shot, allowing to observe how the light is composed by photons. Moreover the SiPM measures the light intensity simply by the number of fired cells.

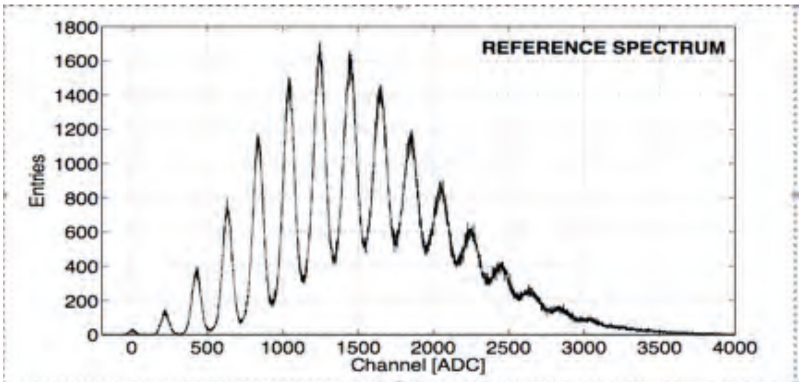

Spectrum of the photons emitted by a LED Driver and detected by a Silicon Photomultiplier.

This experiment is also possible with the following kits

B **SP5600AN**
Educational kits
★ **PREMIUM**

see p. 179

C.2.2 Hands-on Photon Counting Statistics

SG6222

Dedicated kit	
Description	**pp.**
SP5600E Educational Photon Kit	179

Difficulty	Execution Time	Data Analysis	Radioactive Sources
		NO	YES

Requirements

No other tools are needed.

Equipment

SP5600E - Educational Photon Kit

Model	SP5600	DT5720A	SP5601	SP5650C
Description	Power Supply and Amplification Unit 	Desktop Digitizer 250 MS/s 	LED Driver 	Sensor Holder for SP5600 with SiPM 
	p. 190	p. 190	p. 191	p. 191

Purpose of the experiment

pose of the experiment

Statistical properties of the light pulses emitted by a LED driver.

See the Application

Fundamentals

Spontaneous emission of light results from random decays of excited atoms and it is expected to be Poissonian. SiPM can count the number of impacting photons, shot by shot, opening up the possibility to apply basic skills in probability and statistics while playing with light quanta displaying the spectrum of the SiPM response to a high statistics of pulses. The spectrum is composed by a series of peaks, each ones correspond to different number of cells fired at the same time. Each peak is well separated and occurs with a probability linked at first order to the light intensity fluctuations. In SiPM the homogeneity of the response is quite high , however, since fired cells are randomly distributed in the detector sensitive area residual differences in the gain become evident broadening the peak.

A key point in the analysis technique was the estimation of the area underneath every peak, essential to reconstruct the probability density function of the emitted number of photons per pulse. An easy procedure is to consider each peak as a gaussian, so spectra recorded in response to photons impacting on the sensor can be seen as a superposition of Gaussians, each corresponding to a well defined number of fired cells. A binned Gaussian distribution of N_{pk} events may be written as:

$$y_i = y_{max} e^{\frac{-(x_i - x_0)^2}{2\sigma^2}}$$

where yi is the number of events in the bin centred on x_i and y_{max} is the peak value, measured in x_0. Since $y_{max} = N_{pk}/(\sigma\sqrt{2\pi})$, knowing the content of the bin centred in x_0 and estimating σ leads to N_{pk}. The standard deviation can also be calculated in a simple way by the Full Width at Half Maximum (FWHM), obtained searching for the position of the bins with a content equals to $y_{max}/2$ and presuming that FWHM = 2.355σ

Carrying out the experiment

Plug in the SP5650A into one channel of SP5600 and connect the analog output to DT5720A channel 0. Remove the protection cover of the SP5601 and SP5650A, spread the optical grease on both ends of the optical fiber and connect them. Use internal trigger mode on SP5601 and connect its trigger output on the DT5720A trigger IN. Connect via USB the modules to PC and power ON the devices. Use the default software values or optimize the parameters to perform the experiment.

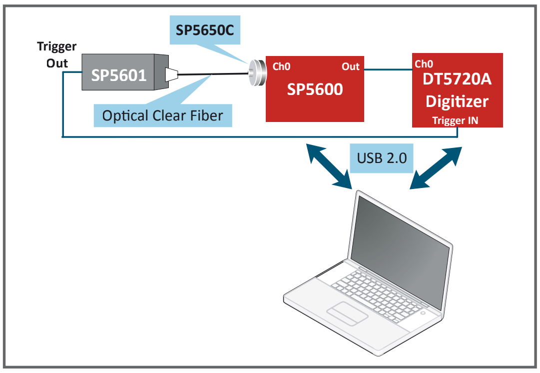

Experimental setup block diagram.

Results

The probability density function of the emitted number of photons per pulse can be estimated by the evaluation of the area underneath every peak.

Two different hypothesis can be investigated to evaluate the statistical model and mean number of photoelectrons: Model Independent (the mean photon number is nothing but the mean) and Poissonian hypothesis (mean value obtained by presuming a pure Poissonian behaviour and by referring to the probability P(0) of having no fired cell when the expected average value).

A complete and more complex analysis that include also considerations about detector structure is reported in the following section in the D.1 note.

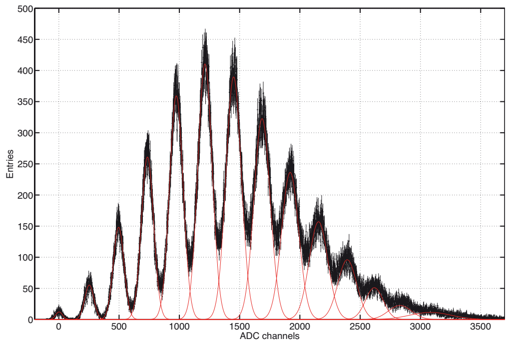

Photoelectron spectrum probing a LED source measured with a Hamamatsu SiPM. The Individual Gaussians are shown in red.

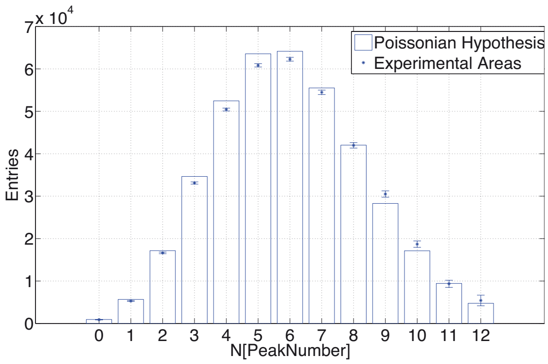

Data from the light spectrum compared to a simple Poissonian.

This experiment is also possible with the following kits

B SP5600AN
Educational kits
PREMIUM

see p. 179

D. Advanced Statistics based on Silicon Photomultiplier Detectors

D. Advanced Statistics based on Silicon Photomultiplier Detectors

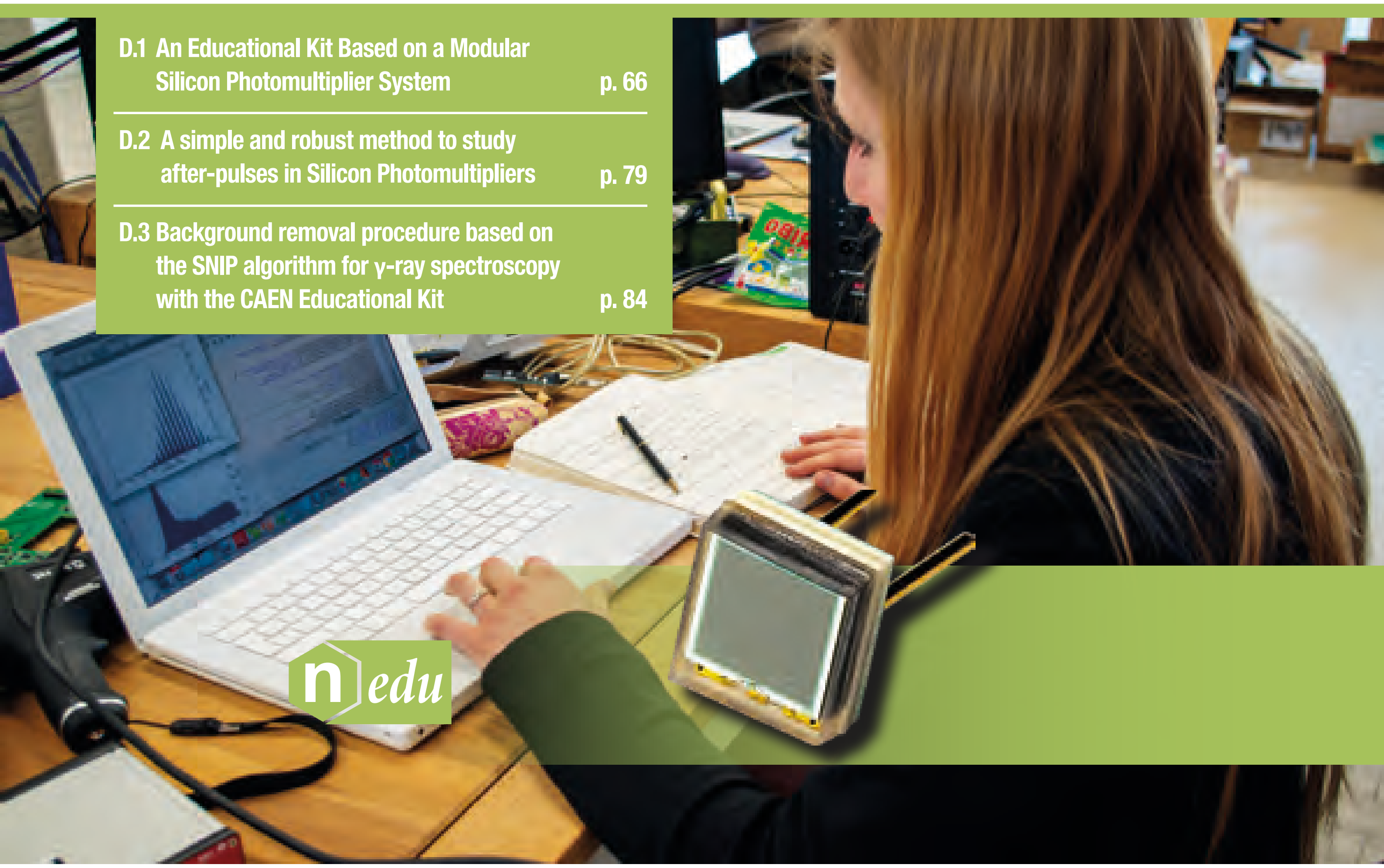

A series of experiments covering several applications has been carried out and are presented in this section through detailed Educational Notes. The collaboration with the University of Insubria allows to offer experiments based on Silicon Photo-Multiplier detectors for advanced laboratories using the latest instrumentation generation developed by CAEN for the major experiments Worldwide.

For every topic, an accompanying suite is being developed, including an instructor' guide, indications on the analysis and a library of routines in MATLAB, a platform widely distributed in the academic community.

EDUCATIONAL KIT - “PREMIUM VERSION”

Model.	Description
SP5600	Power Supply and Amplification Unit
DT5720A	Desktop Digitizer 250 MS/s
SP5601	LED Driver
SP5650C	Sensor Holder for SP5600 with HAMAMATSU SiPM
SP5606	Spectrometer
SP5607	Absorption Tool
A315	Splitter
SP5608	Scintillating tile coupled to SiPM

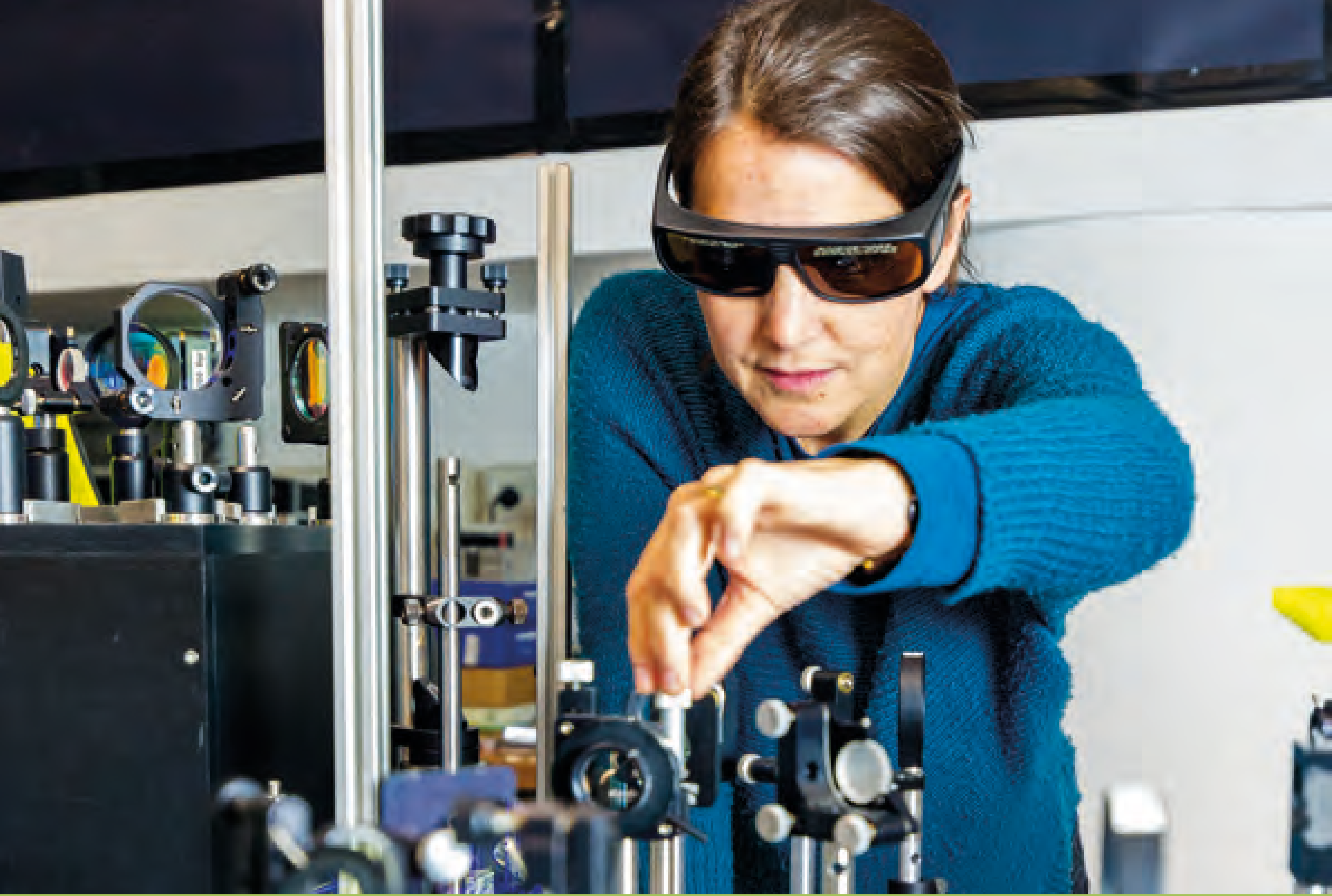

D.1 An Educational Kit Based on a Modular Silicon Photomultiplier System

ED3127

Equipment

SP5600E - Educational Photon Kit

Model	SP5600	DT5720A	SP5601	SP5650A
Description	Power Supply and Amplification Unit	Desktop Digitizer 250 MS/s	LED Driver	Sensor Holder for SP5600 with SiPM
				
	p. 190	p. 190	p. 191	p. 191

Related Experiment
C.2.1
A.1.1

Ordering Options

Equipment	
Code	**Description**
WK5600XEAAAA	SP5600E - Educational Photon Kit
or the all inclusive Premium Version	
WK5600XANAAA	SP5600AN - Educational Kit - Premium Version

Data analysis code developed in MATLAB is available on request.

An Educational Kit Based on a Modular Silicon Photomultiplier System

Valentina Arosio, Massimo Caccia, Valery Chmill, Amedeo Ebolese, Marco Locatelli, Alexander Martemiyanov, Maura Pieracci, Fabio Risigo, Romualdo Santoro and Carlo Tintori

Abstract—**Silicon Photo-Multipliers (SiPM) are state of the art light detectors with unprecedented single photon sensitivity and photon number resolving capability, representing a breakthrough in several fundamental and applied Science domains. An educational experiment based on a SiPM set-up is proposed in this article, guiding the student towards a comprehensive knowledge of this sensor technology while experiencing the quantum nature of light and exploring the statistical properties of the light pulses emitted by a LED.**

Keywords*—*Silicon Photo-Multipliers, Photon Statistics, Educational Apparatus

I. Introduction

EXPLORING the quantum nature of phenomena is one of the most exciting experiences a physics student can live. What is being proposed here has to do with light bullets, bunches of photons emitted in a few nanoseconds by an ultra-fast LED and sensed by a state-of-the-art detector, a Silicon Photo-Multiplier (hereafter, SiPM). SiPM can count the number of impacting photons, shot by shot, opening up the possibility to apply basic skills in probability and statistics while playing with light quanta. After an introduction to the SiPM sensor technology (Section II), the basics of the statistical properties of the random process of light emission and the sensor related effects are introduced (Section III). The experimental and data analysis techniques are described in Section IV, while results and discussions are reported in Section V.

II. Counting photons

SiPMs are cutting edge light detectors essentially consisting of a matrix of photodiodes with a common output and densities up to $10^4/mm^2$. Each diode is operated in a limited Geiger-Muller regime in order to achieve gains at the level of $\approx 10^6$ and guarantee an extremely high homogeneity in the cell-to-cell response. Subject to the high electric field in the depletion zone, initial charge carriers generated by an absorbed photon or by thermal effects trigger an exponential charge multiplication by impact ionization, till when the current spike across the quenching resistance induces a drop in the operating voltage, stopping the process [1], [3], [4]. SiPM can be seen as a collection of binary cells, providing altogether an information about the intensity of the incoming light by counting the number of fired cells.

M. Caccia, V. Chmill, A. Ebolese, A. Martemiyanov, F. Risigo and R. Santoro are with the Dipartimento di Scienza e Alta Tecnologia, Universita' degli Studi dell'Insubria, 22100, Como, Italy (e-mail: massimo.caccia@uninsubria.it).

M. Locatelli, M. Pieracci and C. Tintori are with the CAEN S.p.A., 55049, Viareggio, Italy (e-mail: m.locatelli@caen.it).

Fig. 1 shows the typical response by a SiPM to a light pulse: traces correspond to different numbers of fired cells, proportional to the number of impinging photons. Because of the high gain compared to the noise level, traces are well separated, providing a photon number resolved detection of the light field.

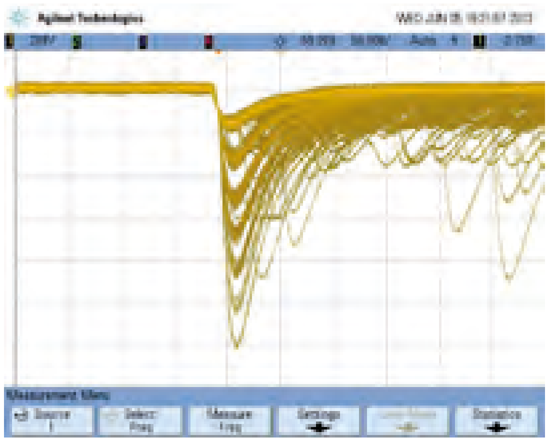

Fig. 1: Response of a SiPM Hamamatsu MPPC S10362-11-100C illuminated by a light pulse.

This is also shown in Fig. 2, displaying the spectrum of the SiPM response to a high statistics of pulses: every entry corresponds to the digitized released charge, measured integrating the electrical current spike during a pre-defined time interval. The peaks correspond to different number of cells fired at the same time. Each peak is well separated and occurs with a probability linked at first order to the light intensity fluctuations. An analysis of the histogram is revealing other significant characteristics:

- The peak at 0 corresponds to no detected photons and its width measures the noise of the system, i.e. the stochastic fluctuations in the output signal in absence of any stimulus. In the displayed histogram, σ_0 = 29±1 ADC channels.
- The peak at 1 detected photon has a width σ_1 = 38.1±0.4 ADC channels, by far exceeding σ_0. The extra

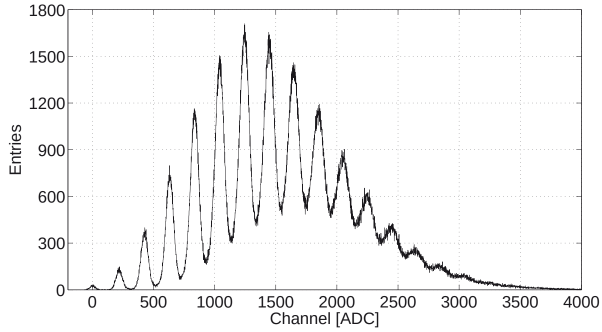

Fig. 2: Photoelectron spectrum probing a LED source measured with a Hamamatsu MPPC S10362-11-100C at a bias voltage of $70.3V$ and temperature of 25^oC.

contribution may be related to the fact that not all of the cells were born equal. In SiPM the homogeneity of the response is quite high [5], [6], however, since fired cells are randomly distributed in the detector sensitive area residual differences in the gain become evident broadening the peak.

- As a consequence the peak width is increasing with the number N of fired cells with a growth expected to follow a $\sqrt{N}$ law, eventually limiting the maximum number *M* of resolved peaks.

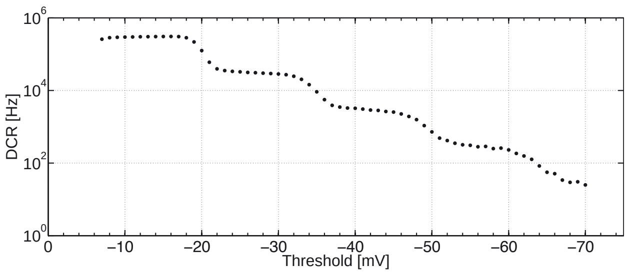

Fig. 3: Measurement of the DCR of the SiPM performed at 25^oC.

The detector working conditions can be optimized to maximize *M*, properly tuning the bias voltage V_{bias} and balancing competing effects. On one hand, the peak-to-peak distance is linked to the single cell gain and it is expected to grow linearly with the over-voltage as:

$$Gain = \frac{C\ \Delta V}{q_e}, \tag{1}$$

where $\Delta V = V_{bias} - V_{Breakdown}$, C is the diode capacitance of the single cell and q_e the electron charge [3]. Effects broadening the peaks may grow faster dumping the expected resolution. Among these effects it is worth mentioning Dark Counts, Optical Cross-Talk and After-Pulsing:

- Free charge carriers may also be thermally generated. Results are spurious avalanches (Dark Counts) occurring randomly and independently from the illumination field. The Dark Count Rate (DCR) does depend from several factors: substrate, processing technology, sensor design and operating temperature [4]. The over-voltage has an impact since the junction thickness volume grows with it together with the triggering probability, namely the probability that a charge carrier develops an avalanche [4], [5]. The DCR can be measured in different ways. A *Stair Case Plot* is presented in Fig. 3 where the output from a sensor is compared to the threshold of a discriminator and the rate with which the threshold is exceeded is counted. A typical DCR is about $0.5\ MHz/mm^2$.

- Dark Counts may be considered as statistically independent. However, optical photons developed during an avalanche have been shown to trigger secondary avalanches [4] involving more than one cell into spurious pulses. This phenomenon is named Optical Cross-Talk (OCT). The OCT is affected by the sensor technology [4], [7], [8], [9] and strongly depends on the bias voltage increasing the triggering probability and the gain forming the optical photon burst. The OCT can be measured by the ratio of the Dark Counts frequencies for pulses exceeding the 0.5 and 1.5 levels of the single cell amplitude, namely:

$$OCT = \frac{\nu_{1.5pe}}{\nu_{0.5pe}}. \tag{2}$$

The OCT typically ranges between 10% and 20% [5], [9], [10].

- Charge carriers from an initial avalanche may be trapped by impurities and released at later stage resulting in delayed avalanches named After-Pulses. For the detectors in use here, an After-Pulse rate at about the 25% level has been reported for an overvoltage $\Delta V = 1\ V$, with a linear dependence on V_{bias} and a two-component exponential decay time of 15 ns and 80 ns [5].

Dark Counts, Optical Cross-Talk and After-Pulses occur stochastically and introduce fluctuations in the multiplication process that contribute to broaden the peaks in the spectrum. An exhaustive study of this effect, also known as Excess Noise Factor (ENF), exceeds the goals of this work and will not be addressed here (see for example [3], [6], [8] and [12]). However, the resolving power that will be introduced in the following may be considered a figure of merit accounting for the ENF and measuring the ability to resolve the number of detected photons.

III. Photon Counting Statistics

Spontaneous emission of light results from random decays of excited atoms. Occurrences may be considered statistically independent, with a decay probability within a time interval

Δt proportional to Δt itself. Being so, the statistics of the number of photons emitted within a finite time interval T is expected to be Poissonian, namely:

$$P_{n,\mathrm{ph}} = \frac{\lambda^n e^{-\lambda}}{n!}, \quad (3)$$

where λ is the mean number of emitted photons.

The detection of the incoming photons has a stochastic nature as well, at the simplest possible order governed by the Photon Detection Probability (PDE) η, resulting in a Binomial probability to detect d photons out of n:

$$B_{d,n}(\eta) = \left(\begin{array}{c} n \\ d \end{array} \right) \eta^d (1-\eta)^{n-d} \ . \quad (4)$$

As a consequence, the distribution $P_{d,\mathrm{el}}$ of the number of detected photons is linked to the distribution $P_{n,\mathrm{ph}}$ of the number of generated photons by

$$P_{d,\mathrm{el}} = \sum_{n=d}^{\infty} B_{d,n}(\eta) P_{n,\mathrm{ph}} \ . \quad (5)$$

However, the photon statistics is preserved and $P_{d,\mathrm{el}}$ is actually a Poissonian distribution of mean value $\mu = \lambda\eta$ [9], [10]. For the sake of completeness, the demonstration is reported in Appendix A.

Detector effects (especially OCT and After-Pulses) can actually modify the original photo-electron probability density function, leading to significant deviations from a pure Poisson distribution. Following [9] and [10], OCT can be accounted for by a parameter ϵ_{XT}, corresponding to the probability of an avalanche to trigger a secondary cell. The probability density function of the number of fired cells, the random discrete variable m, can be written at first order as:

$$P \otimes B = \sum_{k=0}^{floor(m/2)} B_{k,m-k}(\epsilon_{XT}) P_{m-k}(\mu), \quad (6)$$

where *floor* rounds $m/2$ to the nearest lower integer and $B_{k,m-k}(\epsilon_{XT})$ is the binomial probability for $m-k$ cells fired by a photon to generate k extra hit by OCT. $P \otimes B$ is characterized by a mean value and variance expressed as:

$$\bar{m}_{P\otimes B} = \mu(1+\epsilon_{XT}) \qquad \sigma^2_{P\otimes B} = \mu(1+\epsilon_{XT}). \quad (7)$$

In order to perform a more refined analysis, the probability density function of the total number of detected pulses can be calculated taking into account higher order effects [13]. The result is achieved by assuming that every primary event may produce a single infinite chain of secondary pulses with the same probability ϵ_{XT}. Neglecting the probability for an event to trigger more than one cell, the number of secondary hits, described by the random discrete variable k, follows a geometric distribution with parameter ϵ_{XT}:

$$G_k(\epsilon_{XT}) = {\epsilon_{XT}}^k (1-\epsilon_{XT}) \qquad for \quad k = 0, 1, 2, 3.... \quad (8)$$

The number of primary detected pulses is denoted by the random discrete variable *d* and belongs to a Poisson distribution with mean value μ. As a consequence, the total number of detected pulses *m* represents a compound Poisson process given by:

$$m = \sum_{i=1}^{d} (1+k_i). \quad (9)$$

Then, the probability density function of m is expressed as a compound Poisson distribution:

$$P \otimes G = \frac{e^{-\mu} \sum_{i=0}^{m} B_{i,m} \mu^i (1-\epsilon_{XT})^i {\epsilon_{XT}}^{m-i}}{m!}, \quad (10)$$

where

$$B_{i,m} = \begin{cases} 1 & \text{if } i = 0 \text{ and } m = 0 \\ 0 & \text{if } i = 0 \text{ and } m > 0 \\ \frac{m!(m-1)!}{i!(i-1)!(m-i)!} & \text{otherwise} \end{cases}$$

The mean value and the variance of the distribution are respectively given by:

$$\bar{m}_{P\otimes G} = \frac{\mu}{1-\epsilon_{XT}} \qquad \sigma^2_{P\otimes G} = \frac{\mu(1+\epsilon_{XT})}{(1-\epsilon_{XT})^2}. \quad (11)$$

These relations can be calculated referring to the definition of the probability generating function and exploiting its features [13]. The full demonstration is available in Appendix B.

IV. Experimental techniques

In this section the experimental set-up and the analysis methods are presented. The optimization of the working point of a SiPM is addressed together with the recorded spectrum analysis technique.

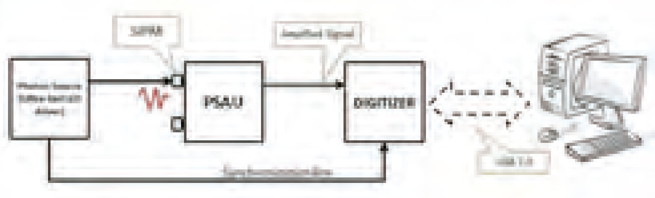

Fig. 4: Schematic layout of the experimental set-up.

A. Set-up and measurements

The experimental set-up is based on the CAEN Silicon Photomultiplier Kit. The modular plug and play system contains:

- The Two channel SP5600 CAEN Power Supply and three-stage Amplification Unit (PSAU) [14], with SiPM embedding head unit. The PSAU integrates a leading edge discriminator per channel and coincidence logic.

- The two channels DT5720A CAEN Desktop Digitizer, sampling the signal at 250 MS/s over a 12 bit dynamic range. The available firmware enables the possibility to perform charge Integration (DPP-CI), pulse shape discrimination (DPP-PSD) and advanced triggering [15].
- The ultra-fast LED (SP5601 [16]) driver emitting pulses at 400 nm with FWHM of 14 nm. Pulses are characterized by an exponential time distribution of the emitted photons with a rising edge at sub-nanosecond level and a trailing edge with $\tau \approx 5\ ns$. The driver is also providing a synchronization signal in NIM standard.

In the current experiments the SiPM that was used is a Multi Pixel Photon Counter (MPCC) S10362-11-100C produced by HAMAMATSU Photonics[1] (see Table I).

TABLE I: Main characteristics of the SiPM sensor (Hamamatsu MPPC S10362-11-100C) at a temperature of 25^{o}C

Number of Cells:	100
Area:	$1 \times 1\ mm^2$
Diode Dimension:	$100\ \mu m \times 100\ \mu m$
Breakdown Voltage:	69.2V
DCR:	600 kHz at 70.3V
OCT:	20% at 70.3V
Gain:	3.3×10^6 at 70.3V
PDE ($\lambda = 440nm$):	75% at 70.3V

The block diagram of the experimental set-up is presented in Fig.4 with light pulses conveyed to the SiPM sensor by an optical fiber.

The area of the digitized signal is retained as a figure proportional to the total charge generated by the SiPM in response to the impacting photons. The integration window (or *gate*) is adjusted to match the signal development and it is synchronized to the LED driver pulsing frequency.

The proposed experimental activities start with the optimal setting of the sensor bias voltage, defined maximizing the resolving power defined as:

$$R = \frac{\Delta_{pp}}{\sigma_{gain}}, \quad (12)$$

where Δ_{pp} is the peak-to-peak distance in the spectrum and σ_{gain} accounts for the single cell gain fluctuations:

$$\sigma_{gain} = (\sigma_1^2 - \sigma_0^2)^{1/2}, \quad (13)$$

being $\sigma_{0,1}$ the standard deviations of the 0- and 1-photoelectron peaks [17]. R is a figure of merit measuring the capability to resolve neighboring peaks in the spectrum. In fact, following the Sparrow criterion [18] according to which two peaks are no longer resolved as long as the dip half way between them ceases to be visible in the superposed curves, the maximum number N_{max} of identified peaks is given by:

$$N_{max} < \frac{R^2}{4}, \quad (14)$$

where it has been assumed the width of the peaks to grow as the squared root of the number of cells (as confirmed by the data reported in Fig. 5).

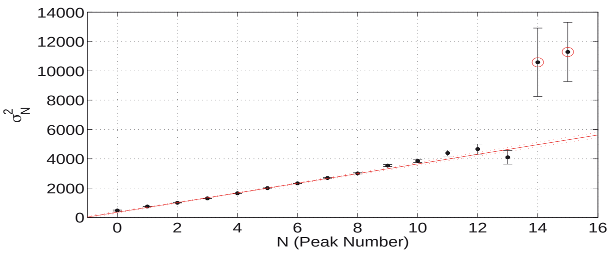

Fig. 5: Peaks width for the spectrum Fig.2 by a multi-Gaussian fit. The dash lines represent the 95% C.L. for the fit, shown with the solid line. The circles indicate the outliers.

The outliers, the data points that are statistically inconsistent with the rest of the data, are identified with the Thompson Tau method [19] and discarded.

A typical plot of the resolving power versus the bias voltage is presented in Fig. 6. The optimal biasing value corresponds to the maximum resolution in the plot and it is used as a working point. After the sensor calibration, spectra for different light intensities are recorded and analyzed as reported below.

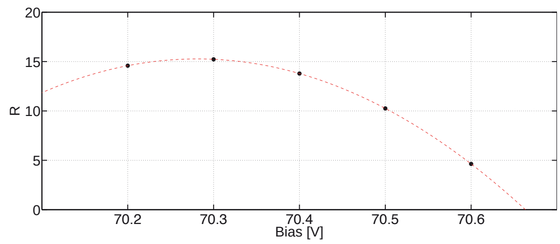

Fig. 6: Scan of the resolution power R as a function of the bias voltage at fixed temperature (25^{o}C) and light intensity. The working point is given by a polynomial fit and equal to 70.28 V.

TABLE II: Acquisition parameters for the reference run presented in this work.

V_{bias}[V]	GateWidth [ns]	Trigger frequency [kHz]	Temperature [C]
70.3	300	100	25.0

B. Multi-peak spectrum analysis

Spectra recorded in response to photons impacting on the sensor can be seen as a superposition of Gaussians, each

[1] http://www.hamamatsu.com/.

corresponding to a well defined number of fired cells. The key point in the analysis technique is the estimation of the area underneath every peak, allowing the reconstruction of the probability density functions.

Initially, areas can be estimated by a *Pick&Play* (hereafter, P&P) procedure on the spectrum. In fact, a binned Gaussian distribution of N_{pk} events may be written as:

$$y_i = y(x_i) = y_{max} e^{-\frac{(x_i - x_0)^2}{2\sigma^2}}, \qquad (15)$$

where $y(x_i)$ is the number of events in the bin centered on x_i and y_{max} is the peak value, measured in x_0. Since $y_{max} = N_{pk}/(\sigma\sqrt{2\pi})$, knowing the content of the bin centered in x_0 and estimating σ leads to N_{pk}. The standard deviation can also be calculated in a simple way by the Full Width at Half Maximum ($FWHM$), obtained searching for the position of the bins with a content equals to $y_{max}/2$ and presuming that $FWHM = 2.355 \times \sigma$. Advantages and limitations of this method are quite obvious: its applicability is straightforward and essentially requires no tool beyond a Graphical User's Interface (*GUI*) for the control of the set-up; on the other hand, it can be applied only to peaks with a limited overlap and uncertainties can only be obtained by repeating the experiment. In order to overcome these limitations, a *Multi-Gaussian Fit* (MGF) procedure was implemented in MATLAB to analyze the full spectrum, according to the following work flow:

- **Initialization**. Robustness and efficiency of minimization algorithms is guaranteed by having an educated guess of the parameter values and by defining boundaries in the parameter variation, a procedure increasingly important as the number of parameters grow. Initial values are provided in an iterative procedure:
  - ○ The user is required to identify by pointing & clicking on the spectrum the peak values and their position for 3 neighboring Gaussians, fitted to improve the estimate.
  - ○ Initial values for every Gaussian are estimated by relying on the peak-to-peak distance from the previous step, presuming the signal from the 0-cell peak to be centered in the origin of the horizontal scale and assuming the standard deviation grows as the squared root of the number of cells.
- **Fit**. Spectra are fitted to a superposition of Gaussians with a non-linear χ^2 minimization algorithm presuming binomial errors in the content of every bin. The most robust convergence over a large number of tests and conditions have been empirically found bounding parameters to vary within 20% of the initial value for the peak position, 30% for the area and 50% for the standard deviation.

V. RESULTS AND DISCUSSIONS.

Exemplary spectra for three light intensities were recorded and the raw data distributions are shown in Fig. 7, where the horizontal scale in ADC channels measures the integrated charge in a pre-defined gate. In the following, the analysis steps are detailed for the distribution corresponding to the highest mean photon number, hereafter identified as the *Reference Spectrum*. Remaining spectra will be used to assess the robustness of the approach and the validity of the model, with the results summarized at the end of the section.

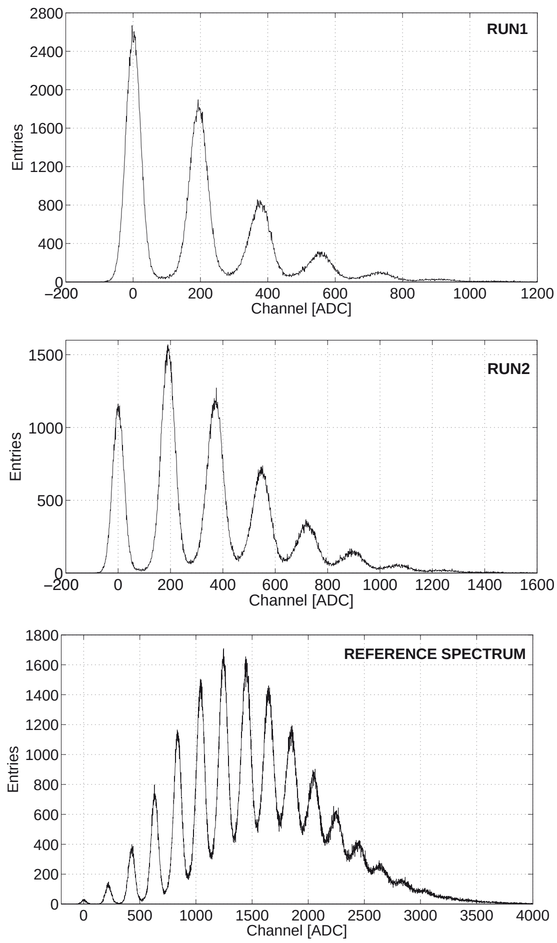

Fig. 7: Exemplary spectra. The mean number μ_{MI} of photo-electrons is measured to be 1.080 ± 0.002 (RUN1), 1.994 ± 0.003 (RUN2) and 7.81 ± 0.01 (Reference Spectrum).

Spectra are seen as a superposition of Gaussians, with parameters estimated according to the methods introduced in Section IV. The outcome of the procedures for the *Reference Spectrum* is reported in Table III for the P&P and the MGF procedures. For the former, uncertainties in the estimated parameters are the standard deviations from five data sets acquired in identical conditions while for the latter errors result from the fitting procedure (Fig. 8).

The characteristics of the experimental distribution can initially be studied referring to the mean number of fired cells. A *Model Independent* (MI) estimate is provided by:

$$\mu_{MI} = \frac{\overline{ADC}}{\overline{\Delta_{pp}}}, \tag{16}$$

where

$$\overline{ADC} = \frac{\Sigma_i y_i ADC_i}{\Sigma_i y_i} \tag{17}$$

is the mean value of the experimental distribution (being y_i the number of events for the i^{th} bin) and $\overline{\Delta_{pp}}$ is the mean peak-to-peak distance, defining the gauge to convert values in ADC channels to number of cells.

TABLE III: Peak position, width and experimental probability of having N photo-electrons from the Pick&Play (P&P) procedure, compared to the results from the Multi-Gaussian Fit (MGF). The results are for the reference spectrum.

	$PeakPosition[ADC]$		$PeakWidth[ADC]$		$Exp.\ Probability$	
N	$P\&P$	MGF	$P\&P$	MGF	$P\&P$	MGF
0	3 ± 1	2.1 ± 0.9	22 ± 1	21.7 ± 0.8	0.092 ± 0.006	0.09 ± 0.01
1	220 ± 1	220.1 ± 0.4	25 ± 1	27.3 ± 0.3	0.53 ± 0.02	0.56 ± 0.01
2	427 ± 1	428.0 ± 0.3	30 ± 1	31.5 ± 0.2	1.75 ± 0.06	1.86 ± 0.02
3	635 ± 1	633.6 ± 0.2	32 ± 1	36.0 ± 0.2	3.8 ± 0.1	4.17 ± 0.02
4	838 ± 2	837.5 ± 0.2	38 ± 1	40.5 ± 0.2	7.0 ± 0.2	7.21 ± 0.04
5	1044 ± 2	1041.3 ± 0.2	41 ± 1	44.7 ± 0.2	9.9 ± 0.2	10.30 ± 0.04
6	1247 ± 2	1243.7 ± 0.2	45 ± 1	48.2 ± 0.2	12.2 ± 0.3	12.67 ± 0.05
7	1449 ± 3	1445.6 ± 0.2	50 ± 3	51.9 ± 0.3	13.4 ± 0.8	13.43 ± 0.06
8	1650 ± 4	1645.8 ± 0.3	57 ± 2	54.8 ± 0.4	13.3 ± 0.5	12.71 ± 0.07
9	1853 ± 4	1846.4 ± 0.4	67 ± 2	59.5 ± 0.6	12.9 ± 0.4	11.2 ± 0.1
10	$--$	2046.5 ± 0.6	$--$	62.0 ± 0.9	$--$	8.7 ± 0.1
11	$--$	2245 ± 1	$--$	66 ± 2	$--$	6.6 ± 0.2
12	$--$	2445 ± 1	$--$	68 ± 2	$--$	4.4 ± 0.2
13	$--$	2632 ± 2	$--$	65 ± 3	$--$	2.4 ± 0.1

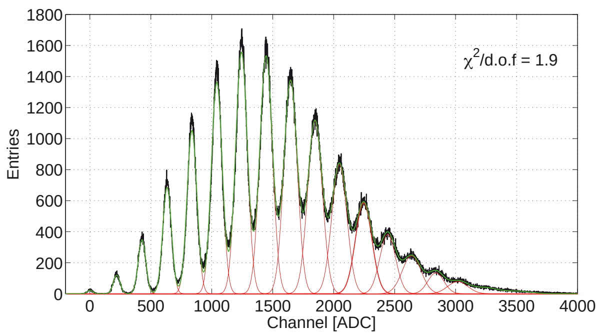

Fig. 8: Outcome of the MGF procedure. Individual Gaussians are in red, while their superposition is displayed in green. The $\chi^2/d.o.f.$ measures the fit quality.

The value of μ_{MI} can be compared to what is estimated presuming a pure Poissonian behaviour and referring to the probability $P(0)$ of having no fired cell when the expected average value is μ_{ZP}, where ZP stands for *Zero Peak*:

$$\mu_{ZP} = -ln(P(0)) \ = -ln\left(\frac{A_0}{A_{tot}}\right), \tag{18}$$

being A_0 the area underneath the first peak of the spectrum and A_{tot} the total number of recorded events. Results are shown in Table IV.

TABLE IV: Estimates of the mean number of fired cells by the average value of the experimental distribution and from the probability of having none, assuming an underlying Poissonian distribution. Errors result from the uncertainties in the peak-to-peak distance and in the area of the zero-cell peak.

	μ_{MI}	μ_{ZP}
P&P	7.6 ± 0.3	6.99 ± 0.06
MGF	7.81 ± 0.01	7.08 ± 0.03

The P&P procedure shows a good compatibility with the hypothesis, while the MGF procedure, due to the smaller errors, presents an evident discrepancy.

The question can be further investigated considering the full distribution and comparing the experimental probability density function with the assumed model distribution by a χ^2 test, where:

$$\chi^2 = \sum_{k=0}^{Npeaks-1} w_k \times (A_{obs,k} - A_{model,k})^2, \tag{19}$$

being $A_{obs,k}$ the number of events in the k^{th} peak of the distribution, $A_{model,k}$ the corresponding number estimated from the reference model and w_k the weights accounting for the uncertainties in the content of every bin. Presuming a Poissonian distribution with mean value μ_{MI}, the returned values of the $\chi^2/d.o.f.$ are ≈ 20 for the $P\&P$ procedure and ≈ 300 for the MGF. The $\chi^2/d.o.f.$ values, even assuming μ as a free parameter, exceeds the 99% C.L. for both methods confirming that the experimental distribution may not be adequately described by a pure Poissonian model.

As a further step, the spectra were compared to the $P \otimes G$ distribution model introduced in Section III, Eq. 10, where the actual number of fired cells results from avalanches triggered by the incoming photons and by the optical cross-talk. The optimal values of the model parameters, namely the cross-talk probability ϵ_{XT} and the mean value μ of the distribution of cells fired by photons, are determined by a grid search according to the following iterative procedure [20] :

- the $\chi^2/d.o.f.$ surface, henceforth referred to as Σ, is sliced with planes orthogonal to the ϵ_{XT} dimension, at values $\tilde{\epsilon}_{XT}$ changed with constant step;
- in each slice, the minimum of the $\Sigma(\tilde{\epsilon}_{XT}, \mu))$ curve is searched and the value $\mu_{min,0}$ corresponding to the minimum is identified;
- the $\Sigma(\epsilon_{XT}, \mu_{min,0})$ curve is scanned and the position ϵ^*_{XT} of the minimum is identified by a local parabolic

fit, to overcome the limitations by the choice of the step in the grid;

- the procedure is repeated for $\Sigma(\epsilon^*_{XT}, \mu)$ vs μ, leading to the determination of the minimum in μ^*.

This method leads to estimate the optimal parameters μ^* and ϵ^*_{XT} by the minimization of the $\chi^2/d.o.f.$ surface for the two variables μ and ϵ_{XT} independently. The surface Σ and the $\Sigma(\epsilon^*_{XT}, \mu)$ and $\Sigma(\epsilon_{XT}, \mu^*)$ curves are shown in Fig. 9. Uncertainties are calculated assuming a parabolic shape of the $\chi^2/d.o.f.$ curves, leading to variances estimated by the inverse of the coefficient of the quadratic term [20], [21]. The results for the reference spectrum are $\mu^* = 7.06 \pm 0.02$ and $\epsilon^*_{XT} = 0.090 \pm 0.004$.

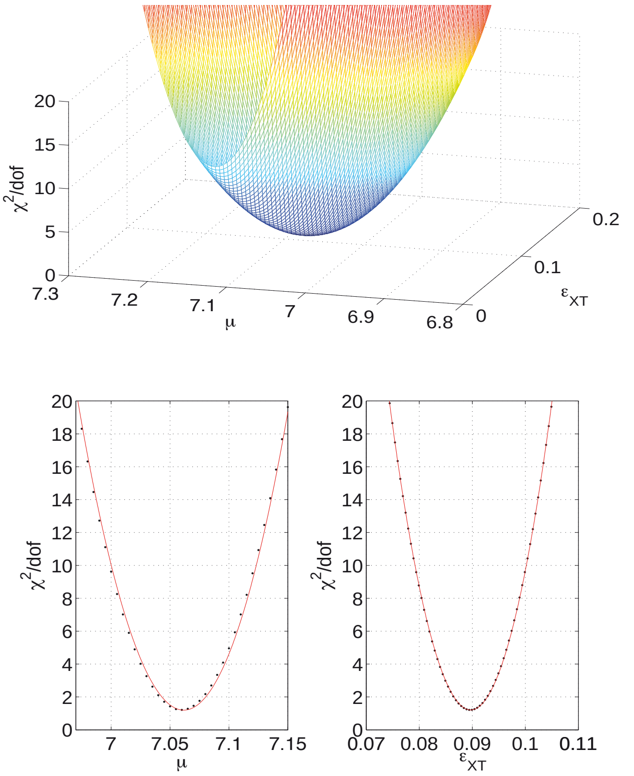

Fig. 9: $\chi^2/d.o.f.$ surface (top panel) and parabolic behavior nearby its minimum (bottom).

In order to account for the two-parameter correlation in the calculation of the uncertainties, it is worth to referring to the *confidence region* of the joint probability distribution [22] [23]. When the parameters are estimated minimizing the χ^2 distribution, confidence levels correspond to regions defined by iso-χ^2 curves. For two parameters, the region assumes an elliptic shape around the Σ minimum, χ^2_{min}. The Σ contour at the constant value of $\chi^2_{\text{min}} + 1$ plays a crucial role due to its specific properties. In fact, the resulting ellipse contains $\sim$ 38.5% of the joint parameter probability distribution and its projections represent the $\sim$ 68.3% of confidence interval for each parameter (σ_1 and σ_2). In addition, the correlation ρ among the parameters may be written as:

$$\rho = \frac{\sigma_1^2 - \sigma_2^2}{2\sigma_1\sigma_2} \tan 2\theta, \tag{20}$$

where θ represents the counter-clockwise rotation angle of the ellipse. The detailed demonstration is reported in Appendix C.

In this specific case, the χ^2_{min} value is determined evaluating the $\chi^2/d.o.f.$ surface at the point of coordinates (μ^*, ϵ^*_{XT}) while the Σ contour at $\chi^2_{\text{min}} + 1$ is shown in Fig.10 (black crosses). The fit curve (red line) returns the value of the ellipse center (μ^0,ϵ^0_{XT}) (black circle). The projections of the ellipse on the μ and ϵ_{XT} axes are the uncertainties on the two values. The results for the reference spectrum are μ^0 = 7.06 ± 0.05 and $\epsilon^0_{XT} = 0.09 \pm 0.01$. Comparing these values with (μ^*,ϵ^*_{XT}) (black cross) it is possible to infer that the correlation does not affect the determination of the parameter central values while increases their standard deviation by a factor of about two. As a consequence, μ^0 and ϵ^0_{XT} with their uncertainties are retained as the best estimate of the model parameter values.

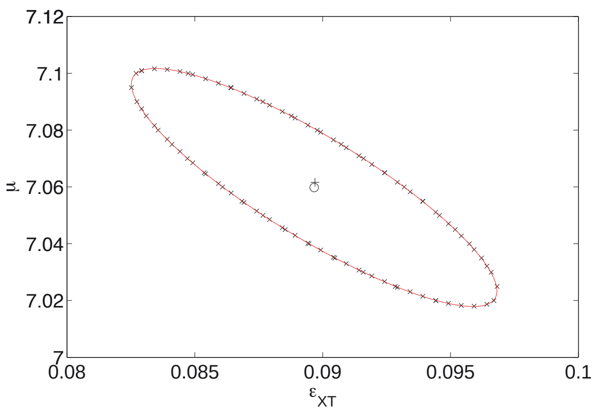

Fig. 10: The point of the $\chi^2/d.o.f.$ surface at the constant value of $\chi^2_{\text{min}} + 1$ are the black crosses, the fit curve is the red line, the center of the ellipse (μ^0,ϵ^0_{XT}) is represented with the black circle and the point (μ^*,ϵ^*_{XT}) is shown with the black cross.

The angle returned by the ellipse fit is used to calculate the correlation ρ between the two parameters through the equation (20). The result for the reference spectrum is $\rho = -0.8$. Then, applying the relation (11) and exploiting the full covariance matrix, the value and the uncertainty of the mean of the $P \otimes G$ model can be obtained. For the reported spectra it results to be 7.76 ± 0.03.

The result of the fit to the data distribution with the $P \otimes G$ probability function is displayed in Fig. 11, showing an excellent agreement between data and model.

The quality of the result is confirmed by the data reported in Table V, where the mean value of the Poissonian distribution obtained by the ellipse fit (μ^0) and by the *Zero Peak* are compared, together with a comparison between μ_{MI} and $\mu^0/(1 - \epsilon^0_{XT})$, the mean value of the $P \otimes G$ distribution.

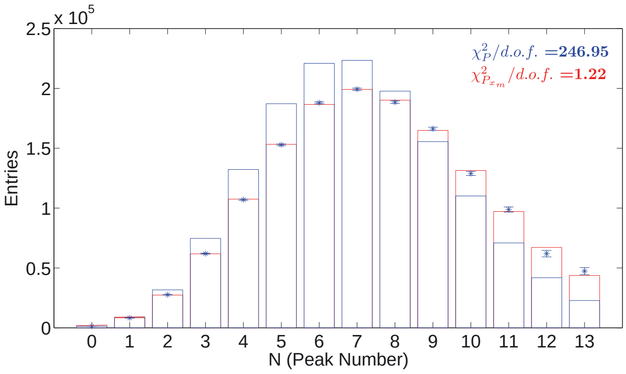

Fig. 11: Data from the reference spectrum are compared to a simple Poissonian model with mean value μ_{ZP} (blue) and to the $P \otimes G$ model (red), accounting for the optical cross-talk. The χ^2 value rule out the former at 99% C.L..

TABLE V: Estimates of the mean number of fired cells for $P \otimes G$ model.

	μ^0	μ_{ZP}
Mean Value of the Poissonian distribution	7.06 ± 0.05	7.08 ± 0.03
	μ_{MI}	$\mu^0/(1-\epsilon^0_{XT})$
Mean Number of Fired Cells	7.81 ± 0.01	7.76 ± 0.03

Results by the other recorded spectra are summarized in Table VI and Fig. 12 for the MGF procedure, confirming the validity of the compound Poissonian model and the need to account for detector effects to have a proper understanding of the phenomenon being investigated.

TABLE VI: Estimate of the mean number of fired cells with the $P \otimes G$ model using the RUN1 and RUN2 data-sets. Also in this case, the $P \otimes G$ model shows an agreement at the 99% C.L.. The measured χ^2 is 12.6 for the RUN1 and 12.0 for the RUN2 respectively.

	μ^0	μ_{ZP}
Mean Value of the Poissonian distribution	0.97 ± 0.01	0.985 ± 0.002
	1.82 ± 0.01	1.823 ± 0.004
	μ_{MI}	$\mu^0/(1-\epsilon^0_{XT})$
Mean Number of Fired Cells	1.080 ± 0.002	1.08 ± 0.01
	1.994 ± 0.003	1.99 ± 0.01

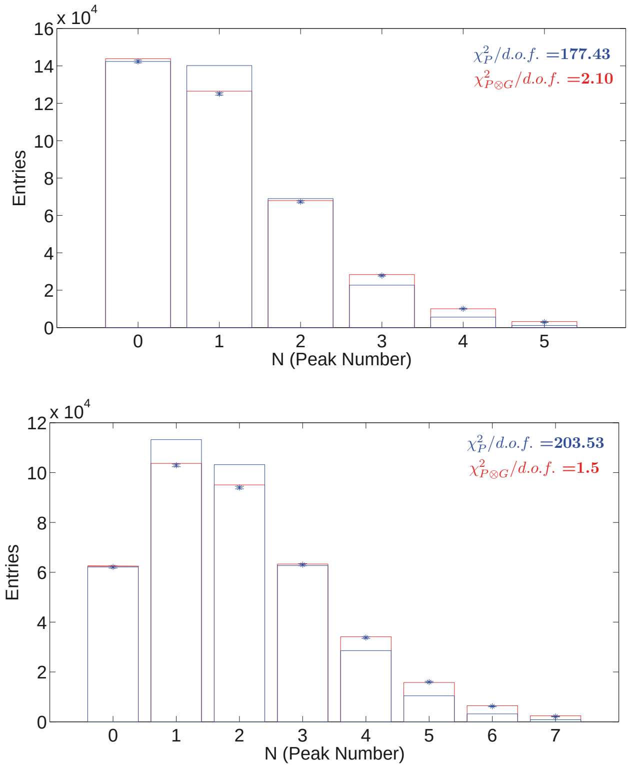

Fig. 12: Results of the MGF procedure on the low and middle intensity, RUN1 and RUN2. The pure Poissonian model with mean value μ_{ZP} (blue) is compared to the $P \otimes G$ model (red).

VI. CONCLUSION

Instruments and methods for the investigation of the statistical properties of the light emitted by an incoherent source have been developed and validated. The experimental set-up is based on Silicon Photomultipliers, state-of-the art light detectors, embedded into a flexible, modular, easy-to-use kit. Methods fold the characteristics of the emitted light and the detector response, with an increasing level of refinement. The model development allows to address advanced topics in statistics and data analysis techniques, targeted to master students in Physics or Engineering.

ACKNOWLEDGMENT

The research reported here has been developed in the framework of a Joint Development Project between CAEN S.p.A. and Universita' degli Studi dell'Insubria. The analysis code developed by the authors in MATLAB®is made available to interested users.

References

[1] B. Dolgoshein et al., *Status report on silicon photomultiplier development and its applications*. Nucl. Instrum. Methods Phys. Res. A 563, 368376. 2006.

[2] P. Buzhan et al., *Silicon photomultiplier and its possible applications*. Nucl. Inst. And Meth. A 504, 48-52. 2003.

[3] D. Renker, *Geiger-mode avalanche photodiodes, history, properties and problems*, 2006, Nuclear Instruments and Methods in Physics Research A, 567, 48.

[4] C. Piemonte, *A new Silicon Photomultiplier structure for blue light detection*, 2006, Nuclear Instruments and Methods in Physics Research A, 568, 224.

[5] P. Eckert, H.-C. Schultz-Coulon, W. Shen, R. Stamen & A. Tadday, *Characterisation studies of silicon photomultipliers*, 2010, Nuclear Instruments and Methods in Physics Research A, 620, 217.

[6] Y. Musienko, S. Reucroft & J. Swain, *The gain, photon detection efficiency and excess noise factor of multi-pixel Geiger-mode avalanche photodiodes*, 2006, Nuclear Instruments and Methods in Physics Research A, 567, 57.

[7] Y. Du & F. Retière, *After-pulsing and cross-talk in multi-pixel photon counters*, 2008, Nuclear Instruments and Methods in Physics Research A, 596, 396.

[8] P. Buzhan, B. Dolgoshein, A. Ilyin, V. Kantserov, V. Kaplin, A. Karakash, A. Pleshko, E. Popova *et al.*, *An advanced study of silicon photomultiplier*, ICFA Instrum. Bull. **23** (2001) 28.

[9] M. Ramilli, A. Allevi, V. Chmill & al., *Photon-number statistics with silicon photomultipliers*, 2010, Journal of the Optical Society of America B Optical Physics, 27, 852.

[10] I. Afek, A. Natan, O. Ambar & Y. Silberberg, *Quantum state measurements using multipixel photon detectors*, 2009, Phys. Rev. A **79**, 043830.

[11] ...

[12] S. Vinogradov, *Analytical models of probability distribution and excess noise factor of solid state photomultiplier signals with crosstalk*, 2012, Nuclear Instruments and Methods in Physics Research A, 695, 247.

[13] S. Vinogradov et al. *Probability distribution and noise factor of solid state photomultiplier signals with cross-talk and afterpulsing*, Nuclear Science Symposium Conference Record (NSS/MIC), 2009 IEEE.

[14] http://www.caentechnologies.com/csite/CaenProd.jsp?showLicence=false&parent=10&idmod=719.

[15] http://www.caen.it/csite/CaenProd.jsp?parent=14&idmod=624.

[16] http://www.caentechnologies.com/servlet/checkCaenManualFile?Id=7624.

[17] A. Vacheret, G. J. Barker, M. Dziewiecki & al., *Characterization and simulation of the response of Multi-Pixel Photon Counters to low light levels*, 2011, Nuclear Instruments and Methods in Physics Research A, 656, 69.

[18] C. M. Sparrow, *On spectroscopic resolving power*, Astrophys. J. 44, 7686 (1916).

[19] nnnn

[20] L. Lyons, *Statistics For Nuclear And Particle Physicists*, Cambridge, Uk: Univ. Pr. (1986).

[21] P. R. Bevington & D. K. Robinson, *Data reduction and error analysis for the physical sciences*, 3rd ed., 2003.

[22] W. H. Press, *Numerical Recipes in C: The Art of Scientific Computing*, Cambridge University Press; 2nd ed., 1992.

[23] G. Cowan, *Statistical Data Analysis*, Clarendon Press, Oxford Science Publications, 1998.

Appendix A

In this appendix it is demonstrated that the convolution of a Poissonian distribution of mean value λ (3) and a Binomial probability η (4) results in a Poissonian distribution of mean value $\lambda\eta$:

- Multiplying and dividing by η^n each element in the series, Eq. 5 can be written as:

$$P_{d,el} = \sum_{n=d}^{\infty} B_{d,n}(\eta)P_{n,ph}(\lambda)$$

$$= \sum_{n=d}^{\infty} \frac{(\lambda\eta)^n \eta^{d-n}(1-\eta)^{n-d}e^{-\lambda}}{d!(n-d)!}.$$

- Hence, defining $n - d = z$:

$$P_{d,el} = \sum_{z=0}^{\infty}(\lambda\eta)^{d+z}\left(\frac{1-\eta}{\eta}\right)^z \frac{e^{-\lambda}}{d!z!} =$$

$$= \frac{(\lambda\eta)^d e^{-\lambda}}{d!} \times \sum_{z=0}^{\infty}\frac{(\lambda\eta)^z}{z!}\left(\frac{1-\eta}{\eta}\right)^z$$

$$= \frac{e^{-\lambda}(\lambda\eta)^d}{d!} \times \sum_{z=0}^{\infty}\frac{(\lambda-\lambda\eta)^z}{z!}.$$

- The series actually corresponds to the Taylor expansion of $e^{\lambda-\lambda\eta}$, so that:

$$P_{d,el} = \sum_{n=d}^{\infty} B_{d,n}(\eta)P_{n,ph}(\lambda) =$$

$$\frac{e^{-\lambda\eta}(\lambda\eta)^d}{d!}$$

Appendix B

This appendix is dedicated to the demonstration of the relations for the probability density function (10), the mean value and variance (11) of the total fired cell number m assuming that every primary events can generate a unique infinite chain of secondary pulses.

This purpose is pursued by applying the probability generating function definition and properties.

For a discrete random variable ϕ, the generating function is defined as:

$$\tilde{\Phi}(s) = \sum_{i=0}^{\infty} P(\phi = i) \times s^i.$$

The probability distribution function, the mean and the variance of the random variable ϕ can be calculated as:

$$\Phi(\phi = m) = \frac{1}{m!} \times \left.\frac{d^m\Phi}{ds^m}\right|_0 \tag{21}$$

$$\bar{m}_\Phi = \Phi(1) \tag{22}$$

$$\sigma_\Phi^2 = \Phi(1)'' + \Phi(1)' - [\Phi(1)']^2. \tag{23}$$

The random variable considered here is the total number of detected pulses, m. Because it is defined by a sum of discrete random variables, its generating function is the composition of the pure Poisson distribution generating function:

$$\tilde{P}(s) = e^{\mu(s-1)}$$

and of the geometric distribution generating function:

$$\begin{aligned}\tilde{G}(s) &= \sum_{i=1}^{\infty} P(g = i-1) \times s^i \\ &= \sum_{i=1}^{\infty} {\epsilon_{XT}}^{i-1} \times (1-\epsilon_{XT}) \times s^i \\ &= \frac{(1-\epsilon_{XT})s}{1-\epsilon_{XT}s}.\end{aligned}$$

Finally, the analytical expression of the generating function for the total number of fired cells result to be:

$$\begin{aligned}\tilde{P} \circ \tilde{G} &= \tilde{P}(\tilde{G}(s)) \\ &= e^{\mu(\tilde{G}(s)-1)} \\ &= e^{\mu\left(\frac{s-1}{1-\epsilon_{XT}s}\right)}.\end{aligned}$$

Using the relation (21) it is possible to derive the probabilities to detect an arbitrary number of total pulses. For 0, 1 and 2 events the result is:

$$P \otimes G(0) = e^{-\mu},$$

$$P \otimes G(1) = e^{-\mu}\mu(1-\epsilon_{XT}),$$

$$P \otimes G(2) = e^{-\mu}\left[\mu(1-\epsilon_{XT})\epsilon_{XT} + \frac{\mu^2(1-\epsilon_{XT})^2}{2}\right].$$

An analysis of these expressions lead to the compact and general formula reported in (10), which refers to the compound Poisson distribution and is valid for m= 0, 1, 2, ... In addition, applying the properties (22) and (23) at $\tilde{P} \circ \tilde{G}$, it is possible to obtain the mean value and the variance of the distribution of the total number of fired cells, as expressed by the relations in (11).

Appendix C: The covariance ellipse

In this appendix the confidence region of two variables is demonstrated to assume the shape of an ellipse. Moreover, the relation between the parameters describing the ellipse, the standard deviation of the variables and their correlation is established.

The joint probability density of two variables x^T=$[x_1, x_2]$ gaussian distributed may be written as:

$$P(x) = k \cdot \exp\Big\{-\frac{1}{2}(x-\mu)^T C^{-1}(x-\mu)\Big\}, \tag{24}$$

where k is a normalization constant, $\mu^T = [\mu_1\mu_2]$ is the vector of the mean values of x and C is the covariance matrix:

$$C = E\{(x-\mu)(x-\mu)^T\} = \begin{bmatrix}\sigma_1^2 & \sigma_{12} \\ \sigma_{21} & \sigma_2^2\end{bmatrix}.$$

The diagonal elements of C are the variances of the variables x_i and the off-diagonal elements represent their covariance, which can be expressed as:

$$\sigma_{12} = \rho\sigma_1\sigma_2,$$

where ρ is the correlation coefficient.

Curves of constant probability are determined by requiring the exponent of the equation (24) to be constant:

$$(x-\mu)^T C^{-1}(x-\mu) = c \tag{25}$$

$$\frac{(x_1-\mu_1)^2}{\sigma_1^2} - 2\rho\frac{(x_1-\mu_1)}{\sigma_1}\frac{(x_2-\mu_2)}{\sigma_2} + \frac{(x_2-\mu_2)^2}{\sigma_2^2} = c',$$

where $c' = c(1-\rho^2)$. This equation represents an ellipse with the center located at (μ_1, μ_2) and the semi-axes placed at an angle θ with respect to the x_1, x_2 axes.

As shown in the folllowing, the equation (25) can be re-written as a sum of squares of two stochastically independent variables, which results to be χ^2 distributed with two degrees of freedom:

$$\frac{\xi_1^2}{a^2} + \frac{\xi_2^2}{b^2} = \chi^2. \tag{26}$$

This relation describes an ellipse centered in the origin of the reference sistem and with the semi-axes of lenght a, b parallel to the ξ_1,ξ_2 axes.

As a first step, the origin of the reference system is translated in the center of the ellipse, resulting in equation:

$$\tilde{x}^T C^{-1}\tilde{x} = c, \tag{27}$$

where $\tilde{x} = x - \mu$.

As a second step, axes are rotated in order to coincide with the (ξ_1, ξ_2) reference sistem by the transformation:

$$\tilde{x} = Q^T\xi,$$

where

$$Q = \begin{bmatrix}\cos\theta & \sin\theta \\ -\sin\theta & \cos\theta\end{bmatrix}.$$

As a consequence, equation (27) is turned to the form

$$\xi^T QC^{-1}Q^T \xi = c,$$

corresponding to the equation (26) as long as

$$QC^{-1}Q^T = \begin{bmatrix} \frac{1}{a^2} & 0 \\ 0 & \frac{1}{b^2} \end{bmatrix},$$

or, equivalently,

$$QCQ^T = \begin{bmatrix} a^2 & 0 \\ 0 & b^2 \end{bmatrix}.$$

The vector of the mean values and the cvariance matrix of ξ results to be:

$$\begin{aligned} \mu_\xi &= E\{\xi\} = QE\{x\} = Q\mu \\ C_\xi &= E\{(\xi-\mu_\xi)(\xi-\mu_\xi)^T\} \\ &= QE\{(x-\mu)(x-\mu)^T\}Q^T \\ &= QCQ^T \end{aligned} \tag{28}$$

So it can be noticed that the eigenvalues of the covariance matrix C_ξ correspond to the squared semi-axes of the canonical ellipse (26).

Because of the symmetry of the covariance matrix, C can be diagonalized exploiting its decomposition in eigenvalues and eigenvectors:

$$C = U\Lambda U^T,$$

where Λ is the diagonal matrix of eigenvalues and U is the rotation matrix constitued by eigenvectors. Comparing this formula with the expression (28) and using the properties of the rotation matrix ($QQ^T = Q^TQ = I$, det$Q = 1$) it can be inferred that:

$$U = Q^T \qquad \Lambda = C_\xi.$$

As a consequence, the eigenvalues of C can be obtained through the quadratic equation:

$$\det(C - \lambda I) = 0,$$

whose solutions are:

$$\lambda_{1,2} = \frac{1}{2}\Big[(\sigma_1^2+\sigma_2^2) \pm \sqrt{(\sigma_1^2+\sigma_2^2)^2 - 4\sigma_1^2\sigma_2^2(1-\rho)}\Big].$$

The lenghts of the ellipse semi-axes result to be the square root of the eigenvalues multiplied by the two degrees of freedom χ^2 value:

$$a = \sqrt{\chi^2\lambda_1} \qquad b = \sqrt{\chi^2\lambda_2}. \tag{29}$$

The eigenvectors of C can be found with the following equation:

$$(C - \lambda_i I)u_i = 0, \quad \text{with} \quad i = 1, 2.$$

For $i = 1$:

$$\begin{bmatrix} \sigma_1^2 - \lambda_1 & \rho\sigma_1\sigma_2 \\ \rho\sigma_1\sigma_2 & \sigma_2^2 - \lambda_1 \end{bmatrix} \begin{bmatrix} u_{1,1} \\ u_{1,2} \end{bmatrix} = 0,$$

and the solution is:

$$u_1 = \alpha_1 \begin{bmatrix} -\rho\sigma_1\sigma_2 \\ \sigma_1^2 - \lambda_1 \end{bmatrix},$$

where α_1 is a normalization constant. In the case of $i = 2$:

$$\begin{bmatrix} \sigma_1^2 - \lambda_2 & \rho\sigma_1\sigma_2 \\ \rho\sigma_1\sigma_2 & \sigma_2^2 - \lambda_2 \end{bmatrix} \begin{bmatrix} u_{2,1} \\ u_{2,2} \end{bmatrix} = 0,$$

and the solution is:

$$u_2 = \alpha_2 \begin{bmatrix} \sigma_2^2 - \lambda_2 \\ -\rho\sigma_1\sigma_2 \end{bmatrix},$$

where α_2 is the normalization constant. Using the eigenvalues definition, it can be proved that $\sigma_2^2 - \lambda_2 = -(\sigma_1^2 - \lambda_1)$. As a result, the U matrix turns out to be equal to Q^T, with $\cos\theta = -\rho\sigma_1\sigma_2$ and $\sin\theta = \sigma_1^2 - \lambda_1$. From these identities it is possibile to calculate the angle θ between the ellipse axis, which lies on ξ_i, and the x_i axis:

$$\tan\theta = -\frac{\sigma_1^2 - \lambda_1}{\rho\sigma_1\sigma_2}.$$

As θ belongs to the range [-π/2, π/2] and the above expression is quite complex, it is more convenient to estimate the $\tan 2\theta$:

$$\tan 2\theta = \frac{2\tan\theta_1}{1 - \tan^2\theta_1} = \frac{2\rho\sigma_1\sigma_2}{\sigma_1^2 - \sigma_2^2}. \tag{30}$$

The angle θ measures the rotation which brings the (x_1, x_2) coordinate system in the (ξ_1, ξ_2) reference system, which represent the rotation undergone by the ellipse. The rotation matrix Q has been completely determined and the ellipse has been entirely defined.

The covariance ellipse of the bivariate normal distribution assumes a particular importance when $\chi^2 = 1$ and its features can be analyzed in two extreme cases:

- if the variables are not correlated ($\rho = 0$), then $\theta = 0$, $a = \sigma_1$ and $b = \sigma_2$, which means that the ellipse axes are parallel to x_i and equal to the variable standard deviations,
- if the correlation is maximum ($\rho = \pm 1$), then the ellipse degenerates into a straight line of lenght $a = \sqrt{\sigma_1^2 + \sigma_2^2}$ (in fact $b = 0$).

In all the intermediate cases the ellipse is inscribed in a rectangle of center (μ_1, μ_2) and sides $2\sigma_1$ and $2\sigma_2$. The projections on the x_i axes of the four intersection points between the ellipse and the rectangle represent the 68% confidence interval for the parameter centered in the mean value μ_i.

All these characteristics of the covariance ellipse can be demonstrated exploiting the conic equations. The general quadratic equation:

$$Ax_1^2 + Bx_1x_2 + Cx_2^2 + Dx_1 + Ex_2 + F = 0 \tag{31}$$

represents the canonical ellipse if $B = 0$ and $AC > 0$. It is always possible to find a new coordinate system, rotated by an angle θ with respect to the x_i axes, in which the equation does not involve the mixed variable product. Calling ξ_i the new set of axis, the x_i variables can be expressed as:

$$x_1 = \xi_1 \cos\theta - \xi_2 \sin\theta \quad x_2 = \xi_1 \sin\theta + \xi_2 \cos\theta.$$

Substituting these relations in (31) and collecting the similar terms a new equation in ξ_i can be obtained:

$$\begin{aligned}
&\xi_1^2(A\cos^2\theta + B\cos\theta\sin\theta + C\sin^2\theta)+\\
&\xi_1\xi_2(-2A\cos\theta\sin\theta + B(\cos^2\theta - \sin^2\theta) + 2C\sin\theta\cos\theta)+\\
&\xi_2^2(A\sin^2\theta - B\cos\theta\sin\theta + C\cos^2\theta)+\\
&\xi_1(D\cos\theta + E\sin\theta) + \xi_2(-D\sin\theta + E\cos\theta) + F = 0.
\end{aligned} \tag{32}$$

In order to eliminate the $\xi_1\xi_2$ term, the angle θ has to satisfy:

$$-2A\cos\theta\sin\theta + B(\cos^2\theta - \sin^2\theta) + 2C\sin\theta\cos\theta = 0.$$

Simplifying the equation:

$$\begin{aligned}
2(A - C)\cos\theta\sin\theta &= B(\cos^2\theta - \sin^2\theta)\\
\frac{2\sin\theta\cos\theta}{\cos^2\theta - \sin^2\theta} &= \frac{B}{A - C}\\
\tan 2\theta &= \frac{B}{A - C}
\end{aligned} \tag{33}$$

In the specific case corresponding to equation (25),

$$A = \frac{1}{\sigma_1^2} \quad B = -\frac{2\rho}{\sigma_1\sigma_2} \quad C = \frac{1}{\sigma_2^2}.$$

As a consequence the expression (33) assume the form of the relation (30). Finally, the coefficients of the second order variables in equation (32) have to be interpreted as the inverse square of the semi-axes lenghts. Replacing the definition of A, B and C and solving for a and b gives:

$$a = \sqrt{\frac{\sigma_1^2\sigma_2^2(1-\rho^2)}{\sigma_2^2\cos^2\theta - 2\rho\sigma_1\sigma_2\cos\theta\sin\theta + \sigma_1^2\sin^2\theta^2}}$$

$$b = \sqrt{\frac{\sigma_1^2\sigma_2^2(1-\rho^2)}{\sigma_2^2\sin^2\theta - 2\rho\sigma_1\sigma_2\cos\theta\sin\theta + \sigma_1^2\cos^2\theta^2}}.$$

Expressing θ as a function of ρ and σ_i it is possible to obtain for the semi-axes the same definition as found previously in equation (29).

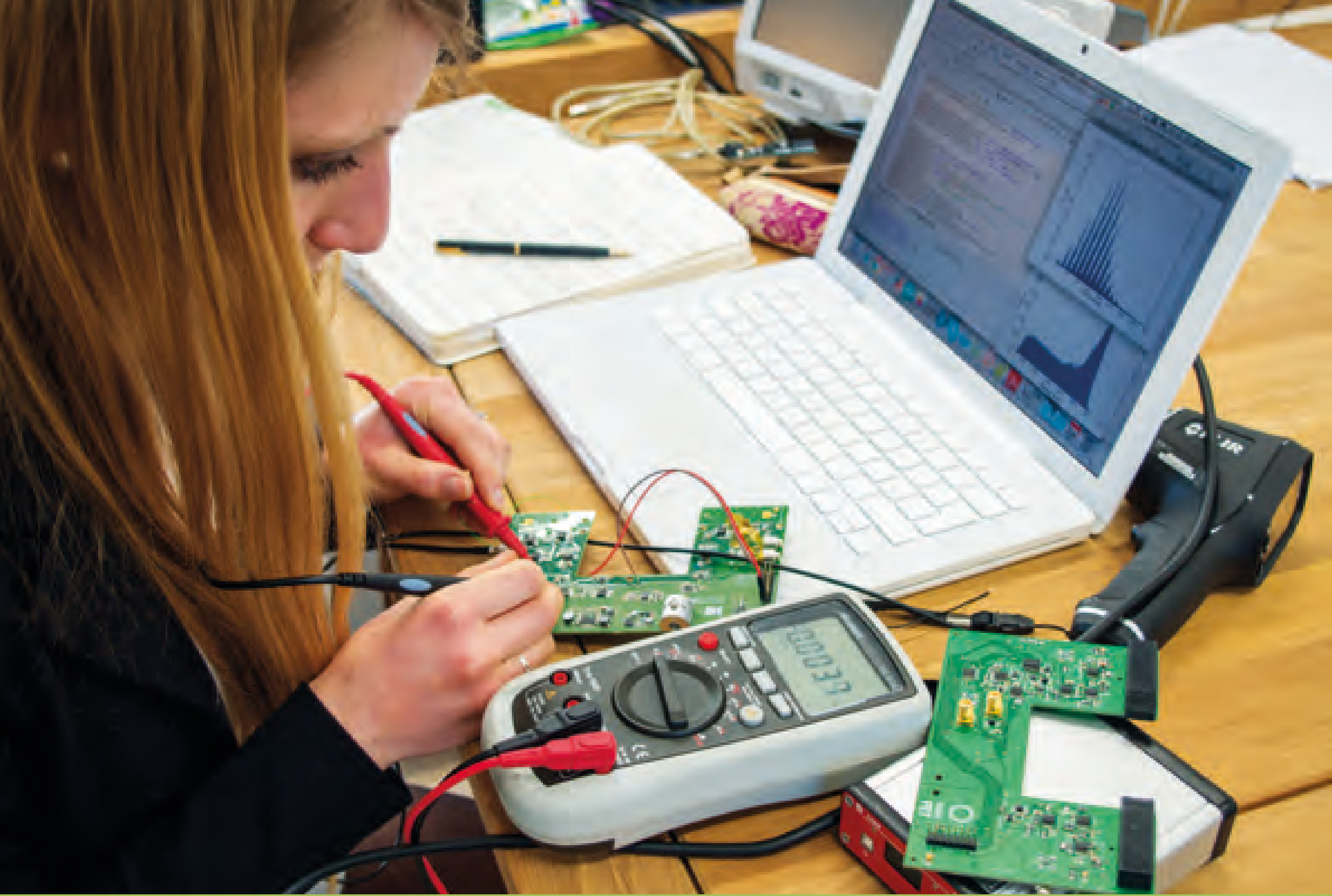

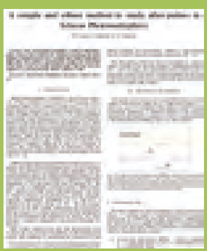

D.2 A simple and robust method to study after-pulses in Silicon Photomultipliers

ED3235

Equipment

SP5600E - Educational Photon Kit and a Timing Unit

Model	SP5600	DT5720A	SP5601	SP5650A	DT993
Description	Power Supply and Amplification Unit	Desktop Digitizer 250 MS/s	LED Driver	Sensor Holder for SP5600 with SiPM	Dual Timer
					
	p. 190	p. 190	p. 191	p. 191	p. 188

Ordering Options

Equipment	
Code	**Description**
WK5600XEAAAA	SP5600E - Educational Photon Kit
WDT993XAAAAA	DT993 - Dual Timer Desktop
or the all inclusive Premium Version	
WK5600XANAAA	SP5600AN - Educational Kit - Premium Version
WDT993XAAAAA	DT993 - Dual Timer Desktop

A simple and robust method to study after-pulses in Silicon Photomultipliers

M. Caccia, R. Santoro, G. A. Stanizzi

Abstract—**The after-pulsing probability in Silicon Photomultipliers and its time constant are obtained measuring the mean number of photo-electrons in a variable time window following a light pulse. The method, experimentally simple and statistically robust due to the use of the Central Limit Theorem, has been applied to an HAMAMATSU MPPC S10362-11-100C.**

Keywords—Silicon Photo-Multipliers, after-pulses, Photon Statistics

I. Introduction

Silicon Photomultipliers (SiPM) are state-of-the-art detectors of light consisting of a matrix of P-N junctions with a common output, with a density of cells up to $\approx 10^4/mm^2$. Each diode is operated in a limited Geiger-Muller regime in order to achieve gains at the level of $\approx 10^6$ and to guarantee an extremely high homogeneity in the cell-to-cell response. Subject to the high electric field in the depletion zone, initial charge carriers generated by an absorbed photon or by thermal effects trigger an exponential charge multiplication by impact ionization. When the current spike across the quenching resistor induces a drop in the voltage across the junction, the avalanche is stopped. SiPM can be seen as a collection of binary cells, providing altogether an information about the intensity of the incoming light by counting the number of fired cells [1] - [4].

SiPM feature an unprecedented photon number resolving capability and offer relevant advantages due to the low operating voltage, the immunity to magnetic field, ruggedness and the design flexibility due to the Silicon Technology. However, they also suffer from drawbacks related to a significant temperature dependence of the gain and a high rate of spurious hits. The latter is due to thermally generated carriers (Dark Counts, DC), Optical Cross-Talk (OCT) and after-pulsing. The OCT is linked to photons generated during a primary avalanche, triggering simultaneous secondaries [3], [5]. The OCT is affected by the sensor design [3], [6] - [8] and strongly depends on the bias voltage. After-pulses are associated to the late release of a charge carrier that has been produced in the original avalanche and trapped by an impurity [3]. After-pulsing is essentially dependent on the sensor technology [3], [6], [8].

Dark Counts, Optical Cross-Talk and after-pulsing occur stochastically and introduce fluctuations in the multiplication process that contribute to deteriorate the resolution in both photon counting and spectrometry. Moreover, after-pulsing may be critical in photon correlation experiments [9] - [11].

The after-pulsing effect has been investigated by various authors, relying on the time correlation of neighbouring pulses [12] - [14]. A simple and statistically robust method is proposed here, based on the sensor current integration and the use of the Central Limit Theorem to estimate the mean number of pulses in a variable time window.

M. Caccia, R. Santoro, G. A. Stanizzi are with the Dipartimento di Scienza e Alta Tecnologia, Universita' degli Studi dell'Insubria, 22100, Como, Italy.

II. Materials and methods

After-pulses can be seen as an excess of fired cells in a time window following the signal due to a light pulse (Figure 1), where the excess is calculated with respect to Dark Counts occasionally appearing. A statistical analysis of the excess, varying the gate length, is expected to lead to a measurement of the after-pulsing probability and of its time constant.

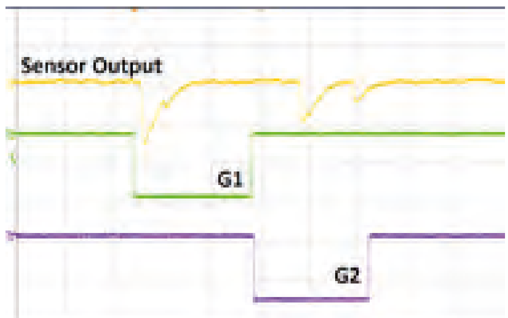

Fig. 1: The figure shows the response of the SIPM to a light burst, synchronised with the leading edge of the gate G_1. Pulses in the G_2 gate may be due to both random Dark Counts and after-pulses. The exemplary event shown here features as well an after-pulse occurring during the recovery time of the sensor. The rate of Dark Counts is measured switching off the LED.

A. Experimental setup

The block diagram of the experimental set-up is shown in Figure 2. A master clock is synchronising the light pulser illuminating the SiPM and the data acquisition, integrating the signal pulses in a variable duration gate G_2 delayed with respect to the light pulse. Results reported here were obtained with the following specific system:

- An ultra-fast LED source (SP5601 - CAEN), emitting $\approx 5\ ns$ long light pulses at $405\ nm$, with intensities in the 1-2000 photon range.

- The SP5600 - CAEN power supply and amplification unit, housing an Hamamatsu MPPC S10362-11-100C.
- A charge digitisation unit, either based on the CAEN - DT5720A waveform digitizer or on the CAEN - V792N QDC.
- A Dual-Timer (N93B - CAEN) to generate the integration gate.

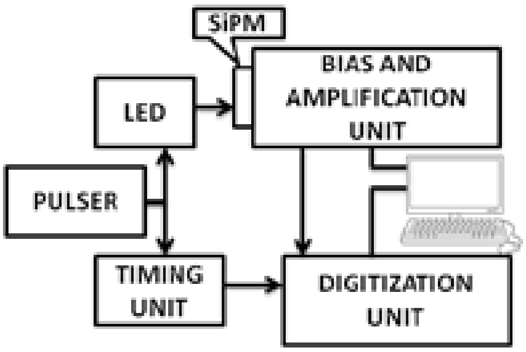

Fig. 2: Block diagram of the experimental setup for the after-pulsing characterization.

B. Experimental procedure

The experimental procedure starts by defining two gates, synchronized to the light pulse (see Figure 1). The first gate G_1 encompasses the time development of the signal due to a light pulse. The de-trapping of charge carriers within G_1 originates avalanches piled-up with the signal from the light pulse and the probability for this to occur is inferred by studying the excess of pulses in a second variable gate G_2, following G_1. The estimation of the mean number of fired cells in G_2 is obtained by the analysis of the spectrum of the released charge, provided integrating the sensor output current. Exemplary spectra for $G_2 = 400\ ns$ are shown in Figure 3, with the LED switched ON and OFF. The peak positions identify the value of the digitized charge for the different number of avalanches while the peak areas measure the corresponding probability.

The spectra clearly show evidence of two statistics characterized by a different mean value. In order to obtain a quantitative information, the data were analysed as follows:

- The average charge $\overline{Q}_N$ by a sequence of N events was retained as the main observable. According to the Central Limit Theorem, $\overline{Q}_N$ is expected to be Gaussian distributed, with the advantage of an easy and robust way to estimate its value and to measure its uncertainty. The value of N was determined studying the evolution of the $\overline{Q}_N$ distribution vs. N and fixing its value at 200, when it was shown to be asymptotically gaussian (Figure 4).
- In order to turn $\overline{Q}_N$ into a number of fired cells, a multi-photon spectrum was recorded illuminating the sensor within G_1. The reference spectrum is shown in Figure 5. This can be fit with a sum of gaussians [15] to find the average peak-to-peak distance $\overline{\Delta}_{pp}$ which provides the conversion factor from ADC channels to number of cells.

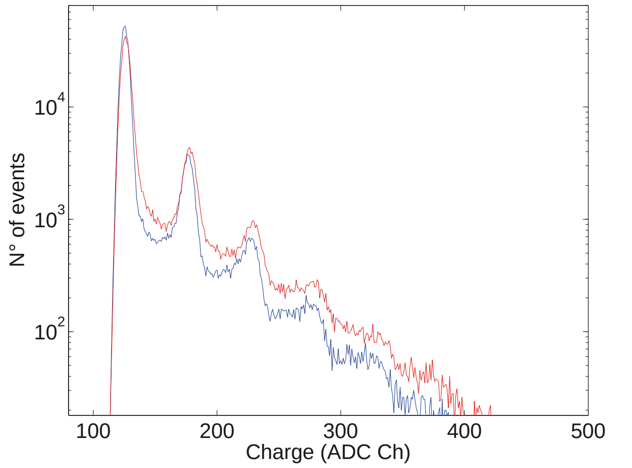

Fig. 3: Spectra of the charge collected in G_2, recorded without illuminating the sensor (blue) and after a light burst (red) pulsed 500 ns before the gate opening. Spectra were normalised to the same number of events.

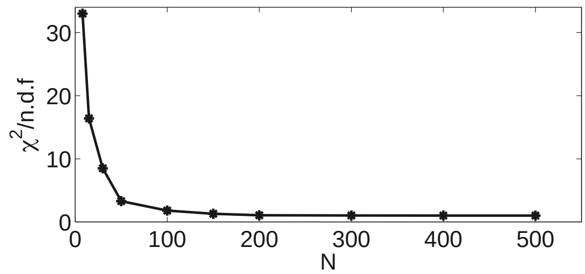

Fig. 4: The $\overline{Q}_N$ distribution was tested against the hypothesis of being Gaussian. The plot shows the $\chi^2/n.d.f.$ vs. N of the fit.

The spectra of $\overline{Q}_N$ are shown in Figure 6, where the shift for the illuminated sensor is very clear. Eventually, the quantity

$$\Delta_{QQ}(G_2) = \frac{\langle \overline{Q}_N(light\ ON, G_2)\rangle - \langle \overline{Q}_N(light\ OFF, G_2)\rangle}{\overline{\Delta}_{pp}} \quad (1)$$

measures the excess of avalanches due to after pulses associated to the light burst with respect to Dark Counts.

The procedure is iterated increasing G_2 till when $\Delta_{QQ}(G_2)$ achieves a constant value, indicating that the after-pulsing phenomenon is exhausted.

In order to cope with possible temperature changes during the experiment, for every value of G_2, a multi-photon spectrum is recorded to have an actual value of $\overline{\Delta}_{pp}$.

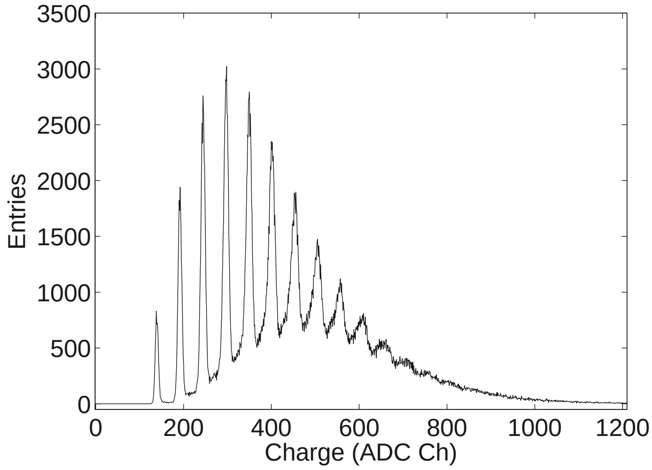

Fig. 5: The distribution of the detected photons used to calibrate the charge in photo-electrons.

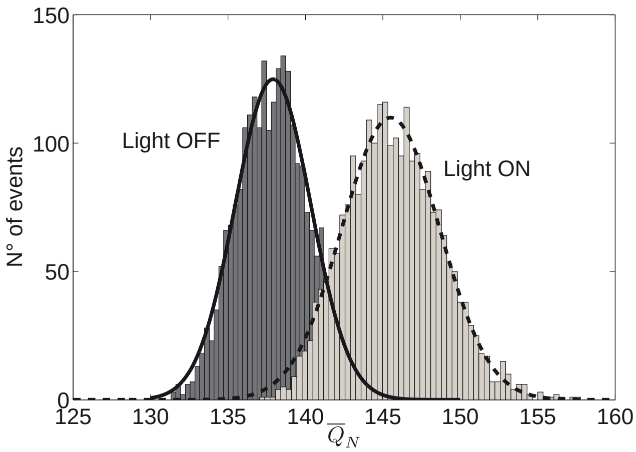

Fig. 6: Exemplary distribution of $\overline{Q}_N$ for $G_2 = 400ns$, having the LED switched ON and OFF.

III. Results

The procedure has been initially qualified measuring the Dark Count Rate (DCR) by the calculation of $\langle\overline{Q}_N\rangle$. The trend of $\langle\overline{Q}_N(light\ OFF)\rangle/\overline{\Delta}_{pp}$ vs. time is shown in Figure 7, where the straight line fit corresponds to a slope $m = 593 \pm 5\ kHz$. The average number of photo-electrons is actually affected by the OCT and $\langle\overline{Q}_N\rangle/\overline{\Delta}_{pp} = n_{p.e.} \times (1+\epsilon)$, where $\epsilon = (22 \pm 1)\%$ is the measured Cross-Talk probability and $n_{p.e.}$ is the number of primary avalanches. As a consequence, the DCR may be calculated as $\frac{m}{1+\epsilon} = 486 \pm 8\ kHz$, in fair agreement with the value of $480 \pm 4\ kHz$ by a direct count of the pulses above the 0.5 photo-electron threshold.

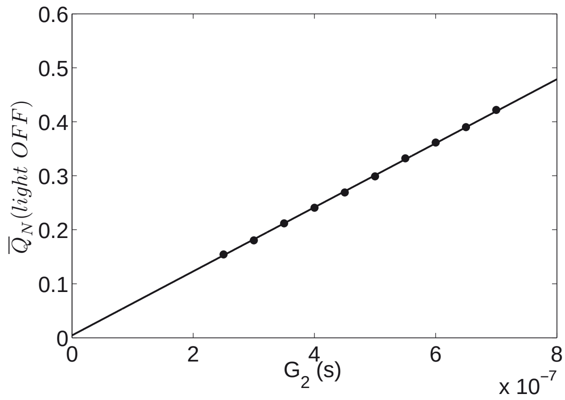

Fig. 7: $\overline{Q}_N(light\ OFF)/\overline{\Delta}_{pp}$ as a function of G_2 (s).

Concerning after-pulses, once the de-trapping of the charge carriers is assumed to have an exponential time dependence, the probability density function may be written as:

$$y(t) = \frac{P}{\tau} e^{-\frac{t}{\tau}}, \tag{2}$$

where **P** is the probability for a single avalanche to originate an after-pulse and τ is the characteristic time constant of the phenomenon. The quantity $\Delta_{QQ}(G_2)$ corresponds to the cumulative distribution function in the integration gate G_2, since:

$$\Delta_{QQ}(G_2) = \int_{G1}^{G1+G2} \frac{N \times P}{\tau} e^{-\frac{t}{\tau}} dt = a(1 - e^{-\frac{G_2}{\tau}}), \tag{3}$$

where N is the mean number of photo-electrons generated by the light burst and $a = N \times Pe^{-\frac{G_1}{\tau}}$ is the asymptotic value of $\Delta_{QQ}(G_2)$.

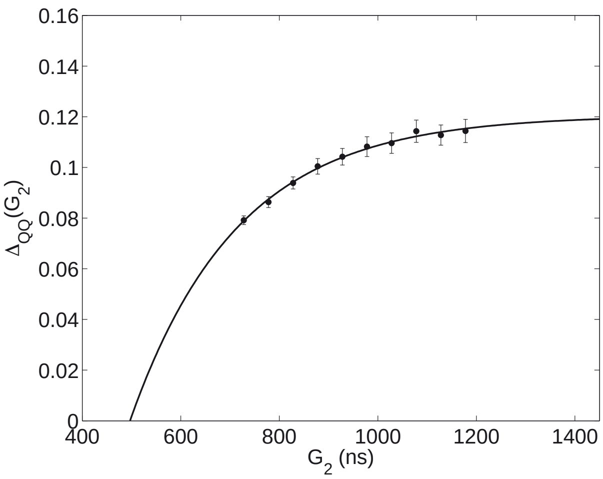

Fig. 8: $\Delta_{QQ}(G_2)$ vs. G_2. Data are fitted by equation 3, with a $\chi^2/n.d.f. = 0.94$

The data resulting by a G_2 scan are shown in Figure 8. A fit to equation (3) yields a value of $\tau = 217.5 \pm 5.9\ ns$ and $a = 0.1206 \pm 0.0010$ photo electrons (p.e.). Since N was measured to be $6.1 \pm 0.1\ p.e.$, this is resulting in an after-pulsing probability of $(19.44 \pm 1.38)\%$ in fair agreement with data found in the Hamamatsu datasheet [16] and in reference [9], [12], reporting values between 17% and 22%.

IV. Conclusions

A method for the characterisation of the after-pulses based on the analysis of the charge distribution in a variable time window has been proposed and qualified. Its advantages are the simplicity and the robustness. Its main limitation is the intrinsic impossibility to probe the after-pulsing components characterised by a short time constant.

References

[1] B. Dolgoshein et al., *Status report on silicon photomultiplier development and its applications*. Nuclear Instruments and Methods in Physics Research A 563, 368376. 2006.

[2] P. Buzhan et al., *Silicon photomultiplier and its possible applications*. Nuclear Instruments and Methods in Physics Research A 504, 48-52. 2003.

[3] D. Renker, *Geiger-mode avalanche photodiodes, history, properties and problems*. Nuclear Instruments and Methods in Physics Research A 567, 48. 2006.

[4] C. Piemonte, *A new Silicon Photomultiplier structure for blue light detection*. Nuclear Instruments and Methods in Physics Research A 568, 224. 2006.

[5] A. L. Lacaita, *On the Bremsstrahlung Origin of Hot-Carrier-Induced Photons in Silicon Devices*. IEEE Trans. Electron Devices, 40, 57782. 1993.

[6] T. Nagano et al., *Timing Resolution Improvement of MPPC for TOF-PET Imaging*. 10.1109/NSSMIC.2012.6551376. IEEE 2012

[7] P. Eckert, *Study of the response and photon-counting resolution of silicon photomultipliers using a generic simulation framework*. arXiv:1206.4154v1. 2012

[8] R. Pagano, *Silicon Photomultiplier: Technology Improvement and Performance*. International Journal on Advances in Systems and Measurements, vol 6 n. 1-2, 124-136. 2013.

[9] T. Niggemann et al., *Status of the silicon photomultiplier telescope FAMOUS for the fluorescence detection of UHECRs*. Proceeding of 33rd International Cosmic Ray Conference. 143.107.180.38/indico/confAuthorIndex.py?confId=0. 2013.

[10] P. Schuck, *Protein Interactions: Biophysical Approaches for the Study of Complex Reversible Systems*. 27-30. Springer, 2007.

[11] T. Toyama et al., *Novel photo multiplier tubes for the Cherenkov Telescope array project*. Proceeding of 33rd International Cosmic Ray Conference. 143.107.180.38/indico/confAuthorIndex.py?confId=0. 2013.

[12] P. Eckert, H.-C. Schultz-Coulon, W. Shen, R. Stamen & A. Tadday, *Characterisation studies of silicon photomultipliers*. Nuclear Instruments and Methods in Physics Research A 620, 217. 2010.

[13] Y. Du, F. Retière, *After-pulsing and cross-talk in multi-pixel photon counters*. Nuclear Instruments and Methods in Physics Research A 596, 396-401. 2008.

[14] C. Piemonte et al., *Development of an automatic procedure for the characterization of silicon photomultipliers*. 978-1-4673-2030-6. IEEE 2012.

[15] M. Caccia et al., *An Educational Kit Based on a Modular Silicon Photomultiplier System*. arXiv:1308.3622. 2013.

[16] hamamatsu.com/eu/en/product/category/3100/4004/4113/index.html

D.3 Background removal procedure based on the SNIP algorithm for γ-ray spectroscopy with the CAEN Educational Kit

ED3163

Equipment

SP5600C - Educational Gamma Kit

Model	SP5600	DT5720A	SP5606	A315	SP5607
Description	Power Supply and Amplification Unit 	Desktop Digitizer 250 MS/s 	Mini-Spectrometer 	Splitter 	Absorption tool 
	p. 190	p. 190	p. 192	p. 192	p. 193

Related Experiment
B.1.3
B.1.4
B.3.1

Ordering Options

Equipment	
Code	**Description**
WK5600XCAAAA	SP5600C - Educational Gamma Kit
or the all inclusive Premium Version	
WK5600XANAAA	SP5600AN - Educational Kit - Premium Version

Requirements

Gamma radioactive source

Data analysis code developed in MATLAB is available.

Background removal procedure based on the SNIP algorithm for $\gamma-$ray spectroscopy with the CAEN Educational Kit.

Massimo Caccia, Amedeo Ebolese, Matteo Maspero, Romualdo Santoro
Dipartimento di Scienza e Alta Tecnologia,
Universita' degli Studi dell'Insubria, 22100, Como, Italy
Marco Locatelli, Maura Pieracci, Carlo Tintori
CAEN S.p.A., 55049, Viareggio, Italy

***Abstract*—In gamma spectra the energy, the intensity and the number of resolved photo peaks depend on the detector resolution and the background from physics processes. A widely used method for subtracting the background under a photo-peak is provided by the Sensitive Nonlinear Iterative Peak (SNIP) algorithm. This paper reports a validation procedure of the SNIP algorithm, based on the invariance of the photo-peak area for different background levels.**

***Index Terms*—Silicon Photo Multipliers, gamma ray spectroscopy**

I. Introduction

GAMMA-RAY spectroscopy is relevant in basic and applied fields of science and technology, from nuclear to medical physics, from archaeometry [1], [2] to homeland security [3], [4].

In recorded $\gamma-$spectra of radioactive samples the number of resolved photo-peaks and the measurement of their energy and intensity is affected by the detector resolution and by background physics processes. In general, the characterization of the photo-peaks implies a robust estimation of the underlying background. Several approaches have been proposed, going from a simple estimate by an analysis of the side bands of the peaks to a spectrum fit with an analytical description of the background.

A flexible and widely used method is provided by the Sensitive Nonlinear Iterative Peak (SNIP) algorithm [5]–[7]. This paper presents a validation procedure of the SNIP algorithm based on the invariance of the photo-peak area when the underlying background changes.

II. Background subtraction in $\gamma-$spectra

For energies of γ below the pair production, the interaction with the detector is dominated by Compton scattering and photo-absorption. Exemplary theoretical and experimental spectra are shown in Fig. 1. The Compton continuum is due to the recoiling electrons with energy

$$E_e = E_0 \times \left(\frac{\frac{E_0}{mc^2}(1-cos\theta)}{1+\frac{E_0}{mc^2}(1-cos\theta)} \right),$$

Corresponding Authors: massimo.caccia@uninsubria.it, m.locatelli@caen.it,

where E_0 is the incoming $\gamma-$ray energy, θ is the scattering angle and mc^2 is the electron rest-mass. The experimental spectrum results by a smearing of the underlying physics distribution [8] [9], implying a photo-absorption peak broadening possibly contaminated by the edge of the Compton spectrum and referred as background in the following.

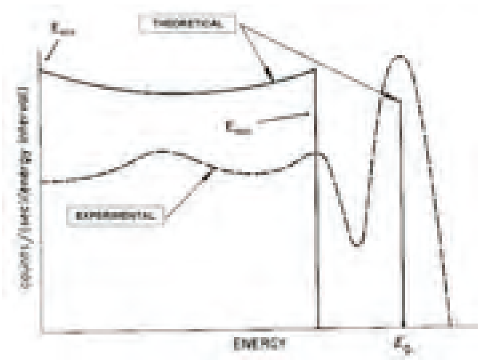

Fig. 1: *Theoretical energy distribution for Compton and photoelectric interaction (continuous line) and experimental pulse-height distribution in a scintillation detector [8].*

The photo-peaks are the signature of a spectrum. Their analysis conveys relevant information about the radioactive sample and the experimental apparatus:

- the peak energies are distinctive of the decaying nuclei in the sample;
- the area of peaks measure the relative concentrations of isotopes;
- the linearity of the system is provided by the spectra for a set of known γ emitters;
- the width of the peaks represents the electronics plus detector resolution. Its dependence against the energy accounts for the poissonian fluctuations in the signal and the detector response.

The SNIP algorithm has been introduced with the aim to separate useless information (i.e.: background, noise and detector artifacts) from useful information contained in the peak.

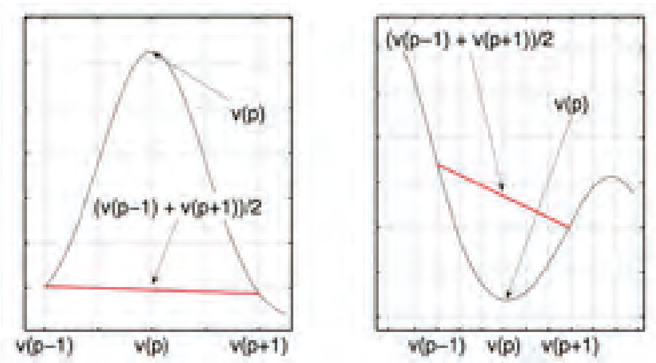

Fig. 2: *Illustration of the SNIP algorithm applied to the peak region (left plot) and to a valley of the spectrum (right plot). Figure adapted from [7].*

The core procedure of the SNIP [7] requires a pre-processing step, where the count $y(i)$ in channel $i-th$ is transformed according to:

$$y(i) \mapsto v(i) \;=\; log(log(\sqrt{y(i)+1}+1)+1).$$

The square-root operator enhances small peaks while the double log operator was introduced to cope with complex spectra with relative intensities over several orders of magnitude.

The background under the peak is evaluated in an iterative way. For the M$-th$ iteration, the content of the transformed bin $v_M(i)$ is compared to the mean of the values at distance equals to $\pm M$ and the updated spectrum is evaluated as:

$$v_{M+1}(i) = min\left\{ v_M(i), \frac{v_M(i-M)+v_M(i+M)}{2} \right\}.$$

In proximity of peaks, as long as the distance is comparable to the peak width, the updated spectrum will result by the shape of the side bands. On the other hand, valleys will be essentially unchanged (see Fig. 2). An exemplary illustration of the outcome of the procedure is shown in Fig. 3, where the raw spectrum, the background estimated with SNIP and the spectrum with the subtracted background are overimposed. Fig. 3 clearly shows that the peak side wings fluctuate around zero as expected after a correct background subtraction.

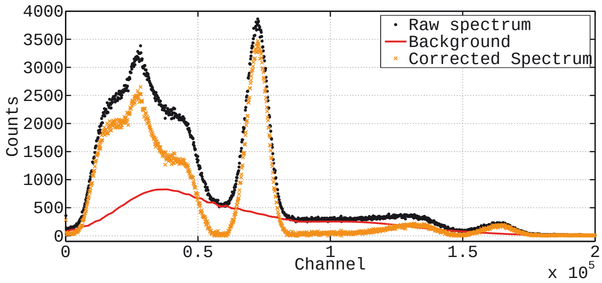

Fig. 3: *Typical ^{22}Na gamma spectrum. The raw data are shown in black, the estimated background in red and the spectrum with the subtracted background in brown.*

The main advantage of the SNIP algorithm is the capability to cope with a large variety of background shapes. Its potential weakness is in the absence of a built-in convergence criterion. In this specific application, the iterative procedure is stopped as long as the estimated background is monotonically changing in the peak region. As a complementary condition, essentially applied for low background spectra where the statistical fluctuations are dominating, the procedure is stopped as long as the background drops below 5% of the total area underneath the peak.

III. Experimental Set-up

The experimental set-up is based on the CAEN Silicon PhotoMultiplier Educational Kit [10], a modular system for undergraduate experiments in nuclear science, photonics and statistics.

Fig. 4: *The CAEN educational kit full package.*

The kit, shown in Fig. 4, include two γ spectrometry heads housing:

- a 3x3mm^2 Hamamatsu MPPC S10362-33-100C with 100 cells and breakdown voltage of 68.5V, optically coupled with 3x3x15mm^3 LYSO/BGO/CsI crystals;
- a 6x6mm^2 SensL MicroSM-60035-X13 (18980 cells, breakdown voltage 27.35V), optically coupled with 3x3x30mm^3 CsI scintillating crystal.

The analog signal generated in the SiPM is amplified by the CAEN SP5600 PSAU Power Supply and Amplification Unit [11] and sampled at 250 MS/s over a 12 bit dynamic range by the CAEN DT5720A Desktop Digitizer [12]. The DT5720A embeds an FPGA for on-board data processing, e.g. baseline calculation and charge integration. The system is controlled by a LabView based Graphical Users Interface and USB interfaced to a computer.

The proposed experiments are based on the use of the head equipped with the 6x6 mm^2 SensL SiPM.

IV. SNIP Algorithm Validation

The validation of the convergence criteria for the SNIP algorithm is based on the assumption that the information in the photo-peak shall be preserved as the underlying background changes. This was established by processing ^{22}Na spectra for different biasing voltages of the SiPM used to detect the scintillation light from the CsI crystal. Data were recorded for ^{22}Na since the interaction of the two $\gamma-$rays by the positron annihilation results in a spectrum featuring a continuous and significant background to the left and right hand side of the 511 keV photo-peak.

Twelve spectra were acquired in the bias voltage range $29.8-31.1$V. A subset is shown in Fig. 5 displaying both raw and background subtracted data. As the over-voltage is raised, the gain of the system is expected to increase together with the photon detection efficiency (PDE), the optical cross-talk and the dark count rate (DCR) [13]–[18]. As a consequence, spectra are expected to change, featuring a shift in the peak position due to the gain change and a width increase associated to the PDE variation and to a different smearing function because of the DCR and the cross-talk.

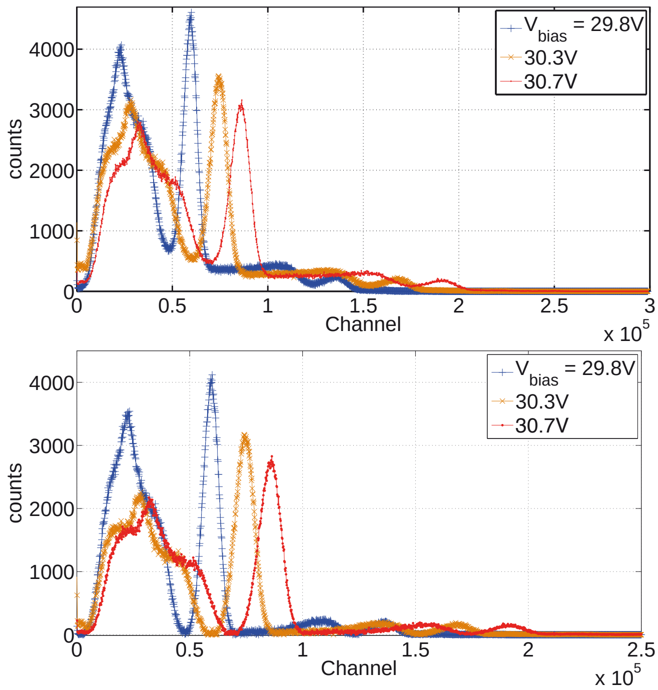

Fig. 5: *Measured ^{22}Na gamma spectra for different bias voltages (upper panel). The SNIP processed spectra for the same subset of data are shown in the bottom panel.*

After the background subtraction by SNIP algorithm, the 511 keV peak was fitted with a gaussian function. The values of the area for the different biasing conditions are presented in Fig. 6, following a normalization to the total number of events for energies higher than the back-scattering peak.

The reported errors account for the poissonian fluctuations ($\sim 0.2\%$) and the effect of the background subtraction ($\sim 1\%$). They correspond to the standard deviation of the values for a set of ten spectra recorded in identical conditions.

Effects due to the convergence criteria of the SNIP algorithm were estimated stopping the procedure one step beyond and behind the iteration corresponding to the convergence step.

The distribution of experimental areas is statistically compliant with the hypothesis of a constant value confirming that

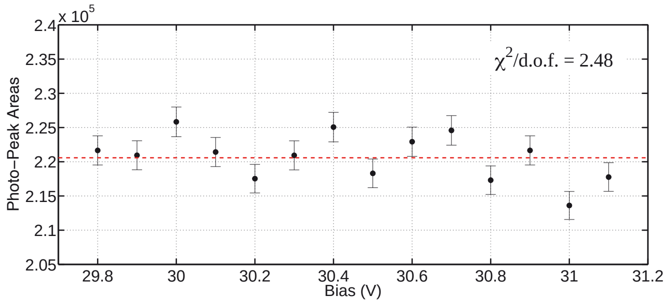

Fig. 6: *Values of the photo-peak areas for different biasing conditions.*

the SNIP background subtraction routine is not introducing any systematic errors.

V. Measurements

The SNIP processed spectra from a series of sources used in educational labs (Tab. I, [19]) were used to calibrate the system response and check its linearity. Results up to the 835 keV from ^{54}Mn are shown in Fig. 7. The linearity of the system can be assessed, and results are shown in Fig. 7, with no indication of saturation.

TABLE I: *Relevant characteristics of the used gamma isotopes.*

Isotope Name	Symbol	Peak Energy (MeV)
Cadmium-109	Cd-109	0.022, 0.025, 0.088
Cobalt-57	Co-57	0.122, 0.136
Sodium-22	Na-22	0.511 (1.275)
Cesium-137	Cs-137	0.662
Manganese-54	Mn-54	0.835

Spectra were also used to verify the energy dependence of the system resolution, where a $dE/E \propto 1/\sqrt{E}$ trend can be assumed by the poissonian fluctuations in the number of scintillation photons. Data are reported in Fig. 8.

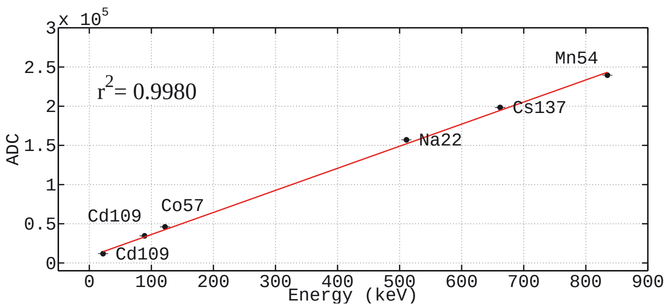

Fig. 7: *Energy calibration.*

The power law fit $f(E) \propto E^{-b}$ gives a value of b=0.57 $\pm$ 0.03, in agreement with the expectations. It is worth mentioning that the resolution at the ^{137}Cs peak is less than 9%, at the level of the standard educational devices.

VI. Conclusions

The flexibility and the potential of the SiPM kit have been confirmed considering its configuration for gamma spectrometry. Basic measurements proving its linearity and assessing

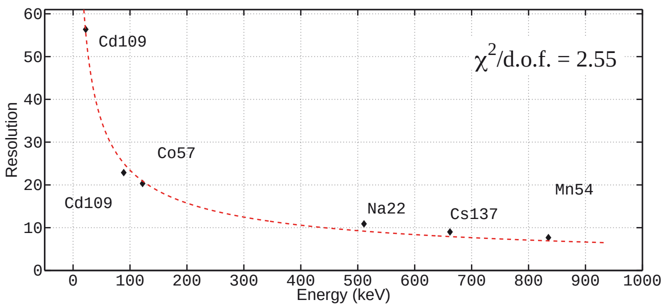

Fig. 8: *Power law fit of data after the SNIP background subtraction.*

its energy resolution have been performed. A MATLAB implementation of the SNIP background subtraction algorithm has been validated, providing altogether a valuable platform for entry-level experiments in gamma spectrometry tailored for undergraduate students in Physics.

References

[1] M. S. Shackley, *Gamma Rays, X-Rays and Stone Tools: Some Recent Advances in Archaeological Geochemistry*, Journal of Archaeological Science, Volume 25, Issue 3, 1998;

[2] M. Moussa, *Gamma-ray spectrometry: a new tool for exploring archaeological sites; a case study from East Sinai, Egypt*, Journal of Applied Geophysics, Volume 48, Issue 3, 2001;

[3] Aage, H., Orsbech, U., *Search for lost or orphan sources based on NaI gamma spectrometry*, Appl. Radiat. Isot. 58, 103113 (2003);

[4] Ely, J., Kouzes, R., Schweppe, J., Siciliano, E., Strachan, D., Weier, D., *The use of energy windowing to discriminate SNM from NORM in radiation portal monitors*, Nucl. Instrum. Methods A 560, 373387 (2006);

[5] Ryan, C. G. and Clayton, E. and Griffin, W. L. and Sie, S. H. and Cousens, D. R., *SNIP, a statistics-sensitive background treatment for the quantitative analysis of PIXE spectra in geoscience applications*;

[6] Ene, A., Badica, T., Olariu, A., Popescu, I. V., & Besliu, C. 2001, Nuclear Instruments and Methods in Physics Research B, 179, 126;

[7] Morháč, M. and Kliman, J. and Matoušek, V. and Veselský, M. and Turzo, I., *Background elimination methods for multidimensional coincidence γ-ray spectra*;

[8] G. F. Knoll, *Radiation Detection and Measurement*, John Wiley & Sons (2000);

[9] Adrian C. Melissinos and Jim Napolitano, *Experiments in Modern Physics, Second Edition*, Academic Press 2003;

[10] http://www.caen.it/jsp/Template2/CaenProd.jsp?parent=61&idmod=719;

[11] http://www.caentechnologies.com/csite/CaenProd.jsp?showLicence=false&parent=10&idmod=719;

[12] http://www.caen.it/csite/CaenProd.jsp?parent=14&idmod=624;

[13] D. Renker, *Geiger-mode avalanche photodiodes, history, properties and problems*, 2006, Nuclear Instruments and Methods in Physics Research A, 567, 48.

[14] P. Eckert, H.-C. Schultz-Coulon, W. Shen, R. Stamen & A. Tadday, *Characterisation studies of silicon photomultipliers*, 2010, Nuclear Instruments and Methods in Physics Research A, 620, 217.

[15] Y. Musienko, S. Reucroft & J. Swain, *The gain, photon detection efficiency and excess noise factor of multi-pixel Geiger-mode avalanche photodiodes*, 2006, Nuclear Instruments and Methods in Physics Research A, 567, 57.

[16] Y. Du & F. Retière, *After-pulsing and cross-talk in multi-pixel photon counters*, 2008, Nuclear Instruments and Methods in Physics Research A, 596, 396.

[17] M. Ramilli, A. Allevi, V. Chmill & al., *Photon-number statistics with silicon photomultipliers*, 2010, Journal of the Optical Society of America B Optical Physics, 27, 852;

[18] Caccia, M. and Chmill, V. and Ebolese, A. and Martemiyanov, A. and Risigo, F. and Santoro, R. and Locatelli, M. and Pieracci, M. and Tintori, C., *An Educational Kit Based on a Modular Silicon Photomultiplier System*, 2013arXiv1308.3622C;

[19] http://www.pasco.com/prodCatalog/SN/SN-7949_gamma-sources-set-of-8/#overviewTab.

PRODUCTS

This section is dedicated to a short description of the advanced instrumentations developed by CAEN and used to perform the experiments proposed in this Handbook.

The devices are put together to form educational kits, suitable to a specified application in Nuclear and Modern Physics fields. Moreover three educational kits, **Educational Gamma Kit**, **Educational Beta Kit** and **Educational Photon Kit**, are included in a **Educational Kit – Premium Version** that allows performing almost entirely of the Handbook experiments.

The **Emulation Kit** allows to perform a series of lab experiments related to gamma spectroscopy with no radioactive source and detector but simulating the signals produced by the interaction of particles with the detecting unit.

The **EasyPET** is the only not modular system. It is a user-friendly and portable PET system that allows users to perform nuclear imaging experiments. The **Environmental Kit** and the **Environmental Kit Plus** are dedicated to the study of gamma radiation produced from material of common use, for example soil samples, and radon indoor measurements.

GammaEDU is a portable detection backpack for revealing the presence of radioactive materials in the environment.

RockyRad is a portable Geiger–Müller counter for nuclear radiation detection with a mobile interface to manage the Geiger counter acquisition.

Cosmic Hunter is a new educational tool through which CAEN wants to inspire young students and guide them towards the analysis and comprehension of cosmic rays.

The **Open FPGA kit** allows performing a series of gamma spectroscopy experiments without using a radioactive source. Moreover, the FPGA on board can be easily configured in order to perform several signal processings.

All the experimental setups are provided by a complete software suite for remote control of the system and data analysis.

The complete list of Physics Experiments and the concerning CAEN Educational Systems is reported in the following table.

Content of the Modular Kits

SP5600C - Educational Gamma Kit

Model	SP5600	DT5720A	A315	SP5606	SP5607
Description	Power Supply and Amplification Unit  p. 190	Desktop Digitizer 250 MS/s  p. 190	Splitter  p. 192	Mini-Spectrometer  p. 192	Absorption tool  p. 193

SP5600D - Educational Beta Kit

Model	SP5600	DT5720A	SP5608
Description	Power Supply and Amplification Unit  p. 190	Desktop Digitizer 250 MS/s  p. 190	Scintillating tile  p. 193

SP5600E - Educational Photon Kit

Model	SP5600	DT5720A	SP5601	SP5650C
Description	Power Supply and Amplification Unit  p. 190	Desktop Digitizer 250 MS/s 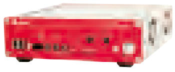 p. 190	LED Driver  p. 191	Sensor Holder for SP5600 with SiPM  p. 191

SP5600AN - Educational Kit - Premium Version

Model	SP5600	DT5720A	A315	SP5606	SP5607	SP5601	SP5650C	SP5608
Description	Power Supply and Amplification Unit  p. 190	Desktop Digitizer 250 MS/s 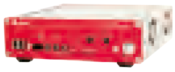 p. 190	Splitter  p. 192	Mini-Spectrometer  p. 192	Absorption tool  p. 193	LED Driver  p. 191	Sensor Holder for SP5600 with SiPM  p. 191	Scintillating tile  p. 193

SP5640 - GammaEDU

Model	SP5640	SP5640
Description	Backpack Radiation Detector  p. 183	Digital MCA Tube Base for Gamma-Ray spectroscopy  p. 183

SP5650 - Open FPGA Kit

Model	DT4800	DT1260
Description	Digital Detector Emulator  p. 194	kit SCI-Compiler SMART  p. 189

SP5630EN - Environmental Kit

Model	i-Spector - S2570B	Samples
Description	Intelligent Silicon Photomultiplier Tube	Samples
		
	p. 187	

SP5630ENP - Environmental Kit Plus

Model	i-Spector - S2570D	Samples	Shielding Kit	BGO Crystal
Description	Intelligent Silicon Photomultiplier Tube	Samples	Shielding Kit	BGO Crystal
		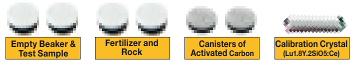		
	p. 187			

SP5620CH - Cosmic Hunter

Model	SP5621	SP5622 (x2)
Description	Coincidence Module	Detection System
		
	p. 182	p. 187

SP5600EMU - Emulation Kit

Model	DT4800	DT5770
Description	Digital Detector Emulator	Desktop Multi-Channel Analyzer
		
	p. 194	p. 194

SP5700 - EasyPET

Model	SP5700
Description	EasyPET
	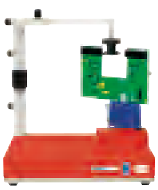
	pp. 178, 195

SP5701 - EasyPET Kit

Model	SP5700	DT5770
Description	EasyPET	Desktop Multi-Channel Analyzer
	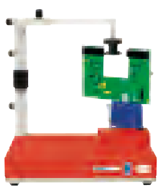	
	pp. 178, 195	p. 194

Additional Tools

Model	SP5608	DT5606	SP5622	SP5609	SP5607	DT993
Description	Scintillating Tile	Mini Spectrometer	Detection System	Telescope Mechanics	Absorption tool	Desktop Dual Timer
						
	p. 193	p. 192	p. 187	p. 189	p. 193	p. 188

SP5700 - SP5701

EasyPET - EasyPET Kit

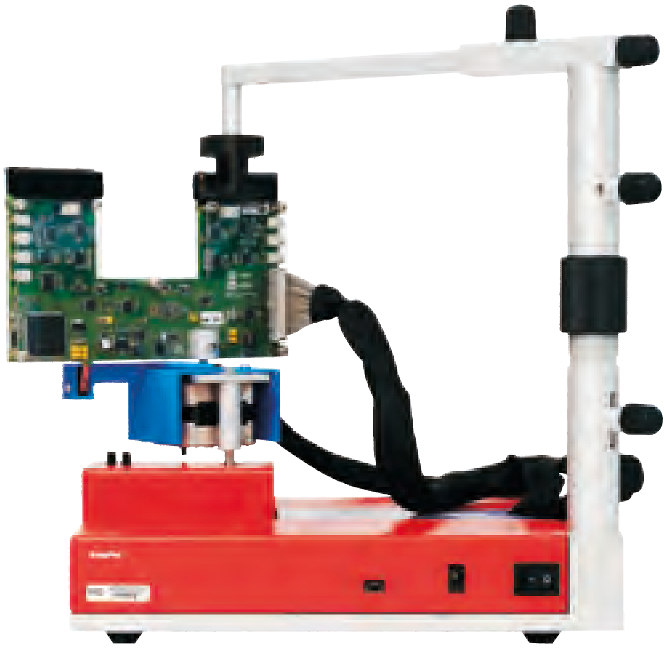

2D image reconstruction in real-time to explore Nuclear Imaging World!

EasyPET is a simple, user-friendly and portable didactic PET system developed for high-level education, to explore the physical and technological principles of the conventional human PET scanners, using the same basic detectors of state-of-the-art systems.

Ordering Options

Code	Description
WSP5700XAAAA	SP5700 - EasyPET
WSP5701XAAAAA	SP5701 - EasyPET Kit

The Positron Emission Tomography (PET) scanner is a state-of-the-art medical imaging system, capable of providing detailed functional information of physiological processes inside the human body.

The EasyPET - SP5700 concept, protected under a patent filed by Aveiro University, is based on a single pair of detector kept collinear during the whole data acquisition and a moving mechanism with two degrees of freedom to reproduce the functionalities of an entire PET ring. The main advantages are in terms of the reduction of the complexity and cost of the PET system. It opens the possibility of teaching by doing the basics behind PET imaging simplifying the set-up to make it accessible to Educational Laboratories.

The EasyPET is also available in a special Educational Kit, EasyPET Kit - SP5701, which includes a compact portable 16k Digital MCA - DT5770 too.

A Graphical User Interface allows the user to easily set the acquisition parameters, visualize the reconstructed image in real-time during acquisition, and perform several didactic experiments related to PET imaging, as well as offline image analysis.

- Two detector cells, each composed of a LYSO scintillator crystal optically coupled to a SiPM
- Software: data analysis and EasyPET and MCA management
- Main applications:

- Basic Measurements: γ Spectroscopy and System Linearity
- Positron Annihilation Detection
- Two-dimensional Reconstruction of Source
- Spatial Resolution

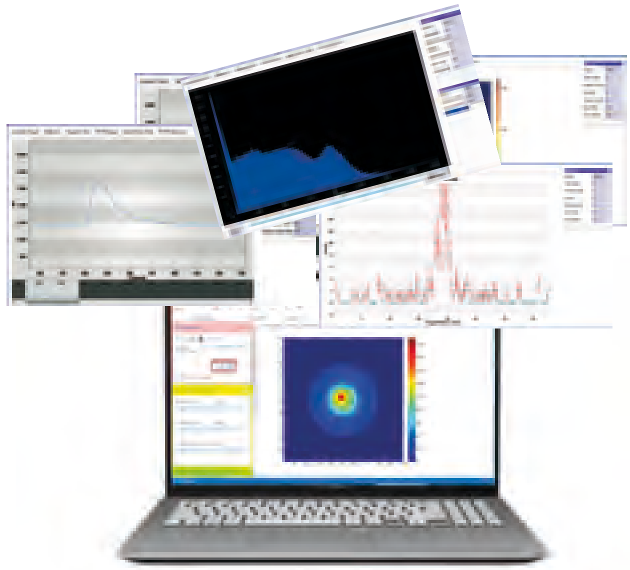

Physics Experiments

Kit Model	Statistics	SiPM Characterization	Photons	Cosmic Rays	γ Spectroscopy	β Spectroscopy	Nuclear Imaging	Environmental Radioactivity Indoor	Environmental Radioactivity Outdoor	Pulse Processing
SPS5700 EasyPET	•	-	-	-	-	-	•	-	-	-
SPS5701 EasyPET Kit	•	-	-	-	•	-	•	-	-	-

[3]Patent pending, Universidade de Aveiro.

SP5600C - SP5600D - SP5600E - SP5600AN

Educational kits

Advanced and compact solutions for Nuclear & Particle Physics experiments!

SiPM Modular

The CAEN Educational kits are modern, digital, and flexible platforms developed by CAEN for teaching the fundamentals of Statistics & Nuclear, and Modern Physics.

The set-ups are all based on Silicon Photomultipliers (SiPM) state-of-the-art sensors of light with single-photon sensitivity and unprecedented photon counting capability.

Ordering Options

Code	Description
WK5600XCAAAA	SP5600C - Educational Gamma Kit
WK5600XDAAAA	SP5600D - Educational Beta Kit
WK5600XEAAAA	SP5600E - Educational Photon Kit
WK5600XANAAA	SP5600AN - Educational Kit Premium Version

CAEN designed several modular Educational Kits:

SP5600C - Educational Gamma Kit, SP5600D - Educational Beta kit, SP5600E - Educational Photon kit, and a Premium version, SP5600AN, which includes all the components of the three kits.

The kits are composed of detectors and electronics modules which can be configured to perform several experiments, covering different Physics fields. What is being proposed has to do with light quanta, radioactive decays (β and γ rays) and cosmic rays.

HERA (Handy Educational Radiation Application) is a user-friendly software allowing the user to manage all mentioned CAEN kits.

The software represents a modern and flexible platform for teaching the fundamentals of Statistics, Particles Detection, and Nuclear Imaging thanks to the simple graphical interfaces and the embedded documentation and analysis tools. The user can easily manage all the parameters of the Power Supply, the Amplification Unit, and the Digitizer. The digitized signals can be monitored for real-time fine-tuning of the setup.

- HERA software for control of the system and for data analysis
- Main experiments:
  - Statistics
  - γ and β Spectroscopy: from energy spectrum to radiation absorption end more
  - Cosmic rays: from cosmic rays detection to cosmic vertical flux measurement
  - Photon detection and light distribution

Physics Experiments

Kit Model	Statistics	SiPM Characterization	Photons	Cosmic Rays	γ Spectroscopy	β Spectroscopy	Nuclear Imaging	Environmental Radioactivity Indoor	Environmental Radioactivity Outdoor	Pulse Processing
SP5600C Gamma Kit	•	-	-	-	•	-	-	•	-	-
SP5600D - Beta Kit	•	-	-	•	-	•	-	•	-	-
SP5600E Photon Kit	•	•	•	-	-	-	-	-	-	-
SP5600AN Premium Kit	•	•	•	•	•	•	-	-	-	-

SP5600EMU
Emulationl Kit

NEW

SP5650
Open FPGA Kit

Create and Analyze a radioactive source!

Ordering Options

Code	Description
WSP5600XEMUAA	SP5600EMU - Emulation Kit

This kit allows the user to perform a series of lab experiments without using a radioactive source and a detector, by simulating the signals produced by the interaction of particles with the detecting unit.

The Emulation kit is based on the CAEN Digital Detector Emulator (DT4800) together with the Digital Multichannel Analyzer (DT5770).

The core of the system is the DT4800, the most compact and cost-effective model of the Detector Emulators family. The unit features one analog output and one digital input. As a Pulser it can generate exponential decay signals with programmable Rise Time and Fall Time up to a rate of 1 Mcps. The rate can be fixed or it can follow a Poissonian distribution. In Emulation mode the unit can reproduce signals from a real energy spectrum. A database of nuclides is provided to generate specific emission lines and Gaussian noise can be added.

The Software interface enables the Emulator to generate an analog output and apply different pulse processing via the MCA.

- No need of radioactive source
- User Friendly Control SW
- γ and ß Spectroscopy
- System Linearity
- Real Energy spectrum emulation
- Noise emulation
- Time distribution Emulation (Poissonian)
- Continuous pre-amplifier emulation
- Pulse processing: Height Analysis and Charge Integration
- Statistic

Programming with SCI-Compiler like setup an experiment!

Ordering Options

Code	Description
WSP5650XAAAA	SP5650 - Open FPGA Kit

The Open FPGA kit allows the user to perform a series of lab experiments without using radioactive source and detector, by simulating the signals and to create specific processing of pulses.

The Open FPGA kit is based on the CAEN Digital Detector Emulator (DT4800) together with a SCI-Compiler SMART starter pack. The kit allows performing a series of lab experiments without using a radioactive source and a detector, by simulating the signals produced by the interaction of particles within the detecting unit. The core of the system is the DT1260, 60 Ms/s, 12 bit General Purpose board with programmable FPGA. Besides DT4800, splitter, and several delay lines are also provided in the kit to reproduce some experimental situations that offer the possibility to configure the FPGA by using several types of pulse processing.

SCI(entific) Compiler is a Windows-based software designed to generate the firmware for signal processing in a simple way. It is an automatic code generator that, starting from a graphical block diagram, generates a VHDL piece of code that implements the required function.

- Complex trigger logic
- Event Counters
- Single Channel (SCA) and Multi Channel Analyser (MCA)
- Time to Digital Converter
- Replacement for any old logic-based system
- Time tagging logic
- Particle real-time Time of Arrival distribution calculation
- Waveform recording digitizer
- Logic Analyzer

Physics Experiments

Kit Model	Statistics	SiPM Characterization	Photons	Cosmic Rays	γ Spectroscopy	ß Spectroscopy	Nuclear Imaging	Environmental Radioactivity Indoor	Environmental Radioactivity Outdoor	Pulse Processing
SP5600EMU Emulation kit	•	-	-	-	•	-	-	-	-	•
SP5650 Open FPGA Kit	•	-	-	-	•	-	-	-	-	•

NEW

SP5630EN

Environmental Kit

Discover the environment that surrounds us!

Ordering Options

Code	Description
WSP5630ENAAAA	SP5630EN - Environmental Kit

To increase the familiarity with Environmental Radioactivity Field, CAEN designed a dedicated educational kit, based on a Silicon Photomultipliers (SiPM) matrix coupled to a CsI Scintillator.

CAEN developed a dedicated kit to discover the environmental radioactivity around us. The goal is to oppose the public imagination that often associates a negative feeling with this natural phenomenon.

The kit is composed of i-Spector- S2570B, a full-featured radiation detector system, and a kit of samples suitable for gamma environmental detection. Teaching and training experiences are performed starting from system calibration in terms of energy and by acquiring gamma spectra to study the emission and the radioactive elements contents of different samples.

Instrumentation Web Interface can be easily controlled through its dedicated web-based interface with no need to install software on your PC. The user can monitor the status of the module, configure the HV and connection parameters, visualize the energy spectrum in real-time, perform online analysis and download the data.

- Indoor Radiation Measurements
- Energy Calibration
- Environmental background measurements
- Passive Radon measurements
- Samples and Photo-peaks identification
- Environmental Sample measurements
- SiPM based

NEW

SP5630ENP

Environmental Kit Plus

Experience the phenomena… Explore the Physics… Discover the essence!

Ordering Options

Code	Description
WSP5630ENAAA	SP5630ENP - Environmental Kit Plus

The Open FPGA kit allows the user to perform a series of lab experiments without using radioactive source and detector, by simulating the signals and to create specific processing of pulses.

CAEN designed a new dedicated Educational kit, the SP5630ENP – Environmental kit Plus, to guide the users towards the development of complementary measurement techniques based on counting and on the analysis of the spectrum.

The kit is composed by the i-Spector Digital (all-in-one detector, electronics and MCA), Shielding Kit (solution to perform several experiments about gamma spectroscopy and shielding materials), CsI and BGO crystals (to be coupled to the SiPM matrix), and a Sample Kit (suitable for gamma environmental detection).

The main goal is the study of the absorption of the gamma rays passing through matter thicknesses and the related observations about the different crossed materials. It is a user-friendly system for Advanced Labs based on the latest technologies and instrumentation.

- Detecting γ-Radiation
- System Calibration: Linearity and Resolution
- γ-Radiation Absorption
- Comparison of different Shielding Materials
- Photonuclear cross-section/Compton Scattering cross-section
- Passive Radon measurements
- Environmental Sample identification & measurements

Physics Experiments

Kit Model	Statistics	SiPM Characterization	Photons	Cosmic Rays	γ Spectrospopy	ß Spectroscopy	Nuclear Imaging	Environmental Radioactivity Indoor	Environmental Radioactivity Outdoor	Pulse Processing
SP5630EN Environmental kit	•	-	-	-	-	-	-	•	-	-
SP5630ENP Environmental kit Plus	•	-	-	-	-	•	-	•	-	-

NEW

SP5620CH

Cosmic Hunter

When CAEN technology meets young talents!

Ordering Options

Code	Description
WSP5620CHAAAA	SP5620CH - Cosmic Hunter

Cosmic Hunter is a simple and portable device from a lab desk to a hot-air balloon! It was indeed employed at the 42nd International Balloon Festival in Château-d'Oex to commemorate cosmic-ray pioneers.

Cosmic Hunter is a new educational tool developed to inspire young students and guide them towards the analysis and comprehension of cosmic rays. Cosmic Hunter, Silicon Photomultipliers (SiPM) based, is composed of one detection coincidence unit together with up to three plastic scintillating tiles.

Muons detection, flux estimation, shower detection and more can be performed thanks to a flexible system geometry.

The Cosmic Hunter needs no Software. All the controls are available on the module and the data can be downloaded via SD card.

CAEN is developing a new dedicated Software for the full control of the system. Through a simple graphical interface, the user can set all the parameters, manage the acquisition, and download the data.-

- Based on SiPM detectors and plastic scintillating tiles
- Up to 3 scintillating tiles management
- Flexible system geometry
- No needs SW interface
- Main experiments:
  - Muons Detection
  - Triple coincidence
  - Muons Vertical Flux on Horizontal Detector
  - Zenith Dependence of Muons Flux
  - Cosmic Shower Detection

SP5600D

Educational Beta Kit

From detector characterization to cosmic rays detection!

Ordering Options

Code	Description
WSP5600DAAAA	SP5600D - Educational Beta Kit

The Educational Beta kit is high-level instrumentation.

The kit addresses experiments on cosmic rays, from simple muons detection to flux estimation and angular distribution, using advanced tools for statistical analysis.

The Educational Beta kit is based on Silicon Photomultipliers (SiPM). The key element is the SP5608 – Scintillating tile. The SP5608 is an assembly with an embedded plastic scintillating tile, directly coupled to a SiPM. The tile is the ideal tool for tests with beta-emitting isotopes and cosmic rays. Thanks to the practical case assembly, SP5608 can be used as a stand-alone detector or in a cosmic telescope with two tile modules, together with the SP5609 - Telescope Mechanics.

HERA (Handy Educational Radiation Application) is a new dedicated control software for the full control of the system and the data analysis. Its "Experiment" area includes also a special section dedicated to Cosmic Rays and Beta Spectroscopy.

- Based on SiPM detectors and plastic scintillating tiles
- Up to 2 scintillating tiles management
- HERA software: remote control of the system and data analysis
- Main experiments:
  - Cosmic Rays
  - Beta spectroscopy
  - Radiation-Matter Interaction
  - Absorption coefficient measurements

Physics Experiments

Kit Model	Statistics	SiPM Characterization	Photons	Cosmic Rays	γ Spectroscopy	ß Spectroscopy	Nuclear Imaging	Environmental Radioactivity Indoor	Environmental Radioactivity Outdoor	Pulse Processing
SP5620CH Cosmic Hunter	•	-	-	•	-	-	-	-	-	-
SP5600D Beta Kit	•	-	-	•	-	•	-	-	-	-

SP5640
GammaEDU

Just one tablet click to perform radioactive measurements outdoor!

A portable detection backpack for revealing the presence of radioactive materials in the environment. The high efficiency of the scintillation crystal allows the user to perform a measurement in few minutes.

GammaEDU can identify industrial, medical, and naturally occurring radioactive isotopes in static and dynamic acquisition

Ordering Options

Code	Description
WSP5640XAAAAA	SP5640 - GammaEDU

The GammaEDU detection backpack includes NaI(Tl) scintillator crystal (0.3 L) coupled with a Photomultiplier Tube (PMT) and the S2580 - GammaStream. The GammaStream integrates High Voltage Power Supply, Preamplifier, and digital Multi-Channel Analyzer for scintillation spectroscopy. The GammaEDU has high detection efficiency, low power consumption, and the data taking can be uninterrupted up to 6 hours, very suitable for outdoor gamma radiation measurements.

A 10'' tablet including CAEN GammaEDU application is part of the product.

With the GammaEDU Android application the students can acquire and analyze in real time a γ-ray spectrum to get the K, U and Th abundances, keep track of the surrounding environment, take the GPS coordinates, and shoot a picture of the on-going measurements. The data are saved in a .kmz file ready to be visualized on Google Earth and shared on Google Drive for producing a radioactivity map of the area.

- Environmental Gamma detection and spectroscopy
- Mapping of potential radon-prone areas
- Environmental monitoring in land field
- Geochemical and mineral exploration
- Statistics
- Customs protection and border control
- Scenario of emergency services
- Homeland security

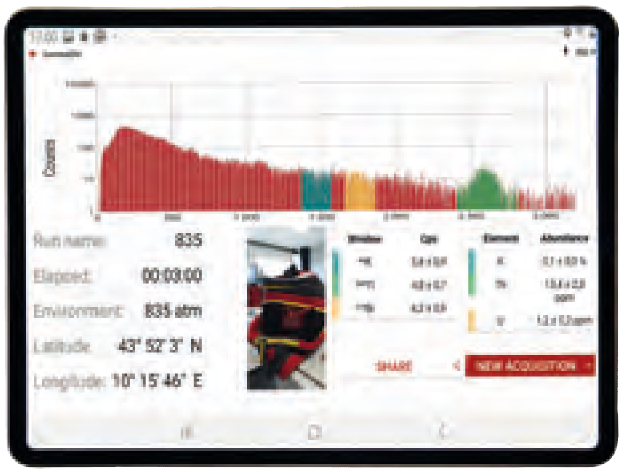

Physics Experiments

Kit Model	Statistics	SiPM Characterization	Photons	Cosmic Rays	γ Spectrospopy	ß Spectroscopy	Nuclear Imaging	Environmental Radioactivity Indoor	Environmental Radioactivity Outdoor	Pulse Processing
SP5640 GammaEDU	•	-	-	-	•	-	-	-	•	-

SP5660

RockyRAD

NEW

Portable Geiger-Müller counter for nuclear radiation

Discover the fascinating world of rock radioactivity and then expand your horizon to detect the unseen radiation in our everyday surroundings.

Ordering Options

Code	Description
WK5660XAAAAA	SP5660 – RockyRAD

RockyRAD, SP5660, is not just a Geiger-Müller counter; it is a portable and compact device that opens a window into the world of gamma and beta radiation. These types of radiation, produced by naturally occurring materials like soil and rocks, can be studied and better understood for various applications. For those who love an interdisciplinary approach, RockyRAD is an invaluable resource. Not only does it promote exciting STEM activities, but it also acts as a catalyst for projects that merge various subjects, such as Physics, Mathematics, Earth Sciences, Statistics, Computer Science, and Geography, creating a comprehensive educational experience.

- Detector: Geiger-Müller Tube
- Display Information: Total Counts, Counts Per Minute, Equivalent Dose Rate
- Bluetooth connection
- Rechargeable Battery (USB-C)
- RockyRAD Androind APP

Physics Experiments

Kit Model	Statistics	SiPM Characterization	Photons	Cosmic Rays	γ Spectrospopy	ß Spectroscopy	Nuclear Imaging	Environmental Radioactivity Indoor	Environmental Radioactivity Outdoor	Pulse Processing
SPS5622B Detection System Plus	•	-	-	•	-	-	-	•	•	-

COMING SOON

SP5622B

Detection System Plus

Portable scintillating tile for cosmic rays detection!

The Detection System Plus, SP5622B, is a user-friendly system for cosmic-ray detection. It can be used as a didactic instrument or as an external trigger system for another experimental setup. The simple design makes it suitable for not only university-level physics labs, but also for high school level physics programs.

Ordering Options

Code	Description
WSP5622BXAAA	SP5622B - Detection System Plus

The Detection System Plus, SP5622B, is a useful tool for introducing people into the world of modern physics, particle physics, special relativity, etc.

It represents a small didactic and complete device for the explanation of the scientific method to the students by performing cosmic rays experiments.

The SP5622B is based on a plastic scintillating tile coupled to a solid-state Silicon Photomultiplier (SiPM), together with all the frontend electronics needed.

This avoids having high voltages, generator, cables, connectors, and offers an additional safety margin for students.

The module management is easily allowed via the selectors and buttons on the front panel. It is equipped with a front display that shows information related to the settings of main parameters and four histograms: charge distribution of the signal, timing distribution of the cosmic rays, cosmic flux rate vs time, and flux distribution per minute.

The data can be recorded on a microSD card.

- Standalone
- Fully compatible with SP5620CH Cosmic Hunter
- Based on SiPM detectors and plastic scintillating tile
- External trigger system for several laboratory setups
- Analog and digital outputs
- No need of SW interface
- SD card to download data

Physics Experiments

Kit Model	Statistics	SiPM Characterization	Photons	Cosmic Rays	γ Spectrospopy	ß Spectroscopy	Nuclear Imaging	Environmental Radioactivity Indoor	Environmental Radioactivity Outdoor	Pulse Processing
SPS5622B Detection System Plus	•	-	-	•	-	-	-	-	-	-

S2580

Gamma stream

Active, stand-alone, fully featured MCA tube base for scintillation spectroscopy

Graphical software tool for digitizers running DPP-PHA firmware

Ordering Options

Code	Description
WS2580XAAAAA	S2580 - GAMMASTREAM - Digital MCA Tube Base for Gamma-Ray Spectroscopy

CAEN Gamma stream is a compact and portable system for gamma ray spectroscopy with scintillation detectors, which provides an active Multi-Channel Analyzer (MCA) integrated in a 14-pin photomultiplier tube (PMT) base. Gamma stream fully integrates in a stand-alone device the high voltage to bias the PMT, the preamplifier to shape the signal from detector, and the MCA for a complete Pulse Height Analysis online.

Gamma stream has been designed to work stand-alone, with no need of additional devices or cables. Gamma stream features internal rechargeable Li-Ion battery providing long-term duration for unattended on-field acquisitions. Once Gamma stream is programmed via computer or mobile phone, it then acquires and logs data in an internal SSD memory.

- High Voltage Power Supply (0 ÷ +1500V/500 µA) - Charge Sensitive Preamplifier - digital Multi-Channel Analyzer (12-bit and 62.5 MHz ADC) for scintillation spectroscopy
- Coupled with NaI(Tl) with a 14-pin PMT
- Full stand-alone operation with embedded CPU, data storage (SSD) unit, and power supply for up to 6/8 hours operation
- Wired and wireless connectivity via USB, Ethernet, Wifi and Bluetooth
- Acquisition modes: PHA, PHA with time stamp, Signal Inspector

S2570B

i-Spector Digital

Ordering Options

Code	Description
WSP5630ENAAAA	S2560B i-Spector 18x18mm – CsI ASSEMBLY

i-Spector is an innovative product designed to operate as full-featured radiation detection systems for Gamma Spectroscopy.

The system is based on a SiPM area 18 ×18 mm^2 [Hamamatsu S14160-60520HS]. All SIPMs of the area are connected in parallel to increase the active area of the matrix.

It integrates a shaper, a peak stretcher and a peak ADC to implement a simple MCA (4K).

A web-based GUI allows the user to set the acquisition parameters, see results on plot and perform basic data analysis.

- All-in-one detector, electronics and signal processing
- Based on a SiPM area up to 18×18 mm^2
- Scintillator Crystal dim: 18 x 18 x 30 mm^3
- 20-80 V Integrated High Voltage for SiPM biasing
- Energy Range: 30 keV to 3 MeV
- Energy Resolution (FWHM): <6 % @ 662 keV
- Ethernet connectivity
- Web-based GUI for unit control and data analysis

S2570D

i-Spector Digital

Ordering Options

Code	Description
WS2560DXAAAA	S2560D i-Spector 18x18mm – CsI ASSEMBLY

i-Spector is an all-in-one unit based on a

scintillating crystal CsI coupled to Silicon Photomultipliers.

i-Spector Digital S2570 is a Gamma Spectrometry unit. It embeds a digital MCA, based on 80 MSps 12-bit ADC and charge integration algorithm. The unit provides as

output an analog amplified signal and a 4k channels energy spectrum calculated onboard and displayed into the Web-Interface.

The unit is enclosed in a light-tight aluminium/plastic tube (Ø 60 mm, h 135 mm), with the possibility to unmount the crystal holder and easily change it.

.

- All-in-one detector, electronics and signal processing
- Based on a SiPM area up to 18×18 mm^2
- Scintillator Crystal dim: 18 x 18 x 30 mm^3
- 20-80 V Integrated High Voltage for SiPM biasing
- Ethernet connectivity
- Web-based GUI for unit control and data analysis

DT993

Desktop Dual Timer

Ordering Options

Code	Description
WS2580XAAAAA	DT993 - Dual Timer Desktop

One of the most useful modules ever made, today in a new and handy form.

The CAEN Model DT993 Dual Timer is a desktop module with two identical triggered pulse generators. It produces NIM/TTL or ECL pulses (selectable via an on-board switch) with widths ranging from 50 ns to 10 s. Output pulses are provided in both normal and negated forms. The timers can be re-triggered by the pulse end marker signal. Coarse width adjustment is done via a 9-position rotary switch, while fine adjustment is done either by a 15-turn dial handle (with lock) or an external voltage. The trigger start can be initiated by an external signal (NIM, TTL, or ECL) or manually via a front panel switch. The module also has VETO and RESET inputs, with RESET available on a front panel switch. The DT993 features LEMO 00 connectors for NIM/TTL signals and male pin couples for ECL signals.

- The Model Dual Timer is a 1-unit module housing two identical triggered pulse generators
- Manual or pulse triggered START (NIM, TTL or ECL)
- NIM, TTL and ECL output pulses from 50 ns to 10 s
- Manual or pulse triggered RESET

(•NIM, TTL and ECL) END-MARKER pulse

- VETO input

SP5609

Telescope Mechanics

The SP5609 Telescope Mechanics is an additional tool for an easy setup of components that need to be on the same axys from different angles. The SP5609 allows the construction of a Muon Telescope using either two SP5608 - Scintillating Tiles or two SP5622 - Detection Systems.

The SP5609 is composed by:

n°1 rotary axis with desk support
n°2 Clamp with screws
n°2 angle bracket kit
n°4 screws TPC 4X25 INOX CROSS DIN 7985
n°4 zinc coated washers [4mm]
n°4 zinc smooth washers
n°4 inox nuts

SP5622

Detection system

The Detection System consists of a plastic scintillator, a photodetector, and a small front-end electronic boards. The charged particles that pass through the unit deposit part of their energy inside the scintillators, producing a light signal. The light produced in the scintillator is then collected and converted into an electrical signal via a photosensor unit.

- Plastic scintillator (15 x 15 x $1cm^2$)
- Frontend electronic board
- AdvanSiD NUV-SiPM (4 x $4mm^2$) mounted in the tile corner at 45°

Ordering Options

Code	Description
WSP5622XAAAA	SP5622 - Detection System

DT1260

Sci-Compiler SMART

Sci-Compiler SMART (SCISMART) is a hardware + software kit for non-expert users who are approaching the open FPGA programming.

We introduce them to an innovative method to simplify the firmware development using Sci-Compiler software, a block-diagram-based programming interface consisting of a prebuilt set of functions (for example oscilloscope, TDC, MCA, charge integration, etc.) specifically developed for physics/engineering applications. Placing and interconnecting the available blocks on a diagram, SCI-Compiler is able to automatically generate a VHDL piece of code that implements the required function and deploy it to the FPGA. In this way, even a non-expert user can write his own firmware code without having any knowledge of the VHDL/Verilog programming language.

A basic, ready-to-use default firmware and readout software is provided for free and open source. The default firmware manages the basic waveform digitization and Pulse Height Analysis. The user can take advantages of examples firmware diagram available in SCI-Compiler, in order to start learning how to program the FPGA and take confidence with the software.

- Beginners' kit to learn how to easily program an open FPGA
- Powered by SCI-Compiler, the block-diagram-based firmware generator and compiler for CAEN programmable boards
- Automatic VHDL code generation starting from logic blocks and virtual instruments
- Very simple generation of complex online pulse processing: schematics-based design
- Hardware included for custom pulse processing firmware testing
- Ideal for non-expert firmware programmer
- Advanced signal processing blocks like PHA based on Trapezoidal Filter, Charge Integration, Oscilloscope …
- Automatic generation of drivers, libraries and demo software
- 2 channel, 65MS/s 12 bit, Open FPGA ADC unit included

Ordering Options

Code	Description
WKSCISMARTXA	SCI-Compiler SMART kit

SP5600

Power Supply and Amplification Unit

The SP5600 is a General purpose Power Supply and Amplification Unit, integrating up to two SiPMs in a mother & daughter architecture allowing for easy mounting and replacement of the sensors. The basic configuration features two channels with independent gain control up to 50 dB and provides the bias voltage (up to 100 V) to the sensors with gain stabilization. Each channel can provide a digital output generated by the fast leading edge discriminators. A timing coincidence of the two channels is also available.

- Variable amplification gain (up to 50 dB)
- Low noise, not to spoil the sensor performances for small signals
- Wideband, to comply with the fast sensor response
- Fast leading edge discriminator and time coincidence
- Provides the bias for the sensors with gain stabilization
- USB 2.0 interface
- Mechanical structure with an embedded SiPM 1 x 1 mm^2
- Dimension: 154 x 50 x 70 mm^3 (WxHxD)
- User Friendly Control Software with all-in-a Window Graphical Interface (together for SP5600 and DT5720A)

Ordering Options

Code	Description
WSP5600XAAAA	SP5600 - 2 Channels General Purpose Amplifier

DT5720A

Desktop Digitizer

The DT5720A is a CAEN Desktop Waveform digitizer housing 2 channels 12 bit 250 MS/s ADC with a dedicated charge integrating firmware (DPP-PSD) for real time pulse processing.

- 2 Channel 12 bit 250 MS/s Digitizer
- Digital Pulse Processing for Charge Integration DPP-PSD
- Best suited for PMT and SiPM/MPPC readout at low and high rates
- Mid-High speed signals (Typ: output of PMT/SiPM)
- Good timing resolution with fast signals (rise time < 100 ns)
- Optical Link and USB 2.0 interfaces
- Dimension: 154 x 50 x 164 mm^3 (WxHxD)
- User Friendly Control Software with all-in-a Window Graphical Interface (together for SP5600 and DT5720A)

Ordering Options

Code	Description
WDT5720AXAAA	DT5720A - 2 Ch. 12 bit 250 MS/s Digitizer: 1.25MS/ch, C4, SE

SP5601

LED Driver

The SP5601 is an ultra-fast LED Driver with pulse width at ns level, tunable intensity and frequency, that provides a low-cost tool for the detector characterization. The LED pulse generation can be triggered by an internal oscillator or by an external pulser.

- Pulse width: 8 ns
- LED color: violet (400 nm) 1500 mcd
- Pulse generator: internal/external
- Optical output connectors: FC
- Optical fiber included
- Dimension: 79 x 42 x 102 mm^3 (WxHxD)

Ordering Options

Code	Description
WSP5601XAAAA	SP5601 - Led Driver for SIPM development kit

SP5650C

Sensor Holder with SiPM

The SP5650C is a sensor holder provided in the Educational Photon kit. The holder hosts a 1.3 x 1.3 mm^2 Silicon Photo-Multipliers; moreover, a probe inside the holders senses temperature variations, thus allowing the user to compensate for possible gain instability. The SP5650C is made of a mechanical structure providing a FC fiber connector and a PCB where the SiPM is soldered. Bias voltage for the SiPM and temperature probe output are provided through a 10 pin female socket, while the analog output connector is MCX.

- Size 20 mm (diameter) x 6 mm (height)
- Analog Out Connector RADIALL: R113425000 (MCX MALE)
- Bias Connector M22-7140542 Female Vertical Socket
- Embedded Hamamatsu MPPC S13360- 1350CS:
  - 1.3 x 1.3 mm^2 Active Area
  - 667 Number of pixel
  - 50 µm Pixel Pitch

Ordering Options

Code	Description
WSP5650XCAAA	SP5650C - Sensor Holder for SP5600 with HAMAMATSU 1.3x1.3mm^2

SP5606

Mini-Spectrometer

SP5606 is mini-spectrometer for gamma ray detection. The spectrometer is composed of a mechanical structure that houses a scintillating crystal, coupled to a dedicated SiPM. Three different crystals are available: CsI, LYSO and BGO. The spectrometer is equipped with a bottom support to allows an easy connection to the SP5600 via the splitter A315, to avoid saturation effects.

- Mechanical structure for optimal SiPM to crystal coupling
- Scintillating Crystals: CsI, LYSO, BGO (6 x 6 x 15 mm^3)
- One SiPM embedded 6 x 6 mm^2

Ordering Options

Code	Description
WSP5606XAAAA	SP5606 - Mini Spectrometer with 6x6 sensor coupled to three scintillating crystals.

A315

Splitter

The Mod. A315 splits one input on two output signals. All the connectors are LEMO female type. The splitter is adapted for 50 Ohm lines. The device is completely passive (no power supply is required); the amplitude on each output is one half of that on the input.

Ordering Options

Code	Description
WA315XAAAAAA	A315 - Splitter

SP5607

Absorption Tool

The Gamma absorption tool allows to perform gamma attenuation measurements. It is a modular tool and its design allows an easy connection to the SP5606 bottom support. It is composed of:

- Spacers: one 4mm thick, five 10 mm thick;
- Aluminum Absorbers: one 4 mm thick, five 10 mm thick;
- PMMA Absorbers: one 4 mm thick, five 10 mm thick.

Ordering Options

Code	Description
WSP5607XAAAA	SP5607 - Absorption Tool for Gamma Applications

SP5608

Scintillating Tile

The SP5608 is a support with a embedded plastic scintillating tile, directly coupled to a SiPM . The tile, with a sensitive volume of 47 x 47 x 10 mm^3, is the ideal tool for tests with beta emitting isotopes and cosmic rays. The support structure allows to use the SP5608 stand-alone or to use two tile modules to build a cosmic telescope. A special source holder allows to perform beta attenuation measurements in a thin thickness material due to 2mm distance from the scintillating tile. It is provided by a paper and aluminum sheets

- Sensitive volume: 47 x 47 x 10 mm^3
- Scintillator: polystyrene
- Directly coupled to a SiPM 6 x 6 mm^2
- 20 Paper and Aluminum sheets

Ordering Options

Code	Description
WSP5608XAAAA	SP5608 - Scintillating Tile

DT4800

Micro Digital Detector Emulator

The DT4800, called Micro Digital Detector Emulator, is the most compact and cost effective model of the Detector Emulators family. It is available only in a one channel version and it is particularly suited for simple emulation needs and educational purposes. The unit features one analog output and one digital input. As a Pulser it can generate exponential decay signals with programmable Rise Time and Fall Time up to a rate of 1 Mcps. The rate can be fixed or it can follow a Poissonian distribution. In Emulation mode the unit can reproduce signals from a real energy spectrum that can be uploaded in the form of CSV or ANSI N42.42 files. A database of nuclides is provided to generate specific emission lines and Gaussian noise can be added. An user friendly control software is provided with the unit.

- Pulser/Emulator operating modes
- Real Energy spectrum emulation
- Time distribution emulation (Poissonian)
- Noise emulation
- Continuous pre-amplifier emulation
- Nuclides database
- Emulation and Detection Educational Software
- Digital Detector Emulator Software

Digital Detector Emulator Software

Ordering Options

Code	Description
WDT4800XAAAA	DT4800 – Micro Digital Detector Emulator

DT5770

Digital Multi Channel Analyzer

The DT5770 is a compact portable Digital MCA for Gamma spectroscopy. It is suited for high energy resolution semiconductor detectors, like HPGe and Silicon Drift Detector, connected to a Charge Sensitive Preamplifier. The unit can also properly operate directly connected to a PMT with inorganic scintillators (e.g. NaI or CsI scintillators), provided exponential pulse shape and decay time above 200 ns. It integrates analog front-end with programmable gain and possible AC coupling.

- Compact portable 16k Digital MCA
- Suited for high resolution Gamma Spectroscopy
- Support continuous and pulsed reset preamplifiers
- Software selectable coarse and fine gain
- DB9 connector for preamplifier power supply
- Features Pulse Height Analysis firmware for energy calculation
- Different acquisition modes available: PHA and signal inspector for an easy setup and signal monitoring
- USB and Ethernet communication interfaces

  Three control software allow to manage the acquisition and perform basic spectrum analysis:

- Emulation and Detection Educational Software
- EasyPET Control Software
- MC^2Analyzer Software

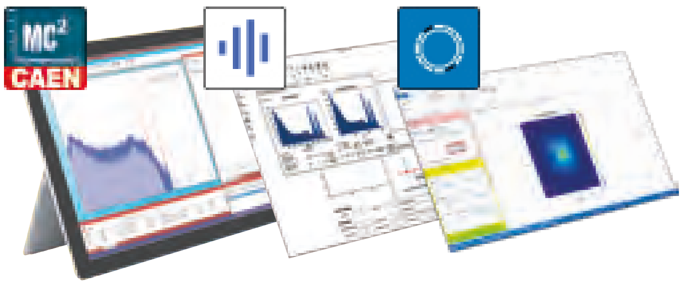

MC^2 Analyzer Software — Emulation and Detection Educational Software — EasyPET Control Software

Ordering Options

Code	Description
WDT5770AXAAA	DT5770 – Digital MCA - 1 LVPS ±12V/100mA ±24V/50mA

SP5700

EasyPET

EasyPET is a simple, user friendly and portable didactic PET system developed for high-level education, which allows exploring the physical and technological principles of the conventional human PET scanners, using the same basic detectors of state-of-the-art systems. The Positron Emission Tomography (PET) scanner is the state-of-the-art medical imaging system, capable of providing detailed functional information of physiological processes inside the human body. Functional imaging has a great impact in cancer diagnostics, monitoring of therapy effects and cancer drug development. The underlying principle to PET systems is the detection of high energy radiation emitted from a chemical marker, a molecule labelled with a radioisotope, administered to a patient. The radioisotope emits positrons which, after annihilating with atomic electrons, result in the isotropic emission of two photons back to back with an energy of 511 keV. The two photons are detected by a ring of detectors, which allows a pair of them to detect two back to back photons in any direction.

The simplicity of EasyPET derives from the innovative characteristics of the system and its acquisition method[1]. EasyPET comprehends only two detector modules that move together and execute two types of independent movements, around two rotation axes, so as to cover a field of view similar to that of a complete ring of detectors. The rotation movements are executed by two stepper motors. The schematic layout of the EasyPET components and acquisition method is shown in the following figure.

The bottom motor (1) has a fixed axis, whose position defines the center of the field of view. The bottom motor supports and performs a complete rotation of a second motor, in predefined steps of amplitude α. The axis of the top motor (2) is thus always

[1]Patent pending, Universidade de Aveiro.

positioned within a circumference of radius equal to the distance between the two axes. The top motor, in its turn, supports and moves a U shaped printed circuit board (3), where a pair of aligned and collinear detector modules (4) is mounted, performing

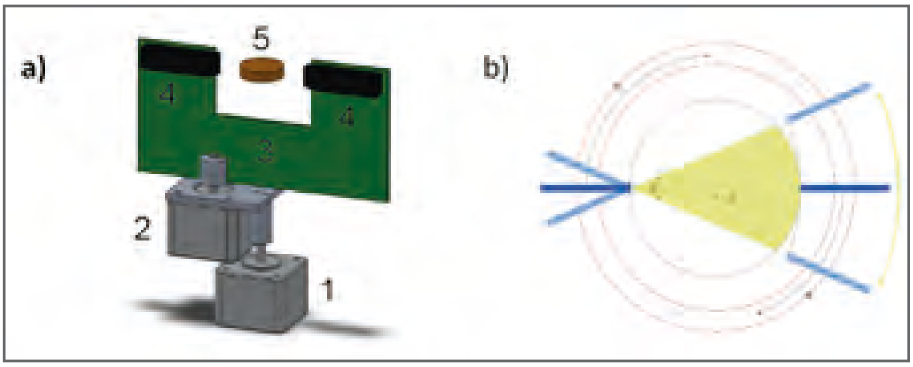

a) The EasyPET component layout:
1 - bottom motor, 2 - top motor, 3 - U-shaped PCB, 4 - pair of detector modules, 5 - radioactive source;

b) Top-view schematics of the EasyPET image acquisition method with two axes of rotation. α represents the angle step of the bottom motor rotation, while θ represents the scanning angle of the top stepper motor. The two axes are used to move one pair of scintillation detectors (blue rectangles) so as to acquire lines of response covering a cylindrical field of view between the detectors.

a symmetric scan of range θ around the center, for each position of the bottom motor. In this way, EasyPET can reconstruct an image of a radioactive source (5) placed anywhere within a cylindrical field of view between the pair of detectors. The diameter of the field of view is defined by the amplitude of θ, the range of the top motor scan.

The EasyPET operation principle is simple: the two small detector cells, each composed of a small scintillator crystal coupled to a silicon photomultiplier (SiPM), develop a signal when they detect a photon emitted by the source. A fast electronic readout system allows detecting coincident events resulting from the same decay process: if the signals from each detector are higher than a reference signal and occur within a specific time validation window, they are considered a coincidence event. For each scanning position, the number of coincidences is counted and an image of the accumulated lines of response is reconstructed in real-time.

EasyPET reduces the number of detectors required for the acquisition of a PET image to the minimum, while at the same time it eliminates the parallax error and the need for determination of depth of interaction in the crystals (DOI), thus allowing the obtainment of high-resolution PET images in all the field of view.

Main EasyPET components:

- Two detectors, each composed of a LYSO scintillator crystal optically coupled to a SiPM;
- Printed Circuit Board (PCB) equipped with electronics used for SiPMs supply voltage, signal readout and coincidence detection;
- Two stepper motors;
- Microcontroller unit responsible for controlling EasyPET parameters, driving the stepper motors and communicating with the computer;
- Holder for radioactive source;
- EasyPET Control Software.

EasyPET Control Software

Ordering Options

Code	Description
WSP5700XAAAA	SP5700 - EasyPET

CAEN global presence

CAEN Worldwide presence CAEN SyS

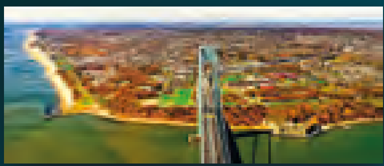

CAEN Technologies, Inc.
Staten Island, NY • USA

CAEN spa
Viareggio • Italy

CAEN GmbH
Solingen • Germany

NEW

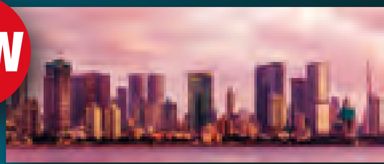

CAENspa INDIA Private Limited
Mumbai City • India

80
Countries where we are present

CAENqs

CAEN quantum Security srl
Torino • Italy

CAENels

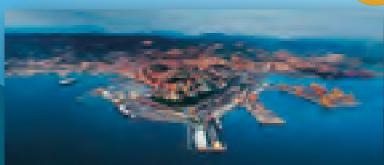

CAEN ELS srl
Basovizza • Trieste (TS)

CAENRFID

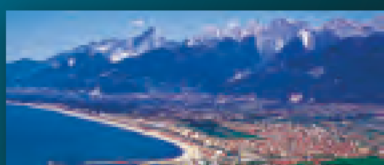

CAEN RFID srl
Viareggio • Italy

Printed in Italy, September 2024
Technical Documentation & Communication Office - CAEN SpA

ADOCUME00170 Educational Handbook 2024

edu CAEN Educational Tools

CAEN Educational Tools is a part of CAEN S.p.A.

CAEN S.p.A.
Via Vetraia 11
55049 - Viareggio
Italy
Phone +39.0584.388.398
Fax +39.0584.388.959
info@caen.it

www.caen.it

CAEN GmbH
Brunnenweg 9
64331 Weiterstadt - Germany
Tel. +49 (0)212 254 4077
Mobile +49 (0)151 16 548 484
info@caen-de.com

www.caen-de.com

CAEN Technologies, Inc.
1 Edgewater Street – Suite 101
Staten Island, NY 10305
USA
Phone +1.718.981.0401
Fax +1.718.556.9185
info@caentechnologies.com

www.caentechnologies.com

CAENspa INDIA Private Limited
B205, BLDG42, B Wing,
Azad Nagar Sangam CHS,
Mhada Layout, Azad Nagar, Andheri (W)
Mumbai, Mumbai City,
Maharashtra, India, 400053
info@caen-india.in

www.caen-india.in

www.caen.it/educational